

Engineering of enzymatic redox cascades involving oxygenases

I n a u g u r a l d i s s e r t a t i o n

zur

Erlangung des akademischen Grades eines

Doktors der Naturwissenschaften

(Dr. rer. nat.)

der

Mathematisch-Naturwissenschaftlichen Fakultät

der

Ernst-Moritz-Arndt-Universität Greifswald

vorgelegt von

Jan Muschiol

geboren am 09.11.1986

in Heide (Holst.)

Greifswald, 22.03.2016

Dekan: Prof. Dr. Werner Weitschies

1. Gutachter : Prof. Dr. Uwe T. Bornscheuer

2. Gutachter : Prof. Dr. Bruno Bühler

Tag der Promotion: 06.06.2016

Contents

Contents.....	IV
List of Abbreviations	VIII
1 Introduction	2
1.1 Enzymes in Biotechnology and Biocatalysis	2
1.1.1 Lipases.....	5
1.1.2 Alcohol dehydrogenases/Keto reductases	6
1.1.3 Old Yellow Enzymes	8
1.1.4 Cytochrome P450-Monooxygenases	10
1.1.5 Baeyer-Villiger-Monooxygenases.....	15
1.1.6 Rieske Non-Heme Iron Dioxygenases	18
1.2 Cascade Reactions.....	20
1.2.1 <i>In vitro</i> Cascades	22
1.2.2 <i>In vivo</i> Cascades.....	24
1.2.3 Combining <i>in vivo</i> and <i>in vitro</i> Cascades.....	27
1.3 Immobilization and Process Engineering	28
1.3.1 Immobilization Techniques.....	29
1.3.2 SpinChem® - A Rotating Bed Reactor	34
1.4 Application of Polymers and Chiral Molecules	35
1.4.1 Chiral Molecules.....	35
1.4.2 Polymers	38
2 Scope of this PhD thesis	40
3 Results	42
3.1 Co-Expression of Three Enzymes for Cascade Optimization	42
3.1.1 Cloning and Co-Expression of Three Enzymes for Application as <i>in vivo</i> Cascade	42
3.1.2 Application of Co-Expressed Enzymes as <i>in vivo</i> Cascade	43
3.2 Extension of a Three-Enzyme Redox Cascade	46
3.2.1 Application of Cytochrome P450-Monooxygenases for Initial Hydroxylation.....	46
3.2.2 Application of a Dioxygenase for Initial Hydroxylation	60
3.3 Immobilization of Two Enzymes for Cascade Reactions	65
3.3.1 General Applicability of Enzymes in a Rotating Bed Reactor.....	65
3.3.2 Optimization of the Whole Cell Encapsulation Process.....	69
3.3.3 Establishment of an <i>in situ</i> Encapsulation Process	73
3.3.4 Application of a Cascade for Oligo-[Caprolactone] Production in a Rotating Bed Reactor	74
4 Discussion.....	83

4.1 Co-Expression of Three Enzymes for Cascade Optimization	83
4.2 Extension of a Three-Enzyme Redox Cascade	85
4.2.1 ...by Cytochrome P450-Monooxygenases	85
4.2.2 ...by Dioxygenases	88
4.3 Immobilization of Two Enzymes for Cascade Reactions	90
5 Summary	94
5 Zusammenfassung	95
6 Materials and Methods	97
6.1 Materials	97
6.2 Microbiological Methods	106
6.3 Molecular Biology Methods	109
6.4 Biochemical Methods	113
6.5 Immobilization and Biocatalysis Reactions in STR, RBR and FBR ..	115
6.6 Analytics	116
6.7 Bioinformatic Methods	118
7 References	119
List of Publications	129
Danksagung	131

List of Abbreviations

AAD	Amino acid deaminase
ADH	Alcohol dehydrogenase
AKR	Aldo-keto reductase
AlaDH	Alanine dehydrogenase
Amp	Ampicillin
Amp ^R	Ampicillin resistance
approx.	approximately
APS	Ammonium persulfate
Aq. bidest.	Twice distilled water
Aq. dest.	Distilled water
ATA	Amine transaminase
B.C.	Before Christ
B.Sc.	Bachelor of Science
BCA	Bicinchoninic acid
BLAST	Basic local alignment search tool
blastn	BLAST based on nucleotide sequence
bp	base pairs
BSA	Bovine serum albumin
BVMO	Baeyer-Villiger monooxygenase
<i>C. cellulans</i>	<i>Cellulosimicrobium cellulans</i>
CAL-A	Lipase A from <i>Pseudozyma antarctica</i>
CAL-B	Lipase B from <i>Pseudozyma antarctica</i>
Cam ^R	Chloramphenicol resistance
CCE	Crude cell extract
cDNA	complementary DNA
CDW	Cell dry weight
CHMO	Cyclohexanone monooxygenase
CHMO _{Acineto}	CHMO from <i>Acinetobacter</i> sp.
CHMO _{DM}	Double mutant of CHMO _{Acineto} C376L/M400I
CHMO _{QM}	Quadruple mutant of CHMO _{Acineto} C376L/M400I/T414C/A463C
CLEA	Cross-linked enzyme aggregate
CLO	Arrangement of genes on pETM6: CHMO _{DM} , LK-ADH, OYE1
CO	Carbon monoxide
COL	Arrangement of genes on pETM6: CHMO _{DM} , OYE1, LK-ADH
Cpd 0/I	Compound 0/I
CPR	Cytochrome P450 reductase
CPR _{apicola}	CPR from <i>Candida apicola</i>
CV	Column volume
CYP	Cytochrome P450-monooxygenase
CYP102A7	P450 from <i>Bacillus licheniformis</i>
de	diastereomeric excess
DFG	Deutsche Forschungsgemeinschaft (German Research Society)
DMSO	Dimethyl sulfoxide

DNA	Deoxyribonucleic acid
dNTP	Deoxynucleoside triphosphate
DOC _{equi}	Dioxygenase cluster from <i>Rhodococcus equi</i>
DOC _{equiAra}	DOC _{equi} with additional pBAD promoter in front of the ferredoxin gene
DOx	Dioxygenase
<i>E. coli</i>	<i>Escherichia coli</i>
<i>e.g.</i>	<i>exempli gratia</i>
EC 1-6	Enzyme class 1-6
EDTA	Ethylenediaminetetraacetic acid
ee	enantiomeric excess
EPR	Electron paramagnetic resonance
ER	Endoplasmic reticulum
ERED	Ene reductase
ESI	Electrospray ionization
<i>et al.</i>	<i>et alii</i>
EtBz	Ethyl benzene
FAD	Flavin adenine dinucleotide
FBR	Fixed bed reactor
FDH	Formate dehydrogenase
FdR	Ferredoxin reductase
Fdx	Ferredoxin
FMN _{ox}	Flavin mononucleotide, oxidized
FMN _{red}	Flavin mononucleotide, reduced
FPLC	Fast protein liquid chromatography
G6P	Glucose-6-phosphate
G6PDH	Glucose-6-phosphate dehydrogenase
GC	Gas chromatography
Glc	D-glucose
GST	Glutathione
GulA	Guluronic acid
Hic	2-hydroxyisocaproate dehydrogenase
IPO	Initial public offering
IPTG	Isopropyl- β -D-thiogalactopyranosid
Kan	Kanamycin
Kan ^R	Kanamycin resistance
kbp	kilo base pairs
kDa	kilo Dalton
KP _i	Potassium phosphate
L+O+C	Cells containing either LK-ADH, OYE1 or CHMO _{DM} mixed in a 1:1:1 ratio
L6H	Limonene-6-hydroxylase (CYP71D18) from <i>Mentha spicata</i>
LB	Lysogenic broth
LCO	Arrangement of genes on pETM6: LK-ADH, CHMO _{DM} , OYE1
LDR	Long-chain dehydrogenase/reductase
LK-ADH	ADH from <i>Lactobacillus kefir</i>
LOC	Arrangement of genes on pETM6: LK-ADH, OYE1, CHMO _{DM}

lpm	Liter per minute
<i>M. spicata</i>	<i>Mentha spicata</i>
M.Sc.	Master of Science
MCP	Microcompartment
MDR	Medium-chain dehydrogenase/reductase
MeOH	Methanol
mRNA	messenger RNA
MS	Mass spectrometry
MW	Molecular weight
NAD(P) ⁺	Oxidized NAD(P)H
NAD(P)H	Nicotinamide adenine dinucleotide (phosphate)
NaP _i	Sodium phosphate
No.	Number
OCL	Arrangement of genes on pETM6: OYE1, CHMO _{DM} , LK-ADH
OD	Optical density
OD _{450/600}	OD at λ = 450 or 600 nm
OLC	Arrangement of genes on pETM6: OYE1, LK-ADH, CHMO _{DM}
OptiTaq	Blend of Taq- and Pfu-polymerase
OYE	Old yellow enzyme
OYE1	OYE 1 from <i>Saccharomyces pastorianus</i>
<i>P. putida</i>	<i>Pseudomonas putida</i>
P3HB	Poly-[3-hydroxybutanoate]
P450	Cytochrome P450-monooxygenase
P450-BM3	P450 3 from <i>Bacillus megaterium</i>
P450 _{cam}	Camphor degrading P450 from <i>P. putida</i>
P450-RhF	P450 from <i>Rhodococcus</i> sp. NCIMB 9784
P450 _{scc}	P450 for cholesterol side-chain cleavage
P4MCL	Poly-[4-methylcaprolactone]
PAGE	Polyacrylamide gel electrophoresis
pB	Arabinose-inducible promoter pBAD
PCL	Polycaprolactone
PCR	Polymerase chain reaction
PDB	Protein data bank
Pfu	<i>Pyrococcus furiosus</i>
PhD	<i>philosophiae doctor</i>
PLA	Polylactate
prim-ADH	primary ADH
Pyr	Pyruvate
<i>R. equi</i>	<i>Rhodococcus equi</i>
RBR	Rotating bed reactor
RBS	Ribosome binding site
RDOx	Rieske non-heme dioxygenase
RNA	Ribonucleic acid
ROP	Ring-opening polymerization
rpm	Revolutions per minute

RR-ADH	ADH from <i>Rhodococcus ruber</i>
SDR	Short-chain dehydrogenase/reductase
SDS	Sodium dodecyl sulfate
sec-ADH	secondary ADH
SLiCE	Seamless Ligation Cloning Extract
SOC	Super Optimal broth with Catabolite repression
sp.	species
STR	Stirred tank reactor
T7	IPTG-inducible T7/lacO promoter
TAE	Tris base, acetic acid and EDTA
Taq	<i>Thermus aquaticus</i>
tB	Terminator rrnBT2
TB	Terrific broth
TfBI/II	Transformation buffer I/II
TG	Transformation salts with glycerol
T _m	Melting temperature
TNT	2,4,6-trinitrotoluene
Tris	Tris(hydroxymethyl)aminomethane
TSB	Tryptic soy broth
tt7	T7 terminator
U	1 Unit = 1 $\mu\text{mol} \cdot \text{min}^{-1}$
UV/Vis	Ultraviolet/visible
WCW	Wet cell weight
XenB	Xenobiotic reductase B from <i>Pseudomonas putida</i> ATCC 17453
YASARA	Yet Another Scientific Artificial Reality Application
δ -ALA	δ -aminolevulinic acid
δ -GL	6-phosphoglucono- δ -lactone
ω -TA	ω -transaminase

In addition the standard single and three letter codes for amino acids and nucleotides as well as SI-units were used.

You've got the power stand up and shout.
Ronnie James Dio (1942 – 2010)

If you think you are too old to Rock'n'Roll then you are.
Ian Fraser 'Lemmy' Kilmister (1945 – 2015)

It's a long way to the top (if you you wanna Rock'n'Roll).
Angus Young (1955 –)

1 Introduction

1.1 Enzymes in Biotechnology and Biocatalysis

In our modern society biotechnology has become highly important for economics, especially for the chemical, pharmaceutical and food industry. But biotechnology has already been important for much longer time. By consideration of brewing and baking also as biotechnology, one might hypothesize that biotechnology was the cradle of our modern settled society. Some historians even said that mankind started farming barley 9000 B.C. to make beer and not to bake bread.^[1] Of course since then this technological field has undergone a tremendous development, which was already foreseen by Malcolm Dixon in 1949, who said:

“[...] purified enzymes have already proved useful to the organic chemist in a number of cases, and it seems likely that they may have an increasing influence on chemical technique in the future as isolation methods improve.”^[2]

Nevertheless, the cradle of modern biotechnology probably might be found in the mid of the 1970s. At that time several milestones in the field can be found:

1. The development of the hybridoma technology for the production of monoclonal antibodies^[3] (Nobel Prize in Physiology or Medicine 1984^[4]);
2. Foundation of Genentech – worldwide the first modern biotechnology company famous for the recombinant production of human insulin^[5];
3. Publication of the first complete genome sequence of an organism – bacteriophage Φ X174 (Nobel Prize in Chemistry 1980^[6]); and
4. The development of gene synthesis.^[7]

Indubitably more breakthroughs were following. Amongst these the development of the polymerase chain reaction (PCR) was probably the most important one (Nobel Prize in Chemistry 1993).^[8] Very recently scientists around J. Craig Venter, who was also responsible for deciphering first the human genome, were able to assemble the first artificial bacterial genome, which can be accounted to as the foundation of modern synthetic biology.^[9]

In Germany one of the pioneering modern biotechnology companies was QIAGEN (founded in 1984) and a lot of other companies in this field were founded within the following decades. The total number of dedicated biotechnology companies and other biotechnology-active companies in Germany reached a value of 710 in 2014 (Figure 1).^[10] In parallel, the total number of employees in biotechnology companies reached a number of 37,130 that year and the development over the last five years showed the same trend. Although the biotechnology industry seems to be quite optimistic concerning its future development, as demonstrated by the BRAIN AG in 2016, which decided to make an IPO at the German stock exchange in Frankfurt/Main, the increase in the number of companies in Germany might have come to stagnation. Especially by having a detailed look on the development since 2005 it becomes obvious that the growth rate decreased the last years (Figure 1). The same trend can be observed for the employees in biotechnology companies, though the maximum is probably not yet reached.

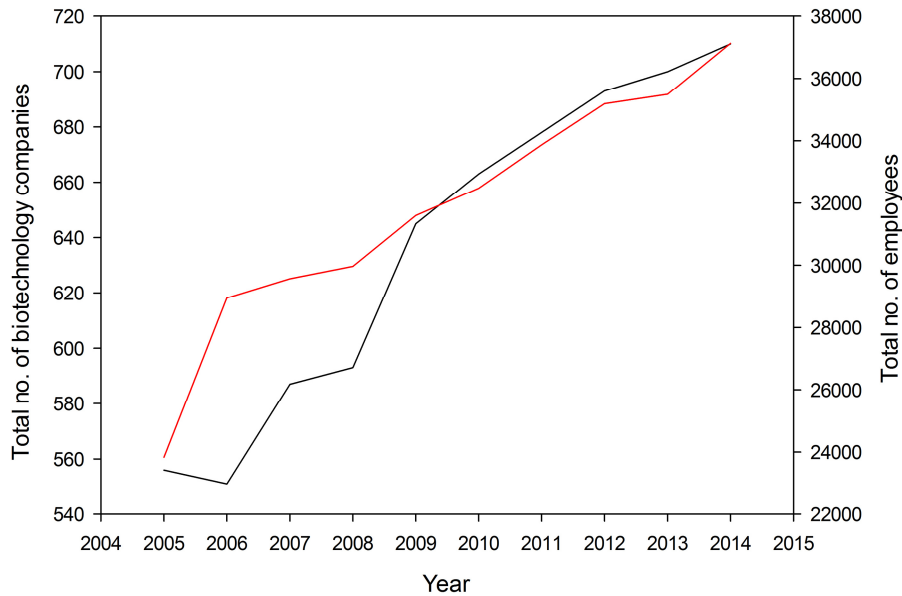


Figure 1: Development of total number of dedicated biotechnology companies and other biotechnology-active companies in Germany from 2005 - 2014 (black: Total no. of dedicated and other biotechnology companies (left y-axis), red: total no. of employees in dedicated and other biotechnology companies (right y-axis)).^[10]

On closer inspection of the trend curve observed for the total number of companies in Germany, this somehow corresponds to the impact of biocatalysis as postulated by Bornscheuer *et al.*^[11] The 'boom' of biocatalysis observed over the last years was correlated to the developed directed evolution methodologies, which were in contrast to the traditional methods in biotechnology. In the early days of biotechnology the process itself was engineered to meet the optimal conditions necessary for the used enzymes. Nowadays the enzymes themselves are engineered. In principle there are two approaches for doing so: rational protein design and directed evolution (Figure 2).

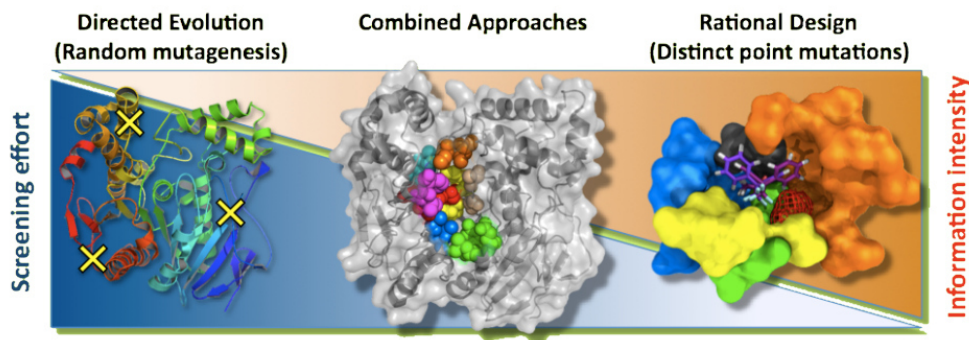


Figure 2: Methodologies for protein engineering (from [12]).

For rational design a lot of information about the protein is needed and only a few hotspots for mutation are selected based for example on structural information, so that the screening effort is kept very low. But the problem is that only for about 20% of the proteins in the Swiss-Prot database (containing 550,299 reviewed sequences), the structure has been determined experimentally. This number even further decreases dramatically to 0.2%, when considering also the TrEMBL database (containing 59,718,159 automatically annotated sequences).^[13] This is probably due to the fact that DNA sequencing has become very fast in the last decade, whereas structure

determination is still rather laborious. Nevertheless modeling of protein structures might close this gap to a certain extent.^[14]

In contrast, for directed evolution very few information about the protein is necessary, because the gene sequence is mutated randomly. Here, the screening effort is very high and several thousand to many million clones have to be analyzed with respect to the desired parameter. To address these high numbers several approaches were made to improve the mutagenesis methods (for details refer to [12]), but also robotics had a certain impact to solve this problem.^[15]

As third methodology a combined approach has to be mentioned, which features for example the use of homology models for rational design or random mutagenesis of only defined enzyme domains ('small, but smart libraries').^[16]

But why has biocatalysis become so important for industry? In general, there are three approaches for the production of chemicals: chemical synthesis, isolation from a natural source or biocatalysis/biotransformation. Of course biocatalysis has certain advantages over chemical synthesis (Table 1) and over natural product isolation (e.g. no landmass needed to grow the desired plants). One of these often mentioned advantages is also the use of water as 'green' solvent. Recently this was questioned by Ni, Holtmann and Hollmann.^[17] They have shown, when considering the wastewater also for calculation, that the *E*-factor^[18] of the biocatalytic route for the production of styrene oxide was ten times higher than the one for an optimized chemical way. Nevertheless, due to their usually high stereoselectivity and the use of very mild reaction conditions in terms of temperature, pressure and pH enzymes often outcompete the chemical processes.

Table 1: Advantages and disadvantages of cells and enzymes as biocatalysts in comparison with chemical catalysts (adapted from [19]).

Advantages	Disadvantages
Stereo- and regioselectivity	Cells and enzymes are:
Low temperatures required	- unstable at high temperature
Low energy consumption	- unstable at extreme pH-values
Active at pH 2-12	- unstable in aggressive solvents
Less byproducts	- inhibited by some metal ions
Non-toxic when used correctly	- hydrolyzed by peptidases
Can be reused (immobilized)	Some enzymes:
Can be degraded biologically	- are still very expensive
Can be produced in unlimited quantities	- require expensive cosubstrates
	When inhaled or ingested enzymes are, as all foreign proteins, potential allergens

In industry the most frequently used enzymes are in general hydrolases, above all lipases and esterases. This is also resembled by the number of commercially available enzyme preparations as surveyed in 2012 (Figure 3).^[20] Here, 59% of the available enzyme formulations belonged to enzyme class 3 (EC 3), in which the hydrolases are classified. These enzymes' popularity is probably due to their outstanding high activities, high stabilities and the fact that usually no co-substrates are needed. In contrast, enzymes belonging to EC 1 usually require a co-factor, e.g. NAD(P)H, which in turn is very expensive. Nevertheless, especially alcohol dehydrogenases/keto

reductases (ADHs, belonging to EC 1) display high activities and stereoselectivities, which make them also very interesting for synthesis.

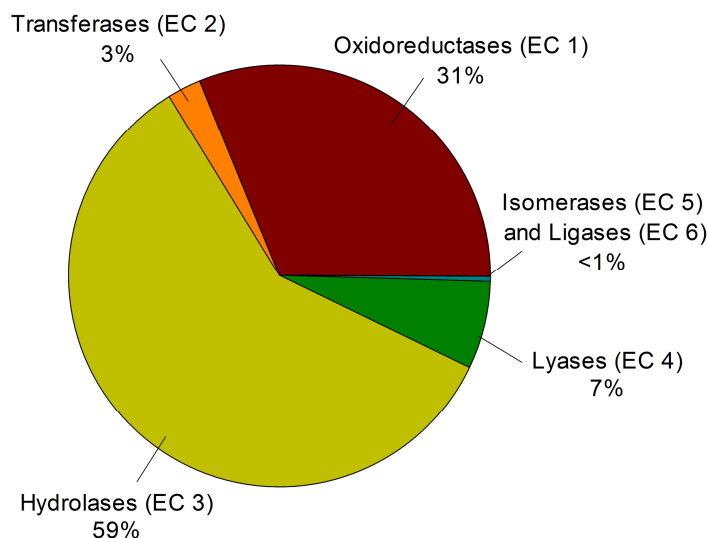


Figure 3: Distribution of enzyme classes of commercially available enzymes as listed in [20].

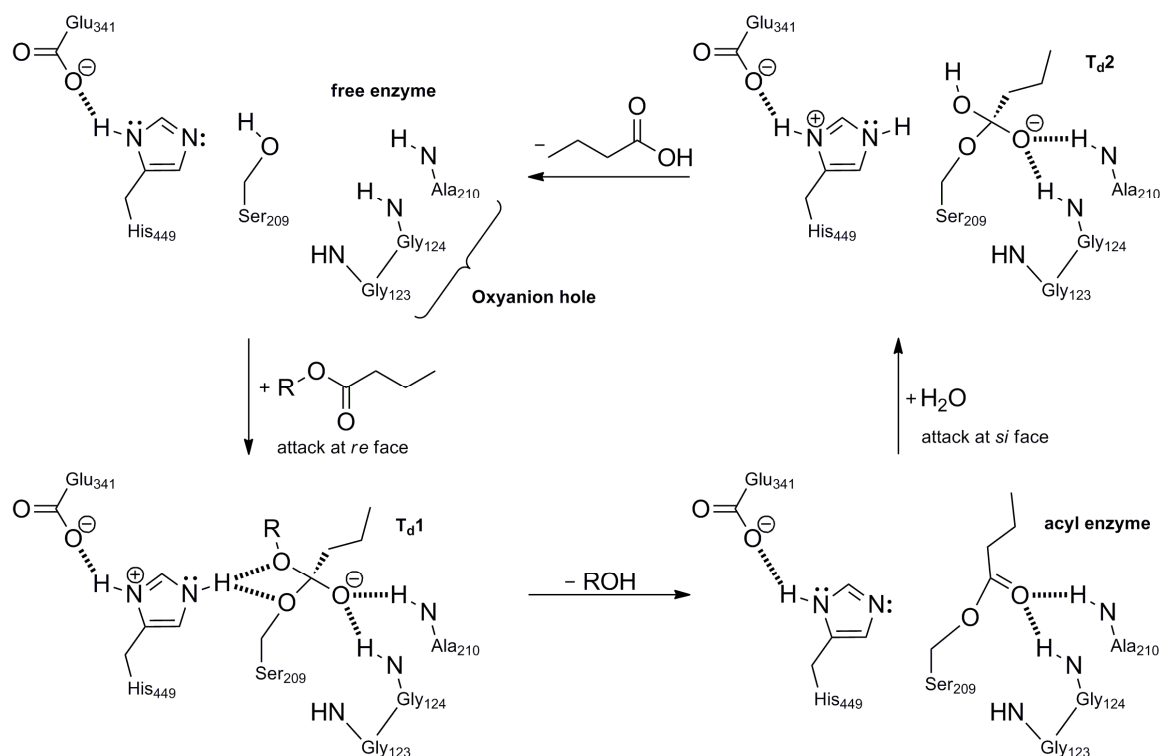
The EC 2 probably was a little bit underrepresented in this survey, because only 3% of the listed enzyme preparations belonged to this class. This number is nowadays possibly higher due to the ‘boom’ of developed transaminase-dependent processes during the last years.^[21] Finally, the enzymes belonging to EC 4 (Lyases) made up a part of 7%. Here, the best known enzymes are the hydroxynitrile lyases, which are used for the stereoselective production of hydroxy acids.^[22] Only <1% of the listed enzymes were isomerases or ligases and therefore these will not be described in detail here.

In the following passages the enzymes used in this thesis will be discussed in more detail.

1.1.1 Lipases

The most prominent enzymes for biocatalysis are lipases. These are used since decades in several industrial sectors, *e.g.* in oleochemical, cosmeceutical, food, health, and pharmaceutical industry.^[23] Here, lipases are mainly applied for lipid modification such as the production of structured triglycerides for human nutrition.^[24] But also their utilization for the production of steroid hormones was demonstrated by several companies (*e.g.* Bayer HealthCare, Pfizer, Essex Pharma), which produce these in a thousand tons range every year (for detailed information refer to [23-25]).

The reaction mechanism of lipases is similar to the one of serine peptidases and carboxyl esterases. These enzymes feature a catalytic triad in their active site, which consists of Ser, His and Asp (or Glu). The mechanism itself proceeds via four steps (Scheme 1). First the substrate ester reacts with the active site serine to a tetrahedral intermediate (T_d1), which is stabilized by the oxyanion hole. In the second step the alcohol is released and the acyl enzyme remains. As third step a nucleophile (*e.g.* water for hydrolysis, alcohol for transesterification) attacks the acyl to give again a tetrahedral intermediate (T_d2). Finally the intermediate collapses and the product acid or ester is released.^[26]



Scheme 1: Mechanism of ester hydrolysis by lipase from *Candida rugosa* (adapted from [26]).

Usually all the established transesterification processes involving lipases require a water-free reaction medium to avoid hydrolysis of the products. On the contrary some transacetylation reactions with lipases in aqueous environment were described recently, like for the lipase A from *Pseudozyma antarctica* (CAL-A; strain formerly known as *Candida antarctica*).^[27] A special case of this reactions in water was described independently by the groups of Uwe T. Bornscheuer^[28] and Wolfgang Kroutil.^[29] In both cases the scientists established biocatalytic routes for the production of poly-[caprolactone] (PCL)/poly-[caprolactam] (Nylon-6) precursors by combining several enzymes. Amongst these there was also a lipase respectively an esterase, which was used for ring opening polymerization respectively transesterification/hydrolysis (Chapters 1.2.1, 1.2.3 and 1.4.2).

1.1.2 Alcohol dehydrogenases/Keto reductases

These enzymes belong to the class of oxidoreductases (EC 1.1.1.1) and up to now several thousand of these enzymes were identified. However, probably only a few of these known ADHs are used for preparative applications. Although in theory ADHs catalyze both, reduction of ketones and oxidation of alcohols, the reductive mode of these enzymes for the production of enantiomerically pure alcohols is favored.^[30] In some cases the term 'ADH' is misleading (e.g. (*R*)-ADH from *Lactobacillus kefir*^[31]), because the equilibrium of the reaction favors the reduction mode, so that for some of these enzymes the nomenclature probably needs to be revised.

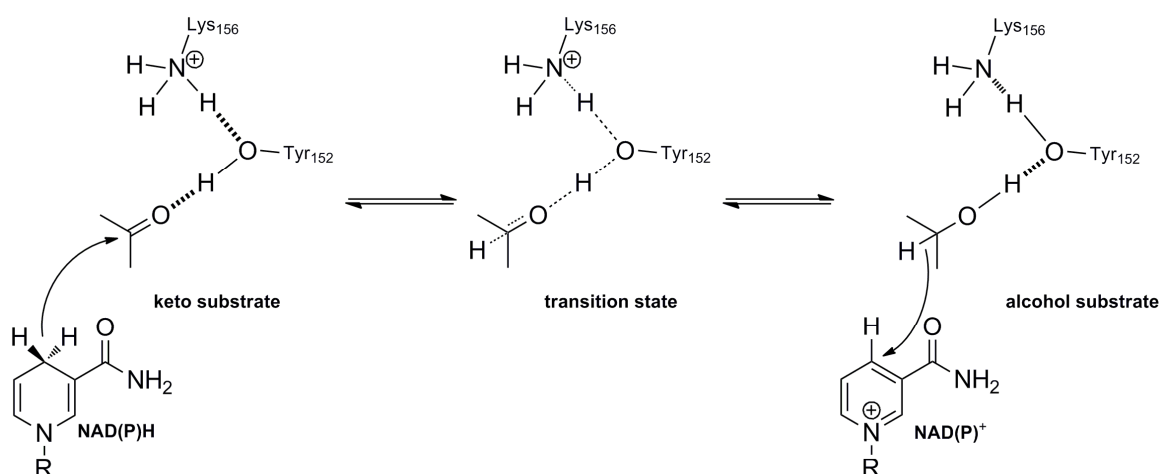
In general, ADHs are classified by structural properties into four groups: aldo-keto reductases (AKR), medium-chain dehydrogenases/reductases (MDR), short-chain dehydrogenases/reductases (SDR) and long-chain dehydrogenases/reductases (LDR). In the following the SDR and MDR are going to be described in more detail.

Table 2: Structural properties and preparatively useful MDR and SDR (adapted from [30a]).

Parameter	MDR	SDR
Amino acid chain length of monomer	350	250
Subunit structure	Di- or tetrameric	Di- or tetrameric
Coenzyme binding motif	Rossmann fold	Rossmann fold
Reference enzyme	Yeast ADH; (horse) liver ADH	<i>Drosophila</i> ADH
Structural catalytic feature	Catalytic metal ion: mostly Zn^{2+}	Catalytic tetrad: Asn, Ser, Tyr, Lys
Examples of preparative useful enzymes available as recombinant proteins	(S)-ADH from <i>Thermoanaerobacter</i> sp., (S)-ADH from <i>Rhodococcus erythropolis</i> /R. <i>ruber</i>	(R)-ADH from <i>Lactobacillus kefir</i> /L. <i>brevis</i> , (R)-ADH from <i>Candida magnoliae</i> , (S)-ADH from <i>Saccharomyces cerevisiae</i>

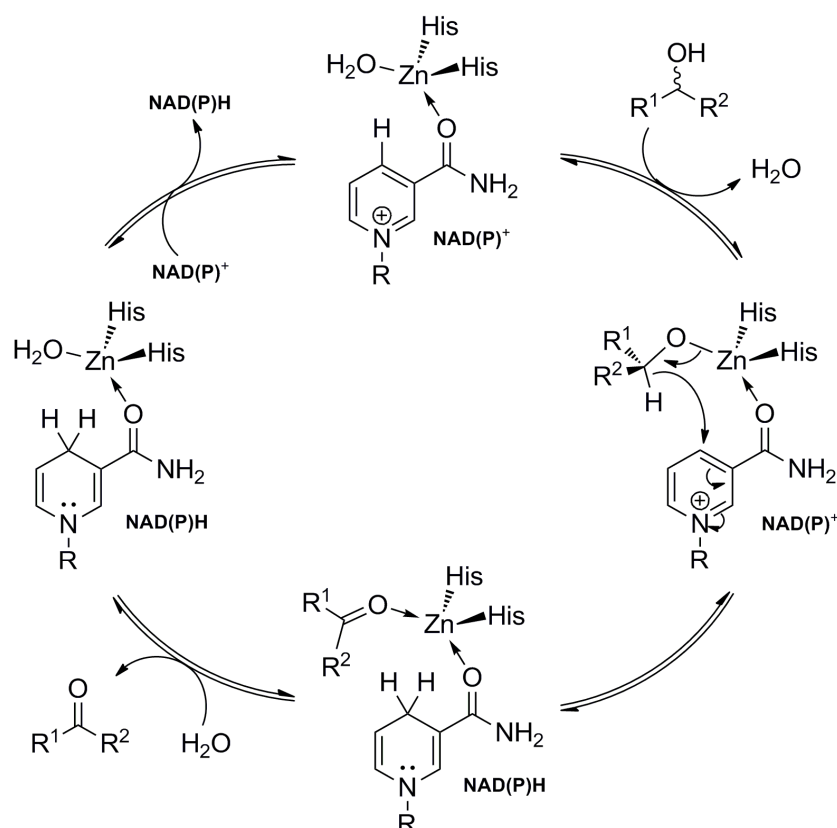
The groups of MDR and SDR have in common that in both classes the cofactor binding motif is a Rossmann fold and that they form di- or tetramers. As the names already suggested the SDR generally have a shorter polypeptide chain than the MDR. The main difference of these enzymes can be found in the catalytic mechanism (Table 2).

The mechanism of SDR involving the catalytic tyrosine and lysine is shown in Scheme 2. The reaction for reduction of a ketone is initiated by hydride transfer from NAD(P)H to the keto substrate. The resulting transition state is stabilized by the catalytic tyrosine and lysine. Finally, a hydrogen is transferred from the tyrosine to the substrate forming the alcohol product and from the lysine to the tyrosine to restore the initial state. The lysine itself is recovered via the catalytic asparagine by a proton from the solvent water.^[32] The reaction can also proceed into the opposite direction.



Scheme 2: Mechanism of 3 α /20 β -hydroxysteroid dehydrogenase from *Streptomyces exfoliatus* (formerly known as *S. hydrogenans*) involving the catalytic Tyr and Lys residues. The catalytic Asn and Ser were left out for simplicity (adapted from [33]).

The mechanism for enzymes from the MDR group is only slightly different (Scheme 3). Here the substrate binds to the catalytic Zn ion, which polarizes the C–O bond instead of the tyrosine as observed for SDR. The remaining mechanism proceeds as described for SDR via the hydride transfer from NAD(P)H.



Scheme 3: Simplified mechanism of alcohol oxidation by a Zn-dependent MDR (adapted from [34]).

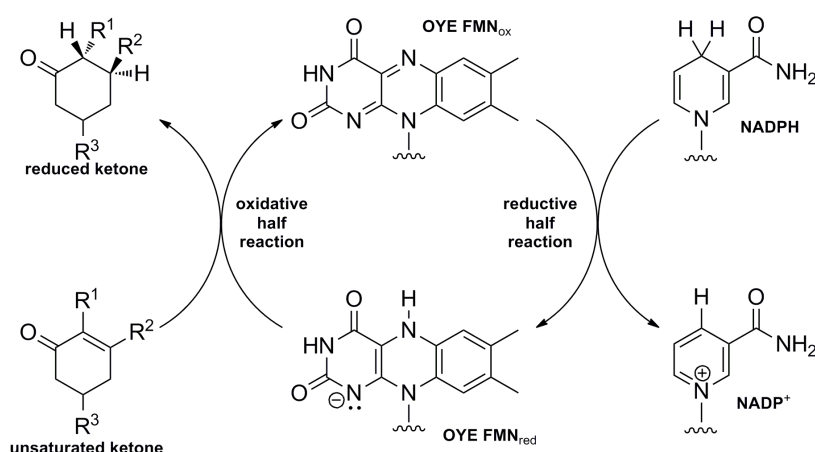
One of the most famous representatives of the SDR group is the (*R*)-ADH from *Lactobacillus kefir* (LK-ADH).^[35] This ADH is NADPH- and Mg-dependent and has already been used for several applications, e.g. the production of (2*R*,5*R*)-hexanediol^[36], in a chemo-enzymatic cascade for the production of hydrophobic allylic alcohols^[37] or in a multi-enzymatic cascade for the production of oligo-[caprolactone].^[28] In contrast, the (*S*)-ADH from *Rhodococcus ruber* (RR-ADH)^[38] belongs to the group of MDR and is NADH- and Zn-dependent. This enzyme's feasibility was also demonstrated in several applications, e.g. the synthesis of enantiopure halohydrins^[39], the synthesis of γ - or δ -lactones, which were in turn used for chemo-enzymatic cascade reactions^[40], or the stereoselective reduction of several ketones in a micro-aqueous environment (99% solvent).^[41]

1.1.3 Old Yellow Enzymes

The old yellow enzymes (OYEs) are also known as enoate reductases or ene reductases, which represent only distant relatives of the OYEs.^[42] The nomenclature goes back to the two first German biochemists, Otto Heinrich Warburg and Walter Christian, who isolated in 1932 the first flavoenzyme from the brewer's bottom yeast *Saccharomyces pastorianus* (formerly known as *S. carlsbergensis*).^[43] Later in 1938 Warburg and Christian and another student of Warburg, Erwin Haas, isolated some new yellow enzymes and compared these new ones to the now so called old yellow enzyme, which was the cradle for this still used nomenclature.^[44] However, only methylene blue was used as substrate by Warburg, Christian and Haas to

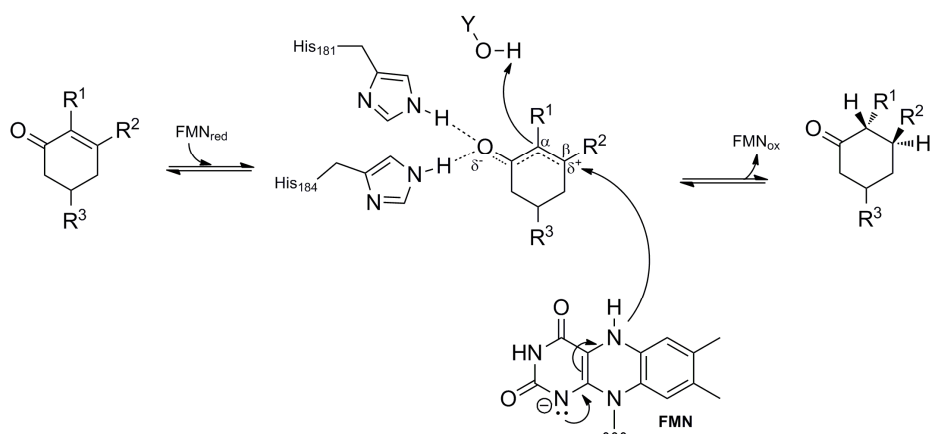
demonstrate the activity of their OYE. The typical activity of these enzymes, the hydration of unsaturated keto acids, ketones or alcohols, was already observed by Fischer and Wiedemann four years before using intact brewer's bottom yeast cells.^[45] They even used already carvone as substrate and were able to detect low activities towards this natural product.

The reaction proceeds via a Ping-Pong-Bi-Bi mechanism (Scheme 4).^[46] First in an oxidative half reaction the unsaturated substrate is reduced by flavin mononucleotide (FMN_{red}) and is released afterwards. As prerequisite for this step the substrate has to carry an electron withdrawing group in α -position to the $\text{C}=\text{C}$ bond. The now oxidized flavin mononucleotide (FMN_{ox}) in turn is restored in the reductive half reaction by NADPH, which binds to the same active site as the alkene substrate.



Scheme 4: Reaction cycle of an old yellow enzyme (adapted from [47]).

The detailed mechanism of the oxidative half reaction can be found in Scheme 5. Here, two conserved histidine residues (or one histidine and one asparagine) coordinate the electron-withdrawing group of the substrate, which leads to a further polarization of the allylic bond. This enables the hydride transfer from FMN_{red} to the $\text{C}\beta$ by a nucleophilic attack. In parallel, a proton from water or a tyrosine residue is transferred to the $\text{C}\alpha$ from the opposing side of the substrate, so that the hydration proceeds in a *trans* fashion.^[47]



Scheme 5: Reaction mechanism for the oxidative half reaction in pentaerythritol tetranitrate reductase from *Enterobacter cloacae* ($\text{Y} = \text{Tyr}$ or H ; adapted from [47]).

As the substrate range of OYEs is very diverse, these of course have been applied in several preparative reactions (for a comprehensive overview refer to [42, 47]). Two examples for OYEs are: OYE1 from *Saccharomyces pastorianus*^[48] and XenB from *Pseudomonas putida* ATCC 17453.^[49]

The XenB from *Pseudomonas putida* ATCC 17453 was identified in 2014 by Christin Peters together with two additional OYEs. The genes were cloned and the enzymes were characterized with respect to pH profile and the substrate range was investigated including 15 linear and cyclic alkenes. Especially the XenB showed high activities towards 2-cyclohexen-1-one, derivatives thereof and the natural product carvone.^[49] As rather unusual application in the field of bioremediation, one homologous enzyme from *Pseudomonas fluorescens* has been shown to degrade nitroglycerine by cleavage of the nitroester^[50] and another one from *Pseudomonas putida* KT2440 to degrade 2,4,6-trinitrotoluene (TNT).^[51] A similar reaction was also observed for the OYE1 from *Saccharomyces pastorianus*,^[52] which also catalyzes the hydration of a huge variety of substrates ranging from substituted and nonsubstituted α,β -unsaturated aldehydes, ketones, imides, nitroalkenes, carboxylic acids, and esters, over cyclic and acyclic enones, nitrate esters, nitroaromatics, terpenoids, and *N*-ethylmaleimide to codeinone.^[47]

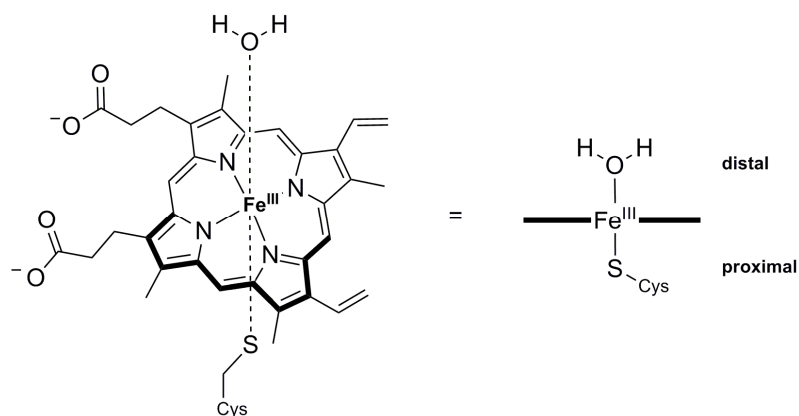
1.1.4 Cytochrome P450-Monooxygenases

In general, monooxygenases are enzymes, which catalyze the oxidation of non-activated C-H groups by utilization of molecular oxygen. Thereby, one oxygen atom is inserted into the substrate and the other one usually is released as water molecule. The largest group of monooxygenases is formed by the cytochrome P450-monooxygenases (P450s) with approx. 53,000 sequences as listed in the CYPED database.^[53] This large number is probably due to the fact that P450s can be found throughout all domains of life, where they have for example important roles in the biosynthesis of natural products or drug metabolism.^[54]

The nomenclature of these monooxygenases goes back to the late 1950s.^[55] At that time P450s were defined as a distinct class of heme-containing proteins, although nothing was known about the structure of the discovered pigment: The described

“CO complex [...] is probably not an iron hemoprotein”.^[55a]

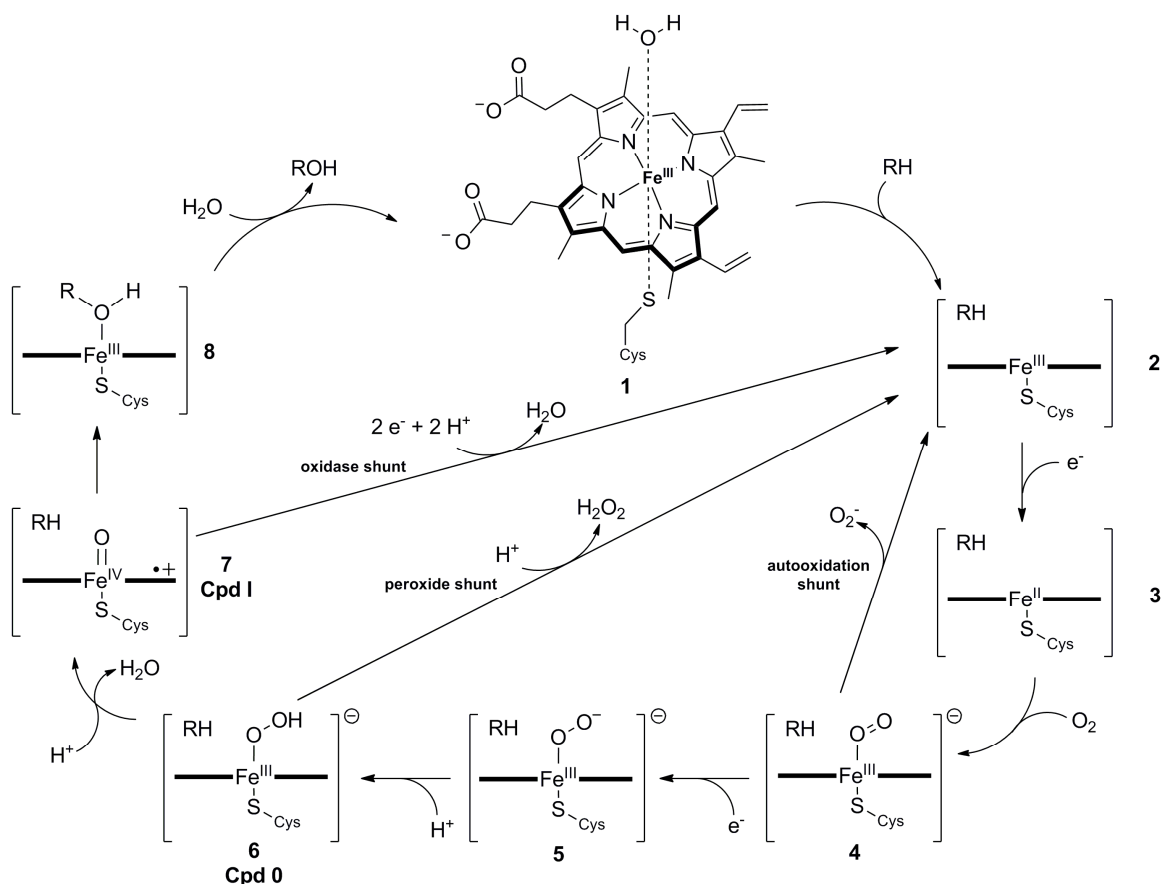
Only three years later, Tsuneo Omura and Ryo Sato reported a first evidence for the presence of a heme group,^[56] which was verified another three years later.^[57] Because they found a maximum of absorption at a wavelength of 450 nm upon carbon monoxide saturation of the reduced solution containing the liver microsomes, these pigments were called P450. Nowadays P450s are well studied and it is known that the reactive center contains a heme *b*, which is bound to the protein via a cysteine. This side of the heme center is referred to as proximal side. The other axial ligand on the distal side of the iron is a water molecule in the inactive state (Scheme 6).



Scheme 6: The heme *b* found in P450s bound to the proximal cysteine ligand and water.

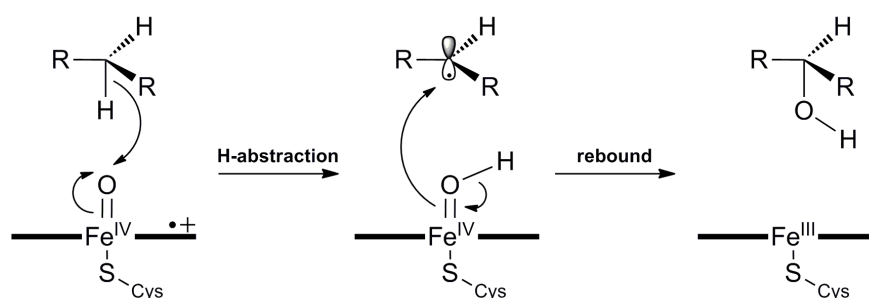
The reaction of a P450 proceeds via the catalytic cycle as shown in Scheme 7.^[58] At first the substrate binding (**2**) leads to dissociation of the bound water molecule (**1**) in the distal heme coordination sphere, which results in a shift of the heme iron spin state from low-spin to high-spin along with a positive shift in the reduction potential. This increased potential allows the oxidation of Fe^{III} (ferric) to Fe^{II} (ferrous, **3**) followed by binding of molecular oxygen, which gives a ferric superoxo-complex (**4**). Upon a second electron delivery this complex is converted into a ferric peroxo anion species (**5**), which after protonation is transformed into a hydroperoxo complex, the so called compound 0 (Cpd 0, **6**). By an additional protonation and heterolytic scission of the dioxygen bond water is released and a high-valent ferryl-oxo-complex is left, the so called compound I (Cpd I, **7**). Nowadays it is widely accepted that this Cpd I is the active species capable of hydroxylating the bound substrate by the 'rebound mechanism' (Scheme 8), especially since the existence of Cpd I has been proven experimentally in the thermophilic CYP119 from *Sulfolobus acidocaldarius* by UV/Vis, Mössbauer and EPR spectroscopy in 2010.^[59] The oxygen insertion itself proceeds probably via a radical intermediate, which was formed by hydrogen abstraction, followed by oxygen rebound to the substrate (**8**). Finally, the starting point of the cycle is restored by replacing the hydroxylated product with a water molecule.

Furthermore, the catalytic cycle of P450s can also be disrupted under certain conditions. These 'shortcut' pathways are called uncoupling reactions. Autooxidation occurs if the second electron is not delivered to reduce the ferric superoxo-complex (**4**). Then a superoxide anion is released, which usually is referred to cause severe damage to the protein. The other two shunts are mainly due to inappropriate positioning of the substrate. If Cpd 0 collapses hydrogen peroxide is released (peroxide shunt) and if Cpd I collapses just water is released (oxidase shunt). Especially the latter two cases display a problem, because without hydroxylating the substrate NAD(P)H is still consumed. Some P450s are even able to use the peroxide shunt to incorporate oxygen deriving from hydrogen peroxide as side activity.^[60]



Scheme 7: Catalytic cycle of P450s (adapted from [61]).

The electrons needed for the catalytic cycle originate from NAD(P)H and are transported to the P450 by distinct redox proteins. Based on these redox partners the P450s are classified. In general the electrons are either delivered by an FAD-containing ferredoxin reductase (FdR) and a corresponding ferredoxin (Fdx) protein or by an FAD/FMN-containing cytochrome P450 reductase (CPR).



Scheme 8: Rebound mechanism of the hydroxylation reaction of P450s (adapted from [58]).

Traditionally the P450-classes are (Figure 4):

- Class I belongs to the FdR/Fdx-dependent P450-system and can be further divided into prokaryotic and eukaryotic systems, which are only distinguished by the membrane-bound nature of the P450. Prominent representatives of this class are the bacterial camphor-degrading P450_{cam}/PdR/Pdx system from *Pseudomonas putida*^[62] and the bovine P450_{scc}/AdR/Adx system, which is involved in steroid metabolism.^[63]
- In class II the CPR and the P450 are both membrane-bound. These systems are usually found in eukaryotic organisms and are located in the ER-membrane. As example for a well-studied P450 belonging to this class the microsomal CYP2B4 can be given, which is involved in drug metabolism.^[64]
- Class III represent a special case of class II, because enzymes belonging to this group are natural fusion enzymes of a CPR and a P450. Probably the most prominent P450 belongs to this class: P450-BM3 from *Bacillus megaterium*. This enzyme has been subject to hundreds of mutagenesis studies and because of the so far highest activity reported for a P450 and due to the fact that it consists of only one polypeptide chain it is of high industrial interest.^[65]
- In contrast, class IV is a special case of class I. These enzymes are also fusion proteins of the respective P450 and its redox proteins. The first enzyme belonging to this class, P450-RhF from *Rhodococcus* sp. NCIMB 9784, was discovered in 2002 by Nicholas Turner and co-workers.^[66]

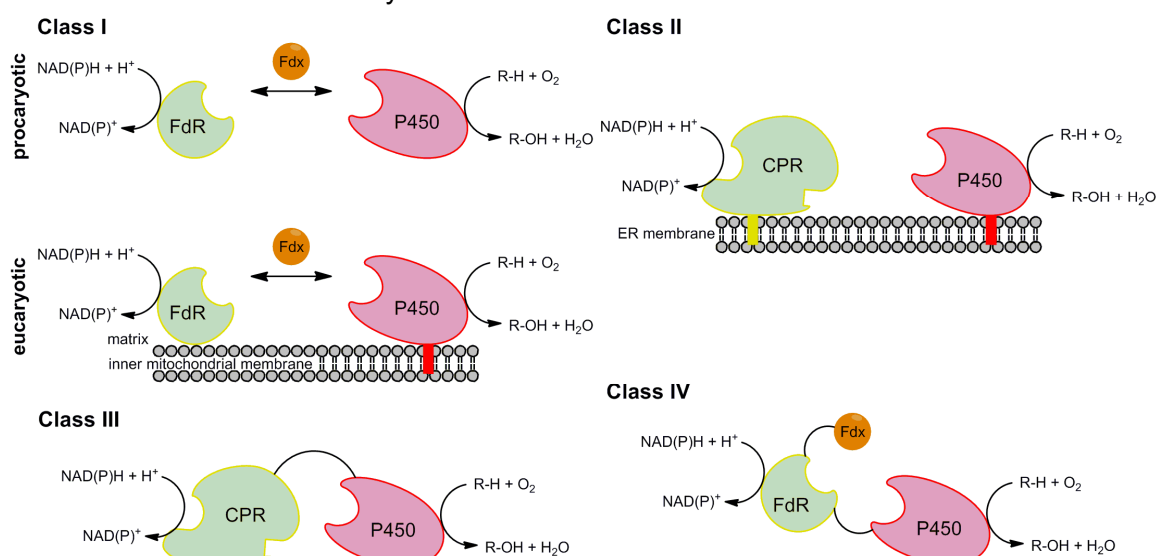


Figure 4: Traditional classification of P450s (adapted from [66-67]).

However, recent developments recommend reclassification of P450s, because a tremendous number of enzymes was described, which could not be grouped into the traditional ones (Figure 5).

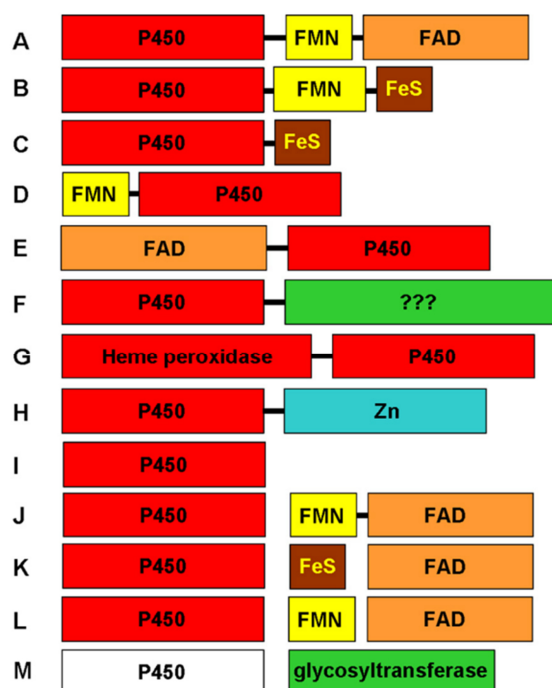


Figure 5: Diversity of P450 redox systems and P450 fusion proteins (from [68]).

The diversity of P450s is not only resembled in their structural organization but also in the range of different reaction types they can catalyze. Amongst these

“oxidation of non-activated sp^3 hybridized carbon atoms, aromatic hydroxylation, epoxidation, C-C bond cleavage, heteroatom oxygenation, heteroatom release (dealkylation), oxidative ester cleavage, oxidative phenol- and ring-coupling, isomerization via (abortive) oxidation, and oxidative dehalogenation, as well as other complex reactions like dimer formation via Diels-Alder reactions of products or Baeyer-Villiger-type oxidations”^[69] (quoted from [58])

are found.

Although P450s are very complex and therefore their use is often limited to whole cell processes, there are some examples of industrial use, e.g. at Sanofi-Aventis and Bayer HealthCare. At Sanofi-Aventis a process for the production of hydrocortisone using an engineered yeast strain expressing several recombinant P450s was established.^[67b, 70] The process for the production of 11β -hydroxy steroids at Bayer HealthCare was already developed in 1982. Here a wild-type strain of the fungus *Curvularia* was used.^[71]

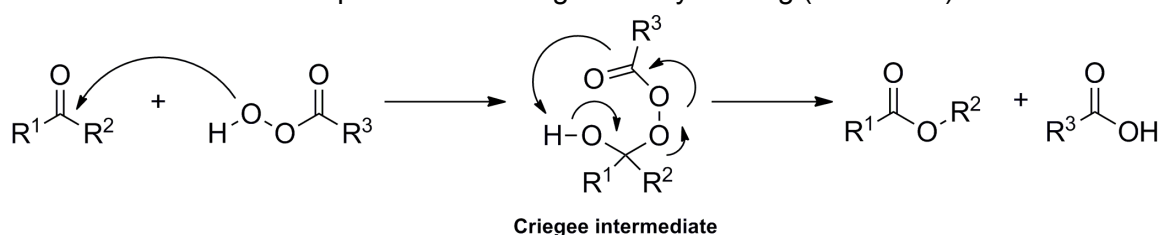
More recently, P450s have been applied for biosynthesis of two ‘blockbuster’ drugs: the anticancer drug Taxol (Paclitaxel) and the anti-malaria drug Artemisinin (Chapter 1.4.1, Table 4). The groups of Blaine Pfeifer and Gregory Stephanopoulos developed a recombinant *E. coli* strain for the production of taxadiene, the first intermediate in Taxol synthesis, with a yield of up to $1 \text{ g} \cdot \text{L}^{-1}$.^[72] The next step in Taxol biosynthesis was realized by application of a fusion engineered plant P450.

The biosynthetic production of Artemisinin was developed by a large consortium of scientists funded by the Melinda & Bill Gates Foundation.^[73] The aim of this project was to establish a biotechnological process for the production of the anti-malaria drug Artemisinin, which traditionally is produced by natural product extraction from *Artemisia annua*. Due to increasing worldwide demand for this drug a new process for

production was needed quickly. However, the aim was also not to replace the traditional agricultural production by the new process and indeed the process developed at Amyris involving several P450s is running now at Sanofi on a 'no profit, no loss' basis.^[74]

1.1.5 Baeyer-Villiger-Monooxygenases

In 1899 Adolf Baeyer and Victor Villiger described the chemical oxidation of ketones and aldehydes by peracids.^[75] Their main interest was to study the effect of Caro's reagent (peroxymonosulfuric acid, H_2SO_5) on menthone, dihydrocarvone, camphor and acetone. Modern oxidants used for Baeyer-Villiger reactions are organic peracids like trifluoroperacetic acid, peroxybenzoic acid and *m*-chloroperoxybenzoic acid. In 1948 Rudolf Criegee proposed a mechanism for this reaction based on his observations on decalin peroxide rearrangement by heating (Scheme 9).



Scheme 9: Mechanism for Baeyer-Villiger oxygenation proposed by Criegee (adapted from [76]).

The mechanism proceeds via two steps: First, a tetrahedral intermediate (the Criegee intermediate) is formed by attack of the carbonyl carbon by the peroxy acid. Then, after migration of one of the substituents to one of the peroxide oxygen atoms, a carboxylic acid is released under retaining of stereochemistry if the migrating carbon atom was chiral. The regioselectivity of this reaction is predictable, because for the migration the stabilization of a positive charge is necessary.^[77] Due to the fact that higher substituted carbon atoms show a better stabilizing effect, usually the higher substituted group is the migrating one.^[78]

Nevertheless, the chemical Baeyer-Villiger reaction has also certain drawbacks like low stereo-, regio-, enantioselectivity and substrate specificity. Additionally, for each equivalent of product also one equivalent of waste acid is produced, which has to be disposed. Furthermore, there are safety issues about peracids, which are often explosive in condensed form, shock sensitive and intrinsically unstable.^[77a] Hence, there is a need to circumvent all these problems, which can be done by the use of Baeyer-Villiger monooxygenases.

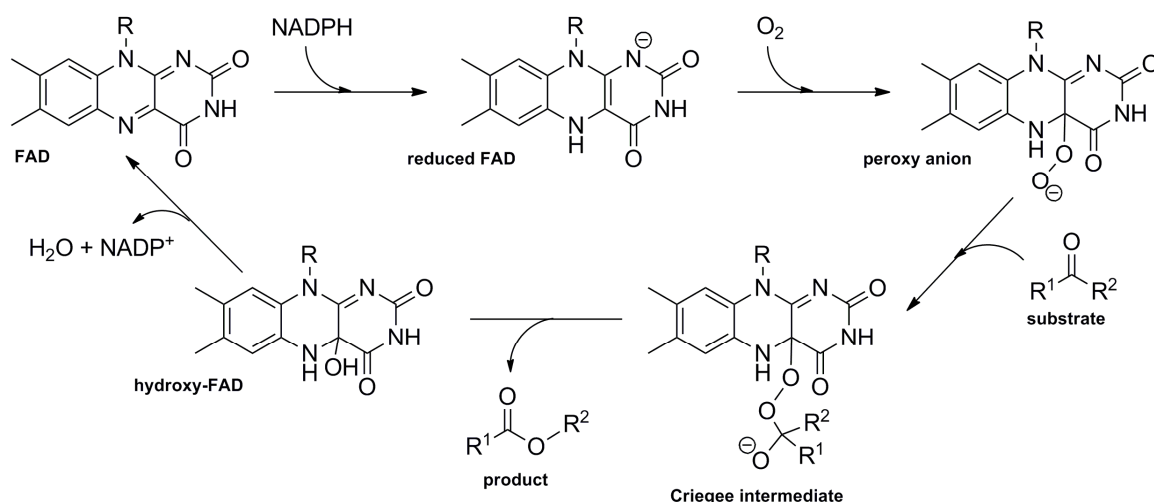
The first biological Baeyer-Villiger oxidation was discovered in 1948 by G. E. Turfitt during his studies on degradation of steroids by *Proactinomyces erythropolis*.^[79] In the late 1960s the first isolated enzymes were described as Baeyer-Villiger monooxygenases (BVMO), which used molecular oxygen and NADPH.^[80] Nowadays, much more BVMOs have been described and these are classified into two groups (Table 3).^[81] Very recently, even the first human flavin monooxygenase with a BVMO activity was described.^[82]

Table 3: General characteristics and classification of Baeyer-Villiger monooxygenases (adapted from [77a, 81a]).

Type 1 (I) BVMO	Type 2 (II) BVMO
single gene product	two separate gene products, reductase and oxygenase
contain a tightly bound FAD co-factor	use reduced FMN generated by the reductase as a co-enzyme
NADPH-dependent	the reductase can use NAD(P)H
NADPH/NADP ⁺ bound during catalysis	
BVMO fingerprint motif sequence: FxGxxxHxxxWP	absence of BVMO fingerprint
two domain structures resembling disulfide oxidoreductases; two dinucleotide-binding domains (Rossmann fold) binding FAD and NADPH	structural core of the oxygenase subunit displays a TIM-barrel fold

A closer sight into the reaction mechanism reveals that the flavin cofactor in BVMOs serves as natural peracid (Scheme 10).^[83] The first step of the reaction is a reduction of the flavin cofactor (FAD) by NADPH. Then a peroxy anion of the FAD is formed by oxygen addition. The Criegee intermediate is generated through nucleophilic attack at the carbonyl substrate by the peroxy anion. Subsequently, the tetrahedral intermediate is rearranged and the product exits the active site leaving the hydroxy-FAD. At this point, also the migratory preference is determined. Finally, the FAD is restored by water elimination and NADP⁺ is released. In principle, the peroxy anion of FAD is in equilibrium with the hydroperoxide. This protonated form is believed to be responsible for electrophilic reactions of flavin monooxygenases, e.g. sulfoxidation.

Recently a structure of the cyclohexanone monooxygenase (CHMO) from *Rhodococcus* sp. was solved containing both co-factors and cyclohexanone as substrate, which supports the proposed reaction mechanism due to the detected distances between flavin and substrate.^[84]



Scheme 10: Reaction mechanism for Baeyer-Villiger monooxygenases (adapted from [83]).

In contrast to the chemical Baeyer-Villiger oxidation, the enzymatic one is able to overcome the electronic effect leading to the preferred migration by conformational and stereoelectronic rearrangements of the substrate in the active site, which leads in the end to the formation of the so called abnormal lactone. The only two prerequisites for this reaction are an antiperiplanar position of the migrating group to the peroxy group and a lone electron pair of the carbonyl oxygen in anti position (Figure 6).

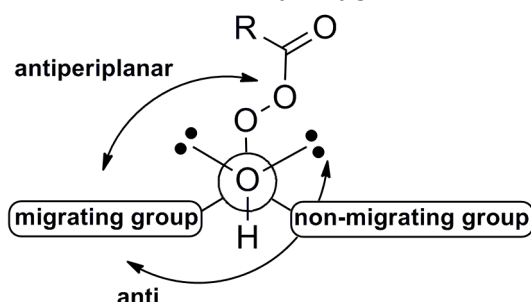


Figure 6: Stereoelectronic requirement of the Criegee intermediate for successful migration (adapted from [83]).

There are several examples, in which BVMOs were used as stereoselective catalysts (for further reading refer to [77a, 81, 83, 85]). Especially their selectivity and the fact that BVMOs can be altered with respect to thermostability and specificity by protein engineering, make them advantageous over the chemical Baeyer-Villiger oxidation. Hence, there were several attempts in the last years to especially enhance thermo- and oxidative stability of the CHMO from *Acinetobacter* sp. (CHMO_{Acineto}), which is due to the high interest for industry probably the most studied one. It is used for example for the production of ϵ -caprolactone, which in turn can be used as monomer for polymerization to PCL^[86] or it can be transformed to ϵ -caprolactam, a Nylon-6 precursor.^[87] Nevertheless, the CHMO_{Acineto} has one certain drawback: its low stability. Therefore, several studies dealt with the improvement of the thermo- as well as the oxidative stability of this enzyme, with more or less success.^[88] The first study was carried out by Opperman & Reetz. They succeeded in creating more stable variants with respect to temperature and oxidative stability by site-directed mutagenesis. One of the most interesting variants was the double mutant C376L/M400I (CHMO_{DM}). Interestingly, in the last two years there were two studies using the same attempt by introduction of *in silico* designed disulfide bonds to enhance stability. The first example by van Beek *et al.* described one double mutant, which had a significantly higher thermostability, but unfortunately the activity was also lowered.^[88c] In contrast, Schmidt *et al.* found different 'hot spots' for disulfide bridging and indeed found one double mutant having increased stability while retaining wild type-like activity. Furthermore, the single mutants out of this double mutant were also characterized and these revealed that the single mutant T415C showed an even higher improvement and detailed studies on the hypothetical disulfide bridge suggested that this was not formed in the enzyme. So that the stabilizing effect was probably due to the scavenging property of the thiol group.^[88a] One successful implementation of a BVMO into an industrial process was demonstrated at Codexis Inc. The scientists succeeded in creating a BVMO mutant for the production of Esomeprazol (Table 4).^[89] This drug is mainly used for treatment of gastric acid related disorders due to its inhibitory effect on proton pumps. The ancestor of this new drug is Omeprazol, which contains the racemic mixture of the same molecule. The advantage of the pure (S)-enantiomer (Esomeprazol) is the lower

metabolization rate, although the general benefit of the enantiopure drug has been questioned. Both enantiomers act as prodrugs, which are metabolized to the active pump inhibitor in the parietal cells, so that the sufficient dose of Esomeprazol is only lower in comparison to Omeprazol. However, application of a higher dose of Omeprazol has the same effect and side effect as the lower one for Esomeprazol.^[90]

1.1.6 Rieske Non-Heme Iron Dioxygenases

Like P450s the dioxygenases (DOx) are very versatile enzymes for stereospecific hydroxylation reactions. As the name already suggests these enzymes catalyze the incorporation of both oxygen atoms from molecular oxygen into the substrate. In general, DOx contain either one or more heme iron units or non-heme iron units. The latter ones are further classified into intradiol and extradiol DOx, which differ in the used iron cofactor and its coordination (Fe^{III} bound to 2-tyrosine-2-histidine motif for intradiol DOx and Fe^{II} bound to 2-histidine-1-carboxylate motif for extradiol DOx). As part of bacterial aromatic degradation pathways the Rieske non-heme dioxygenases (RDOx) are the most prominent representatives of this enzyme class.^[58] Furthermore, the natural substrates are used for classification of RDOx into four families: the toluene/biphenyl family, the naphthalene family, the benzoate family, and the phthalate family.^[91]

The RDOx usually consist of three to four protein components: The oxygenase itself containing the non-heme iron center and the Rieske center (Scheme 11) is assembled by two subunits, which form ($\alpha\beta$)-multimers. Furthermore, an electron supply chain for activation of molecular oxygen is required, which is built by a soluble reductase and, if a three-component system is described, a ferredoxin protein (Figure 7).

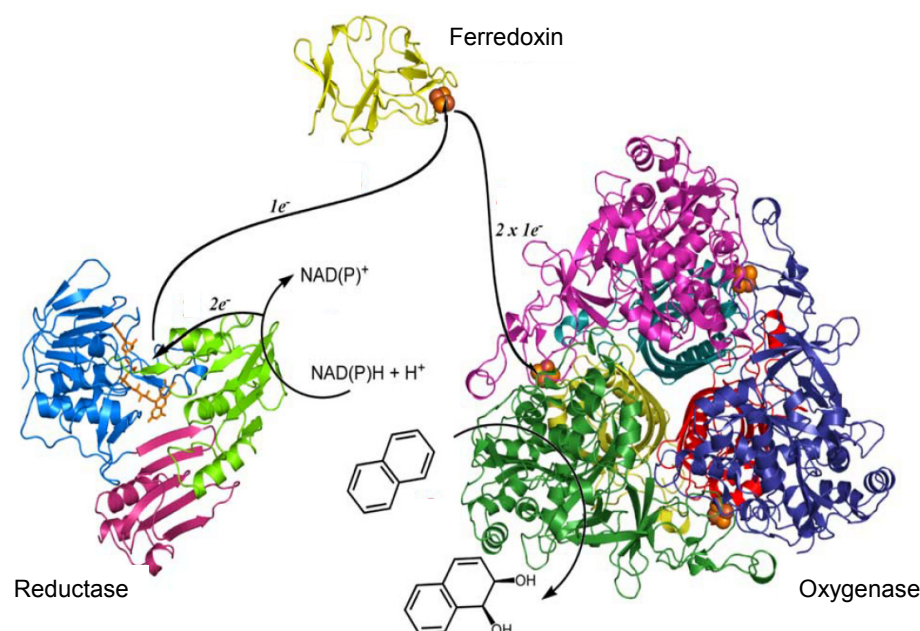
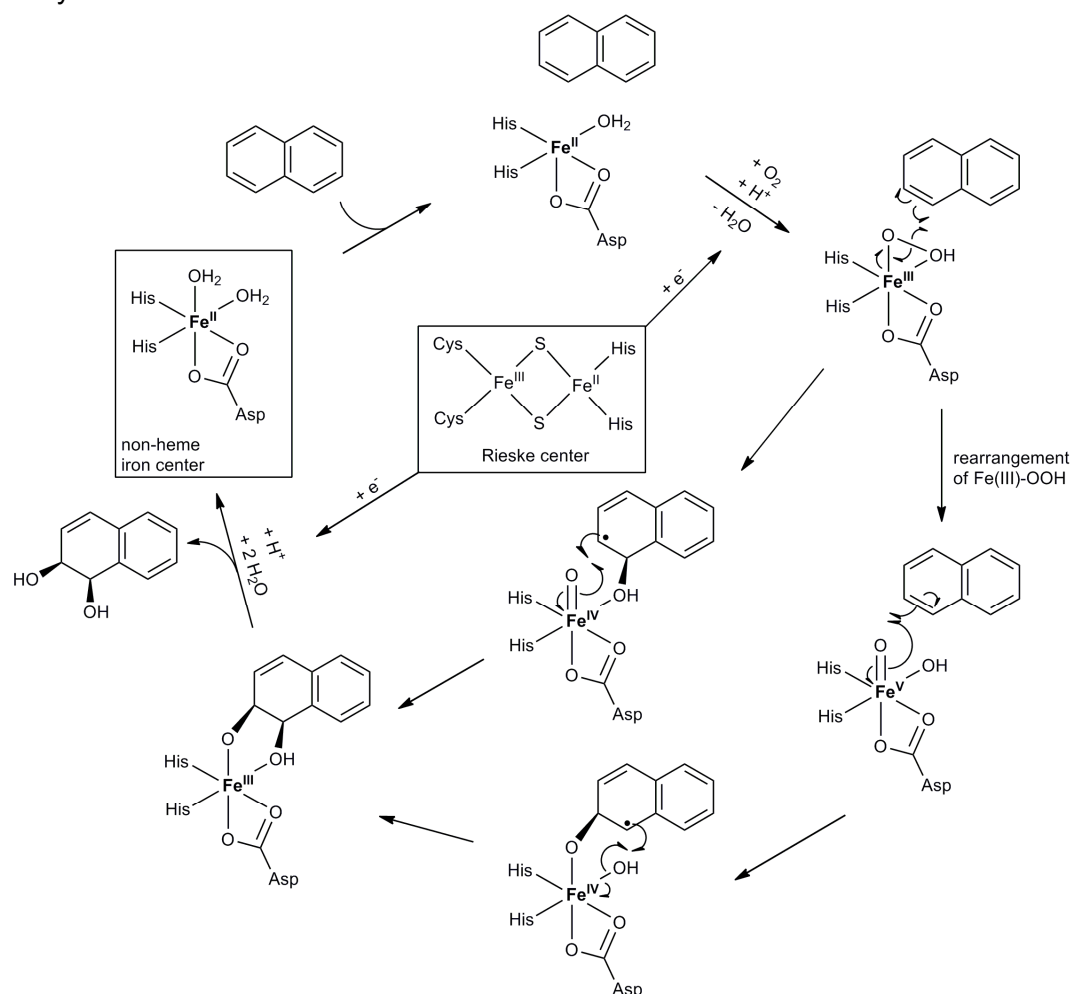


Figure 7: Total reaction of a three component Rieske non-heme dioxygenase system (reductase from *Pseudomonas* sp. KKS102, PDB 1F3P^[92]; ferredoxin component from *Burkholderia xenovorans* LB400, PDB 1FQT^[93]; oxygenase Rieske cluster from *Rhodococcus* sp. RHA1, PDB 1ULJ^[94]; Flavin shown as sticks, Rieske cluster and mononuclear iron shown as spheres; adapted from [95]).

An exemplified three-component RDOx system is shown in Figure 7. The required electrons are recruited by NAD(P)H oxidation carried out by the flavin-containing reductase. The electrons are stored by a ferredoxin (containing a [2Fe-2S] cluster), which shuttles these to the RDOx. Here the electrons are passed to the catalytic center.

The detailed reaction mechanism of RDOx is still unknown. Therefore, two proposed mechanisms are shown in Scheme 11. Both routes proceed via a reactive Fe^{III} -peroxy species. In one of the proposed mechanisms a similar Fe^{IV} -oxo-hydroxy species was hypothesized as observed in P450s to be formed as intermediate in a radical mechanism, which further reacts to the *cis*-diol bound Fe^{III} complex. The alternative route describes a rearrangement of the Fe^{III} -peroxy species to a Fe^{V} -oxo-hydroxy one, which also reacts in a radical mechanism over a Fe^{IV} -oxo-hydroxy species to the *cis*-diol product. However, until now there was experimental proof for neither of these proposed mechanisms, although recently a Fe^{V} -oxo-hydroxy species was detected by variable-temperature mass spectrometry using a synthetic Fe-cluster, which showed enzyme-like C-H and C=C oxidation reactions.^[96]



Scheme 11: Proposed reaction scheme of a Rieske non-heme dioxxygenase (adapted from [97]).

In industry, DOx are often used due to their outstanding stereoselectivity, which was demonstrated for several substrates, *e.g.* naphthalene, indole, nitroarenes, phenanthrene, toluene, cumene, biphenyl, polychlorinated biphenyls, benzene,

benzoate, toluate and phthalate.^[98] Because of the high number of necessary proteins for proper activity, whole cells are preferred as catalysts for biotransformation reactions. One example of an industrial process involving a DOx is the production of 1,2-dehydrocatechol by a *Pseudomonas putida* strain as carried out at Avecia.^[99]

A rather unexpected monooxygenation reaction by a DOx was used at Genencor International for the microbial production of indigo using a naphthalene dioxygenase from *Pseudomonas putida*, which was cloned into *E. coli*. The process itself was further optimized by metabolic engineering and site-directed mutagenesis.^[100]

Very recently, Marco Fraaije and co-workers identified another dioxygenase from *Pseudomonas* sp. PWD32^[101], which is capable of monooxygenating limonene very stereo- and also regioselectively to (+)-*trans*-carveol.^[102]

1.2 Cascade Reactions

In the last few years, cascade reactions using enzymes were amongst the hot topics in biocatalysis. Though this concept is not a new one, because every natural metabolic reaction is a cascade reaction and the latter are also essential for life. Chemists just copied this concept and applied it to organic synthesis. The first example of a biomimetic total synthesis was the one of tropinone by Robert Robinson in 1917.^[103]

The term 'cascade' in a biotechnological process was first used in a patent by the Denka Engineering Co. Ltd. in 1978, in which the cascaded use of immobilized enzymes in a packed bed reactor was optimized.^[104] Thirty years before that, Malcolm Dixon was already talking about multi-enzyme systems, so that the real first example of a synthetic cascade involving enzymes still is elusive:

„But in recent years there has been a tendency to move on to the synthetic phase, that is to build up systems consisting of two or more enzymes linked together functionally, to study the special phenomena which appear in such *systems* and the manner in which the constituent enzymes work together in producing them, and to build up trains or chains of enzyme reactions which will reproduce *in vitro* many of the metabolic transformations which occur in the living cell.“^[105]

For a better understanding of cascade reactions there were several recent attempts for the classification of the reaction concept.^[106] In general, the reactions can be grouped into multistep syntheses and one-pot cascades (Figure 8). The first one resembles the classical chemical multistep synthesis, in which for a reaction from substrate A to product D the intermediates B and C are synthesized and isolated separately to serve as substrates for the next step. This work-flow is obvious a rather laborious one, despite the fact that a lot of solvents are needed for isolation of the substances. In contrast, a one-pot cascade contains all reactants and catalysts in the same reaction vessel, so that the reaction can proceed directly from substrate A to product D, which in the end is the only substance that has to be isolated. Of course by using this concept a lot of time and auxiliary chemicals are saved. But the disadvantage of this system is to find a compromise of the optimal reaction conditions for the separate catalysts.

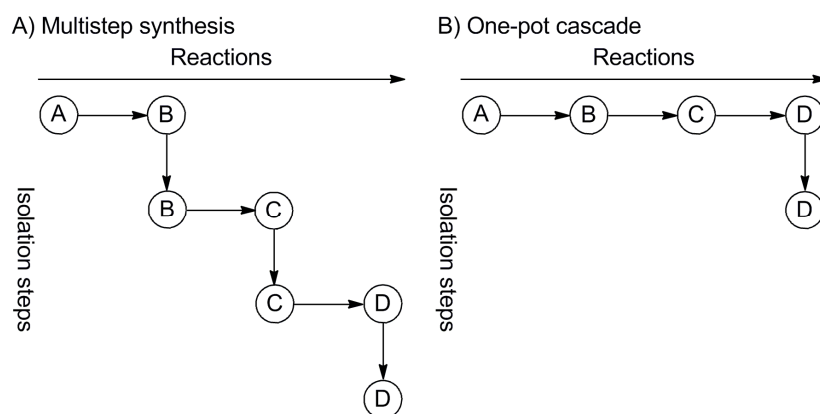


Figure 8: General classification of cascade reactions (adapted from [106e]).

One-pot reactions will be described in more detail in the following passages. A first simple classification for one-pot multi-enzymatic systems was described by Malcolm Dixon in 1949, which still can be applied nowadays:

“In forming, let us say, a two-enzyme system from the separate enzymes it is of no use just to take any two enzymes and mix them. In all probability they will be unconnected; they will not form a *system* and we shall learn nothing more from the mixture than from the separate enzymes. In order that a system may be formed, the enzymes must have some functional connection which will couple them together. The results will only be of interest if the enzymes form a system which will do things which neither of the two enzymes will do singly. [...]

The direct coupling of two enzymes together is brought about when the two enzymes possess a *common substrate*, which acts as a link. This occurs when the product of the reaction catalysed by the first enzyme is the starting-point of the reaction catalysed by the second enzyme. In other words, we have simply the case of successive or consecutive enzyme reactions. Now there are two fundamentally different types of substrate-linked reactions. The first and most obvious type, (a), is where the second enzyme takes the substance which forms the link *on* to form a new substance, that is to say it takes it a step forward in its metabolism. [...]

The second type (b) is where the second enzyme simply undoes what the first enzyme does, as far as the linking substrate is concerned. In other words, it takes this substrate back to what it was initially. If the first enzyme reaction reduces it, the second reoxidises it; if the first phosphorylates it, the second dephosphorylates it, and so on. Of course this does not occur by a reversal of the first enzyme reaction, but by a different reaction (two different enzymes being involved), which, nevertheless, brings the common substrate back to its starting-point.”^[107]

Obviously Dixon was already talking about, what Woodley & Santacoloma recently suggested on multienzyme system classification.^[106c] The first Dixon-type (a) apparently describes the use of primary enzymes, which are those enzymes directly involved in product synthesis. Cascade reactions involving only primary enzymes are the linear ones (Figure 9A). This kind of cascade can be carried out in three different modes. First in a two-pot mode, which is similar to the classical multistep synthesis and has the mentioned drawbacks; second the one-pot sequential mode, where the enzyme for the second step is added after completing the first step; and third the one-pot simultaneous mode, where all enzymes are present from the start of the reaction. Also the parallel cascade reactions (Figure 9D) make use of only primary enzymes,

but here these are coupled by a co-factor to produce two products *in situ*. The latter mode and also the orthogonal and cyclic cascades (Figure 9B and C) belong to the Dixon-type (b). These systems involve so called secondary enzymes, which are mainly included in the reactions either, as already mentioned, to recycle necessary co-factors (e.g. NAD(P)H), or supply/remove toxic/inhibitory substrates/intermediates/(by-)products.

A)

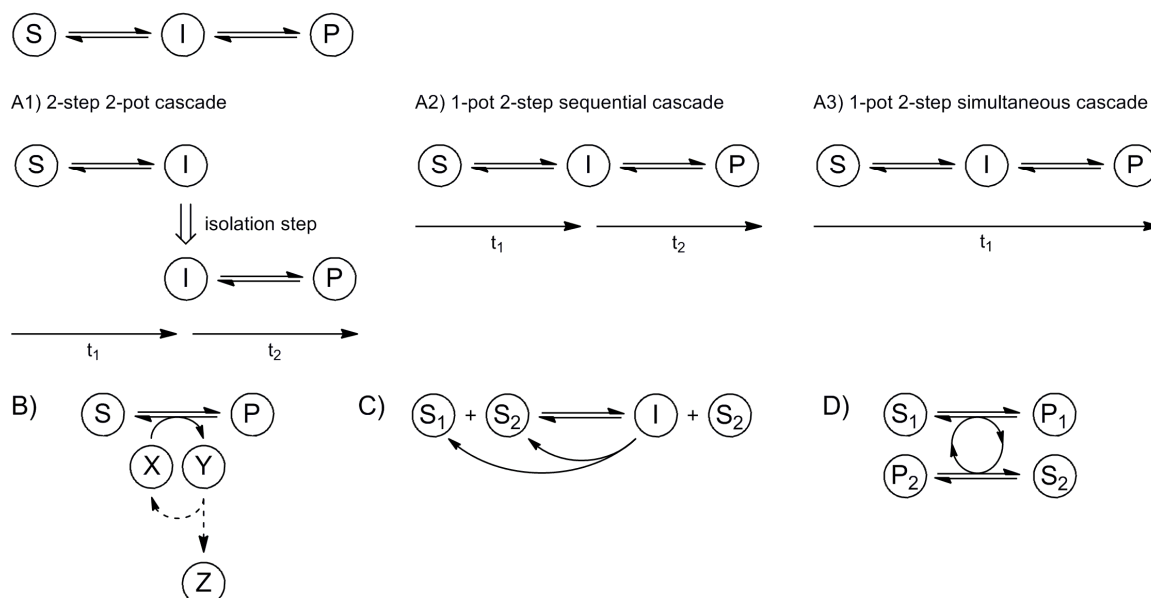


Figure 9: Enzymatic cascade 'designs' (A: linear cascades, B: orthogonal cascade, C: cyclic cascade, D: parallel cascade; adapted from [106b, 106d]).

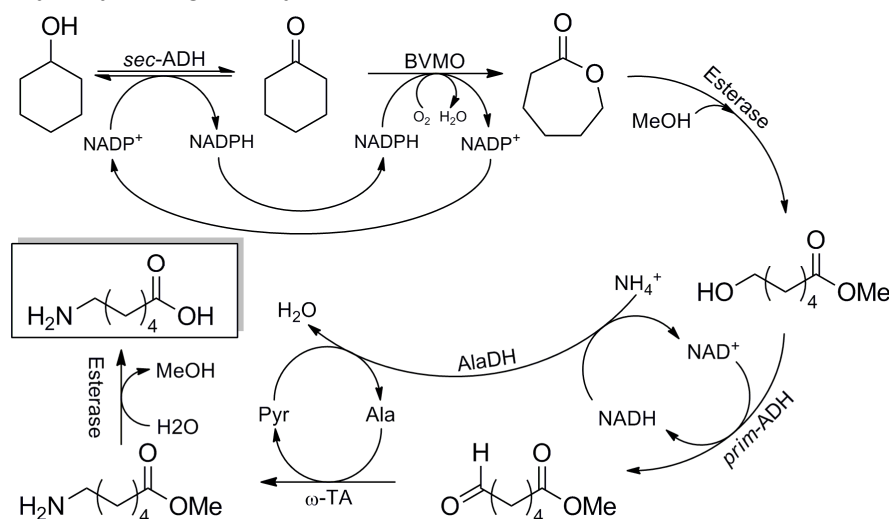
Of course at this point the possibilities of classifying cascade reactions are not yet tapped. These reactions can also be grouped depending on the used catalysts: *in vitro* cascades, *in vivo* cascades and chemo-enzymatic cascades.^[108] The latter one describes reactions, which combine the two worlds of chemo- and biocatalysis. Nevertheless, there are only a few examples described in literature over the last years, which will not be discussed here. The other two groups are going to be described in more detail in the following passages.

1.2.1 *In vitro* Cascades

In general, for *in vitro* cascades either purified enzymes, crude cell extracts (CCE) or lyophilized recombinant cells are applied. These cascade systems had a high impact in the past years, ranging from simple combinations of two enzymes forming an orthogonal cascade to the complex combination of up to 13 different enzymes.^[109] Hence, not all of these can be discussed here. Instead two examples are going to be described further.

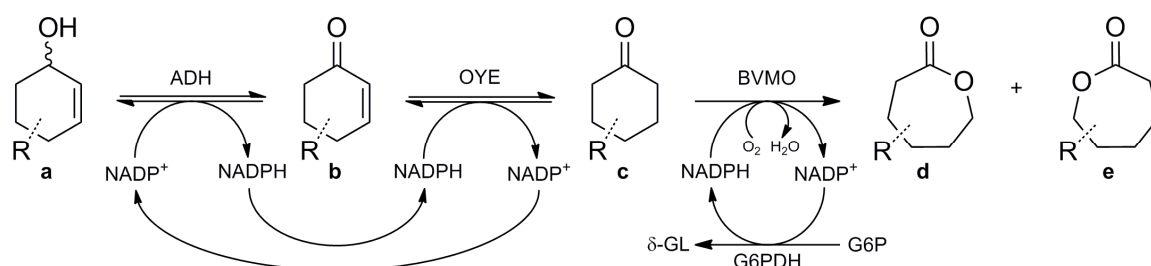
As first example the production of 6-aminohexanoic acid applying an *in vitro* cascade was demonstrated by Sattler *et al.* in a joint project with Evonik (Scheme 12).^[29] Here, the cascade reaction was divided into two modules: NADPH-dependent production of ϵ -caprolactone and NADH-dependent 6-aminohexanoic acid production applying an *in situ* capping strategy. The first module contained two steps using an ADH and a BVMO. The production of ϵ -caprolactone by this strategy was already described in

literature and proved to be an elegant way to circumvent the substrate inhibition of the BVMO, so that the way to a large-scale process using high substrate concentrations was paved.^[110] Nevertheless, Sattler *et al.* could further show that the application of the CHMO double mutant C376L M400I (CHMO_{DM}) with higher oxidative stability^[88e], and that a subsequent product removal were necessary to reach satisfying conversions with high substrate concentrations. The second module started with ring-opening of the lactone applying an *in situ* capping strategy using methanol and an esterase. The capping of the carboxylic acid function was necessary, because all tested ADHs for the following step did not accept the 6-hydroxyhexanoic acid as substrate, but the methyl capped one. In the following steps the hydroxy group was first oxidized to the aldehyde and then the amino group was introduced using a transaminase. Finally, the methyl ester was hydrolyzed again to yield the desired 6-aminohexanoic acid.



Scheme 12: *In vitro* cascade for production of 6-aminohexanoic acid as nylon-6 precursor (*sec*-ADH: secondary alcohol dehydrogenase, BVMO: Baeyer-Villiger monooxygenase, *prim*-ADH: primary alcohol dehydrogenase, ω -TA: ω -transaminase, AlaDH: alanine dehydrogenase, Ala: L-alanine, Pyr: pyruvate, MeOH: methanol; adapted from [29]).

The second cascade to be described here was the *in vitro* characterization of an *in vivo* cascade established by Oberleitner *et al.* to identify possible bottlenecks.^[111] Here, the combination of ADH, OYE and BVMO led to the successful production of enantiopure chiral lactones starting from 2-cyclohexen-1-ol and derivatives thereof (Scheme 13). Furthermore, it has to be pointed out that the combination of ADH and OYE led to a self-sufficient system, which supplied itself with the needed co-factor. As the third enzyme also required NADPH an additional co-factor regeneration system using the glucose-6-phosphate dehydrogenase was applied. As already described for the *in vivo* version of this cascade^[112] (see next chapter) the chiral lactones could be synthesized in perfect enantiopurities (up to >99% ee/de), although the conversions ranged from 55 to >99%. However, the most important finding in this study was the detailed characterization of the ADH reaction, which revealed that first in general the ADH activity towards the unsaturated substrate/intermediate (Scheme 13, compounds **a/b**) was significantly lower than the one towards the intermediate **c**, which led secondly to the discovery of an unwanted side-reaction by the ADH reducing intermediate **c** to the saturated cyclic alcohol. Nevertheless, application of the BVMO was sufficient to convert almost quantitatively the saturated ketone intermediate in an irreversible reaction to the final product (**d** or **e**).



Scheme 13: *In vitro* cascade for the production of chiral lactones (G6P: glucose-6-phosphate, G6PDH: G6P dehydrogenase, δ -GL: 6-phosphoglucono- δ -lactone; adapted from [111]).

1.2.2 *In vivo* Cascades

In this group of cascade reactions the enzymes are applied in their natural environment, which is the cytoplasm of the host organism. Hence, it should be distinguished between classical metabolic engineering and *in vivo* cascades in a synthetic biology sense. Whereas by metabolic engineering only the cell's metabolism is engineered to channel metabolites towards the production of a certain product, *in vivo* cascades in synthetic biology aim to introduce reactions not occurring in nature by the use of naturally unconnected enzymes in a host organism. As a matter of fact, scientists are facing additional challenges when using whole cells for cascade reactions:

1. Host background: Naturally occurring enzymes of the used host organism might catalyze unwanted side-reactions. To solve this problem there are two possibilities: use of a different cascade host organism or knock-out of the gene(s) encoding the unwanted enzyme(s), although the latter one might also lead to the next problem:
2. Growth deficiency: As consequence of a knock-out or by the introduction of the cascade itself cell growth might be impaired, which is mainly due to competition with the host enzymes for metabolites or the production of toxic intermediates. Here, intracellular scaffolding, protein fusion engineering or compartmentalization of the cascade might contribute positively to the host viability.
3. Expression levels: Obviously it is quite easy to balance enzyme ratios of *in vitro* systems by just mixing these in the optimal ratios. But this becomes an issue when using *in vivo* systems, where balancing of expression levels is not trivial. Nevertheless, there are possibilities towards this problem, e.g. plasmids based on the BioBricks principles^[113] containing different architectural elements like promoters and origins of replication, which can be used for different expression modes.
4. Additional diffusion barrier: Rather obvious the cell membrane, which forms the beneficial environment for *in vivo* cascades, might impair substrate uptake and product release. To let substrate and product pass this barrier, enzymes or transport systems for uptake and release can be introduced. Also permeabilization of the cells might enhance transport over the membrane.^[114]

As part of this DFG-funded overall project an *in vivo* cascade reaction for the production of chiral lactones (Figure 10) was established by Christin Peters in cooperation with our project partners Nikolin Oberleitner, Florian Rudroff and Marko D.

Mihovilovic (Vienna Technical University, Austria). They set up an enzymatic toolbox containing two ADHs, two OYEs and one BVMO, which enabled desymmetrization, kinetic resolution and regiodivergent biotransformation reactions. Like in the described *in vitro* version (Scheme 13) of this cascade the ADH and the OYE form a self-sufficient system for co-factor supply. The NADPH for the BVMO reaction was in this case recycled by the host enzymes using glucose as co-substrate. The substrates used were 2-cyclohexen-1-ol and the 2-, 3- and 4-methyl derivatives thereof as well as three out of four carveol diastereomers. All substrates were converted by 63 to >99% in perfect enantiopurities of >99%ee/de to the corresponding lactones. Furthermore, it has to be mentioned that the used BVMO exclusively produced either the normal or the abnormal lactone depending on the used substrate, so that in theory almost all possible lactones could be synthesized by this cascade when the used BVMO is exchanged with another regiocomplementary one.^[115]

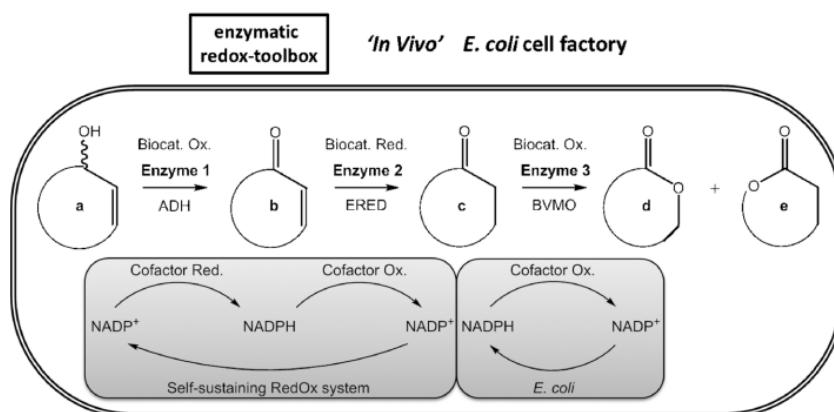


Figure 10: Principle of the *in vivo* cascade reaction for the production of chiral lactones (ADH: alcohol dehydrogenase, ERED: ene reductase, BVMO: Baeyer-Villiger monooxygenase; from [112]).

Nevertheless, during this research project some of the mentioned problems still needed to be addressed: The first one was an observed background reaction by an endogenous OYE from *E. coli*, which even showed opposite enantioselectivity for some of the substrates. This side-reaction was especially a problem for the substrates, which only were converted slowly. Changing the cascade host was not an option, because all the expression constructs were already created for *E. coli* and adopting these to another host organism would have been too tedious. Hence, the gene encoding the responsible enzyme had to be inactivated and indeed a knock-out of the gene *nemA*, which encodes the *N*-ethylmaleimide reductase A, nullified the background activity. The same background reaction was also observed by others and seems to be a general problem when performing OYE reactions in *E. coli*.^[115c, 116]

Furthermore, for this cascade reaction a proper co-expression strategy had to be applied, because the available plasmids carrying the single genes were not compatible among each other. To enable the *in vivo* reaction co-expression was done by application of a two plasmid strategy, where the OYE and the BVMO were encoded on one plasmid and the ADH on another one. Although the expression levels of all enzymes were sufficient to demonstrate the feasibility of this cascade, further optimization was performed. In her PhD thesis Christin Peters created fusion proteins of the OYEs and the BVMO, so that at least these two enzymes were available in

equal amounts, and indeed the fusion enzymes showed the same activities as observed for the single enzymes.^[117]

Another option to lower the metabolic burden for the host is the use of a single plasmid. In literature the feasibility of this strategy has already been demonstrated. Very recently, Wolfgang Kroutil and co-workers showed that the production of α -hydroxy acids by an *in vivo* cascade could be realized using the single plasmid strategy for co-expression (Figure 11A). They used different arrangements of the genes under the same promoter, introduction of engineered ribosomal binding sites (RBS) and application of promoters with different strengths for their optimization study (Figure 11B). They identified the plasmid pCAS3 to be the optimal expression strategy for their cascade. Here, the primary enzymes were encoded together under a weaker promoter (pBAD) and the secondary enzyme for co-factor regeneration was expressed under the strong IPTG-inducible T7 promoter. This way also the bottleneck in this reaction could be identified, which was the co-factor regenerating formate dehydrogenase. By the use of the strong T7 promoter this enzyme was expressed in much higher yields compared to the other genes under the control of pBAD.^[118]

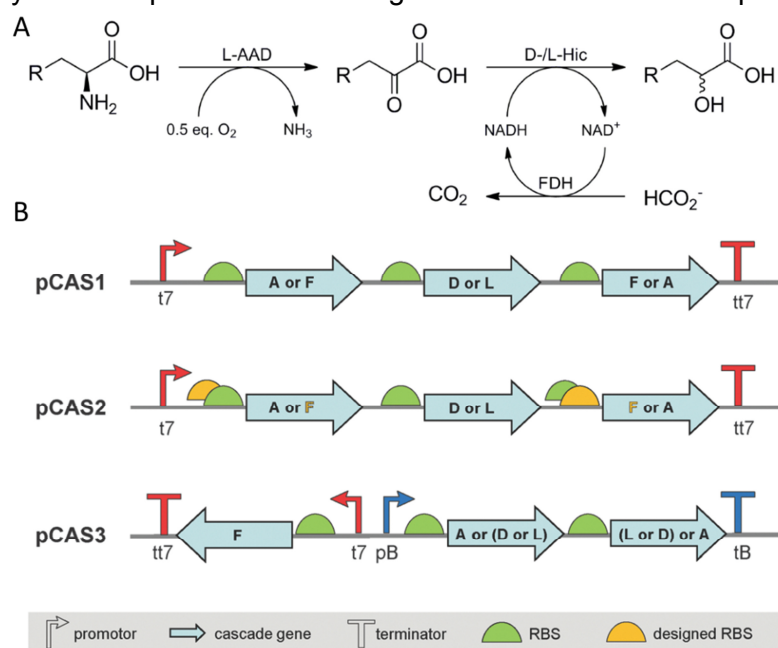


Figure 11: Cascade reaction for the production of α -hydroxy acids (A; L-AAD: L-amino acid deaminase, D-/L-Hic: 2-hydroxyisocaproate dehydrogenase, FDH: formate dehydrogenase; adapted from ^[118]) and single plasmid co-expression strategy (B; t7: IPTG-inducible T7/lacO promoter; tt7: T7 terminator; pB: arabinose-inducible promoter pBAD; tB: terminator rrnBT2, A: L-AAD, F: FDH, D/L: D-/L-Hic; from ^[118]).

Another strategy for co-expression optimization was developed by Mattheos Koffas and co-workers. They created a set of plasmids based on the Duet expression vectors from Novagen. The plasmids were redesigned in a way that the target genes could be easily cloned using four compatible restriction enzymes to be expressed in three different modes: operon mode, pseudo-operon mode and monocistronic (Figure 12). When assembling the genes in operon mode (Figure 12A), there is one promoter upstream of all genes and one terminator downstream. This mode of expression results in the transcription of one long mRNA product for all genes, out of which the first one usually shows highest expression due to parallel transcription/translation in bacteria. Introducing an additional promoter in front of each individual gene leads to

the pseudo-operon assembly (Figure 12B). In this way three mRNA products are transcribed of different lengths carrying the information of one to three genes. Hence, the expression of the last gene is expected to be the highest. The last mode of expression is the monocistronic one, which is created by additional introduction of a terminator sequence followed by a promoter behind each gene, so that these are all expressed individually (Figure 12C). This mode results in three single short mRNAs, which are expected to be translated equally. The feasibility of this concept was shown by application of a cascade reaction for the production of flavonoids.^[113b]

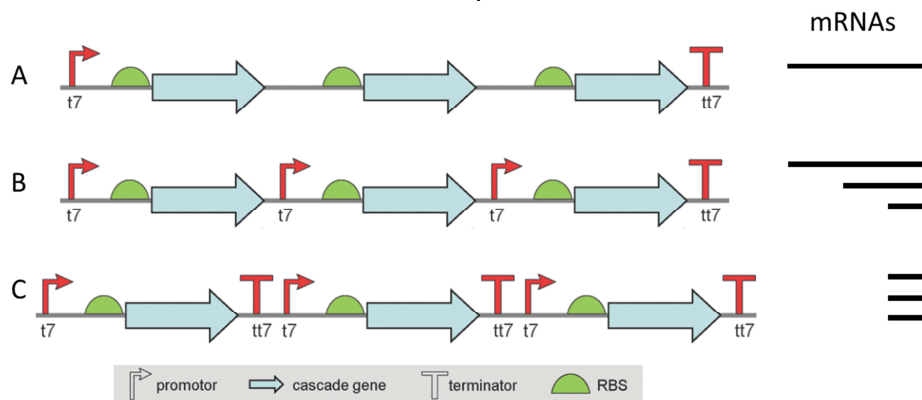
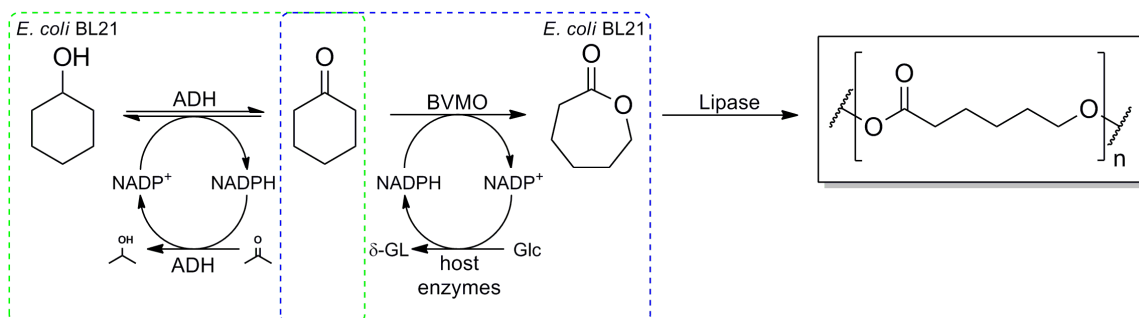


Figure 12: Possible modes of gene assembly for co-expression as designed by Mattheos Koffas and co-workers (A: operon mode, B: pseudo-operon mode, C: monocistronic; RBS: ribosome binding side, t7: IPTG-inducible T7/lacO promoter; tt7: T7 terminator; adapted from [113b]).

1.2.3 Combining *in vivo* and *in vitro* Cascades

Of course the two concepts of *in vivo* and *in vitro* cascades obviously also might be combined. This especially can be practical, if for example one of the enzymes is only poorly expressed in the desired cascade host and even probably easily available as commercial formulation.

Schmidt *et al.* described a cascade reaction, where exactly the problem described above had to be faced. The reaction for the production of PCL precursors applying an ADH, a BVMO and a lipase was developed in parallel to the one developed by Sattler *et al.* (Scheme 12).^[29] Their aim was also the production of polymer precursors, but a different concept was developed for this purpose. In both studies it was necessary to use the above described CHMO_{DM} for efficient conversions. The difference of this cascade to the above described one is the application of whole cells for the first two steps instead of isolated enzymes and the product removal strategy used. Here, the ADH and the BVMO were expressed separately in individual host cells, which just were mixed for the reactions as resting cells. The lipase A from *Pseudozyma antarctica* (CAL-A) for ring-opening polymerization to facilitate product removal was added as lyophilized enzyme preparation, because this enzyme shows only poor expression in *E. coli*. Co-factor regeneration for the ADH was realized by addition of acetone, which was transformed by the same ADH to *iso*-propanol, and for the co-factor recycling of the BVMO glucose was added, which was metabolized by the host enzymes. Furthermore, in this study also the co-expression of ADH and BVMO was investigated, but mixing the individual cells led to significantly higher production rates and of course this way the ratio of the enzymes could be adjusted more easily.^[28]



Scheme 14: Combined *in vitro* and *in vivo* cascade for the production of PCL precursors (ADH: alcohol dehydrogenase, BVMO: Baeyer-Villiger monooxygenase, Glc: glucose, δ -GL: 6-phosphoglucono- δ -lactone; adapted from [28]).

Interestingly, in the study by Sattler *et al.* also the CAL-A was tested for activity on ϵ -caprolactone, but found to be not active, which was obviously only true for the formation of the methyl ester. Hence, the saying

“You get what you screen for”^[119]

can also be true for cascade reaction engineering and not only for protein engineering.

1.3 Immobilization and Process Engineering

“Why immobilize? – The simplest answer may be: Because nature does it! While scientists are requested to be mobile it is obviously advantageous for many biocatalytic systems to be immobile.”^[120]

After reading this citation by Christian Wandrey probably nothing more needs to be said about immobilization. But of course the question needs to be commented. The use of immobilized cells is not an invention of the 20th century. The first reported use of immobilized cells dates back to 1670^[121] and this probably is not far enough. In that time beechwood shaves, charcoal or coke was used as matrix for the cells, which were used for vinegar production. The first immobilized isolated enzymes came up in the 1960s^[122] and the first large-scale process using immobilized enzymes was described in 1969 by the Tanabe Company (Japan).^[123] Immobilized catalysts simplify transfer of batch-processes into continuous ones, isolation of product and furthermore the immobilization contributes to stability of the catalysts.^[124] In principle, when deciding on either the use of isolated enzymes or whole cells as immobilized biocatalyst the following questions should be considered: How many steps are involved in the biocatalytic process? Is co-factor regeneration required?^[124a]

For multistep reactions generally whole cells are preferred, because often co-factor recycling is necessary in such reactions, which usually can be done by the cell metabolism. In simpler setups using single- or two-step reactions the above described problems when using whole cells can be circumvented by the use of isolated enzymes, although the isolation process itself is a laborious one. So that the pros and cons of both systems always have to be considered when setting up an immobilization process. In the following passages the commonly used immobilization techniques will be described.

1.3.1 Immobilization Techniques

Over the last 60 years a vast number of immobilization methods was developed, which generally can be divided into the following groups (Figure 13):

- Adsorption on solid matrices
- Covalent attachment to solid matrices
- Cross-linking with bifunctional reagents
- Entrapment in polymeric gels
- Encapsulation
- Immobilization by bio-specific recognition and more complex biological techniques

In general, all these techniques can be applied to immobilize either isolated enzymes or whole cells.

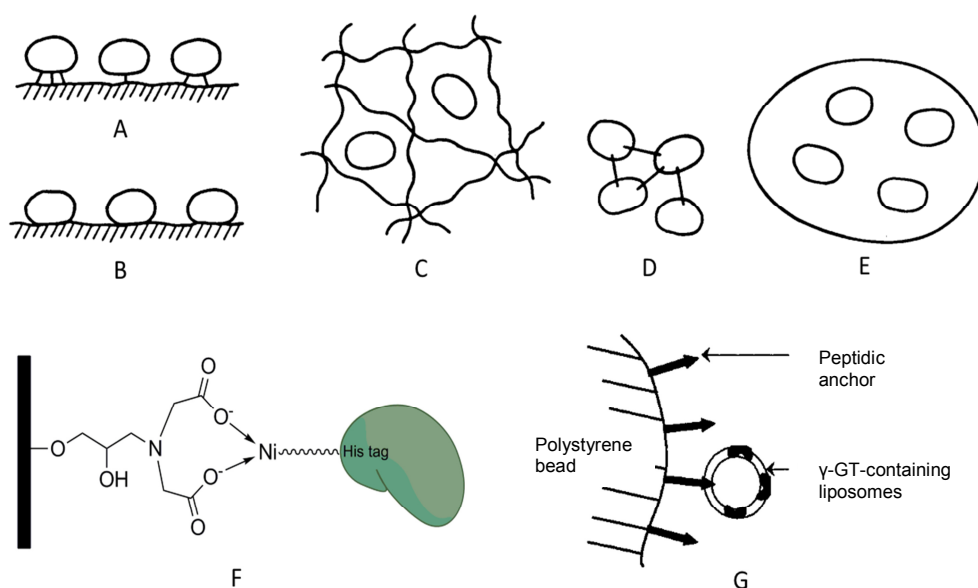


Figure 13: Immobilization methods (A: adsorption, B: covalent attachment, C: cross-linking, D: entrapment, E: encapsulation, F: affinity-tagged, G: lipid vesicle immobilization; adapted from [124a, 125]).

1.3.1.1 Adsorption on and Covalent Attachment to Solid Matrices

Immobilizing cells on solid supports by adsorption is probably the oldest (e.g. vinegar production above) and also easiest method, although often the adsorption of micro-organisms to for example filter or reactor walls by biofilm formation is unwanted. Nevertheless, the first modern attempts of cell immobilization for industrial use were described in the 1960s by Hattori & Furusaka, who succeeded in adsorbing *E. coli* and *Azotobacter agilis* cells to ion exchange resins.^[126]

Due to its simplicity this technique seems to be superior to all other ones, because in principle it is just mixing a biocatalyst solution with the desired resin and incubating for a while, during which the cells adsorb to the surface. However, this process is much more complex. The forces, which are responsible for efficient immobilization, are mainly electrostatic (van der Waals) and ionic or even natural covalent interactions of the cells with the surface. The latter one especially is involved in biofilm formation,^[127] which shows high complexity due to the fact that also the cell surface has an important

role with respect to its flexibility depending on cell and nutritional state and environmental circumstances.^[124b, 128] In parallel, the properties of the support, like chemical composition, hydrophobicity, charge and structure, also have to be considered.^[128] Furthermore, these can be modified by chemical and physical treatments.^[129]

For covalent immobilization adsorption is somehow a prerequisite, because the cells of course have to be in contact to a surface to be linked covalently. Therefore, usually reactive reagents are used. The most common one is probably glutaraldehyde, which cross-links amino groups of the enzyme or cell wall to amino groups of the matrix. In contrast, if there are epoxy groups available on the support's surface, no cross-linker is necessary due the reactivity of the oxirans. In general, when using covalent immobilization, the surface is activated first by the reactive reagent, so that the introduced functional groups can react with the biocatalyst surface. However, the optimal ratio between cross-linker and biocatalyst has to be found, because too many reactive functionalities at the surface might lead to inactivation.^[130] For further functionalization of course the used resin has to carry already certain groups on its surface (e.g. polysaccharides) and for these modifications several methods either physical or chemical were described in literature.^[129]

As there is a huge number of commercial and natural matrices available, finding an adequate supporting material is mostly based on the trial-and-error principle. To lower the number of materials to choose from the exact requirements for the planned immobilization have to be figured out. The following parameters might give a kind of guideline: price, biocompatibility, hydrophilicity, toxicity, biodegradability, mechanical stability, possible functionalization, surface area and pore size. In general, there are three groups of different materials: inorganic supports, synthetic polymers and natural macromolecules. The use of the inorganic ones can be limited sometimes due to low stability or low biocompatibility. Nevertheless, there are also special ceramics for medical purposes, which are indeed stable and show high biocompatibility, but are very expensive. Natural macromolecules on the one hand generally are biodegradable, have a high hydrophilicity, are not toxic and inexpensive. On the other hand, they sometimes show low mechanical stability, which might be undesired for certain processes. Finally, synthetic polymers are often superior due to their general high stability and often already existing functional surface groups. If these are not yet available they can be introduced rather easily, which makes them most suitable for covalent immobilization. Furthermore, already during their production process the geometrical configuration and shape can be introduced. Nevertheless, one drawback definitively can be the high hydrophobicity. But again this can also be modified by functionalization.

1.3.1.2 Cross-Linking with Bifunctional Reagents

In contrast to the two techniques described so far no solid material is needed for cross-linking. Here, the biocatalysts are directly cross-linked by inter- and/or intramolecular covalent bonds. The most common reagents used for this are glutaraldehyde, dimethyl adipimide, dimethyl suberimide, aliphatic amines and toluene diisocyanate.^[124] Especially the intramolecular cross-links might have a negative effect due to the fact that after reaching a certain threshold of the cross-linking degree these might lead to severe changes in the structure of the biocatalyst and finally to inactivation.^[130]

Furthermore, the cytotoxicity of the linking molecules makes this method inadequate for cell immobilization. Nevertheless, especially Roger Sheldon, who also founded CLEA Technologies B.V. (Delft, The Netherlands), promoted this technique during the last years. There were several studies by this scientist and his co-workers using the so called cross-linked enzyme aggregates (CLEAs) for biocatalysis, which demonstrated the feasibility of this technique.^[131] Nowadays the portfolio of CLEA Technologies contains several enzymes, e.g. lipases, proteases, keto reductases and many others.

1.3.1.3 Entrapment and Encapsulation in Polymeric Gels

The main difference of these methods to the previously described ones is that the catalyst itself is not attached to the supporting matrix. Thus, the biocatalysts are generally entrapped inside a gel-like structure. For both procedures the catalyst solution is simply mixed with a water-soluble polymer and the gelation is either induced by a shift of temperature, pH or the addition of inducing agents. The difference between entrapment and encapsulation is the fact that using entrapment methods generally a gel block containing the catalysts is produced, whereas in encapsulation processes small beads containing the catalyst are made.

For entrapment typically gel-forming molecules like acrylamide or vinyl alcohol and natural polymers like alginate, agar, gelatin or carrageenan are used.^[124a] However, this method suffers from several disadvantages, like extreme conditions for gelation (e.g. very high pH values used in sol-gel processes^[132]), which might lead to inactivation. Additionally, diffusional limitations might impair catalytic efficiency and leakage of especially enzymes from the gel might become a problem. These problems can be solved by adjustment of the balance between pore size and leakage of catalyst. However, entrapment of enzymes and cells is still applied frequently due to the low costs and simplicity of the method.

Likewise, the same principles as described above are used for encapsulation. Both techniques facilitate the inclusion of biocatalysts in a semi-permeable compartment. Here, gelling agents, but also lipids, are used to form capsule structures, which contain the catalysts. This is also the main difference between the entrapment and the encapsulation technique. Furthermore, the conditions used for encapsulation usually are milder in comparison to the ones for entrapment and therefore advantageous due to the reduced loss of activity. Especially for immobilization of cells such gentle conditions are beneficial. Probably the most wide-spread applied natural polymer for encapsulation is alginate.

The first alginates isolated from *Laminaria vesiculosus* and *Fucus stencphylla* were described in 1883.^[133] Nowadays, the commercially available alginate mainly is extracted from the giant kelps *Macrocystis pyrifera*, *Ascophyllum nodosum*, and various types of *Laminaria hyperborea*.^[134] From 1929 to 1955 the structure of alginate was described to be built up by 1,4-linked β -D-mannuronic acid and α -L-guluronic acid residues.^[135]

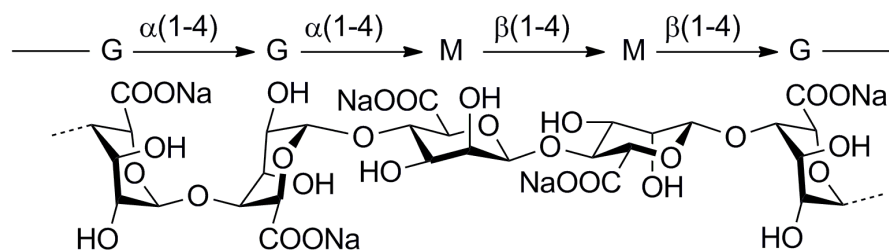


Figure 14: Structure of alginate sodium salt (G: α -L-guluronic acid, M: β -D-mannuronic acid; adapted from [136]).

Gelling of this natural polysaccharide is induced by addition of divalent cations (e.g. Ca^{2+}), which is based on coordination of these by the carboxy and hydroxy groups of the sugar monomers as well as by the glycosidic and lactonic oxygen atoms (Figure 15 A). Intermolecular binding of the cations by different polysaccharide chains is preferred over the intramolecular one, which leads to the formation of buckled-shaped cavities perfect for Ca^{2+} coordination. This phenomenon is called ‘egg-box’ model for obvious reasons (Figure 15 B).^[137]

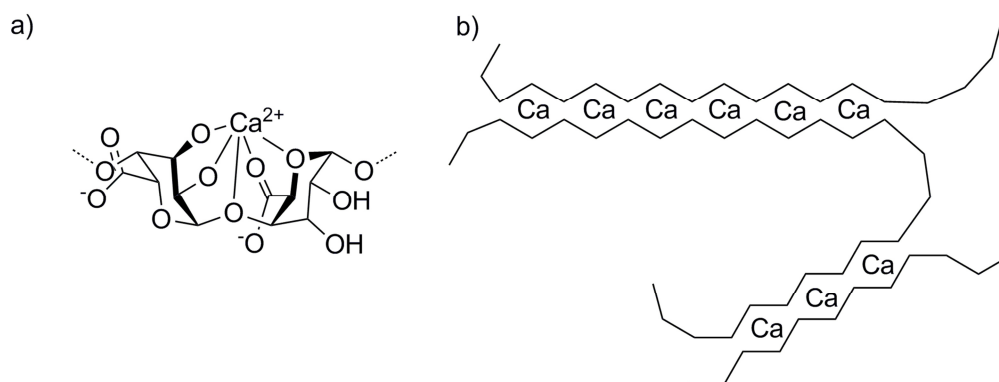


Figure 15: Coordination of Ca^{2+} -ions by alginate (A: Binding of Ca^{2+} to α -L-GulA-(1-4)-I-GulA (GulA: guluronic acid), B: ‘egg-box’ model of polyGulA in gel state; adapted from [137]).

For the encapsulation procedure itself there are several methods. At first the solution containing the biocatalyst has to be mixed with a sodium alginate solution, which subsequently is dropped into the Ca^{2+} -containing solution, where the capsules are formed immediately. In laboratory scale this dropping process often is carried out manually just using a syringe (Figure 16 A), which results in capsules of a size in the millimeter range. Smaller particles often enhance mass transfer due to the increased size to surface ratio. To realize the production of smaller capsules (micrometer range) in lab-scale a co-axial air current can be applied (Figure 16 C). But the availability of commercial devices for application of a co-axial air stream is limited. The second method for production of micrometer-scaled capsules is the use of a JetCutter system (Figure 16 B), which usually is also the choice of method for industrial processes.^[138] Here, the alginate solution is extruded from a nozzle and the so called liquid jet is simply cut off by a high-speed rotating cutting wire wheel. This way a throughput of up to $20 \text{ kg} \cdot \text{h}^{-1} \cdot \text{nozzle}^{-1}$ can be reached.^[139]

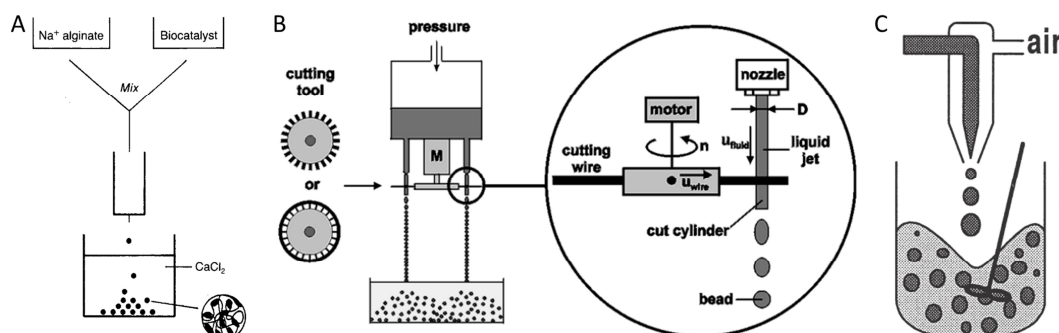


Figure 16: Procedures for encapsulation in alginate (A: 'drop-method' as used in laboratory scale, B: jet-cutting device as used in industry, C: principle of co-axial air current applied to nozzle; adapted from [136, 138-139]).

The alginate encapsulation technique has been used for several applications, e.g. water treatment^[140], biological ammonia production^[141], artificial plant seeds^[142] or hydrolysis of whey^[143]. Rather exotic applications of the alginate technology came up in the last years, where it was used in the so called 'molecular kitchen' movement^[144] and also in bubble teas for encapsulation of flavors.^[145]

1.3.1.4 Immobilization by Bio-Specific Recognition and Complex Biological Techniques

Immobilization techniques belonging to this group are probably the most sophisticated ones. Here, the biocatalyst usually is immobilized via a very specific one-point attachment. These bio-specific recognition methods are especially necessary, if the native conformation of the biomolecule is required, e.g. immobilization of antibodies.^[146] In the field of protein technology the most obvious method for immobilization of enzymes is the use of an affinity tag, which originally was introduced for purification. For this purpose the Avidin-tag^[147], cellulose binding domain^[148] and metal affinity tag (e.g. His-tag)^[125a, 149] have already been described. However, the degree of complexity can be further increased, like immobilization of lipid vesicles, which contain a membrane enzyme, using a peptide anchor.^[125b] Very recently the intracellular immobilization or cell surface immobilization of enzymes came up to enhance catalytic efficiency via substrate/intermediate channeling. Therefore, either so called bacterial microcompartments (MCPs)^[150] or scaffolds based on specific protein-protein^[151], protein-DNA^[152] or protein-RNA^[153] interactions were used. In all cases the enzyme(s) of interest was fused to a foreign protein domain, which guides it towards a certain scaffolding partner molecule.

The first example of a bacterial MCP, which could be engineered to encapsulate foreign proteins, was found in the 1,2-propanediol utilization pathway from *Salmonella enterica* (Figure 17).^[150f] This pathway is completely encapsulated in a 'protein cage', because that way the cell components are protected from the reactive intermediate propionaldehyde. For encapsulation of foreign enzymes these just have to be fused to one of the natural anchor peptides and by co-expression with the shell proteins these are automatically encapsulated.

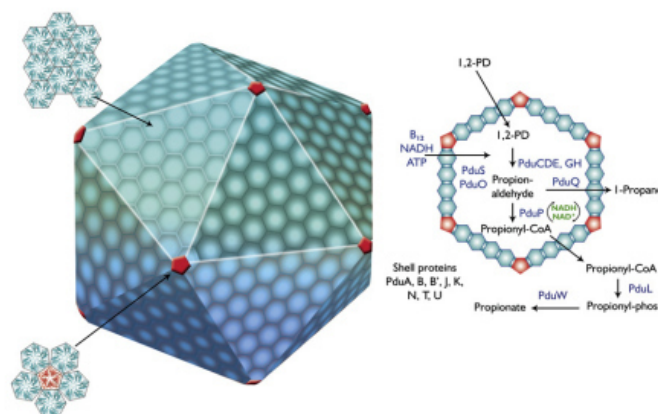


Figure 17: Microcompartment for 1,2-propanediol utilization from *Salmonella enterica* (from [150h]).

1.3.2 SpinChem® - A Rotating Bed Reactor

As pointed out above, the immobilization of biocatalysts often contributes to long-term stability and facilitates their reuse. In general, when using these immobilized biocatalysts a proper reactor system has to be chosen. The classical reactor concepts therefor are a simple stirred tank reactor (STR) and a fixed bed reactor (FBR, Figure 18).

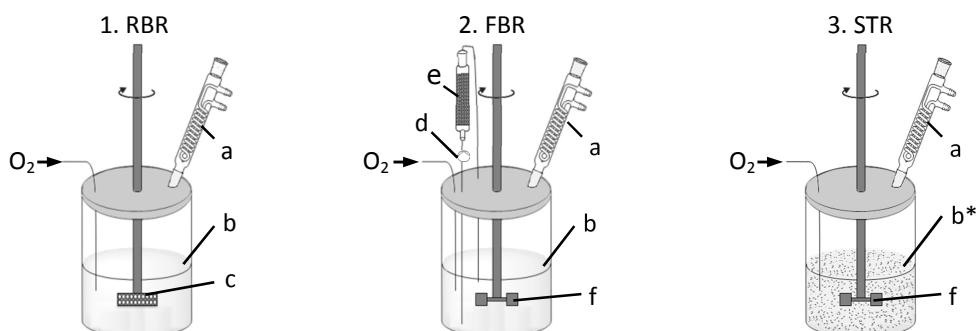


Figure 18: Schematic drawing of the three reactor setups (RBR: rotating bed reactor, STR: stirred tank reactor, FBR: fixed bed reactor, a: reflux cooler, b: reaction solution, b*: reaction solution containing catalyst particles, c: RBR packed with catalyst particles, d: pump, e: column packed with catalyst particles, f: Rushton-type stirrer; adapted from [154]).

The STR is a very simple setup, where the solid particles are added to the liquid reaction medium, which is mixed by a certain stirring device. In contrast to its simplicity the use of an STR obviously is encountered with the mechanical stress, to which the catalysts are exposed. This often leads to abrasion or even severe damage of the particles. Beside this the recycling process is rather laborious, because the medium has to be separated from the catalysts by filtration or centrifugation, which especially for industrial processes is unwanted.

The tedious work-up process when using an STR can be avoided by application of an FBR. Here, the immobilized catalysts are simply packed into a usually tempered column, which is fluidized by the reaction medium. Nevertheless, with the ease of separation certain disadvantages depending on the properties of the column (e.g.

length, diameter), particles (e.g. size, squeezability) and process parameters (e.g. flow rate) like pressure drop, reactant and pH gradients have to be considered.

As a kind of 'reactor chimera' combining the advantageous features of STR and FBR the rotating bed reactor (RBR) was developed. The RBR concept was first described in 1960 by Pilo & Dahlbeck.^[155] They patented an apparatus to enhance the contact of two fluids (or one fluid and a gas) with different specific weights. Later this concept was further developed for the use in heterogeneous catalysis as basket reactor, which features baskets rotating inside a well for gas/solid and liquid/solid reactions.^[156] Furthermore, the use of an 'insolubilized' enzyme in an RBR was first described in a patent filed by Corning Inc. at the same time.^[157] Very recently, this reactor concept was rediscovered by scientists from Nordic Chemquest AB (Umeå, Sweden) and further optimized with respect to handling and mass transfer.^[158]

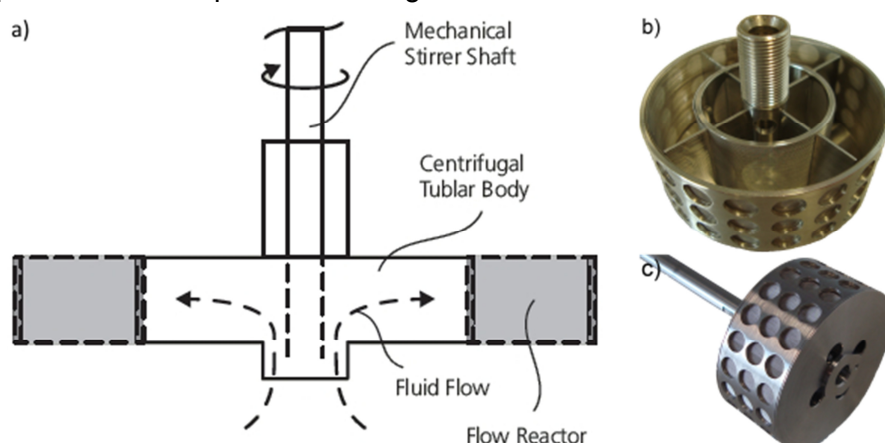


Figure 19: Schematic drawing of the SpinChem[®] rotating bed reactor (A), inside view (B) and outside view (C) (adapted from [154, 158a]).

The working principle of the RBR designed at Nordic Chemquest AB (SpinChem[®]) is depicted in Figure 19. The catalytic particles are simply packed into the outer void of the cylinder (Figure 19 A, flow reactor), which is confined by a filter with a defined mesh size. After closing the filled compartment and attaching it to an overhead stirrer this is rotated, thus leading to a flow of reaction medium through the packed bed driven by the centripetal forces. Thereby, not only the mass transfer is improved, but also the particles themselves are protected from any mechanical forces and gradients are avoided due to the fact that the compartment is also used for mixing. Furthermore, the work-up respectively the recycling of the catalysts becomes obviously very simple in comparison to an STR, because the SpinChem[®] just has to be lifted out of the medium.

1.4 Application of Polymers and Chiral Molecules

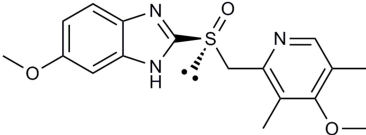
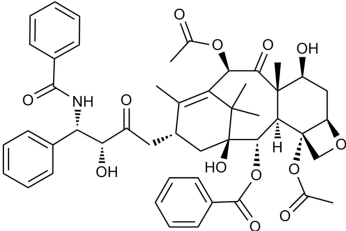
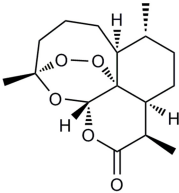
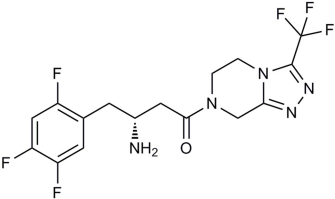
1.4.1 Chiral Molecules

Chirality is of great importance especially for the pharmaceutical industry, which was realized in the 1960s in Germany during the Contergan scandal.^[159] In that case, the tranquilizer and sleep-inducing drug thalidomide was especially administered to pregnant women as a racemic mixture to alleviate morning sickness. After the sale launch in 1957, the cases of newborns with phocomelia increased, but this was

mislinked to nuclear weapon tests during world war II. In 1961, the cases were connected to Contergan application and therefore it was taken off the market. Later the effects of the single enantiomers were described: the sedative effect was linked to the (*R*)-enantiomer^[160], whereas the teratogenic one was ascribed to the (*S*)-enantiomer, although there have been contradictory results in literature^[161] and it could not be absolutely discriminated between the two molecules, because both enantiomers easily undergo chiral inversion when applied *in vivo*.^[162]

In the list of 'Top 200 Drugs by Worldwide Sales 2013' 41.5% of the molecules featured one or more chiral center.^[163] Examples for chiral drug molecules, which are produced via biocatalytic or biotransformation processes, are listed in Table 4. For details on Esomeprazol refer to chapter 1.1.5 and for Taxol and Artemisinin refer to chapter 1.1.4. Especially the process for Sitagliptin synthesis has drawn attention in the last years, because the researchers at Merck & Co. and Codexis Inc. succeeded in creating an amine transaminase variant (with 27 mutations), which accepts a so called bulky-bulky substrate.^[164] This biocatalyst even outperformed the established chemical process using transition metals due to the fact that less steps are required.^[165] At that point the described mutant was the first transaminase being able to use sterically demanding substrates.

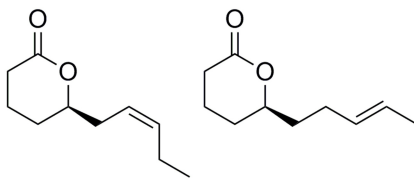
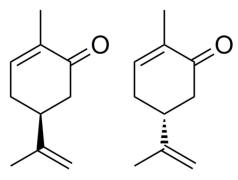
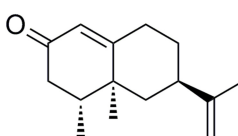
Table 4: Examples of chiral drug molecules produced by biocatalytic or biotransformation processes (ATA: amine transaminase).

Structure Name	Enzyme(s) for Synthesis	Application	Reference(s)
 Esomeprazol	BVMO or DOx or P450	Proton pump inhibitor used in the treatment of gastric acid-related disorders	[89, 166]
 Taxol (Paclitaxel)	Synthases, P450s and Transferases (biosynthesis not yet deciphered completely)	Cancer drug for treatment of breast, lung and non-small cell cancers	[72, 167]
 Artemisinin	Synthases, dehydrogenases, reductases and P450s	Anti-malaria drug	[73]
 Sitagliptin	ATA	Anti-diabetic drug	[164, 168]

The flavor and fragrance industry is another branch using chiral molecules. Three selected examples are given in Table 5. The synthesis of the Jasmin lactones shown was realized by Fink *et al.* screening a panel of different BVMOs.^[169] All possible enantiomers were accessible via kinetic resolution reactions starting from the racemic cyclic ketones with E-values ≥ 100 . These pure lactones are of special interest for organoleptic studies by perfumers as they are also part of natural fragrances.

Another example of biocatalysis used in flavor industry is the synthesis of (+)-nootkatone combining a P450 and an ADH.^[170] Therefore, in the group of Vlada Urlacher first a P450 catalyzing the regioselective hydroxylation of (+)-valencene was identified, which at first sight could have been problematic due to the fact that (+)-nootkatone was found to be an inhibitor of human P450s.^[171] This is also the reason for the recommendation not to take medication together with grapefruit juice. Nevertheless, it was demonstrated that CYP109B1 and a P450-BM3 mutant were capable of regioselective hydroxylation with notable activity. Combining the P450-BM3 with an unselective ADH further improved the conversion rate and yield.^[170b]

Table 5: Examples of chiral flavor and fragrance molecules with possible industrial interest accessible by biocatalytic or biotransformation processes.

Structure Name	Enzyme(s) for Synthesis	Natural Occurrence and/or Application	Reference(s)
 (R)-cis- Jasmin lactone (R)-trans- Jasmin lactone	BVMO	(R)-cis: part of <i>Jasminium grandiflorum</i> essential oil, (S)-cis: part of <i>Polianthes tuberosa</i> tuberose oil, (R)-cis/trans: both found in gardenia flowers, part of natural mango aroma	[169]
 (S)- Carvone (R)- Carvone	P450 and ADH	(S): main constituent of caraway seed oil, (R): main constituent of spearmint essential oil; Precursor for synthesis of dihydrocarvide	[111-112, 172]
 (+)-Nootkatone	P450 and ADH	Found in grapefruit juice, high added-value commercial flavoring compound	[170]

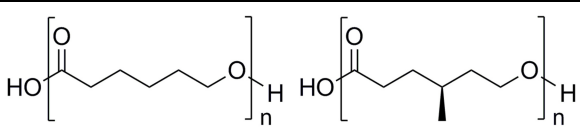
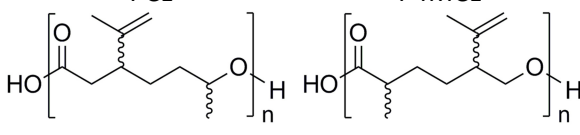
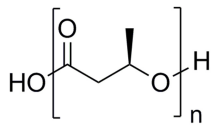
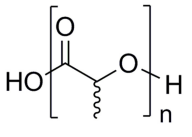
As a last example the synthesis of the monoterpene carvone will be described. In nature both enantiomers can be found: the (S)-enantiomer is the main constituent of caraway seed oil,^[173] whereas the (R)-enantiomer is responsible for the scent of spearmint (*Mentha spicata*) essential oils.^[174] The biosynthesis reaction for carvone is initiated by a P450, which regioselectively hydroxylates limonene in C6-position. The resulting carveol is then further oxidized by an ADH to carvone. Interestingly, Schalk & Croteau could identify the amino acid residue, which is responsible for regioselectivity in the *M. spicata* enzyme and they even could create a mutant (F363I) showing the C3-regioselectivity of the enzyme from *Mentha × piperita* (peppermint).^[175] Surprisingly, introduction of the homolog mutation (F364I) in the peppermint P450 led

to deactivation of the enzyme. The carvone itself cannot only be used as fragrant, but also as precursor for interesting polymers, which are described in the following chapter.

1.4.2 Polymers

Due to the fact that the global plastic production reached 311 mega tons in 2014^[176] and assuming that the global demand has grown in the same way, it is obvious that the oil-based production cannot suffice the market forever. Hence, renewable sources and sustainable processes are necessary for the production of polymers, which are desirably also biodegradable. In Table 6 some examples for biodegradable polymers either produced by biocatalysis/biotransformation and/or based on natural sources are summarized.

Table 6: Examples of biodegradable polymers (PCL: poly-[caprolactone], P4MCL: poly-[4-methylcaprolactone], P3HB: poly-[3-hydroxybutanoate], PLA: poly-[lactate]).

Structure Name	Application(s)	Reference(s)
 <p>PCL P4MCL</p>	Tissue engineering, drug delivery, microelectronics, adhesives, packaging, 3D printing	[28, 86a, 177]
 <p>normal abnormal</p> <p>Poly-[dihydrocarvide]</p>	Shape memory polymers, cross-linking, additive for co-polymers, tissue engineering, (not yet biocatalytically produced)	[178]
 <p>P3HB</p>	Wound management, vascular system materials, orthopedics, drug delivery, packaging, adhesives, coatings	[179]
 <p>PLA</p>	Packaging, coating, fibers, prosthetics, drug delivery, 3D printing	[179-180]
Plastics based on natural polymers, <i>e.g.</i> starch, cellulose, soy protein, sugar beet pulp	Additives for composite polymers	[179, 181]

PCL is a very important polymer and it is widely applied for several purposes, *e.g.* tissue engineering and drug delivery. On the one hand it is so popular due to its biodegradability by microorganisms^[182] and on the other hand its biocompatibility and persistence in the human body, which makes it predestinated for use in orthopedics.^[183] PCL is traditionally produced by ring-opening polymerization (ROP) of ϵ -caprolactone using metals, organic acids or enzymes as catalysts. Due to the relevance to this thesis only the enzyme-mediated reactions will be discussed here.

The first described ROP reactions by lipases in organic solvent are from 1995.^[184] Of course a process in an aqueous environment would contribute to the 'greenness' of such a reaction. Hence, there were some recent successful attempts to perform ROP using a lipase in water.^[28, 185] The mechanism for the ROP reaction in solvent is shown in Figure 20. It is assumed that in the first step the acyl-enzyme intermediate is formed by hydrolysis of the lactone. Next, the 6-hydroxyhexanoic acid alkyl ester is released, which acts also as the monomer for the polymerization. For elongation of the polymer-chain the acyl-enzyme intermediate is hydrolyzed by the alcohol function of a mono- or oligomer.

1. Formation of acyl-enzyme intermediate



2. Release of 6-hydroxyhexanoic acid alkyl ester



3. Elongation of oligomer

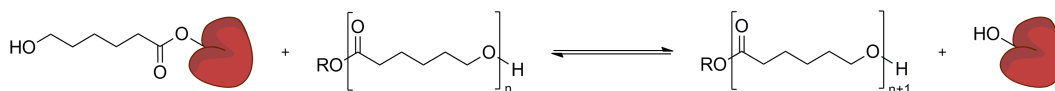


Figure 20: Proposed mechanism of ring-opening polymerization by a lipase in neat organic solvent (red bubble: lipase).^[186]

The applicability of ROP in water has been demonstrated for a set of chiral and achiral lactones by Schmidt *et al.* In this study, even the formation of an enantiopure polymer (P4MCL, Table 6) was shown by application of the above described cascade reaction (Scheme 14) using the prochiral 4-methyl-cyclohexanol as substrate. However, the mechanism of the ROP in an aqueous environment still stays elusive. In this case it is eventually more likely that the free hydroxy acid is due to its stability not released, but the acyl-enzyme intermediate gets hydrolyzed directly by the lactone.

The polymerization of the natural product derived lactones dihydrocarvide and menthide was until now only demonstrated by chemical reactions,^[178a-c] although in principle the lipase-mediated ROP should be possible. The monomers for this reaction can be synthesized already in a biocatalytic cascade reaction,^[111-112] so that only the lipase reaction needs to be established. The polymers resulting from the chemical polymerization reactions were already characterized, e.g. these showed a good shape memory ability.

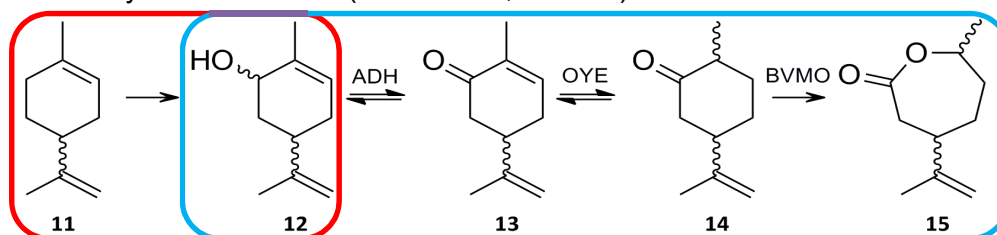
Other highly investigated biodegradable polymers from renewable sources are poly-[3-hydroxybutanoate] (P3HB) and poly-[lactate] (PLA). Both polymers are used nowadays for several purposes. Especially PLA, since the production costs went down, has become popular as renewable alternative in packaging.^[180] In contrast to the other described polymers, P3HB is produced naturally by several microorganisms under nutrient-limiting conditions, which makes it an interesting alternative to petroleum-based processes.^[179]

Naturally produced polymers, mainly deriving from waste streams, were also subject to several studies. But due to their usually high hydrophilicities, it was difficult to apply these as neat polymers. Here, the combination of for example sugar beet pulp with PLA led to a significant increase of the composite strength compared to PLA alone.^[187]

2 Scope of this PhD thesis

The aim of this PhD thesis was to further optimize two different redox cascade reactions concerning the establishment of new enzymes for additional reaction steps, process engineering and overall work-flow improvement.

The first cascade was established in a DFG-funded project (grant no. Bo1862/6-1) in cooperation with the Vienna Technical University (Figure 10). In this cascade it was planned to utilize limonene **11** as renewable, chiral precursor for the production of chiral lactones by coupling of a hydroxylating enzyme, an alcohol dehydrogenase (ADH), an old yellow enzyme (OYE) and a Baeyer-Villiger monooxygenase (BVMO). In this thesis especially the initial hydroxylation step should be studied with respect to regioselectivity of this reaction (Scheme 15, red box).



Scheme 15: Desired redox cascade reaction for the synthesis of chiral lactones using limonene as substrate (involved co-factors are not shown; red box: reaction step studied in this thesis; blue box: reaction steps optimized by co-expression in this thesis).

Therefore a highly regioselective enzyme was subject to search. The most prominent enzymes for hydroxylations in biotechnology are cytochrome P450-monooxygenases, above all the P450-BM3 from *Bacillus megaterium*. This enzyme and a homologous one should be the first ones to be studied for the desired reaction.

Nevertheless, in literature there are further bacterial wild-type strains, e.g. *Cellulosimicrobium cellulans* EB-8-4, described to be capable of highly regioselectively hydroxylating limonene. However, the enzymes responsible for this reaction still are elusive. The strain should be further studied and the hydroxylating enzyme(s) identified and possibly further characterized.

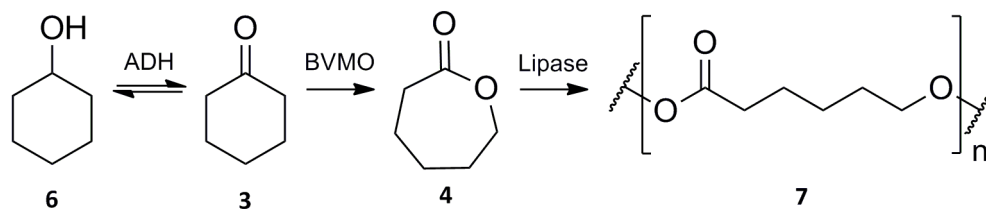
Furthermore, the expression of the enzymes involved in the latter three steps of the established cascade should be optimized. Until now a two plasmid strategy was used for co-expression of these enzymes. However, a single plasmid strategy was expected to lower the metabolic burden of the host organism and thereby further optimizing the reaction steps. In this thesis especially the expression ratio should be addressed by creation of a single plasmid system carrying all three necessary genes encoding for the desired enzymes.

In the second part of the thesis another redox cascade reaction for the synthesis of poly-[caprolactone] (PCL) precursors (Scheme 16) was aimed to be further optimized by immobilization, so that the catalysts could be applied in a rotating bed reactor (RBR). Therefore, the general applicability of the RBR for enzymatic reactions should be demonstrated and an immobilization method should be established for *in vivo* cascade reactions using the well-known alginate encapsulation technique.

For a future application in an industrial environment the process itself was also planned to be further optimized. Therefore, the immobilization procedure should be improved with respect to activity of the catalysts. Hence, a method leading to

decreased particle size of the alginate capsules containing the catalytic cells should be established. To further pave the way *en route* to industry the work-flow also should be a subject of optimization, so that possibly not only the reaction would be carried out in one-pot but also the beforehand steps of catalyst preparation.

Finally, the feasibility of the developed methods should be demonstrated in biocatalysis reactions using the catalytical capsules produced by application of the *in situ* process.



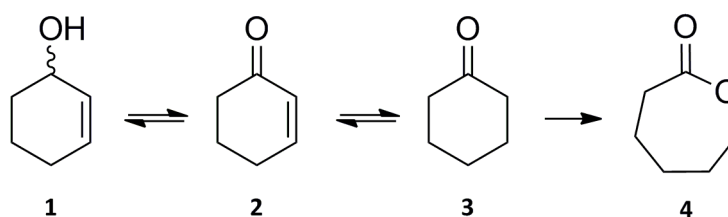
Scheme 16: Redox cascade reaction for the synthesis of oligo-[caprolactone] (involved co-factors are not shown).

3 Results

As already outlined in chapter 2 the scope of this thesis was the further optimization of recently developed cascade reactions. First of all, the cascade for production of chiral lactones as potential polymer precursor (Scheme 13, Figure 10) was subjected to expression optimization. Therefore, all three involved enzymes should be expressed as a single plasmid construct to lower the expression burden for the cells (chapter 3.1). Secondly, the same cascade should be extended by introduction of an initial hydroxylation step to enable the use of limonene as 'renewable' chiral precursor (chapter 3.2). Finally, another described cascade for the production of PCL precursors (Scheme 14) was subject to process optimization. Here, the catalysts should be transformed into an immobilized one to enable the application of a rotating bed reactor (chapter 3.3).

3.1 Co-Expression of Three Enzymes for Cascade Optimization

In the first part of this thesis the cascade reaction shown in Scheme 13 and Figure 10 was aimed to be optimized. Therefore, three involved enzymes were planned to be co-expressed in one host cell using a single plasmid. To balance the different expression levels and activities all possible arrangements of the genes on the plasmid following the pseudo-operon strategy (see chapter 1.2.2, Figure 12) were created. The reaction producing ϵ -caprolactone **4** from cyclohexenol **1** was used as model reaction (Scheme 17), which required the following enzymes from the 'tool-box': the alcohol dehydrogenase from *Lactobacillus kefir* (LK-ADH), the old yellow enzyme 1 from *Saccharomyces pastorianus* (OYE1) and the more stable double mutant C376L/M400I of cyclohexanone monooxygenase from *Acinetobacter* sp. (CHMO_{DM}).



Scheme 17: Model reaction for optimization of co-expression.

3.1.1 Cloning and Co-Expression of Three Enzymes for Application as *in vivo* Cascade

For further optimization of the established *in vivo* redox cascade (Figure 10) the co-expression of the three involved genes was established. Therefore, these were cloned by classical cloning, FastCloning or SLiCE into pETM6 onto one single plasmid in all theoretical arrangements: CLO, COL, LCO, LOC, OCL, OLC (C: CHMO_{DM}, L: LK-ADH, O: OYE1). Subsequently, the vectors were transformed into *E. coli* BL21 (DE3) $\Delta nemA$, which was created by Nikolin Oberleitner (Vienna Technical University, Austria) due to the fact that in previous experiments a concurring background reaction by this endogenous OYE was observed.

To analyze the expression levels the cells were cultivated at 25°C, because at this temperature all of the single enzymes showed reasonable expression. To ensure a high ratio of soluble to insoluble protein the induced culture was harvested after 8 h. At this time point also samples normalized to OD (7/OD) for SDS-PAGE analysis were collected.

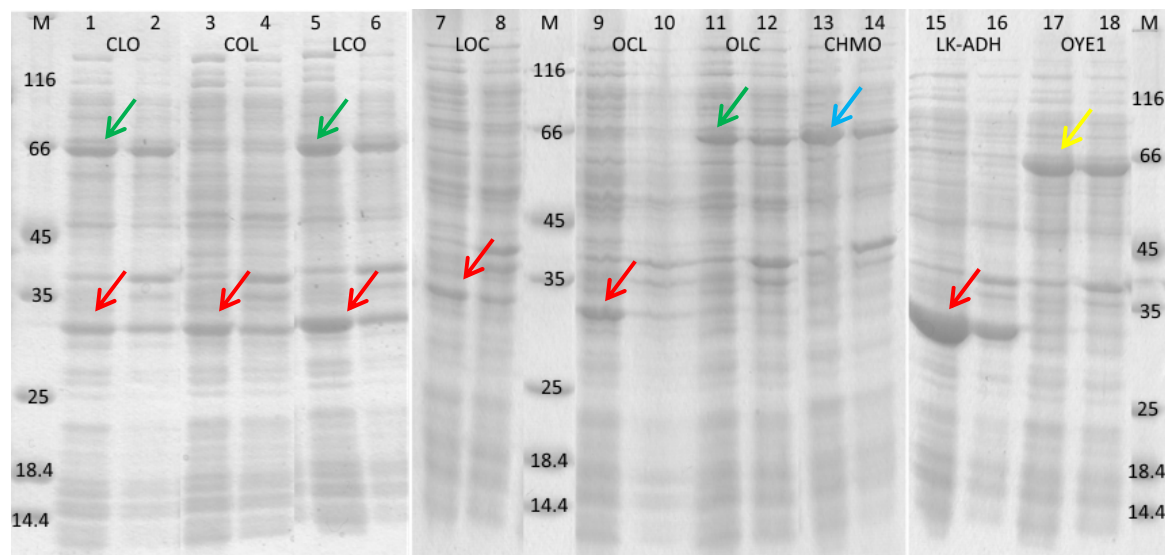


Figure 21: Electrophoregram of 7/OD-samples from co- and single expression of LK-ADH, OYE1 and CHMO (odd lanes: soluble protein fraction, even lanes: insoluble protein fraction, blue arrow: CHMO_{DM}, red arrow: LK-ADH; yellow arrow: OYE1, green arrow: CHMO_{DM}/OYE1, M: protein marker in kDa).

As shown in Figure 21 all three enzymes could be co-expressed successfully when using the combinations CLO and LCO. These two constructs showed reasonable amounts of soluble protein at the calculated sizes for LK-ADH (27 kDa, red arrow) as well as for CHMO (62 kDa, green arrow) and OYE1 (72 kDa, green arrow), which showed the same behavior in SDS-PAGE analysis (lanes 13-14 and 17-18). This observation was due to the fact, that OYE1 was expressed as GST-tagged protein to enhance the solubility and this tag was described to be usually degraded when analyzed by SDS-PAGE,^[188] so that it was not possible to distinguish between these two enzymes. For these two combinations the highest activity was expected. The combinations COL, LOC and OCL showed only soluble expression for the LK-ADH, whereas for OLC only bands for the CHMO and/or OYE1 were observed. When combining XenB with LK-ADH and CHMO for co-expression in the same way, the OYE was expressed as insoluble protein only (data not shown). This approach was not further investigated.

3.1.2 Application of Co-Expressed Enzymes as *in vivo* Cascade

The activity of the co-expressed enzymes in the described cascade (Scheme 17) was determined by cultivating the cells at 25°C for 8 h and subsequently using these as resting cells for biocatalysis with 20 mmol · L⁻¹ **1** as substrate. For comparison, each enzyme was singly expressed in a separate host and used for reaction by mixing in a ratio of 1:1:1. All reactions were done in triplicates and analyzed after 2 h by GC for product formation.

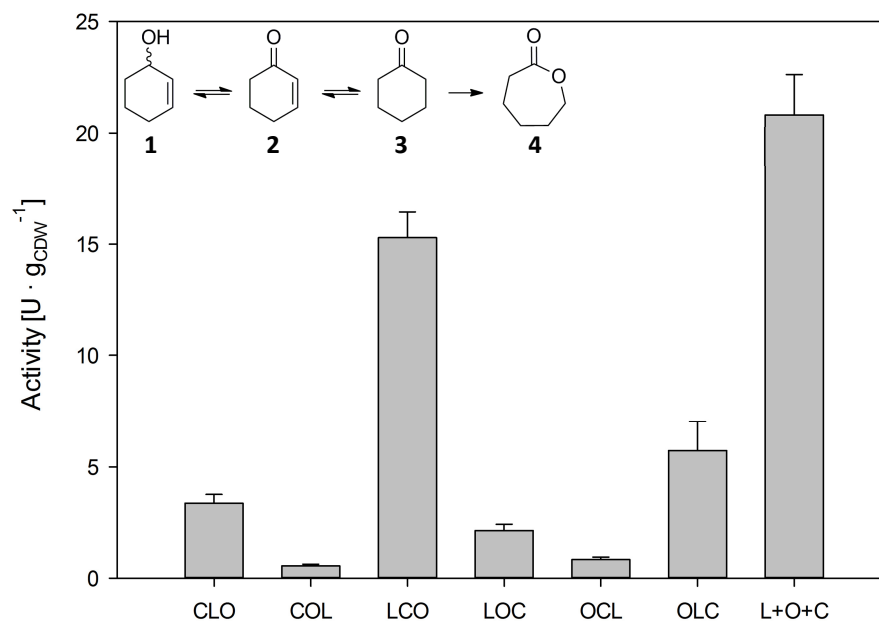


Figure 22: Initial activities of co-expressed enzymes used in a cascade reaction utilizing 20 mM **1** for the production of **4** (CLO - OLC: constructs for co-expression with various arrangements, L+O+C: cells harboring each single enzyme mixed 1:1:1; n=3).

As expected the combination LCO showed the highest initial activity of $15.3 \pm 1.2 \text{ U} \cdot \text{g}_{\text{CDW}}^{-1}$ in comparison to the other ones. In contrast, for CLO only a low initial activity of $3.4 \pm 0.4 \text{ U} \cdot \text{g}_{\text{CDW}}^{-1}$ was observed. Rather unexpected OLC showed a relatively high initial activity of $5.7 \pm 1.3 \text{ U} \cdot \text{g}_{\text{CDW}}^{-1}$. Unfortunately, when comparing the activity of the co-expressed cascade with the one of the singly expressed enzymes, these showed the highest initial activity of $20.8 \pm 1.8 \text{ U} \cdot \text{g}_{\text{CDW}}^{-1}$.

For detailed investigation of the reaction the concentrations of substrate, intermediates and (side-)products was analyzed by GC after 24 h.

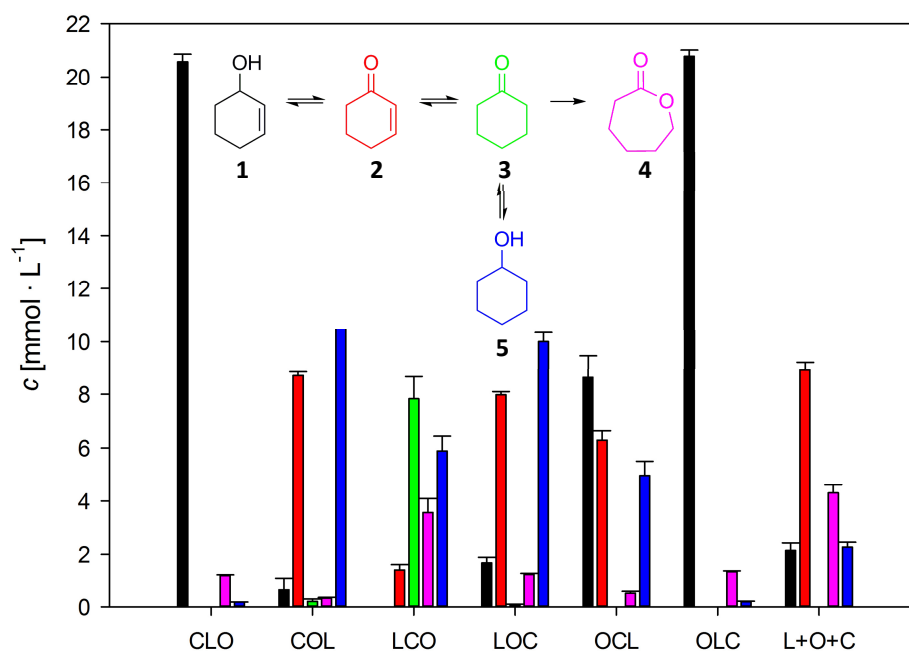


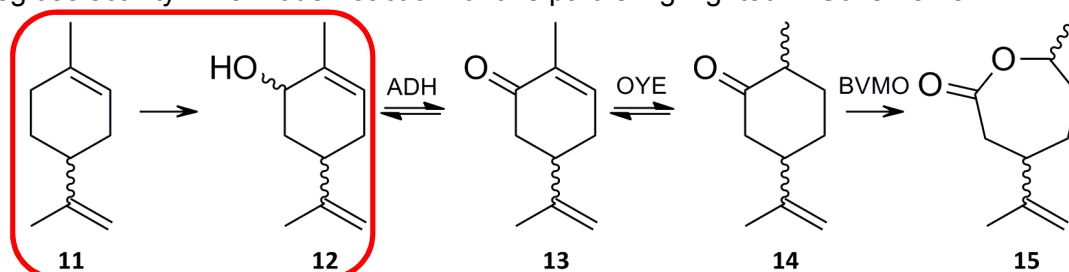
Figure 23: Concentrations of substrate, intermediates and (side-)product after 24 h (initial concentration of **1**: 20 mM; CLO - OLC: constructs for co-expression with various arrangements, L+O+C: cells harboring each single enzyme mixed 1:1:1; black: 2-cyclohexenol; red: 2-cyclohexenone; green: cyclohexanone; purple: ϵ -caprolactone; blue: cyclohexanol; $n=3$).

The distribution of all substances shown in Figure 23 gives a detailed view into the limiting steps for the co-expressed cascade reaction. As expected for the OLC-construct, which showed no expression of LK-ADH (Figure 21), substrate **1** was not consumed during 24 h, although approx. $1 \text{ mmol} \cdot \text{L}^{-1}$ **4** was formed. The CLO-construct showed unexpectedly the same behavior. In contrast, in reactions with the COL-, LCO- and LOC-constructs the substrate was almost completely consumed. For COL and LOC only up to $1 \text{ mmol} \cdot \text{L}^{-1}$ **4** was found. Additionally up to $11 \text{ mmol} \cdot \text{L}^{-1}$ **5** and up to $9 \text{ mmol} \cdot \text{L}^{-1}$ **2** were detected. Obviously the low expression of the CHMO led to this result (Figure 21), so that the ADH also used **3** as substrate to form the side-product **5**. Among the co-expressed approaches the LCO-construct showed the highest amount of **4**. But in this case, there were $8 \text{ mmol} \cdot \text{L}^{-1}$ **3** left and also $6 \text{ mmol} \cdot \text{L}^{-1}$ **5** were formed. Here, the stability of the CHMO still could be the limiting factor. The cells harboring the OCL-construct showed similar behavior as COL and LOC, except that after 24 h still $9 \text{ mmol} \cdot \text{L}^{-1}$ **1** was found. Using the mixed approach (L+O+C) $4 \text{ mmol} \cdot \text{L}^{-1}$ **4** and in addition $9 \text{ mmol} \cdot \text{L}^{-1}$ **2** were detected. For all reactions, in which significant amounts of **2** were found, the OYE could be either inhibited by substrate and/or product or the expression of this enzyme was too low.

In summary, the co-expression of all three enzymes for a cascade reaction in a single host was successfully realized by construction of a single plasmid. Unfortunately, the co-expression led to no further improvement of the reaction itself, because in the mixed cell approach the same amounts of **4** were produced after 24 h. For further cascade optimization alternative ways have to be investigated.

3.2 Extension of a Three-Enzyme Redox Cascade

The second part of this thesis deals with the extension of a described cascade reaction (Figure 10) by introduction of an initial hydroxylation step to enable the use of limonene **11** as renewable chiral precursor. Therefore, different enzymes should be tested with respect to their applicability for the cascade reaction in terms of activity and regioselectivity. The model reaction for this part is highlighted in Scheme 18.



Scheme 18: Cascade reaction for the production of chiral lactones using limonene as renewable chiral precursor (red box: model reaction used in search for an applicable enzyme).

3.2.1 Application of Cytochrome P450-Monooxygenases for Initial Hydroxylation

3.2.1.1 Expression and Characterization of Product Distribution of P450-BM3 and a Homologous Enzyme

The first possibility for extension of the described three-enzyme cascade^[112] (Figure 10) was the use of a cytochrome P450-monooxygenase (P450) for the initial hydroxylation. Therefore, the most prominent representative of this enzyme class (P450-BM3) and one homologous enzyme from *Bacillus licheniformis* (CYP102A7) were investigated with respect to the desired reaction.

For expression of P450-BM3 an established protocol already available in the group was used, so that no further optimization for this enzyme was needed. In contrast, for CYP102A7 an expression optimization was necessary, because a described method from literature^[189] was not sufficient for the use of this enzyme in an *in vivo* cascade. Therefore, a first trial for the optimal expression parameters was carried out with respect to expression temperature (17/30°C), expression host (*E. coli* TOP10, BL21, C41, C43, SHuffle) and expression vector (pET28_CYP102A7_N-his/pBAD_CYP102A7_N-his). After first problems with expression of CYP102A7 it turned out, that using conical flasks at slow shaking (135 rpm) and addition of δ -aminolevulinic acid at induction were crucial for proper expression. Induction was carried out at OD 1.0 - 1.2 and the cultivation was continued for 24 h (30°C) or 48 h (17°C).

In general CYP102A7 showed higher soluble expression at 30°C in comparison to 17°C. As detected by SDS-PAGE the highest soluble expression was reached using the pET28 construct in *E. coli* C43 at 30°C (Figure 24, lanes 7 - 8). In contrast to the reported method in literature, using the pET28 construct in *E. coli* BL21 led to nearly no expression. Interestingly using *E. coli* TOP10, which cannot use the T7 promoter, showed relatively high expressions with the pET28_CYP102A7_N-his construct. Furthermore, high expressions were already visible by eye in the bacteria culture,

which showed, if high amounts of active P450 were produced, a dark blue color (Figure 24, inset).

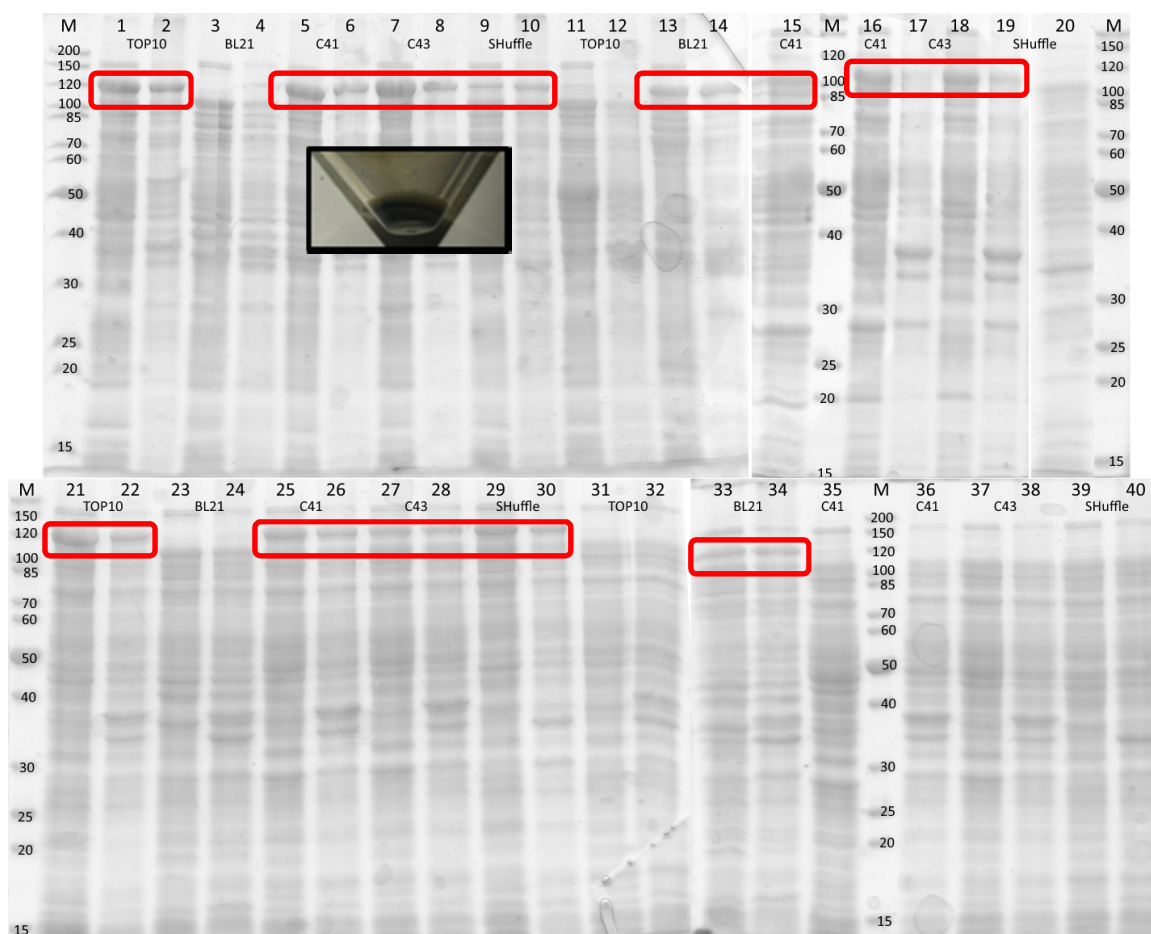


Figure 24: Electrophoregram of 7/OD-samples from the first expression trials for CYP102A7 (odd lanes: soluble protein fraction, even lanes: insoluble protein fraction, lanes 1 - 20: expression at 30°C, lanes 21 - 40: expression at 17°C, lanes 1 - 10/21 - 30: expression vector pET28, lanes 11 - 20/31 - 40: expression vector pBAD, red box: overexpression of CYP102A7, M: protein marker in kDa; inset: harvested cells with active CYP102A7).

After SDS-PAGE analysis the samples from the first expression trial were analyzed by CO-difference spectra to measure the concentration of correctly folded P450. As shown in Table 7 the measured P450 concentrations were in good agreement with the observations from SDS-PAGE. The highest amount of P450 ($4.3 \mu\text{mol} \cdot \text{L}^{-1}$) was found for the *E. coli* C43 using the pET28 construct and expression at 30°C. Also the C41 strain under the same conditions ($4.1 \mu\text{mol} \cdot \text{L}^{-1}$) and the TOP10 at 17°C ($3.58 \mu\text{mol} \cdot \text{L}^{-1}$) showed high contents of the desired enzyme.

Table 7: P450 content from first expression trial measured by CO-difference spectra.

Temperature	Construct	Strain	P450 [$\mu\text{g} \cdot \text{mL}^{-1}$]	P450 [$\mu\text{mol} \cdot \text{L}^{-1}$]
30° C	pET28_CYP102A7_N-his	TOP10	237	1.96
		BL21	0	0
		C41	496	4.1
		C43	520	4.3
		SHuffle	58	0.48
	pBAD_CYP102A7_N-his	TOP10	11	0.09
		BL21	149	1.23
		C41	0	0
		C43	0	0
		SHuffle	1	0.01
	pET28_CYP102A7_N-his	TOP10	433	3.58
		BL21	0	0
		C41	315	2.6
		C43	134	1.11
		SHuffle	101	0.84
17° C	pBAD_CYP102A7_N-his	TOP10	0	0
		BL21	137	1.13
		C41	0	0
		C43	0	0
		SHuffle	0	0
	pET28_CYP102A7_N-his	TOP10	0	0
		BL21	137	1.13
		C41	0	0

For validation of the previous results and to further extend the expression parameters a second trial was conducted. Therefore, the best result from the first round (30°C, *E. coli* C43, pET28_CYP102A7_N-his) was reproduced and the gene was cloned into two additional expression vectors. These new constructs carried in contrast to the pET28 the codon optimized CYP102A7 gene with a C-terminal (pET22_CYP102A7opti_C-his) or without a His-tag (pET22_CYP102A7opti_no-his). Both constructs were transformed into *E. coli* TOP10, BL21, C41 and C43 as most promising hosts. The SHuffle strain was not used, because for this one only low expressions were found in the first trial. An expression temperature of 30°C was chosen.

Again using strains C41 and C43, the highest soluble expression was observed as documented by SDS-PAGE analysis (Figure 25). As expected, no expression was observed using the TOP10 strain, *E. coli* BL21 showed significant lower expression than C41 and C43. There was no difference observed by SDS-PAGE when comparing the different constructs in the same strain (*E. coli* C43), except that using the two pET22 constructs led to more insoluble protein compared to the pET28 one.

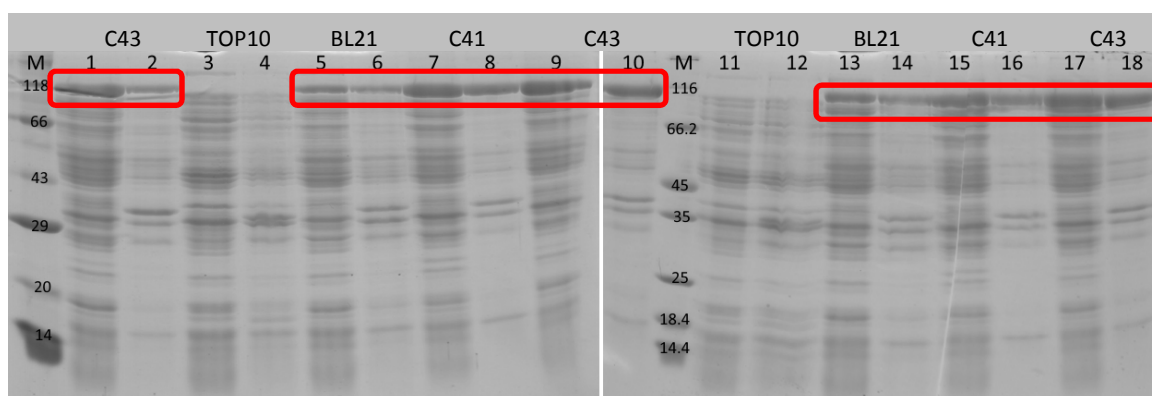


Figure 25: Electrophoregram of 7/OD-samples from the second expression trial for CYP102A7 (odd lanes: soluble protein fraction, even lanes: insoluble protein fraction, lanes 1 - 2: *E. coli* C43 with pET28_CYP102A7_N-his, lanes 3 - 10: pET22_CYP102A7opti_C-his, lanes 11 - 18: pET22_CYP102A7opti_no-his, red box: overexpression of CYP102A7, M: protein marker in kDa).

The samples from the second expression trial were analyzed for activity and the concentration of correctly folded P450. Although the high amount of P450 from the first expression trial using the pET28 construct in *E. coli* C43 could not be reproduced, an activity of $957.6 \text{ U} \cdot \text{g}_{\text{P450}}^{-1}$ was calculated (Table 8). The C-terminal tagged enzyme showed the highest activity in *E. coli* C41 ($1080.6 \text{ U} \cdot \text{g}_{\text{P450}}^{-1}$). Surprisingly, the untagged enzyme showed significantly lower activities of $290.8 \text{ U} \cdot \text{g}_{\text{P450}}^{-1}$ for C41 and $592.5 \text{ U} \cdot \text{g}_{\text{P450}}^{-1}$ for C43 as expression host. Although in the BL21 strains up to $1.21 \mu\text{mol} \cdot \text{L}^{-1}$ P450 was detected by CO-difference analysis, no activities were determined. As expected the enzyme expressed in TOP10 showed no activity.

Table 8: P450 content measured by CO-difference spectrum and activity against 4 mM limonene from second expression trial (activity measured with NADPH depletion assay).

Construct	Strain	P450 [$\mu\text{g} \cdot \text{mL}^{-1}$]	P450 [$\mu\text{mol} \cdot \text{L}^{-1}$]	Activity [$\text{U} \cdot \text{g}_{\text{P450}}^{-1}$]
pET28_CYP102A7_N-his	C43	58	0.48	957.6
pET22_CYP102A7opti_C-his	TOP10	0	0	n.d.
	BL21	113	0.93	n.d.
	C41	362	2.99	1080.6
	C43	200	1.66	659.5
pET22_CYP102A7opti_no-his	TOP10	0	0	n.d.
	BL21	146	1.21	n.d.
	C41	557	4.6	290.8
	C43	241	1.99	592.5

n.d. – not determinable

After optimization of expression both enzymes, CYP102A7 and P450-BM3, were used for biocatalysis reactions either as crude cell extracts (CCE) or as resting cells. Therefore, the cells were cultivated as described in 50 mL scale and harvested after 8 h. After resuspending the cells in 5 mL KPi buffer (50 mM, pH 7.5), 1 mL of this was added to 9 mL of reaction solution containing $3 \text{ mmol} \cdot \text{L}^{-1}$ NADPH and $3 \text{ mmol} \cdot \text{L}^{-1}$ *rac*-limonene and incubated at 30°C at 120 rpm. The reactions were analyzed by GC after 2 h.

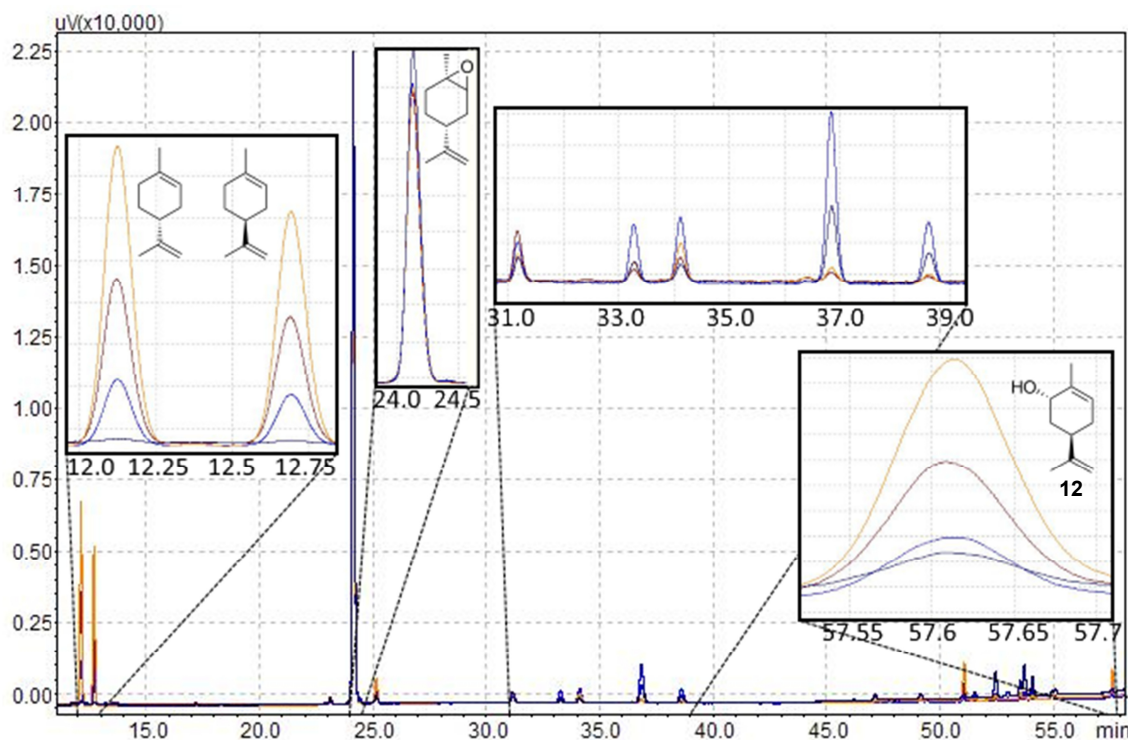


Figure 26: GC-Chromatogram of biocatalysis reactions using P450-BM3 or CYP102A7 after 2 h (orange line: CYP102A7 concentrated CCE, dark red line: CYP102A7 resting cells, blue line: P450-BM3 resting cells, black line: P450-BM3 purified CCE).

The GC analysis of the P450 catalyzed reactions revealed that the desired product **12** was produced in low amounts. Additionally both enzymes showed only low regioselectivity, because several unidentified side-products were detected. These probably correspond to other possible oxidation products like dihydrocarvone, carvone, isopiperitenol, perillyl alcohol or limonene-8,9-oxide (Figure 62). Nevertheless, the main product of all reactions was (+)-*cis*-limonene-1,2-oxide (Figure 26). In summary, due to the low regioselectivity of these P450s alternative enzymes had to be investigated for the application in cascade reactions.

3.2.1.2 Homology Model of Limonene-6-hydroxylase from *Mentha spicata*

Due to the fact, that the P450s investigated so far showed only bad regioselectivity, the natural enzyme for (–)-*trans*-carveol production from *Mentha spicata* (limonene-6-hydroxylase, L6H; CYP71D18) was studied.^[174b] First of all, homology models were prepared to compare the distal heme environment and the substrate tunnel of L6H to the one of CYP102A7 to finally provide a basis for protein engineering. Therefore, the homology modeling function of YASARA was used with ten different templates and five different alignments for each template. After preparation of 50 models, the software combined the best results in a hybrid model. This hybrid model was then subject to refinement using the YASARA macro `md_refine` with the standard parameters. Finally, the refined model with the lowest calculated energy was analyzed by MolProbity^[190] to estimate the quality.

The results from this analysis for the model of L6H showed that the prepared model in general was of good quality (Table 9). Although some mediocre rotamers and Ramachandran values as well as some bad bonds, bad angles and one twisted

peptide were found, the overall scores were of good quality. So that in summary the prepared model (Figure 27) could be used for further investigations.

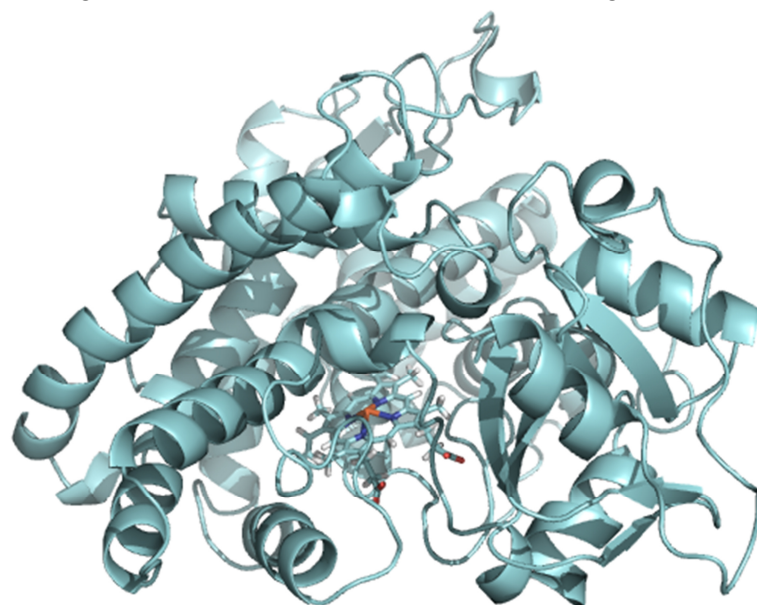


Figure 27: Homology model of L6H from *Mentha spicata* (heme shown as sticks; model prepared with YASARA based on pdb structures: 1PO5, 2HI4, 2PG5, 3CZH, 3MDM; picture prepared with PyMol).

The same procedure was carried out for the preparation of a CYP102A7 model. For this model the MolProbity^[190] analysis gave even better results (Table 10). Here, the rotamers and Ramachandran values had the same quality as for the L6H model, but the only poor parameters found were eight bad bonds. This result was rather unexpected, because the linker peptide between the heme domain and the cytochrome P450 reductase (CPR) domain for this enzyme class was not crystallized yet and high flexibility was assumed for this part of the polypeptide chain. Nevertheless, also this model (Figure 28) could be used for further investigations.

Table 9: MolProbity^[190] analysis output summary for L6H homology model.

All-Atom Contacts	Clashscore, all atoms:	0.38	100 th percentile* (N=355, 2.30Å ± 0.25Å)	
	Clashscore is the number of serious steric overlaps (> 0.4 Å) per 1000 atoms.			
Protein Geometry	Poor rotamers	3	0.71%	Goal: <0.3%
	Favored rotamers	403	95.50%	Goal: >98%
	Ramachandran outliers	2	0.42%	Goal: <0.05%
	Ramachandran favored	463	96.66%	Goal: >98%
	MolProbity score^	0.85	100 th percentile* (N=8909, 2.30Å ± 0.25Å)	
	Cβ deviations >0.25Å	0	0.00%	Goal: 0
	Bad bonds:	5 / 3989	0.13%	Goal: 0%
	Bad angles:	7 / 5414	0.13%	Goal: <0.1%
Peptide Omegas	Cis Prolines:	1 / 30	3.33%	Expected: ≤1 per chain, or ≤5%
	Twisted Peptides:	1 / 480	0.21%	Goal: 0

In the highlighted column results, the left column gives the raw count, right column gives the percentage.

* 100th percentile is the best among structures of comparable resolution; 0th percentile is the worst. For clashscore the comparative set of structures was selected in 2004, for MolProbity score in 2006.

[^] MolProbity score combines the clashscore, rotamer, and Ramachandran evaluations into a single score, normalized to be on the same scale as X-ray resolution.

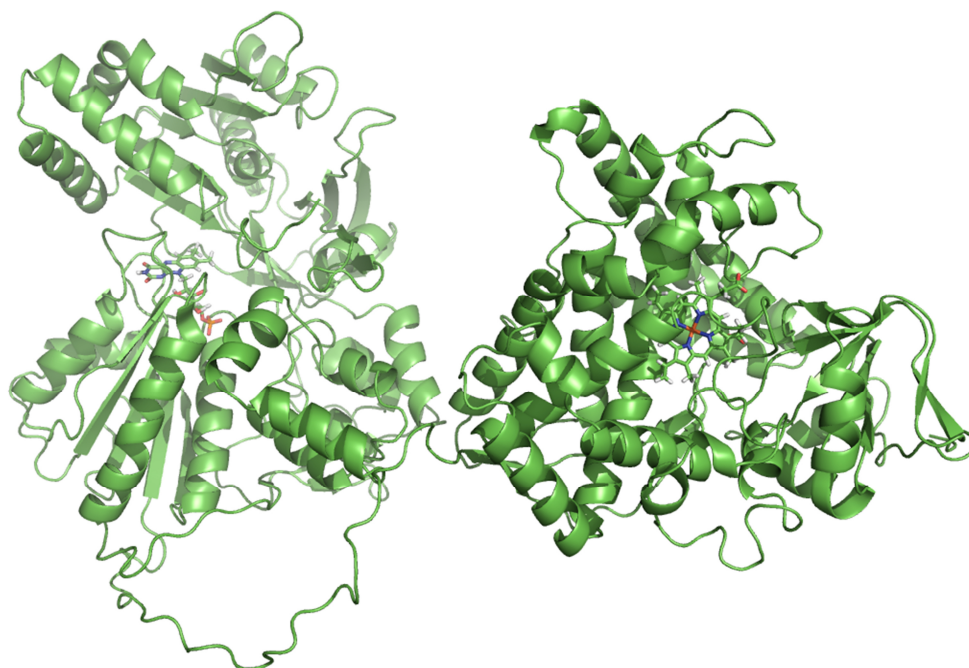


Figure 28: Homology model of CYP102A7 from *Bacillus licheniformis* (foreground in dark green: heme domain, background in light green: CPR domain; heme/FMN shown as sticks; model prepared with YASARA based on pdb structures: 1JA1, 1ZO9, 2IJ2, 3NPL, 4DQL; picture prepared with PyMol).

After preparation of the models these were subject for sequence and structure alignments. Because L6H did not contain its CPR as natural fusion enzyme, only the heme domain of CYP102A7 (the first 497 amino acids) was used for alignment. The software calculated an identity of 20.8%. As Figure 30 shows both enzymes had very few conserved residues, which belong mainly to structurally important loops or the heme coordinating residues, like the proximal cysteine ligand. More interesting were the non-aligning regions (loop A and C). Additionally, structure alignment revealed another loop (loop B), which showed improper superposition (Figure 29 and Figure 31).

Table 10: MolProbity^[190] analysis output summary for CYP102A7 homology model.

Table 16: MolProbity analysis output summary for 6H1VZ17 homology model.				
All-Atom Contacts	Clashscore, all atoms:	0.12		100 th percentile* (N=677, 2.03Å ± 0.25Å)
	Clashscore is the number of serious steric overlaps (> 0.4 Å) per 1000 atoms.			
Protein Geometry	Poor rotamers	13	1.43%	Goal: <0.3%
	Favored rotamers	867	95.59%	Goal: >98%
	Ramachandran outliers	4	0.38%	Goal: <0.05%
	Ramachandran favored	1032	96.81%	Goal: >98%
	MolProbity score^	0.86		100 th percentile* (N=12152, 2.03Å ± 0.25Å)
	Cβ deviations >0.25Å	0	0.00%	Goal: 0
	Bad bonds:	8 / 8720	0.09%	Goal: 0%
	Bad angles:	11 / 11815	0.09%	Goal: <0.1%
Peptide Omegas	Cis Prolines:	1 / 63	1.59%	Expected: ≤1 per chain, or ≤5%

In the highlighted column results, the left column gives the raw count, right column gives the percentage.
 * 100th percentile is the best among structures of comparable resolution; 0th percentile is the worst. For clashscore the comparative set of structures was selected in 2004, for MolProbity score in 2006.

[^] MolProbity score combines the clashscore, rotamer, and Ramachandran evaluations into a single score, normalized to be on the same scale as X-ray resolution.

By having a closer look on the conserved FXGXG motif of loop A (Figure 30 and Figure 31-A) it seemed that these amino acid residues might have been conserved, although they structurally had not aligned at all. In L6H this motif belonged to the N-terminal part of the α -helix and in CYP102A7 to the C-terminal part.

The same drastic gap between sequence and structure alignment was found for loop C (Figure 30 and Figure 31-C). In L6H the conserved motif MTXXPG belongs to a C-terminal unordered loop of the enzyme, whereas this loop in CYP102A7 was built by completely different amino acid residues even forming two β -strands. Furthermore, the motif was modeled into the connecting linker sequence between heme and CPR domain.

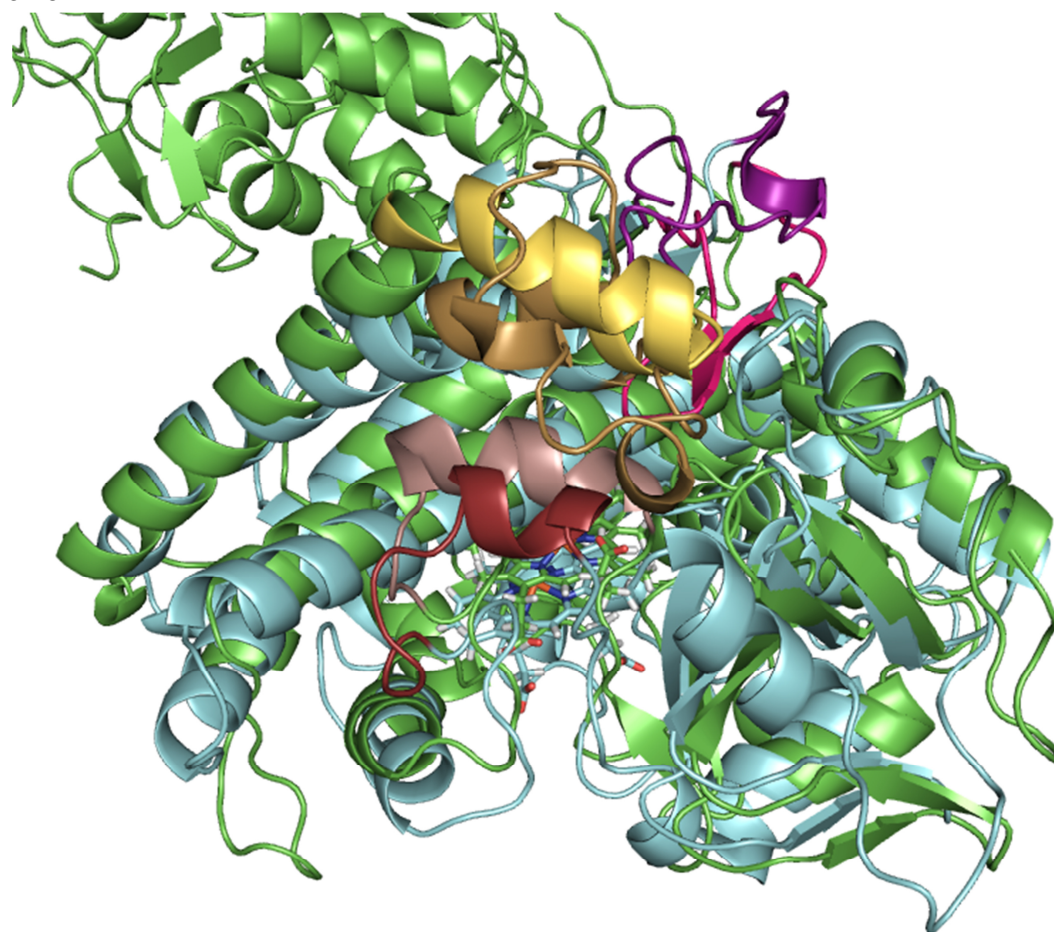


Figure 29: Alignment of the homology models of L6H and CYP102A7 (cyan/darker colored loops: L6H, green/lighter colored loops: CYP102A7, red: loop A, yellow: loop B, magenta: loop C; heme shown as sticks; models prepared with YASARA; alignment and picture prepared with PyMol).

Finally, structure alignment revealed improper superposition of loop B, but the sequence alignment for this region showed a high agreement (Figure 30 and Figure 31). Here for the CYP102A7 a bent α -helix followed by a turn and another α -helix was modeled. In contrast for L6H an unbent α -helix followed by an unstructured longer loop and another α -helix was introduced. Having a closer look into the conserved amino acid residues revealed that here the sequence and structure alignment had not shown the drastic disagreements as observed before.

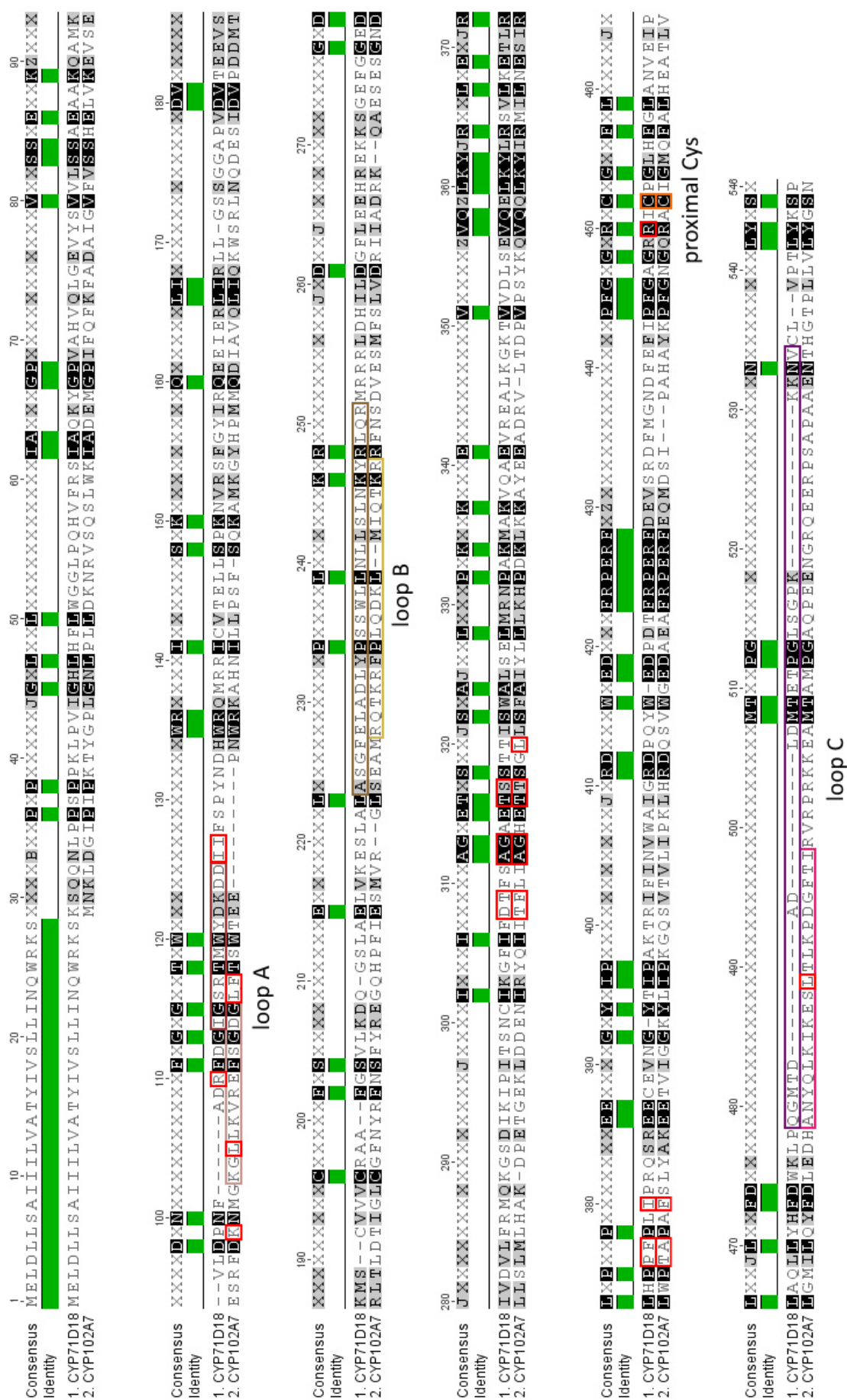


Figure 30: Sequence alignment of L6H (CYP71D18) and heme domain of CYP102A7 (red boxes: distal heme environment; picture prepared with Geneious).

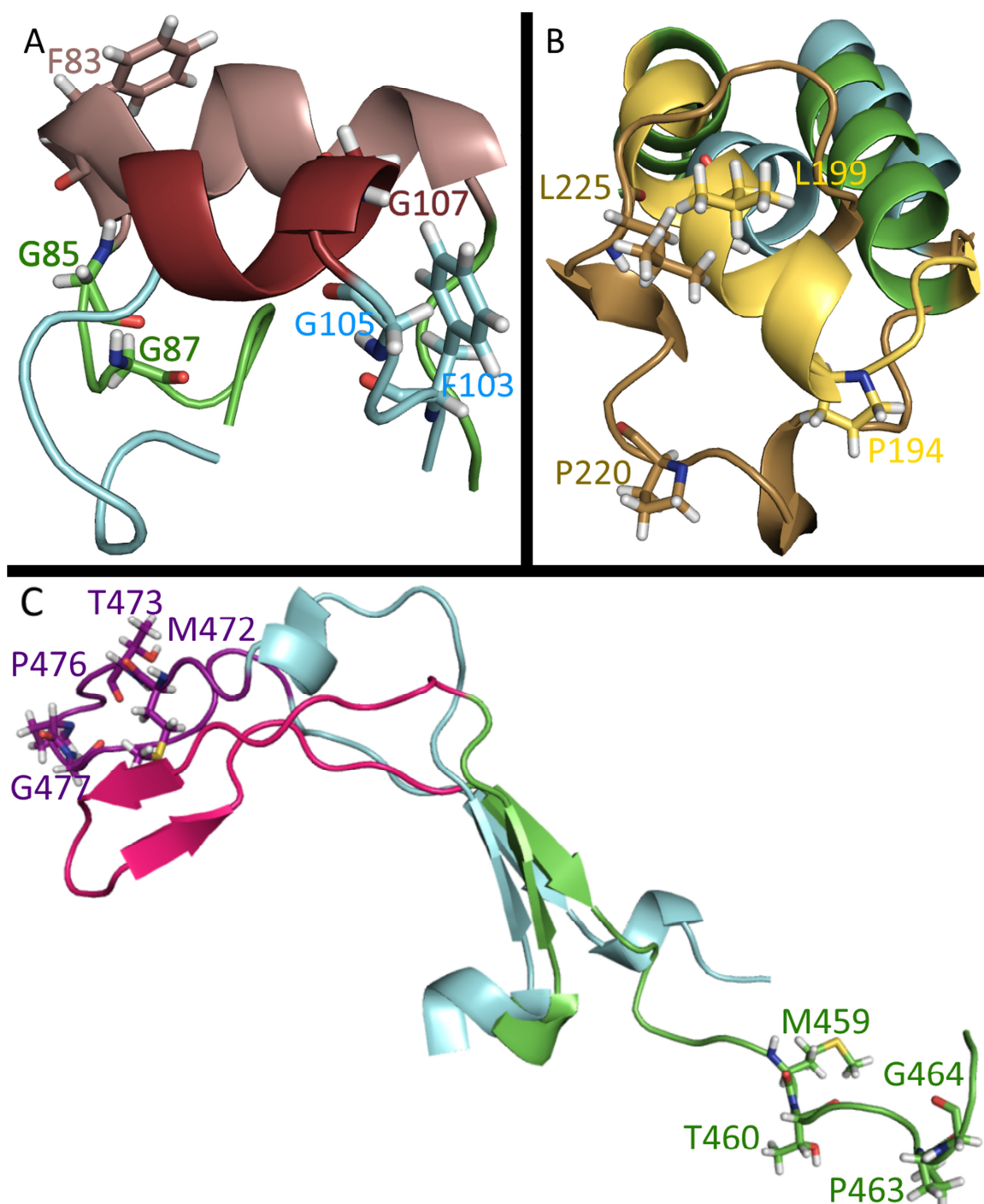


Figure 31: Detailed view of the non-aligned loops from L6H and CYP102A7 (A: loop A from sequence alignment, B: loop B from sequence alignment, C: loop C from sequence alignment; conserved residues from the sequence alignment shown as sticks; dark colors/cyan: L6H, light colors/green: CYP102A7; picture prepared with PyMol).

Next to comparison of the alignments the amino acid residues forming the distal heme environment were analyzed (Figure 30, red boxes). First of all, the heme co-factors in the two models showed a different binding mode (Figure 32). The propionate groups of the heme in L6H both showed a proximal orientation, whereas in CYP102A7 one of these was in proximal, the other one in distal orientation, as already observed in crystal structures of P450-BM3. So that in summary, at least on that side of the heme a different environment was expected. By having a closer look at the amino acid

residues of the distal heme environment, only four of these were conserved in both enzymes: AGXXT(S/T). A detailed analysis of these residues revealed that these were part of the highly conserved, long α -helix typically found in the distal heme environment of P450s. The other residues identified to be involved in formation of the distal heme environment were mainly part of loop A. So that, this loop would be an interesting region for mutagenesis studies with the aim to improve regioselectivity in CYP102A7. But also loop C might be interesting for this purpose, because there was one residue found in CYP102A7 to be involved in distal heme environment formation. Furthermore, there were five additional positions, which were different and might be of interest for protein engineering.

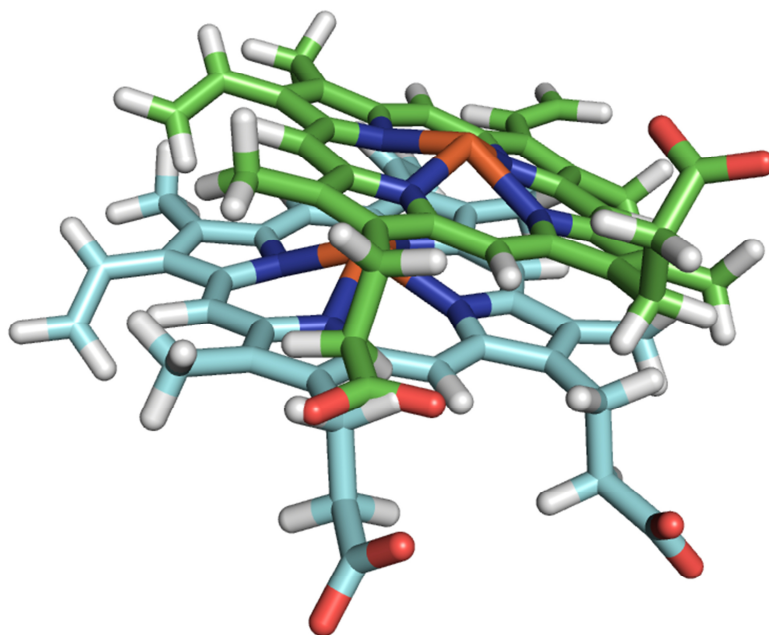


Figure 32: Close view on the modeled hemes from L6H (cyan) and CYP102A7 (green; picture prepared with PyMol).

Several studies showed that the substrate tunnel in P450s has an important role also for activity.^[191] That was why these tunnels were also computed using the PyMol plugin Caver 3.0^[192] for comparison. For CYP102A7 eight tunnels were computed, which lead a way from the heme center to the surface of the protein. Three of these were omitted, because these were tunnels leading to the surface from the proximal site of the heme. Superposition of the five distal tunnels revealed that there were three main tunnels leading from the heme center to the surface (Figure 33A).

The same procedure was carried out for L6H. Again eight tunnels were computed by the plugin, out of which three were omitted because these were proximal tunnels. Superposing the left five tunnels showed that there were also three main distal tunnels leading to the protein surface (Figure 33B).

For comparison of the substrate tunnels, these were overlaid in the structure-aligned models (Figure 33C). The direct comparison of both 'tunnel-systems' clearly showed that the substrate had completely different possibilities of getting to the active site. Having a closer look led on the one hand to the conclusion that the substrate tunnels of L6H would be blocked in CYP102A7 by the loops A and C (Figure 29). On the other hand the tunnels of CYP102A7 would be blocked in L6H by loop B and an additional opposing loop. In summary, the substrate tunnels of the analyzed homology models

were completely different, which even more raised the interest of mutating the described loops.

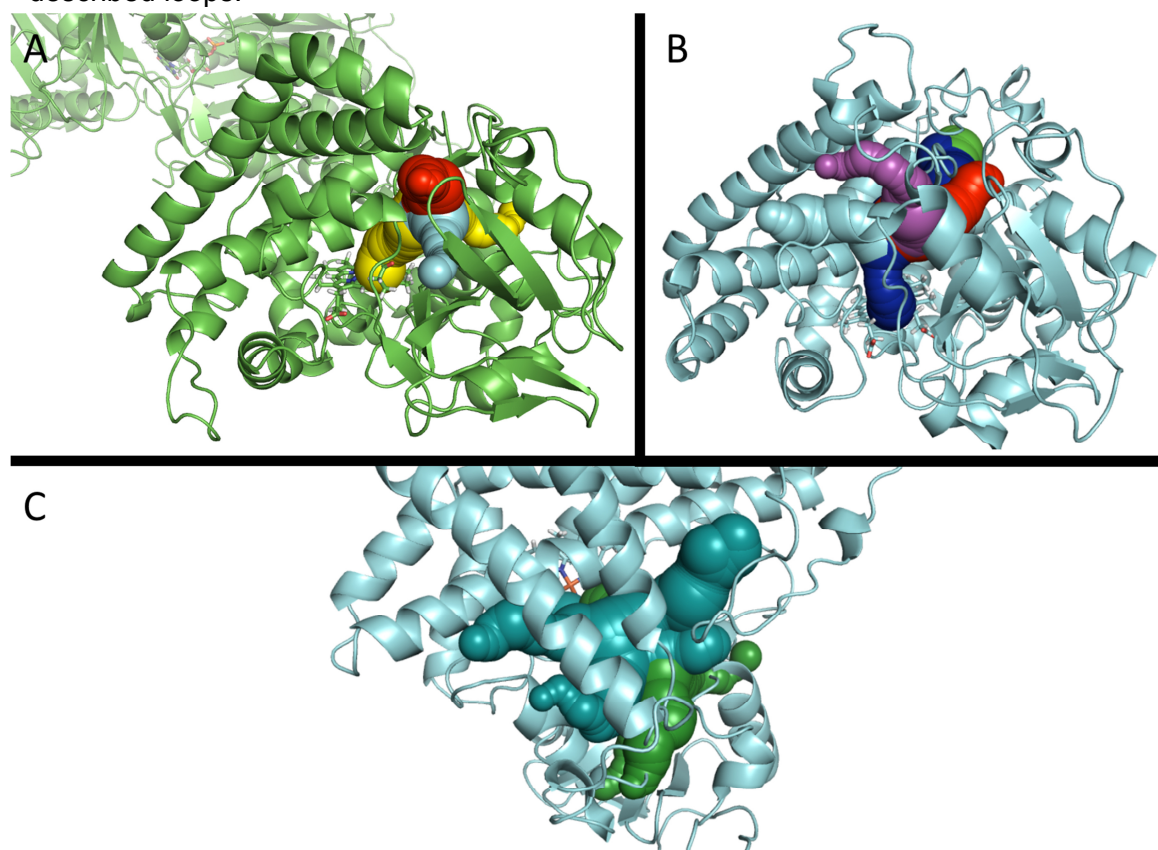


Figure 33: Computed substrate tunnels for CYP102A7 (A), L6H (B) and overlay of these viewed from distal heme site in the model of L6H (models prepared with YASARA; tunnels calculated with CAVER 3.0^[192]; pictures prepared with PyMol).

3.2.1.3 Expression of Limonene-6-hydroxylase from *Mentha spicata*

For studies of the regioselectivity of L6H establishment of expression of this enzyme was necessary. Therefore, the codon-optimized gene was purchased readily cloned into pET22 and transformed into *E. coli* BL21 (DE3). The expression was carried out according to the standard cultivation protocol. Due to the fact that L6H has been described as a membrane-bound enzyme mainly insoluble expression was expected. As shown in Figure 34 already after 2 h there was expression of a protein in the insoluble fraction at approx. 55 kDa (calculated MW: 56.2 kDa). The intensity of this band increased over the 24 h of expression.

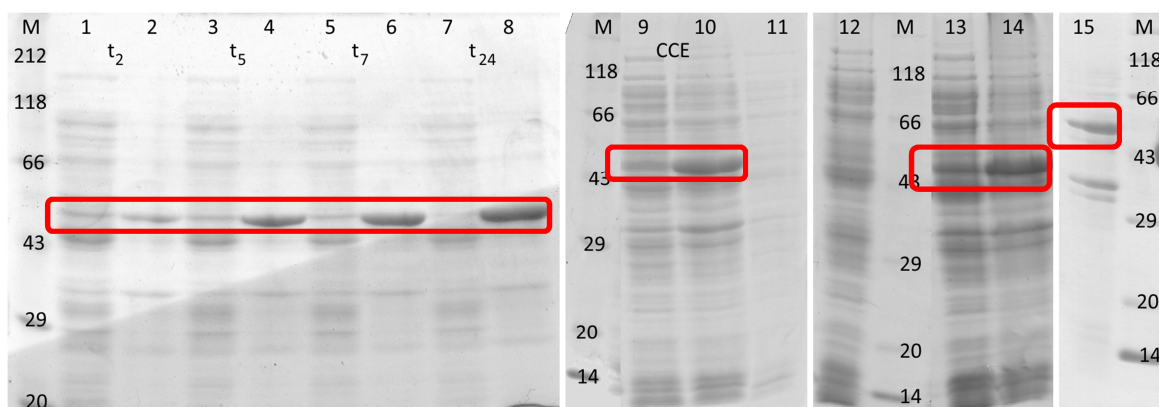


Figure 34: Electrophoregram of L6H expression and membrane purification (red boxes indicate overexpressed protein, lanes 1-10: odd lanes: soluble fraction, even lanes: insoluble fraction; lanes 9-10: crude cell extract (CCE) used for membrane preparation; lane 11: cells before lysozyme treatment, lane 12: supernatant after membrane sedimentation, lane 13: supernatant after lysozyme treatment, lane 14: pelleted spheroblasts, lane 15: resuspended membrane preparation, M: protein marker in kDa).

The membrane fraction of the cells was prepared to proof that the insoluble protein fraction was membrane-bound and not just inclusion bodies. Therefore, a protocol from literature was modified, so that neither ultracentrifugation nor Potter Elvehjem homogenizer was needed.^[174a, 193] The different fractions of the membrane preparation showed that the observed band indeed was overexpressed and membrane-bound protein (Figure 34, lanes 9-15). In summary, expression of L6H was established without any further optimization. Further validation by CO-difference spectra and optimization of expression as well as verification of the expected activity were carried out by the visiting student Anna Kluza (Jagiellonian University, Kraków, Poland) during an ERASMUS+ traineeship. In her project she was able to express the L6H in a yield of approx. $4 \text{ mg}_{\text{P450}} \cdot \text{L}^{-1}$. Furthermore, for expression optimization the N-terminus of the enzyme was modified as described by Croteau and co-workers.^[174a] Unfortunately, this led to no further improvement of the yield of correctly folded P450. Also the introduction of chaperones did not improve expression, so that in the end both enzymes should be checked for activity. Therefore, the establishment of a proper reductase system was needed.

3.2.1.4 Identification of the Natural Redox System for Limonene-6-hydroxylase from *Mentha spicata*

Due to the fact that the natural redox system of L6H was unknown, the enzymes involved in the electron supply chain should be identified. Therefore, a cooperation with the group of Prof. Christine Stöhr (Institute of Botany, University of Greifswald) was set up. For the generation of plant material the green houses of the Institute of Botany were used. Young apical buds of *Mentha spicata* were collected during a period of five months and immediately snap-frozen in liquid nitrogen. These were used later for isolation of DNA and RNA. The gene encoding the CPR should be identified by gene walking. Therefore, three gene fragments annotated as *Mentha*-CPRs found in the TrichOME database were aligned to 38 sequences of known plant CPRs.^[234] Based on these alignments degenerated primers were designed, which turned out to

have too high degeneracy. So that based on another alignment using 114 sequences two primers were designed using the hyden software^[194].

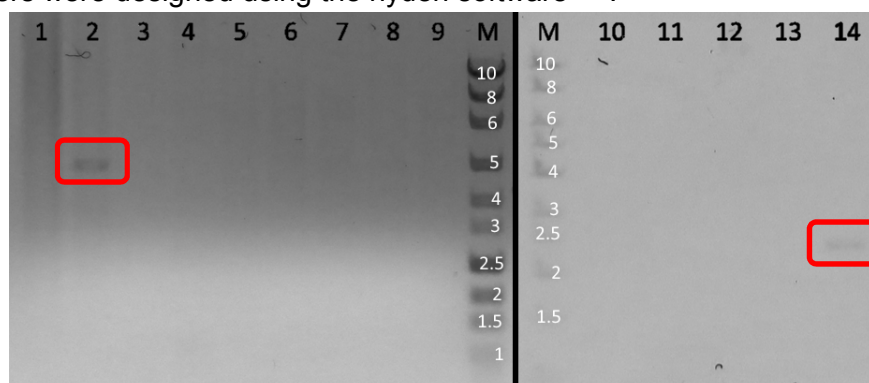


Figure 35: Electrophoregram of PCR samples for identification of *Mentha spicata* CPR (red boxes indicate specific PCR products, lanes 1-9: PCRs using 5'-primer 09048, lanes 10-14: PCRs using 3'-primer 09049, M: DNA marker in kbp).

For both primers one specific PCR product was detected by agarose electrophoresis (Figure 35). These were purified from the gel and cloned using the TOPO[®] TA Cloning[®] Kit (Thermo Fisher Scientific). Subsequently, the resulting vectors were sequenced. Here it turned out, that the 5 kbp product from the reaction with the 5'-primer was only partially inserted into the vector. Furthermore, blastn/blastx analysis of this short fragment revealed that probably a bacterial contamination was responsible for the PCR product. In contrast, for the 3'-primer a fragment of 2.4 kbp was found as insert in the vector, which resembled the PCR product for this primer (Figure 35). A blastn analysis of this fragment gave only two hits (Table 11), which covered only 1% of the queried sequence. But at least the results belonged to plant genes.

Although one potential hit was found for the PCR product with the 3'-primer, no further effort was put into the identification of the natural CPR from *Mentha spicata*, because the obtained results so far were not very promising. Furthermore, there was no information about potential intronic sequences for *Mentha* sp.

Table 11: Blastn hits for the PCR product with 3'-primer.

Description	Max score	Total score	Query cover	E value	Ident	Accession
<i>Triteleia hyacinthine</i> NADH-plastoquinone oxidoreductase subunit 3 (ndhC) gene, complete cds: chloroplast	63.9	63.9	1%	1e-05	91%	JQ276576.1
<i>Anemarrhena asphodeloides</i> NADH-plastoquinone oxidoreductase subunit 3 (ndhC) gene, complete cds: chloroplast	63.9	63.9	1%	1e-05	91%	JQ276531.1

Due to the fact that the natural redox system for L6H could not be identified, the visiting student Anna Kluza also studied the applicability of a foreign CPR from *Candida apicola* (CPR_{apicola}) to serve as a proper reductase. Unfortunately, in biocatalysis reactions using either the N-terminal modified or the wild-type L6H in combination with the CPR_{apicola} no activity could be detected. Finally also the studies

involving P450s were stopped at this point, because the use of an alternative hydroxylating enzyme seemed to be more promising.

3.2.2 Application of a Dioxygenase for Initial Hydroxylation

3.2.2.1 Cultivation of *Cellulosimicrobium cellulans* EB-8-4 and Identification of the Limonene-hydroxylating Enzyme

Due to the low regioselectivity of the P450s, which were tested for their applicability in cascade reactions, alternative enzymes were investigated. Amongst others there was one strain of *Cellulosimicrobium cellulans* described to produce highly regioselective (1*R*,5*S*)-carveol from limonene, when grown on ethyl benzene as sole carbon source.^[195] This specific strain was provided by Prof. Dr. Zhi Li (National University of Singapore, Singapore). To verify the described activity, the *C. cellulans* strain EB-8-4 was cultivated in M9 minimal medium either containing glucose and/or ethyl benzene as sole carbon source. The supplementation of the medium with ethyl benzene had to be carried out by vaporization of 1 mL from a 15 mL-tube, which was placed into the Erlenmeyer flask (Figure 37). Furthermore, this flask was sealed with a rubber stopper. If the medium was supplemented directly with 1 mL ethyl benzene, no growth was detected due to the toxicity of the substance.

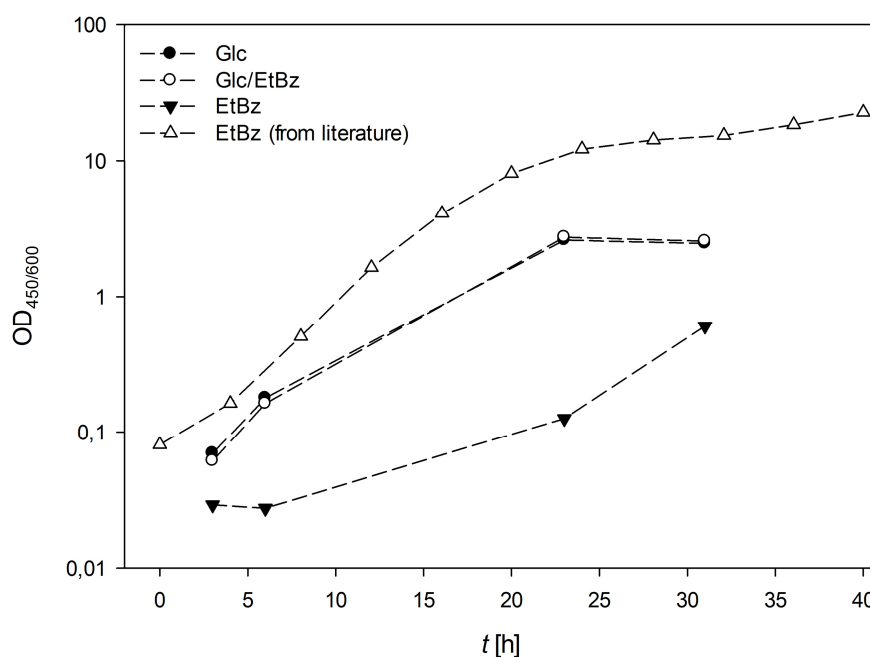


Figure 36: Growth curves for *Cellulosimicrobium cellulans* EB-8-4 either grown on glucose (Glc), ethyl benzene (EtBz) or both (Glc/EtBz) measured at OD₆₀₀. White triangles represent a reference curve from literature measured at OD₄₅₀.^[195a]

As depicted in Figure 36 the ability of the strain from Singapore to utilize ethyl benzene as sole carbon source could be reproduced, although the final optical densities of the cultures were significantly lower than the reported ones. The cultivations with glucose reached an OD₆₀₀ of 2.5, whereas the one with ethyl benzene reached a value of 0.6 after 31 h. In literature a value of OD₄₅₀ = 15 was reported after 32 h. Interestingly, the

cultures showed different colors when harvested (Figure 37). Only the cells grown on glucose showed the typical yellow color of *C. cellulans* cultures.^[196]

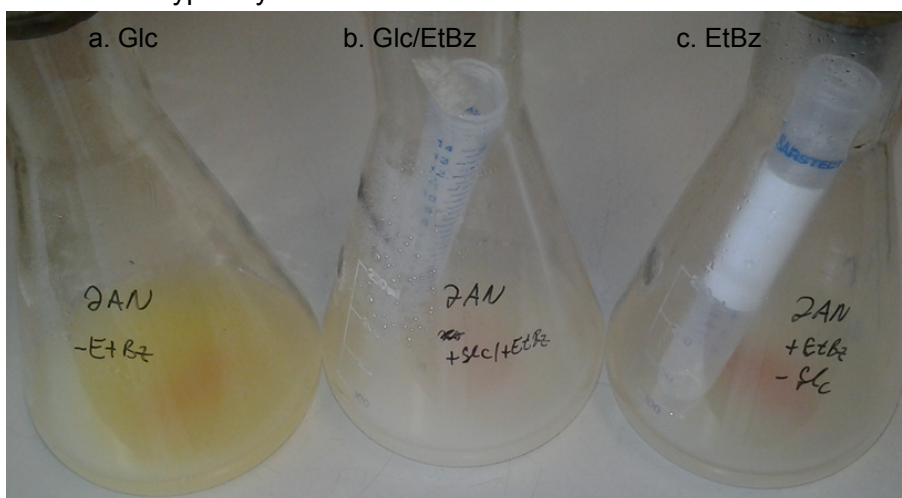


Figure 37: Cultures of *C. cellulans* EB-8-4 grown on glucose (Glc), ethyl benzene (EtBz) or both (Glc/EtBz) after 31 h.

The strain's ability to convert limonene into (1*R*,5*S*)-carveol was verified by using resting cells from these cultivations for biotransformation reactions. These revealed, that only the ethyl benzene grown cells were able to produce the desired carveol (Figure 38). There, a concentration of $50 \mu\text{mol} \cdot \text{L}^{-1}$ after 18 h was reached. Whereas in the other two reactions no product was detected by GC.

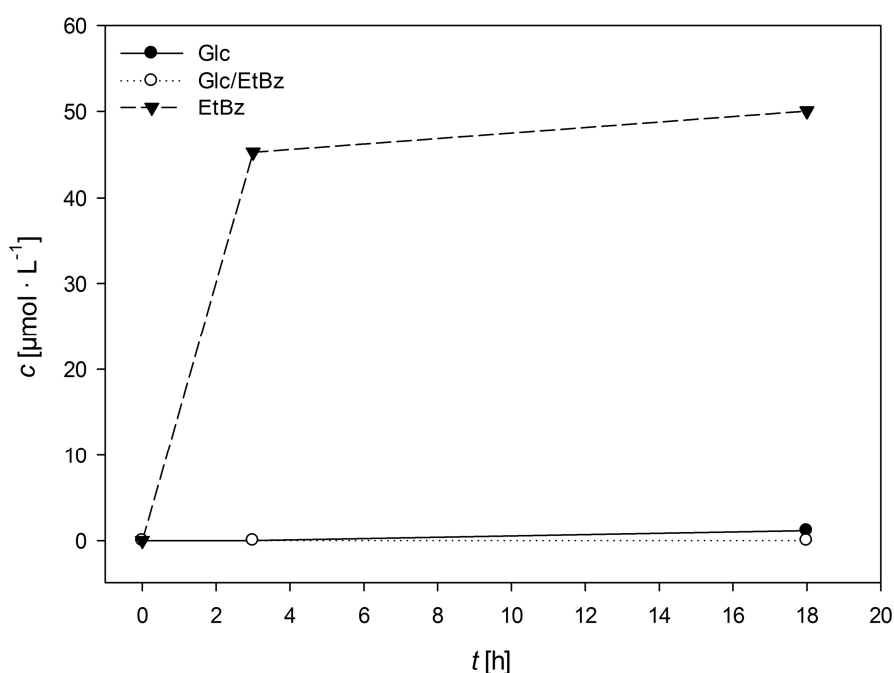


Figure 38: Concentration of (1*R*,5*S*)-carveol in biotransformations over 18 h using resting cells of *C. cellulans* EB-8-4 grown on glucose (filled circles), ethyl benzene (triangles) or both (open circles).

To identify and study the responsible enzyme(s) in more detail and to simplify the combination of this reaction with an established redox cascade by heterologous expression, the *C. cellulans* EB-8-4 genome was partially sequenced by Dr. Andrea Thürmer (Göttingen Genomics Laboratory, University of Göttingen). Therefore,

glucose grown cells were used for isolation of genomic DNA. The result of the sequencing contained approx. 3.9 million short reads of 75 bp. These were mapped by Dr. Johannes Kabisch (Institute of Biochemistry, University of Greifswald) to a reference genome of *C. cellulans* LMG16121 (BioProject accession: PRJEB571), which was not reported to grow on ethyl benzene. The unused reads after the mapping were subject to InterProScan 5^[197] and subsequently analyzed for the content of oxygenases, other hydroxylating enzymes or NAD(P)-dependent enzymes.

Table 12: List of genes encoding for NAD(P)-dependent enzymes found among the unused reads.

#	Sequence	Length	Description
1	Contig_5__5_ORF12 CRC64: 00BE4626C9310061	551 aa	adh_short, Rossmann fold
2	Contig_9__1_ORF2 CRC64: F3D24275C3F3AEBA	338 aa	Aldo/Keto reductase, NAD(P)-linked oxidoreductase
3	Contig_21__6_ORF2 CRC64: 96770564BC31137D	582 aa	dehydrogenase, Rossmann fold
4	Contig_35__6_ORF4 CRC64: 3795EB4434505BBA	453 aa	Rossmann fold
5	Contig_41__4_ORF4 CRC64: 6C0505BC861A1ACC	473 aa	Rossmann fold
6	Contig_53__4_ORF1 CRC64: BE946C41CE951092	135 aa	ADH_zinc_N, Rossmann fold
7	Contig_64__1_ORF2 CRC64: 73DDFDE5E728DFC8	166 aa	adh_short_C2, Rossmann fold
8	Contig_64__5_ORF3 CRC64: 75F6671A48165F8C	273 aa	adh_short, Rossmann fold
9	Contig_76__6_ORF1 CRC64: E81D238057DF2A94	839 aa	ADH_zinc_N, Rossmann fold
10	Contig_86__2_ORF4 CRC64: 11090C1E2337AA94	346 aa	Ferric reductase, FAD_binding
11	Contig_87__5_ORF8 CRC64: 973A237BC8E60CE1	458 aa	Nucleotide sugar dehydrogenase, Rossmann fold
12	Contig_89__5_ORF2 CRC64: 47BE0705FE6DB615	318 aa	adh_short, Rossmann fold
13	Contig_96__4_ORF3 CRC64: 52260C27A34CC4C2	325 aa	Aldo/Keto reductase, NAD(P)-linked oxidoreductase
14	Contig_110__1_ORF1 CRC64: 646E7681D3B70BE4	439 aa	Ferredoxin reductase-like, NAD_binding
15	Contig_132__2_ORF2 CRC64: 51281A92FF6CE9D2	447 aa	Lactate dehydrogenase, Rossmann fold
16	Contig_149__5_ORF4 CRC64: 39F2B58D11A68016	336 aa	adh_short, Rossmann fold
17	Contig_176__4_ORF1 CRC64: A904E362A1D9FA0C	548 aa	2-Hydroxyacid dehydrogenase, Rossmann fold
18	Contig_207__5_ORF1 CRC64: 237B1E810BD73003	240 aa	ADH_zinc_N, Rossmann fold
19	Contig_216__6_ORF1 CRC64: 47FFBE8BF958C7BA	180 aa	adh_short, Rossmann fold
20	Contig_229__1_ORF2 CRC64: DAA47B31A36E7D23	170 aa	Pyr_redox_2, FAD/NAD(P)-binding domain
21	Contig_239__2_ORF2 CRC64: 82233BD626002BB0	479 aa	GAP dehydrogenase-like, Rossmann fold
22	Contig_249__1_ORF1 CRC64: 57466ACDB916947E	286 aa	GAP dehydrogenase-like, Rossmann fold
23	Contig_266__5_ORF1 CRC64: 3C2009874327DD34	112 aa	adh_short_C2, Rossmann fold
24	Contig_273__2_ORF1 CRC64: 2E4C94A9CAEF81F9	247 aa	Oxidoreductase, FAD/NAD(P)-binding domain
25	Contig_282__6_ORF1 CRC64: A483C4033E104292	295 aa	Aldo/Keto reductase, NAD(P)-linked oxidoreductase
26	Contig_354__1_ORF3 CRC64: DDB3E612518FBF4F	217 aa	Saccarop_dh, Rossmann fold
27	Contig_359__3_ORF1 CRC64: 1E74BC01280186D4	317 aa	adh_short, Rossmann fold
28	Contig_360__1_ORF2 CRC64: AF001C8BA308D803	68 aa	Pyr_redox, FAD/NAD(P)-binding domain
29	Contig_383__6_ORF1 CRC64: 811934A81E375ACE	214 aa	GFO_IDH_MocA, Rossmann fold
30	Contig_410__6_ORF1 CRC64: 02C6F225B0838206	188 aa	GDHRDH, Rossmann fold
31	Contig_425__4_ORF2 CRC64: D2E69394865F6821	213 aa	Isomerase/Epimerase, Rossmann fold
32	Contig_430__5_ORF2 CRC64: CA0A351AF6B709D6	196 aa	Rossmann fold
33	Contig_459__5_ORF1 CRC64: E78C6A505FA00882	254 aa	Rossmann fold
34	Contig_478__2_ORF1 CRC64: A9093C6E6580ACA6	320 aa	Nitrite reductase, FAD/NAD(P)-binding domain
35	Contig_510__4_ORF1 CRC64: 55E8060E474E15DD	169 aa	2-Hydroxyacid dehydrogenase, Rossmann fold
36	Contig_516__1_ORF1 CRC64: 8F4C47A0FE7D1503	215 aa	adh_short, Rossmann fold
37	Contig_535__2_ORF1 CRC64: E3ACE3C76B0CB8D5	183 aa	F420_oxidored, Rossmann fold
38	Contig_555__6_ORF1 CRC64: 7508EE91ADC7D22F	202 aa	Rossmann fold
39	Contig_576__6_ORF1 CRC64: 967F5C6A67814A72	253 aa	Nitrite reductase, FAD/NAD(P)-binding domain
40	Contig_864__6_ORF1 CRC64: 472B30BDA77C46D6	127 aa	Pyr_redox_2, FAD/NAD(P)-binding domain
41	Contig_888__1_ORF1 CRC64: 17F052DCE2B004BC	148 aa	Nitrite reductase, FAD/NAD(P)-binding domain
42	Contig_971__4_ORF1 CRC64: 25C9AFC48BEAA971	101 aa	GFO_IDH_MocA, Rossmann fold
43	Contig_1198__5_ORF1 CRC64: 2A949D3132D3B7E8	108 aa	2-Hacid_dh_C, Rossmann fold
44	Contig_8171__3_ORF1 CRC64: 601280F24E488B60	53 aa	AdoHcyase_NAD
45	Contig_8171__6_ORF1 CRC64: 71BCF82399E880B6	53 aa	AdoHcyase_NAD
46	Contig_8190__2_ORF1 CRC64: 74F1E35C4576D2C8	52 aa	adh_short, Rossmann fold

Within the unused reads no oxygenases or oxidases were found. There were only hits for genes encoding NAD(P)-dependent enzymes (Table 12). However none of these encoded a probable relevant enzyme, so that an alternative approach for identification of the enzyme(s) had to be used. Therefore, it was decided to analyze directly the proteins by MS, which were expressed when growing the cells on ethyl benzene. This work was subject of a supervised M.Sc. thesis by Katja Zorn (University of Greifswald, Germany) in cooperation with Dr. Dirk Albrecht (Institute of Microbiology, University of Greifswald).^[198]

3.2.2.2 Cloning and Heterologous Expression of a Dioxygenase

In her M.Sc. thesis Katja Zorn (University of Greifswald, Germany) identified the dioxygenase cluster, which was responsible for the selective limonene hydroxylation by gene walking. It turned out, that the microbe responsible for this reaction was a *Rhodococcus equi* strain and not the previously described *C. cellulans* EB-8-4! Furthermore, the identified cluster showed a 100% sequence identity to a benzene-1,2-dioxygenase from *Rhodococcus opacus* B4!^[198]

Due to the fact that *R. equi* is an S2 organism, the cluster was expressed heterologously in *E. coli*. Though this was not successful until now.^[198] In addition, *Pseudomonas putida* S12 was used as host organism for the recombinant expression, which was reported by Hugo van Beek and Prof. Dr. Marco W. Fraaije (University of Groningen, The Netherlands) to functionally express a homologous dioxygenase cluster from *P. putida* PWD32 (formerly known as *Rhodococcus opacus* PWD4).^[101-102] The *P. putida* S12 strain and a suitable plasmid (pBTBx-2) were also provided by the Fraaije group. The identified dioxygenase cluster from *R. equi* (DOC_{equi}) was cloned into the vector by FastCloning and transformed into *P. putida* S12.^[199]

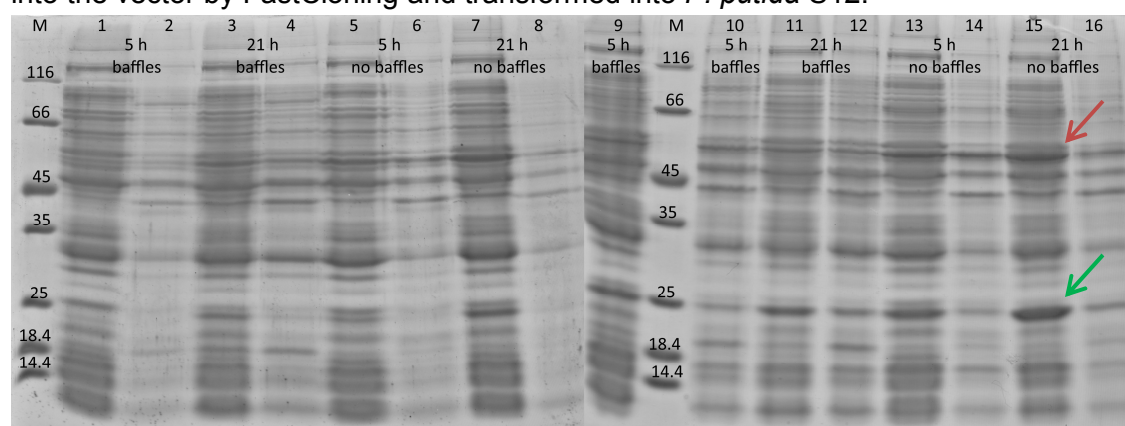


Figure 39: Electrophoregram of 7/OD-samples from recombinant expression of DOC_{equi} in *P. putida* S12 at various temperatures (odd lanes: soluble protein fraction, even lanes: insoluble protein fraction, lanes 1 - 8: expression at 20°C, lanes 9 - 16: expression at 30°C, red arrow: large subunit of DOC_{equi}, green arrow: small subunit of DOC_{equi}, M: protein marker in kDa).

The recombinant expression of DOC_{equi} was carried out at different temperatures (20/30°C), in different flasks (conical/baffled) and over different time periods (5/21 h). The cells were cultivated at 30°C until OD 0.5 - 0.6, then expression was induced by 0.2% L-arabinose and the cultivation was continued either at 20°C or 30°C. According to Figure 39 expression in conical flasks and at 30°C generally seemed to result in high yields of soluble protein at least for the large (51.6 kDa, Figure 39: red arrow) and small subunit (22.0 kDa, Figure 39: green arrow) of the dioxygenase. Expression of the

ferredoxin (11.5 kDa) and the ferredoxin reductase (43.5 kDa) was not detected by SDS-PAGE.

Nevertheless, the cells from the expression experiments were used for resting cell biocatalysis reactions. These were carried out in a total reaction volume of 1 mL KPi buffer ($50 \text{ mmol} \cdot \text{L}^{-1}$, pH 7.0) in closed 10 mL-glass vials containing $40 \text{ mmol} \cdot \text{L}^{-1}$ *rac*-limonene and $20 \text{ mmol} \cdot \text{L}^{-1}$ glucose. The total reaction medium was extracted after 24 h and analyzed by GC. However, no product was detected probably due to the missing ferredoxin and ferredoxin reductase, which might have been caused by the low concentration of L-arabinose used for induction.

To increase the expression of these two proteins an additional L-arabinose inducible promoter was inserted downstream of the gene for the small subunit and in front of the ferredoxin gene by FastCloning, which resulted in $\text{DOC}_{\text{equiAra}}$. Again, the cells were cultivated at 30°C until OD 0.5 - 0.6, then expression was induced by 0.5 - 2% L-arabinose and the cultivation was continued at 30°C . The expression was analyzed by SDS-PAGE.

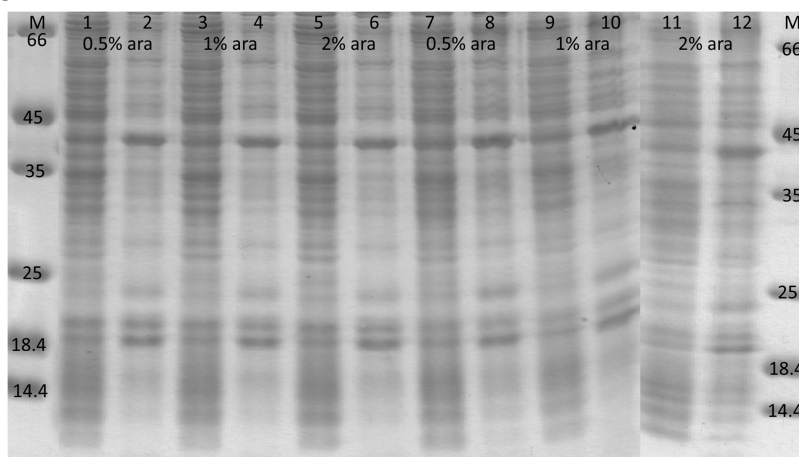


Figure 40: Electrophoregram of 7/OD-samples from recombinant expression of $\text{DOC}_{\text{equiAra}}$ in *P. putida* S12 induced with various L-arabinose concentrations (odd lanes: soluble protein fraction, even lanes: insoluble protein fraction, lanes 1 - 6: 8 h expression, lanes 7 - 12: 27 h expression, M: protein marker in kDa).

As depicted in Figure 40 no expression, either after 8 h or 27 h, was detected for the $\text{DOC}_{\text{equiAra}}$ genes. Nevertheless, biocatalysis reactions using the resting cells were carried out as described above except that 2 or $20 \text{ mmol} \cdot \text{L}^{-1}$ *rac*-limonene and equimolar amounts of glucose were used. After 24 h the reaction medium was extracted and analyzed. Unfortunately no product formation was detected by GC probably due to the missing expression of all required proteins, so that no further attempts were made to express DOC_{equi} recombinantly. Nevertheless, combined biocatalysis reactions using resting cells of *R. equi* and the recombinant *E. coli* carrying the genes for expression of the enzymes involved were carried out by Nikolin Oberleitner (Vienna Technical University, Austria) as part of her PhD thesis.

In summary, the described redox cascade for the production of chiral lactones (Scheme 12) was successfully extended to a certain extent after identification of a suitable hydroxylating catalyst and in mixed culture reactions the production of chiral lactones was realized by the project partner in Vienna.

3.3 Immobilization of Two Enzymes for Cascade Reactions

The last part of this thesis deals with the immobilization of two enzymes as whole cell biocatalysts, which was used in a cascade reaction for the production of PCL precursors (Scheme 14). Furthermore, the reaction should be upscaled by application of a rotating bed reactor. Therefore, several model reactions were studied, which are outlined in the corresponding chapters.

3.3.1 General Applicability of Enzymes in a Rotating Bed Reactor

As mentioned before in chapter 1.4, immobilization of (bio-)catalysts might lead to a substantial increase of stability and reusability of these. During my diploma thesis a method for encapsulation of cells using alginate was developed and the general applicability of these in a rotating bed reactor (RBR) was demonstrated in two preliminary experiments. However optimization of the process itself and demonstration of the general applicability of an RBR for different biocatalysts, especially concerning the reusability of these, still were necessary.

To demonstrate the feasibility of the RBR (SpinChem[®]) three different immobilized enzymes were selected: the (*R*)-selective amine transaminase (*R*-ATA) from *Gibberella zeae* immobilized on chitosan^[200], cells harboring the CHMO from *Acinetobacter* sp. encapsulated in Ca-alginate^[201] and the commercially available lipase B from *Pseudozyma antarctica* (CAL-B; strain formerly known as *Candida antarctica*) immobilized on an acrylic resin. The studies involving the *R*-ATA were in cooperation with Dr. Hendrik Mallin.^[202] All these biocatalysts were used in three different reactor setups (Figure 18) for comparison and subsequently for recycling studies using the stirred tank reactor (STR) and the RBR.

3.3.1.1 Process Optimization of Reactions Using the SpinChem[®]

Before studying the applicability of the SpinChem[®], the biocatalytic process concerning the stirring speed of the flow cell needed to be optimized. Therefore, biocatalysis reactions using the CHMO or the lipase were carried out over 2 h or 1 h respectively, so that full conversion was not reached. As shown in Table 13 the stirring speed had no significant influence on the conversion. Based on this result it was decided to use 500 rpm as standard stirring speed for reactions applying the RBR.

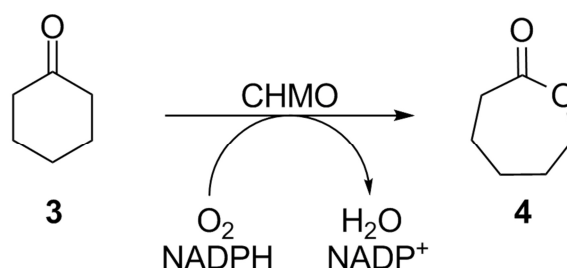
Table 13: Influence of stirring speed on conversion (from [154]).

Stirring Speed [rpm]	Conversion [%]	
	CHMO ^a	Novozyme [®] 435 ^b
100	3.4	n.d.
250	3.5	7.7
500	3.3	7.6
750	2.7	7.8
1000	n.d.	7.5

^a-after 2 h, ^b-after 1 h, n.d.-not determined

3.3.1.2 Application of a BVMO in a Rotating Bed Reactor

The application of CHMO_{Acineto} was studied first, because this enzyme was one of the key enzymes in the studied cascade reactions. Furthermore, these multi-enzymatic systems were designed as *in vivo* pathways, that was why encapsulated cells harboring the CHMO_{Acineto} were used for these experiments. The cells were encapsulated in Ca-alginate using the 'drop method' and subsequently used for biocatalysis reactions for the production of **4** in three different reactor setups (Scheme 19, Figure 18).



Scheme 19: BVMO model reaction for production of ϵ -caprolactone.

The production of **4** catalyzed by the CHMO_{Acineto} showed approx. the same conversions of 66% to 69% after 24 h in both the RBR and the STR (Figure 41). In contrast, for the FBR a significant nine-fold lower conversion was obtained. This drastic decrease could be explained by the decreased oxygen supply in the column.

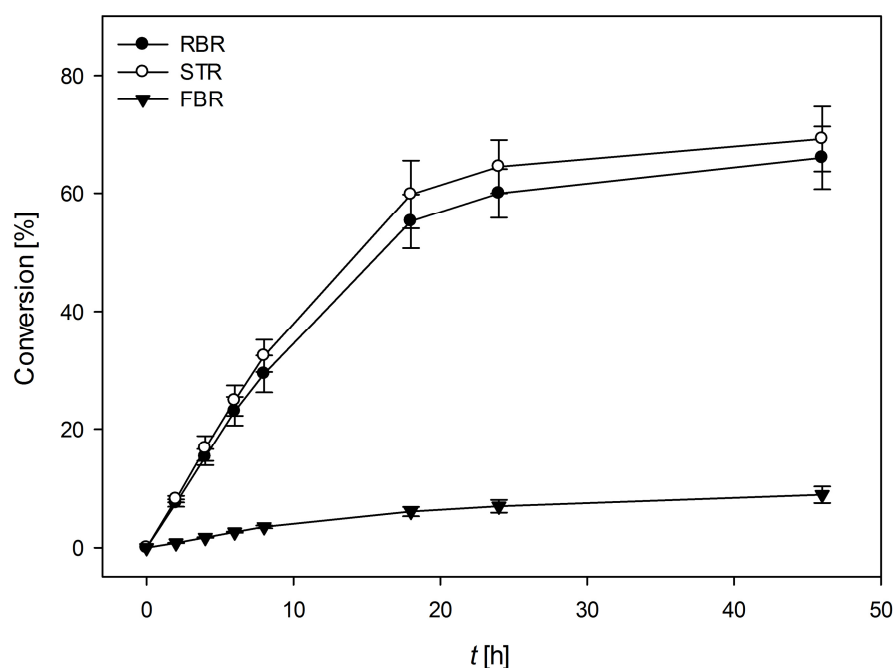


Figure 41: Conversion of cyclohexanone to ϵ -caprolactone by using Ca-alginate encapsulated resting *E. coli* cells harboring a CHMO (RBR: Rotating bed reactor, STR: Stirred tank reactor, FBR: Fixed bed reactor; $n=3$; from [154]).

Next, reuse and downstream processing were studied in the RBR and the STR under identical conditions. Therefore, the encapsulated cells were used in six successive

biocatalytic reactions each of 2 h. Between each cycle the capsules were recovered from the reaction medium, washed in buffer and used directly for the next reaction.

The recycling of the Ca-alginate encapsulated cells was significantly improved by using the SpinChem[®] reactor (Figure 42). The beads used in the rotating flow cell showed a residual activity of 41% after six cycles. In contrast, for the catalyst used in the STR only 14% residual activity was observed. In addition, it was observed that the capsules used in RBR were protected completely from any mechanical forces, because these showed no significant change in morphology. The beads used in STR showed a drastic change in shape due to the mechanical stress by the stirrer. Furthermore, the downstream processing of the RBR reactions was much easier and faster than the STR ones. Here, especially the separation of the catalysts from the reaction medium by filtration was very tedious and time-consuming.

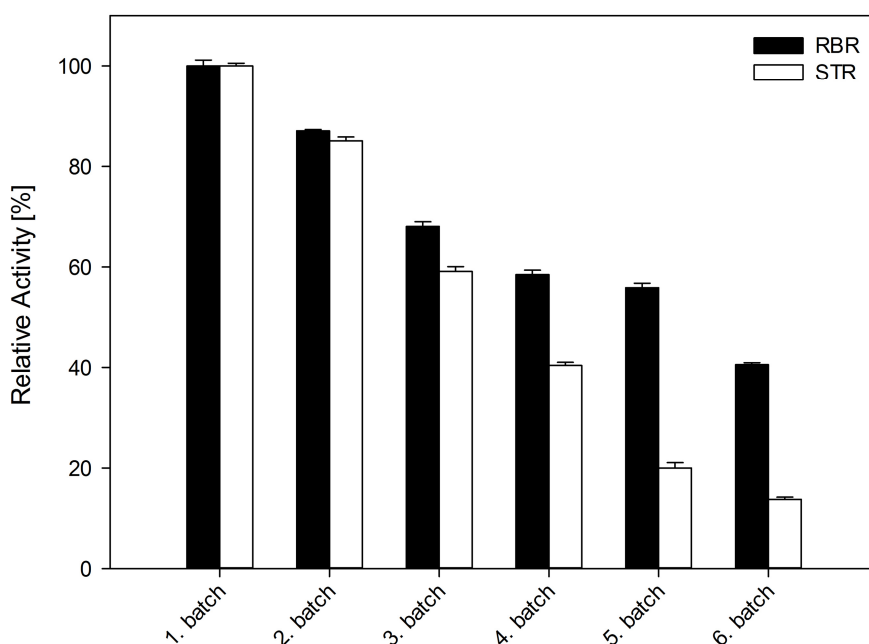
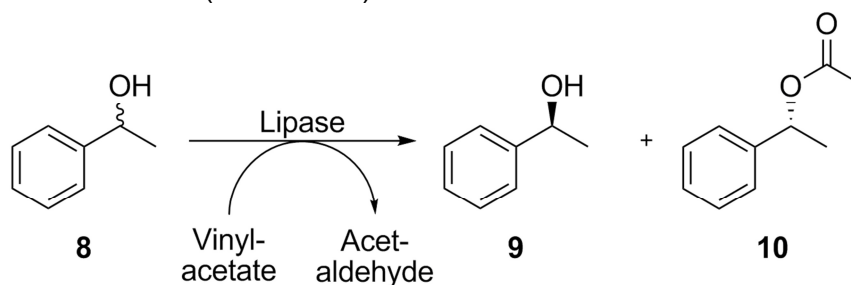


Figure 42: Recycling study with encapsulated resting *E. coli* cells containing the CHMO_{Acineto} in the RBR and the STR (2 h per batch; 100% relative activity \equiv 7.5% conversion of **3** in the first batch; RBR: Rotating bed reactor, STR: Stirred tank reactor; n=3; from [154]).

3.3.1.3 Application of an Immobilized Lipase in a Rotating Bed Reactor

One of the thesis' projects was the biocatalytic production of polymers using a lipase. Therefore, the transesterification reaction of *rac*-**8** by an immobilized lipase (Novozyme[®] 435) was studied in neat organic solvent using a rotating bed reactor (RBR) as model reaction (Scheme 20).



Scheme 20: Model reaction for transesterification by immobilized lipase.

Again the reaction in the RBR was compared with a classical stirred tank reactor (STR). In this case the fixed bed reactor was not studied, because it showed in the preceding experiments using BVMO and (*R*)-ATA lower conversions and the available FBR equipment was not suitable for reactions with neat organic solvent. For proper comparison of the chosen reactor systems it was necessary to slow down the reaction of the lipase. Therefore, a substrate concentration of 1 M and a reaction temperature of 30°C were used. This way it was possible to follow the reaction over at least 4 h.

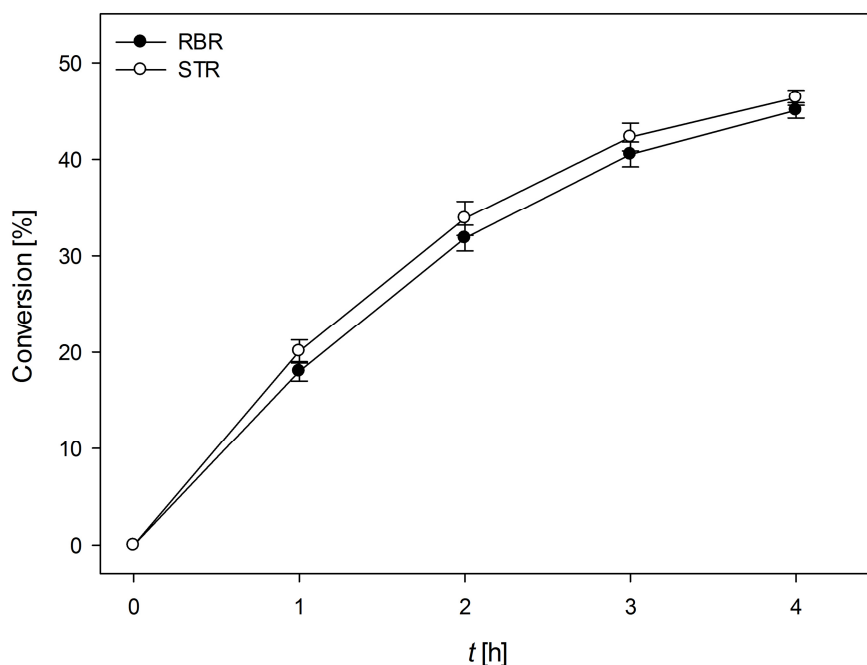


Figure 43: Transesterification of *rac*-**8** into the (*R*)-**10** by using immobilized lipase CAL-B in RBR and STR (from [154]).

The transesterification reaction by the lipase in the STR and the RBR showed similar conversions as observed before in the BVMO reaction. In both experiments a

conversion of approx. 45% was reached after 4 h. This result indicated that the well-studied lipase reaction could be transferred into an RBR.

Next to the comparison of RBR and STR with respect to conversion the recyclability of the lipase was studied in both reactors. Therefore, the immobilized CAL-B was used in five successive biocatalytic reactions each of 2 h. Between each cycle the catalytic particles were recovered from the reaction medium, washed in cold acetone and used directly for the next reaction.

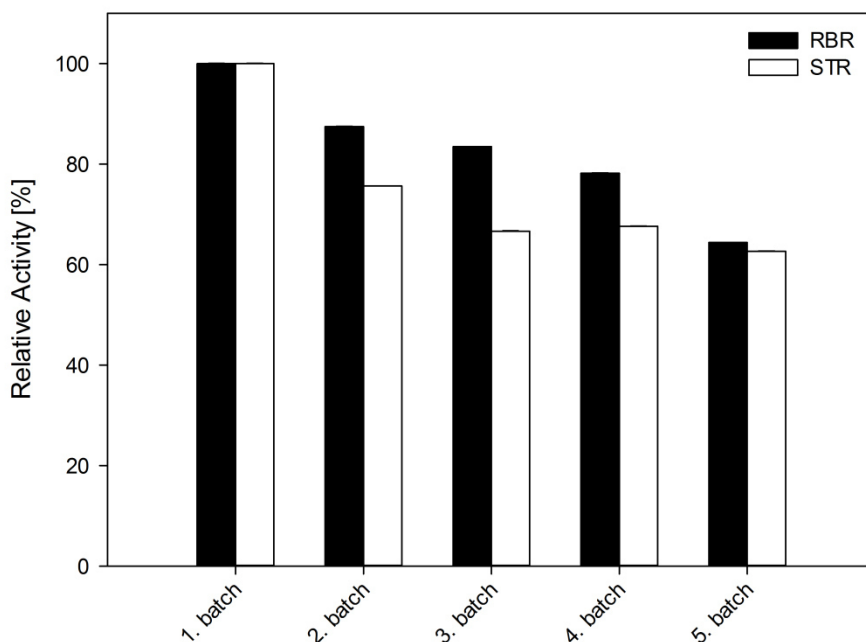


Figure 44: Recycling study with immobilized lipase CAL-B (2 h per batch) in RBR and STR (100% relative activity \equiv 33% (RBR) and 39% conversions (STR) of *rac*-8 in the first batch; from [154]).

The advantage of using the SpinChem[®] after five cycles of recycling was not as obvious as for the other reactions, because both attempts showed a relative activity of approx. 63% after five cycles. But after the second to fourth batch the activity recovered from RBR was 11 - 17% higher than for STR. The fact, that after five cycles both systems showed similar activities, was probably due to the nature of the used immobilization method, which was to our knowledge adsorptive. For this methodology high 'leaching' was reported often.^[203]

3.3.2 Optimization of the Whole Cell Encapsulation Process

A simple encapsulation process for cells harboring the CHMO using the 'drop method' was already established during my diploma thesis.^[201] Furthermore, these immobilized cells were successfully applied in reactions using an RBR (SpinChem[®]) as described above and in a publication.^[154] Due to the high particle size of about 2 - 3 mm the immobilization yield was only 26%.^[201] It was assumed that the oxygen supply within the particles was limited due to the high diameter. To address this problem alternative encapsulation processes were established, which resulted in smaller particles. First, Stefanie Becker could show in her B.Sc. thesis using an emulsion process for encapsulation that smaller particles indeed had higher activities.^[204] But this procedure

was rather laborious, so that a simpler process was developed. In literature the application of a co-axial gas stream was described to decrease the capsule size.^[139, 205] Due to the fact that the prices of commercial gas shear devices were very high, a home-made one was set up (Figure 45).

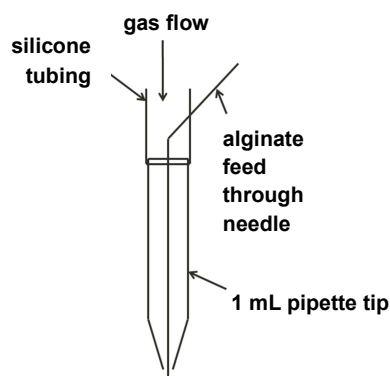


Figure 45: Schematic drawing of 'home-made' gas shear device.

Therefore, the cone end of a 1 mL-pipette tip was cut, so that a hole of about 1 mm was created. This prepared pipette tip was attached to a silicone tubing (outer Ø: 8 mm, inner Ø: 5 mm), which in turn was attached to an air flow meter (Key Instruments, Langhorne, USA). The needle, which was also used for the 'drop method', was simply pierced through the silicone tubing (Figure 45) and the tip of the needle was moved to the end of the pipette tip, so that approx. 1 mm of the needle was out of the pipette tip again.

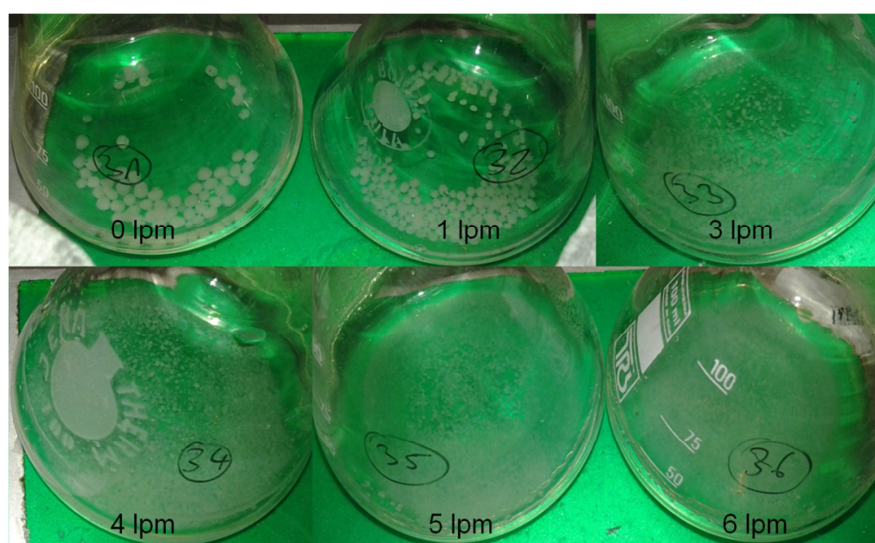


Figure 46: Calcium alginate capsules produced with the 'home-made' gas shear device at different flow rates (lpm: $\text{L} \cdot \text{min}^{-1}$).

Already by eye the decreased particle size could be observed (Figure 46). Here, various flow rates of the air stream ($0 - 6 \text{ L} \cdot \text{min}^{-1}$) were applied. Already the application of $1 \text{ L} \cdot \text{min}^{-1}$ led to a definite decrease in particle size. By applying higher flow rates the particle size was decreasing further as observed by eye.

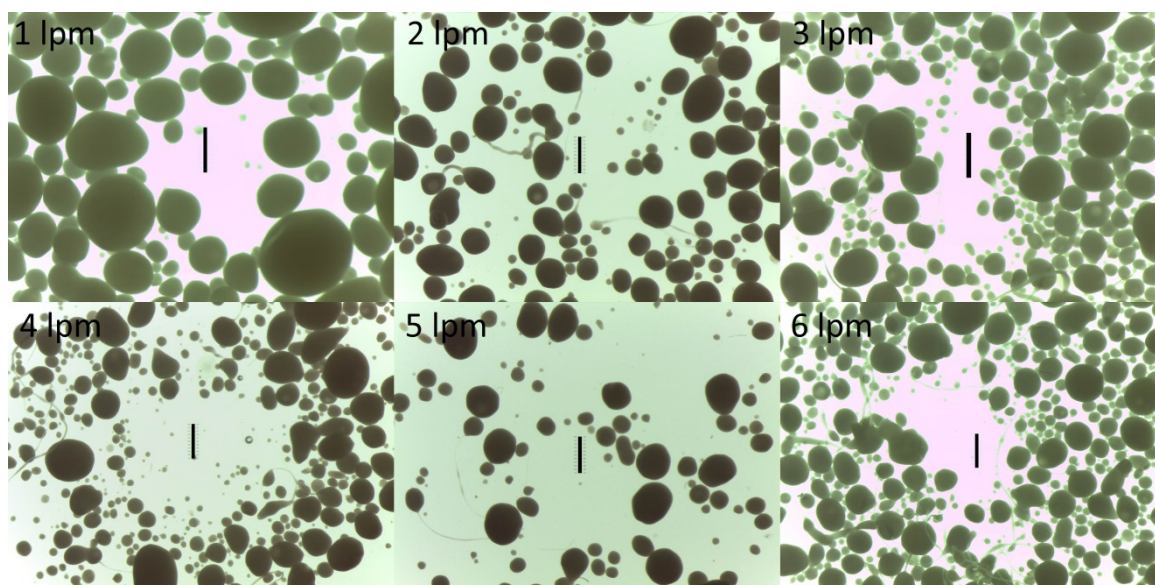


Figure 47: Microscopic pictures of alginate beads produced by application of different gas flow rates. (lpm: $\text{L} \cdot \text{min}^{-1}$; Black bar $\equiv 1 \text{ mm}$).

To determine the mean particle size, these were measured using a microscope slide with ruler (Figure 47). The diameter of at least thirteen beads of each batch with different flow rates was measured to determine the mean diameter of the capsules and further validate the results.

Table 14: Mean diameters of calcium alginate capsules produced by application of various gas flow rates ($n \geq 13$, except $0 \text{ L} \cdot \text{min}^{-1}$).

Flow rate [$\text{L} \cdot \text{min}^{-1}$]	Mean diameter [mm]
0.0	2.0-3.0 ^a
1.0	0.931 ± 0.45
2.0	0.657 ± 0.66
3.0	0.488 ± 0.35
4.0	0.418 ± 0.33
5.0	0.405 ± 0.25
6.0	0.387 ± 0.19

^aestimated using a desk ruler

As shown in Table 14 the mean diameter of the particles was successfully decreased to $<1 \text{ mm}$. Application of a co-axial gas flow at $1.0 - 2.0 \text{ L} \cdot \text{min}^{-1}$ resulted in particles with an approx. diameter of 1 mm . A further increase of the flow rate up to $6.0 \text{ L} \cdot \text{min}^{-1}$ led to even smaller capsules of approx. $0.5 - 0.7 \text{ mm}$.

After establishment of the gas shear process to produce alginate capsules with a diameter $<1 \text{ mm}$, the positive effect of the decreased particle size needed to be validated. This was done by using the small alginate beads for biocatalysis reactions in shake flasks (Figure 46). Therefore, resting cells harboring the $\text{CHMO}_{\text{Acineto}}$ were encapsulated in alginate using the 'home-made' gas shear device at different air flow rates ($0.0 - 6.0 \text{ L} \cdot \text{min}^{-1}$). The biocatalysis reactions were carried out in 100 mL -conical Erlenmeyer flasks at 25°C and 120 rpm shaking. As reaction medium Tris-HCl buffer ($20 \text{ mmol} \cdot \text{L}^{-1}$, pH 7.5, $1\% \text{ NaCl}$, $10 \text{ mmol} \cdot \text{L}^{-1} \text{ CaCl}_2$) containing $20 \text{ mmol} \cdot \text{L}^{-1}$ cyclohexanone and $20 \text{ mmol} \cdot \text{L}^{-1}$ glucose as (co-)substrates. Samples of $500 \mu\text{L}$ were collected and analyzed by GC.

According to Figure 48 the activity of the encapsulated cells was drastically increased by the application of the co-axial gas stream. Without the gas shear device only an activity of $1.5 \pm 0.1 \text{ U} \cdot \text{g}_{\text{WCW}}^{-1}$ was reached. Using $1 \text{ L} \cdot \text{min}^{-1}$ gas flow during the process gave no significant increase of activity. In contrast, the use of $2 - 5 \text{ L} \cdot \text{min}^{-1}$ led to increasing activities. The capsules produced at $5 \text{ L} \cdot \text{min}^{-1}$ even had doubled activity ($3.0 \pm 0.2 \text{ U} \cdot \text{g}_{\text{WCW}}^{-1}$) than the ones without applied gas stream. However, the free cells still featured slightly higher activity of $4.0 \pm 0.1 \text{ U} \cdot \text{g}_{\text{WCW}}^{-1}$. So that in summary the activity of the immobilized cells could be doubled by the application of the ‘home-made’ gas shear device.

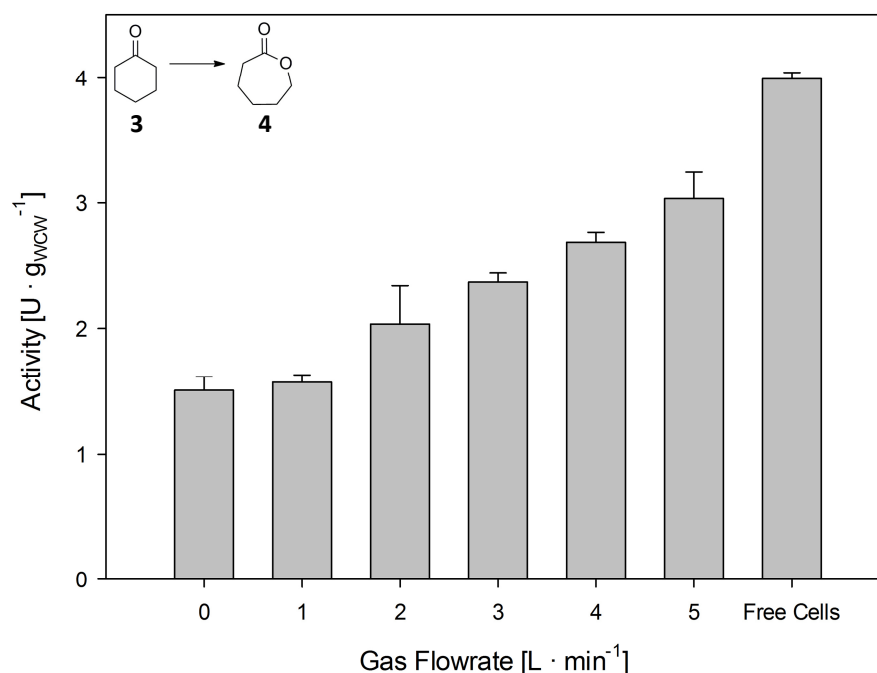


Figure 48: Initial activities of micro-scale Ca-alginate beads dependent on applied gas flow ($20 \text{ mmol} \cdot \text{L}^{-1}$ **3** initial concentration, 2 h reaction time; $n=3$).

As next step the influence of the used cell weight was investigated, because it was reported that a high cell load ($25 \text{ g}_{\text{WCW}} \cdot \text{L}^{-1}$) was needed for the production of oligo-[caprolactone] by coupling of CHMO and ADH.^[28] Up to now the cells for biotransformation were resuspended to a concentration of $100 \text{ g}_{\text{WCW}} \cdot \text{L}^{-1}$. Higher cell densities were applied for encapsulation by resuspending the cells after cultivation to a concentration of $500 \text{ g}_{\text{WCW}} \cdot \text{L}^{-1}$. Subsequently, this cell suspension was diluted, so that concentrations from $100 - 500 \text{ g}_{\text{WCW}} \cdot \text{L}^{-1}$ were used. The alginate beads containing the cells were used for biocatalysis reactions over 24 h in 10 mL scale.

According to Figure 49 the absolute concentration of **4** after 24 h was increased from $11.2 \text{ mmol} \cdot \text{L}^{-1}$ to $12.2 - 13.2 \text{ mmol} \cdot \text{L}^{-1}$ by using a cell weight $>100 \text{ g}_{\text{WCW}} \cdot \text{L}^{-1}$. However the yield using free cells was higher with $13.8 \text{ mmol} \cdot \text{L}^{-1}$. Still the final yield using encapsulated cells was increased to approx. the one when using free cells. With respect to the normalized concentrations (Figure 49, left y-axis) the results were completely different. Here the final yield ($\mu\text{mol} \cdot \text{mg}_{\text{WCW}}^{-1}$) was decreasing gradually with increasing used cell weight. Although the capsule size was decreased to enhance oxygen supply within the bead, this still might have been the problem when using higher cell densities for encapsulation. Nevertheless a cell density of $500 \text{ g}_{\text{WCW}} \cdot \text{L}^{-1}$ was used for all subsequent encapsulation experiments.

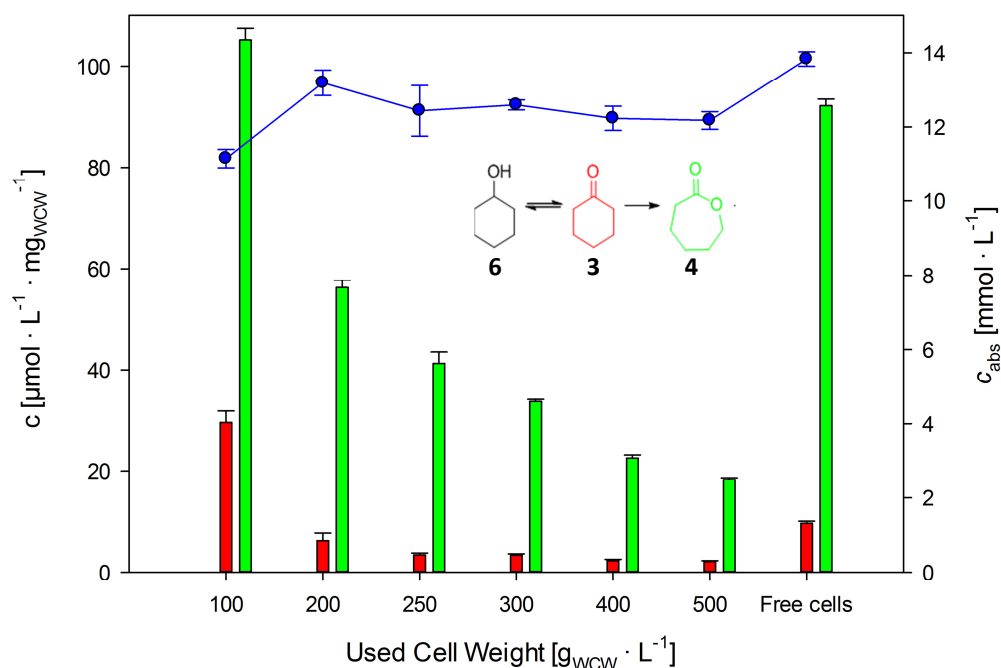


Figure 49: Concentrations after 24 h with micro-scale alginate beads containing various total amounts of cells with ADH and CHMO (bars represent normalized concentrations on the left y-axis; black bars: **6**, red bars: **3**, green bars: **4**; the blue line represents absolute concentrations of **4** on the right y-axis; n=3).

3.3.3 Establishment of an *in situ* Encapsulation Process

After improvement of the encapsulation process *ex situ* in terms of capsule size and cell load this was transformed into an *in situ* process. That means that the capsule formation was carried out within the actual reaction vessel containing the reaction medium. Therefore the 'home-made' gas shear device was attached to the reaction vessel through one of the fittings. The encapsulation was done, while the RBR (without inner net) was stirred, so that the empty compartments of the SpinChem® were filled with the solid beads (Figure 50).

As reaction vessels either the SpinChem® V211 (Nordic Chemquest AB, Umeå, Sweden) for reactions up to 200 ml or the BioFlo 110 1 L-fermenter (Eppendorf AG, Hamburg, Germany) for larger volumes were used. Furthermore, the process was established for two different RBRs (SpinChem® S221 and S311).

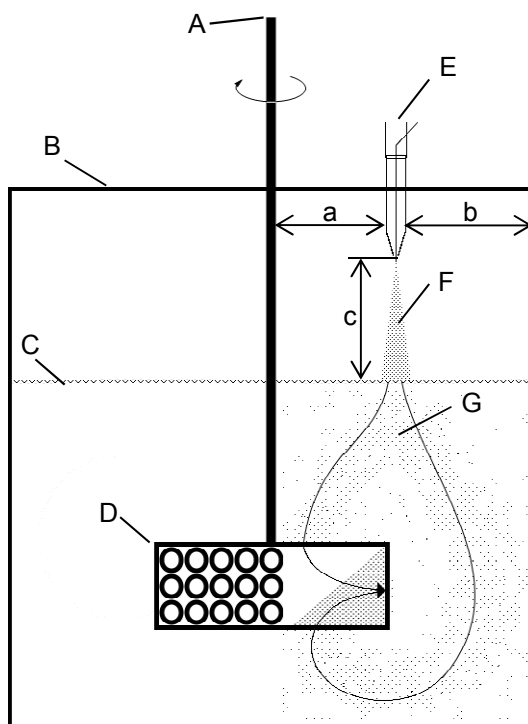


Figure 50: Schematic drawing of the *in situ* encapsulation process (A: Stirring bar attached to overhead stirrer, B: Reaction vessel, C: Reaction medium, D: Rotating bed reactor (SpinChem[®]), E: 'Home-made' gas shear device, F: Spray containing alginate/cell droplets, G: Solid alginate capsules; the arrows describe the way of the capsules into the empty compartments of D; a: Distance A to E, b: Distance E to B, c: Distance tip of E to C).

The most important parameters when setting up the *in situ* encapsulation were the distances a-c as shown in Figure 50. Setting up the distances a and b too narrow led to attachment of alginate droplets on the inside of the vessel wall or on the stirring bar. The distances for the use of both setups are listed below (Table 15).

Table 15: Distance parameters for *in situ* encapsulation process in two different setups.

Rotating Flow Cell	Reaction Vessel	Distance [mm]		
		a	b	c
SpinChem [®] S221	SpinChem [®] V211	12	15	65
SpinChem [®] S311	BioFlo 110	30	25	40

3.3.4 Application of a Cascade for Oligo-[Caprolactone] Production in a Rotating Bed Reactor

After optimization and establishment of the *in situ* encapsulation process, the feasibility of the cascade for oligomer production was validated by use of the reaction in a rotating bed reactor. Furthermore, instead of the CHMO_{Acineto} wild-type the quadruple mutant (CHMO_{QM}) created by Hanna Büchsenschütz in her M.Sc. thesis,^[177, 206] which showed a higher stability, was applied for all subsequent experiments. Therefore, three different setups were compared (Figure 51).

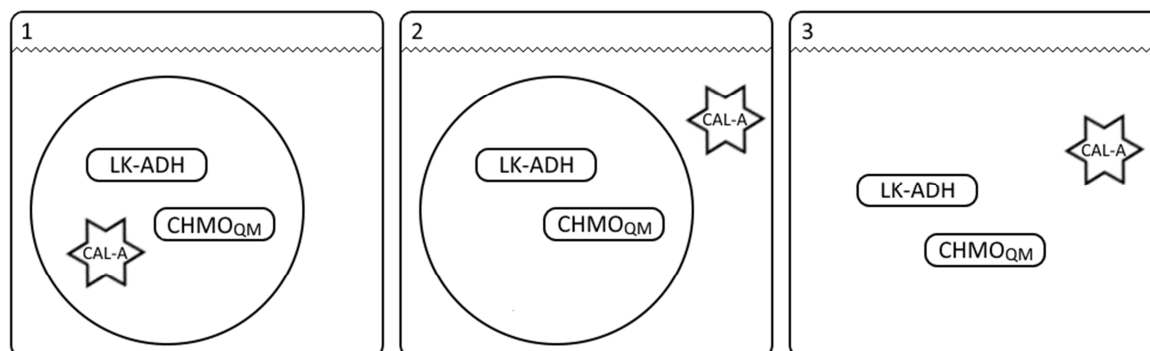


Figure 51: Schematic drawing of setups used for application of the cascade in a rotating bed reactor (Rounded bars: cells containing ADH or CHMO, circle: alginate capsule, start: isolated enzyme; 1: Co-immobilization of cells containing LK-ADH, cells containing CHMO_{QM} and CAL-A; 2: Co-immobilization of cells containing LK-ADH and cells containing CHMO_{QM}, external addition of CAL-A; 3: Free cells containing LK-ADH and free cells containing CHMO_{QM}, addition of CAL-A).

For the first experiments the cells harboring ADH and CHMO_{QM} were mixed in a ratio of 1:10 and resuspended in Tris-HCl buffer either containing lyophilized CAL-A (Figure 51, setup 1) or no CAL-A (Figure 51, setup 2 and 3). Mixing the suspension with Na-alginate solution (3.6%) in a ratio of 1:1 resulted in the optimal final Na-alginate concentration of 1.8%. For biocatalysis reaction an initial concentration of $60 \text{ mmol} \cdot \text{L}^{-1}$ of **6** and acetone as co-substrate was used and further fed over 16 h up to a final concentration of $200 \text{ mmol} \cdot \text{L}^{-1}$.

As Figure 52 - 55 show the substrate **6** was not consumed completely, because in all three setups approx. $60 \text{ mmol} \cdot \text{L}^{-1}$ **6** was detected after 48 h. Interestingly, the concentration of the substrate first decreased within 10 - 20 h to $24 - 42 \text{ mmol} \cdot \text{L}^{-1}$. After that the concentration increased again up to the final value of $52 - 58 \text{ mmol} \cdot \text{L}^{-1}$. The intermediate **3** was detected in low concentrations within the first 5 h. In all later samples **3** was not found. The concentration of intermediate **4** reached a maximum at approx. $20 \text{ mmol} \cdot \text{L}^{-1}$ after 10 h. The final oligomeric product was not isolated due to the high amounts of substrate **6**, which was also extracted by the used method. So that in summary based on substrate depletion a theoretical yield of 71 - 74% was reached.

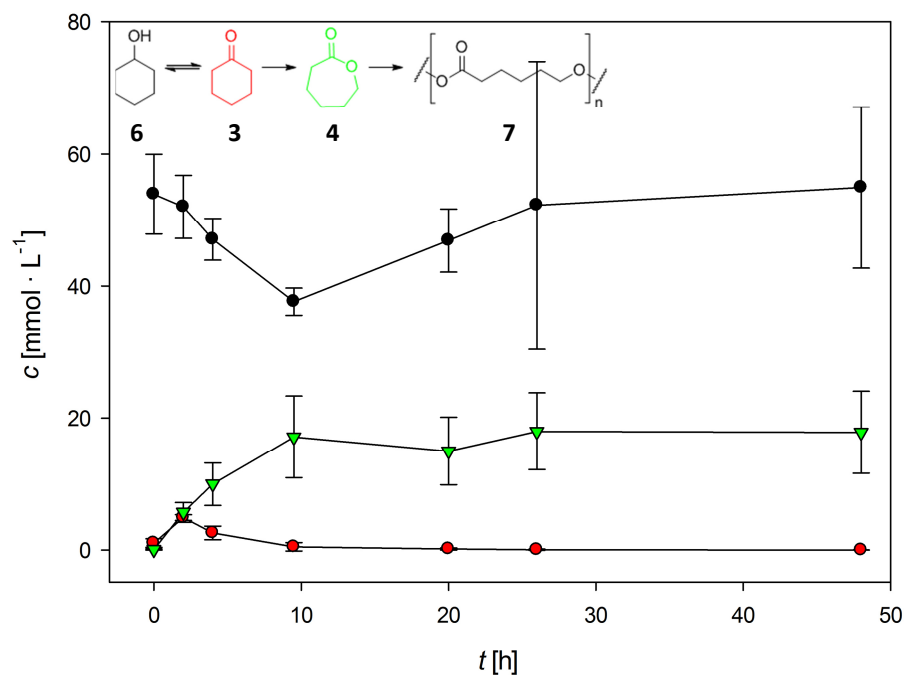


Figure 52: Reaction time course for co-immobilized cells (ratio LK-ADH:CHMO_{QM}=1:10) and CAL-A (setup 1). Substrate **6** was fed over 16 h up to 200 $\text{mmol} \cdot \text{L}^{-1}$, initial concentration: 60 $\text{mmol} \cdot \text{L}^{-1}$ (black: **6**, red: **3**, green: **4**; $n=3$).

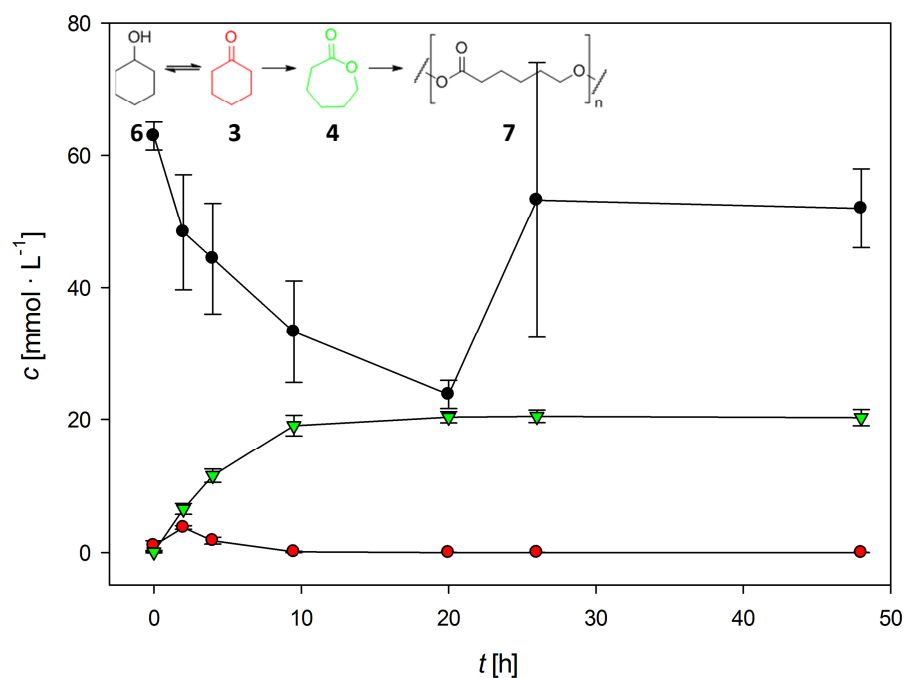


Figure 53: Reaction time course for immobilized cells (ratio LK-ADH:CHMO_{QM}=1:10) and external CAL-A (setup 2). Substrate **6** was fed over 16 h up to 200 $\text{mmol} \cdot \text{L}^{-1}$, initial concentration: 60 $\text{mmol} \cdot \text{L}^{-1}$ (black: **6**, red: **3**, green: **4**; $n=3$).

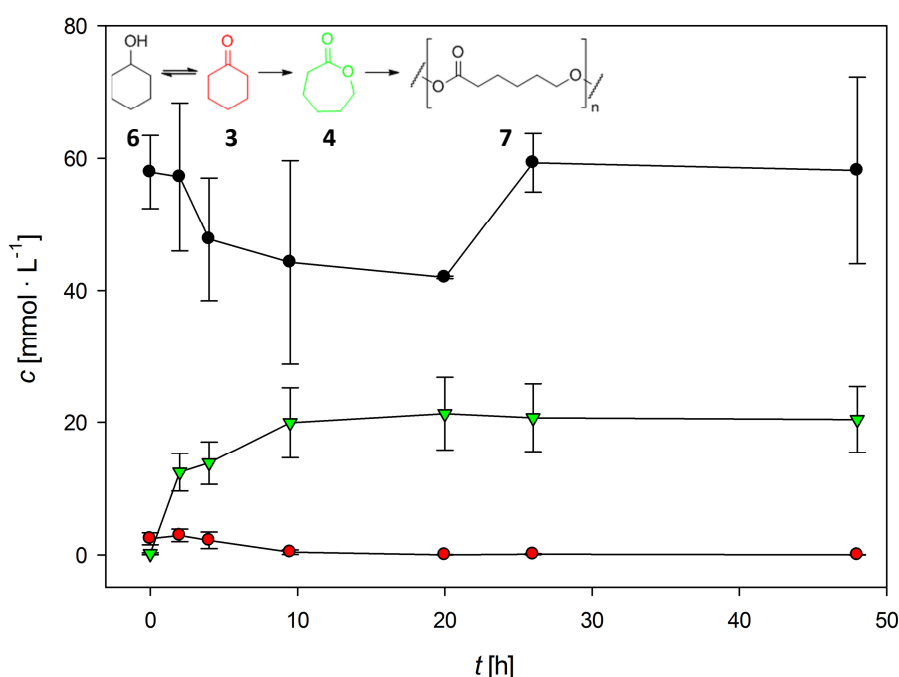


Figure 54: Reaction time course for free cells (ratio LK-ADH:CHMO_{QM}=1:10) and external CAL-A (setup 3). Substrate **6** was fed over 16 h up to 200 mmol · L⁻¹, initial concentration: 60 mmol · L⁻¹ (black: **6**, red: **3**, green: **4**; n=3).

Since the ADH reaction seemed to be the limiting step in the reaction due to the observed final concentrations of **6** after 48 h in the first experiments, the ratio of the cells was raised to LK-ADH:CHMO_{QM} = 1:5. The encapsulation and the biocatalysis reaction were carried out as described before. Furthermore, the reaction time was elongated until 96 h to increase the chance that the substrate was consumed completely.

Unexpectedly in all setups the substrate **6** still was detected after 96 h in concentrations from 40 - 53 mmol · L⁻¹ (Figure 55 - 58). In this case, the concentration first decreased within 6 - 20 h down to 4 - 7 mmol · L⁻¹ and after that it showed an increase up to the final values mentioned before. The concentrations of the two intermediates **3** and **4** showed a comparable behavior to the first experiments. Whereas **3** could be hardly detected at all, intermediate **4** showed a stable concentration of 9 - 12 mmol · L⁻¹ already after 4 h. Again the final oligomeric product was not isolated due to the high substrate concentrations. Nevertheless, the final theoretical yield based on substrate depletion could be increased up to 74 - 80%.

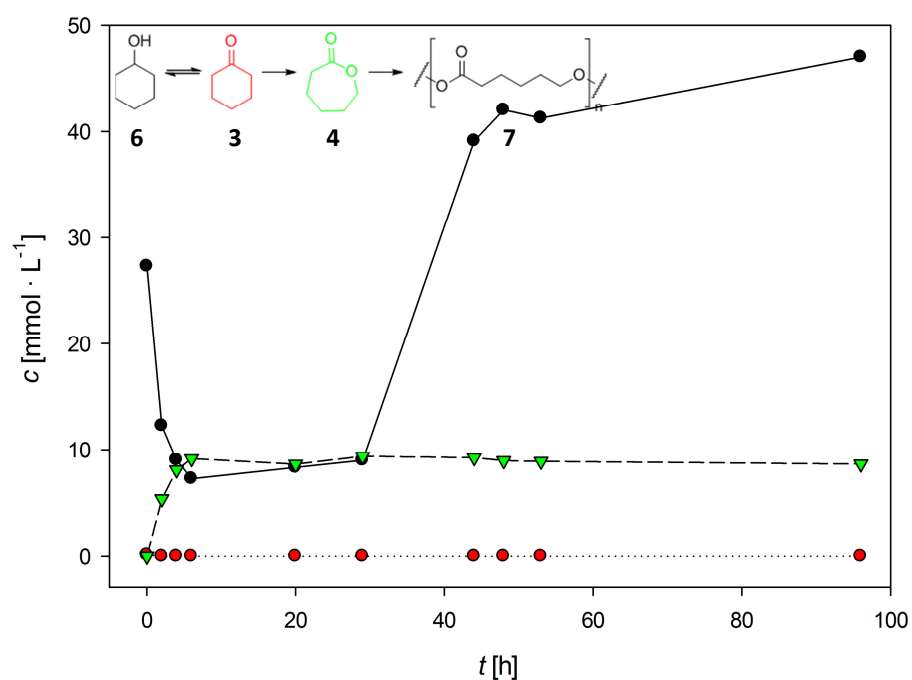


Figure 55: Reaction time course for co-immobilized cells (ratio LK-ADH:CHMO_{QM}=1:5) and CAL-A (setup 1). Substrate **6** was fed over 16 h up to 200 mmol · L⁻¹, initial concentration: 60 mmol · L⁻¹ (black: **6**, red: **3**, green: **4**).

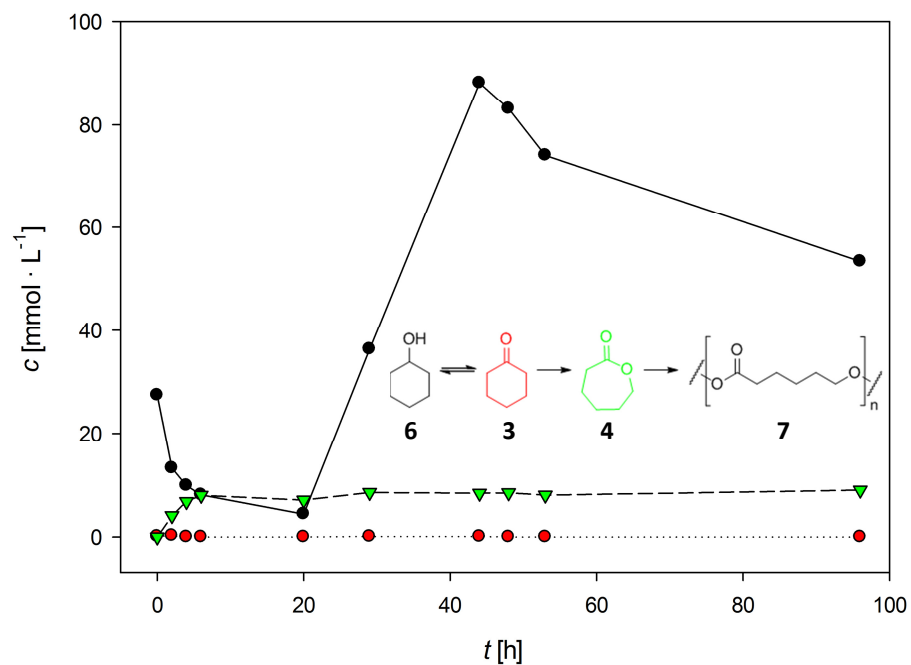


Figure 56: Reaction time course for immobilized cells (ratio LK-ADH:CHMO_{QM}=1:5) and external CAL-A (setup 2). Substrate **6** was fed over 16 h up to 200 mmol · L⁻¹, initial concentration: 60 mmol · L⁻¹ (black: **6**, red: **3**, green: **4**).

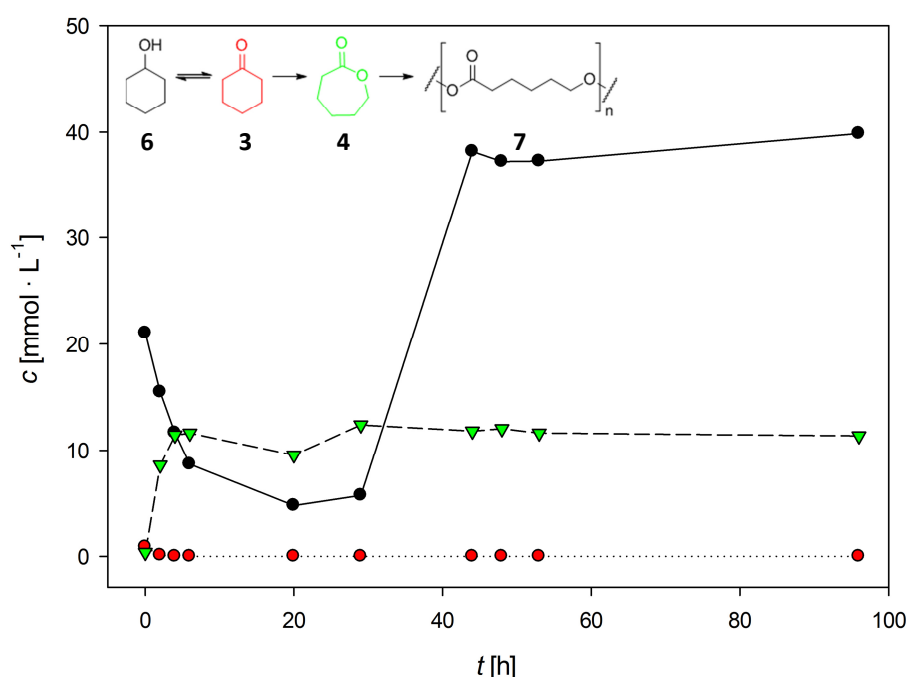


Figure 57: Reaction time course for free cells (ratio LK-ADH:CHMO_{QM}=1:5) and external CAL-A (setup 3). Substrate **6** was fed over 16 h up to 200 mmol · L⁻¹, initial concentration: 60 mmol · L⁻¹ (black: **6**, red: **3**, green: **4**).

The previous results have shown that an increase of the ratio LK-ADH:CHMO_{QM} only slightly improved the reaction behavior. That was why the ratio of LK-ADH:CHMO_{QM} was changed again to 1:2. Additionally, after 24 h an exchange of the cells with freshly prepared ones was carried out to exclude that the enzymes were inactivated during that time. For all these experiments the setup 2 (Figure 51) was used, because the general influence of the varied parameters was subject to the investigation. Furthermore, the substrate-feed initial concentration of **6** was lowered to 0 mmol · L⁻¹, because experiments from Christian Scherkus (Institute of Technical Biocatalysis, Technical University Hamburg-Harburg) revealed that the activity of the CHMO was already severely impaired at 5 mmol · L⁻¹ of **6**.

Comparison of Figure 56 and Figure 58 reveals, that changing the cell ratio from 1:5 to 1:2 and decreasing the initial concentration of the substrate-feed led to no improvement of the reaction time course. The concentration of **6** after 24 h was found to be 84 mmol · L⁻¹, which was even higher compared to the previous experiment (Figure 56), although the intermediates **3** and **4** were detected in low concentrations up to 3 mmol · L⁻¹. In the end, changing the cell ratio to 1:2 did not further improve the reaction.

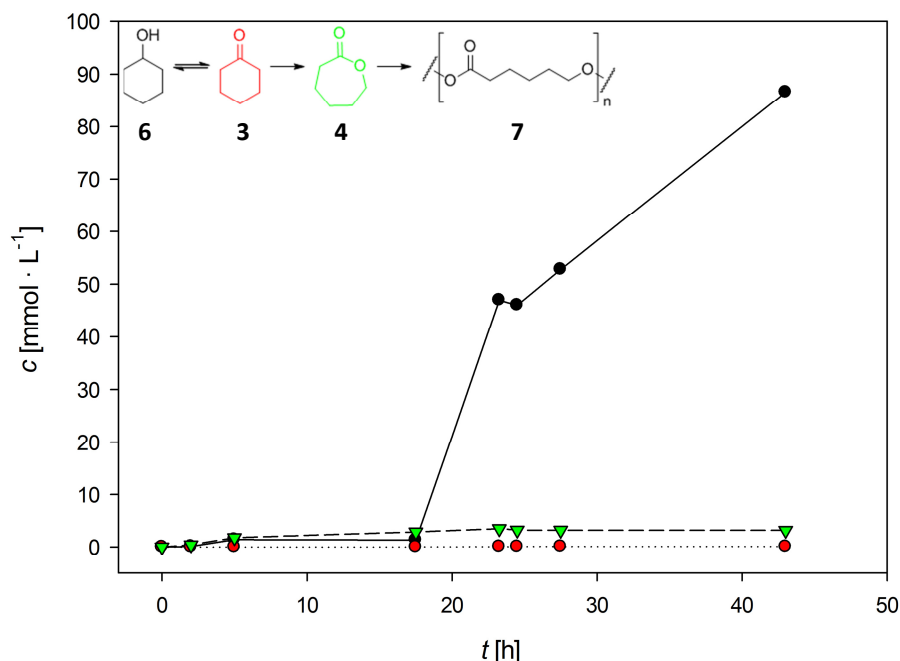


Figure 58: Reaction time course for immobilized cells (ratio LK-ADH:CHMO_{QM}=1:2) and external CAL-A (setup 2) without exchange of cells after 24 h. Substrate **6** was fed over 16 h up to 200 mmol · L⁻¹, initial concentration: 0 mmol · L⁻¹ (black: **6**, red: **3**, green: **4**).

In contrast, an exchange of the cells in the reactor after 24 h with freshly prepared ones led to a distinct improvement of the reaction. When using a cell ratio of 1:2 (Figure 59) the concentration of substrate **6** was 24 mmol · L⁻¹ and the ones of the intermediates **3** and **4** were <1.6 mmol · L⁻¹. Changing the ratio to 1:5 (Figure 60) led to further improvement in terms of residual substrate concentration, which in this case was 14 mmol · L⁻¹ after 24 h. Also the intermediate **3** was not observed at all and the intermediate **4** had a maximum concentration of 3 mmol · L⁻¹. Interestingly, the concentration of substrate **6** was almost 0 mmol · L⁻¹ up to 28 h, which was the point of time where the substrate-feed was already finished for at least 10 h. After that in both experiments the concentration increased again to its final value. Possibly substrate **6** accumulated by adsorption in one of the reactor parts and was slowly released over the last 15 h of reaction.

In summary, by the exchange of cells after 24 h the yield based on substrate depletion was increased to 88 - 93%.

To sum up this last part of the results, the most promising ones so far were obtained in a reaction, in which the cells were replaced after 24 h with fresh ones. Furthermore, the feasibility of a rotating bed reactor (SpinChem[®]) was demonstrated for single and cascade biocatalytic reactions, especially with respect to stabilization and protection of the catalyst particles. Also the immobilization process itself was simplified and optimized by the establishment of a gas-shear device, which improved the oxygen transfer within the capsules, and the *in situ* encapsulation process, which especially saved a lot of time.

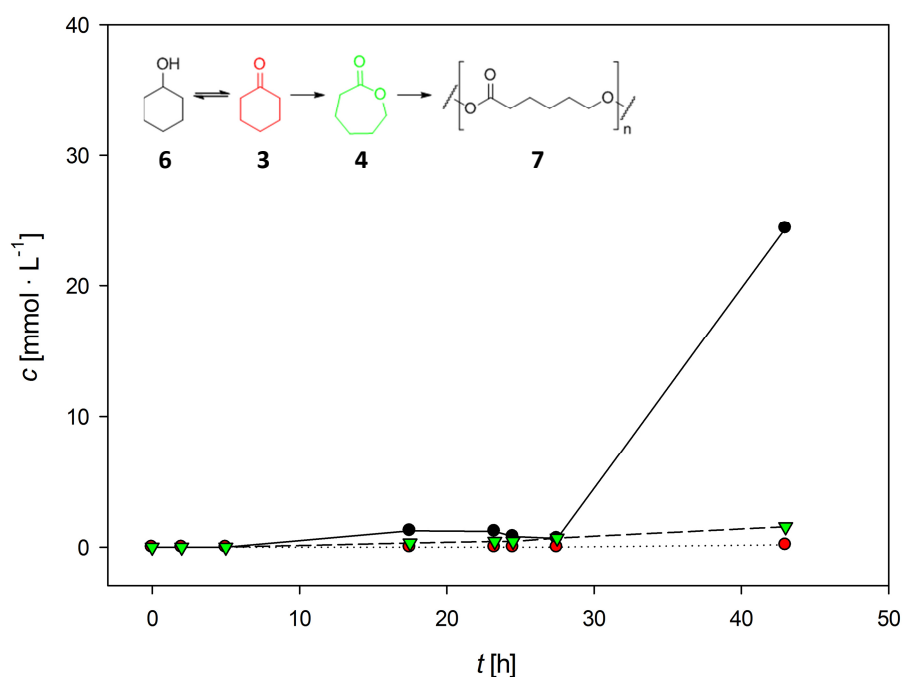


Figure 59: Reaction time course for immobilized cells (ratio LK-ADH:CHMO_{QM}=1:2) and external CAL-A (setup 2) with exchange of cells after 24 h. Substrate **6** was fed over 16 h up to 200 mmol · L⁻¹, initial concentration: 0 mmol · L⁻¹ (black: **6**, red: **3**, green: **4**).

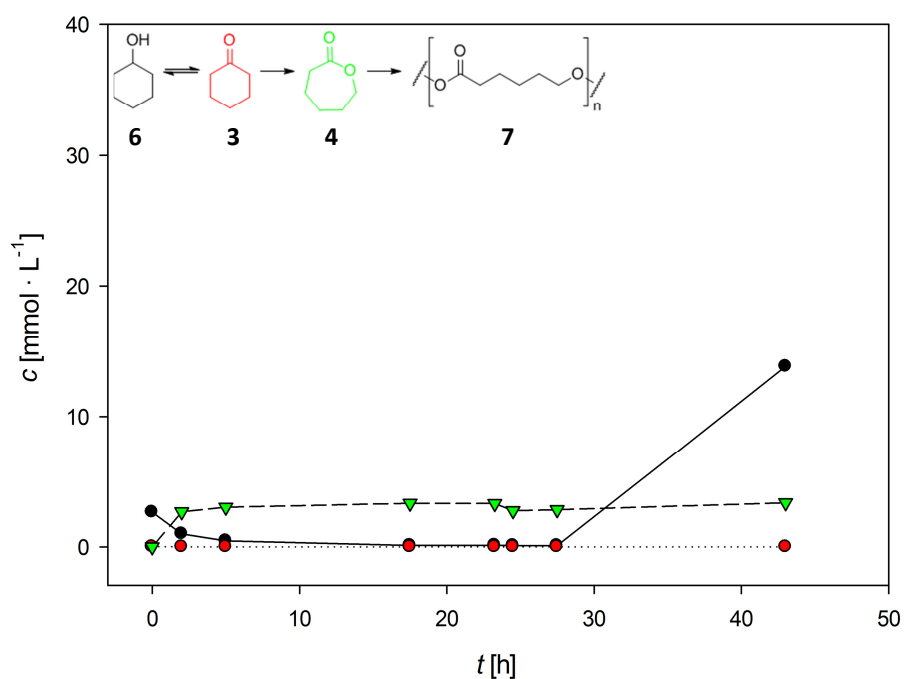


Figure 60: Reaction time course for immobilized cells (ratio LK-ADH:CHMO_{QM}=1:5) and external CAL-A (setup 2) with exchange of cells after 24 h. Substrate **6** was fed over 16 h up to 200 mmol · L⁻¹, initial concentration: 0 mmol · L⁻¹ (black: **6**, red: **3**, green: **4**).

And this?

What is this for?

It's blue light.

What does it do?

It turns blue.

I see.

(Rambo III, 1988)

4 Discussion

4.1 Co-Expression of Three Enzymes for Cascade Optimization

The *in vivo* three enzyme cascade described above (Figure 10) was subject to further optimization by establishment of a co-expression system based on a single plasmid. Thereby, the metabolic burden for the host organism was expected to be lowered due to the fact that only one plasmid has to be maintained. In her PhD thesis, Christin Peters already established the co-expression of all three enzymes using a two plasmid strategy.^[207] Therefore, she simply cloned the respective OYE gene with an additional ribosome binding side between the BVMO gene and the terminator, which results in an operon expression mode. Here the expression of the CHMO was expected to be the highest one, but for the combination of CHMO and XenB the opposite result was found. As also observed in this thesis CHMO and OYE1 could not be discriminated in SDS-PAGE analysis due to their similar molecular weights, so that for this combination the co-expression could not be evaluated properly. When combining the plasmids carrying two genes with the one carrying only the ADH gene, the co-expression of OYE and BVMO was not impaired, although the expression of the ADHs from separate vectors was observed to be much higher. Nevertheless, in cooperation with the project partners Nikolin Oberleitner, Florian Rudroff and Marko D. Mihovilovic (Vienna Technical University, Austria), the feasibility of the recombinant *E. coli* strains was demonstrated for the above described cascade reaction (Figure 10).

In this work a single plasmid carrying all three genes (LK-ADH, OYE1, CHMO_{DM}) for co-expression in a pseudo-operon mode was successfully constructed and further used for biocatalysis reactions to demonstrate its general feasibility. By SDS-PAGE analysis it was observed that the expression for all possible arrangements of the genes differed significantly. From these results only the constructs LCO and CLO were expected to have a thorough activity towards the model substrate **1**, out of which the LCO-construct had the highest activity with $15.3 \pm 1.2 \text{ U} \cdot \text{g}_{\text{CDW}}^{-1}$, so that this construct (LCO) could be identified as best variant in the co-expression screening. Especially the analysis of the substrate, intermediate and product concentrations after 24 h revealed that for the other construct (CLO) obviously the ADH was not expressed sufficiently, although a significant amount of soluble protein was found in the SDS-PAGE analysis. In reactions using most of the other less active constructs (COL, LOC, OCL) and also for LCO and the separately expressed enzymes (L+O+C), side-product **5** was found with up to $11 \text{ mmol} \cdot \text{L}^{-1}$, thus leading to the assumption that the CHMO_{DM} was the rate-limiting enzyme in these cases. As already mentioned above (Chapter 1.1.5) it is well known that the CHMO_{DM} has only low thermo- and oxidative stability, which was very probable the reason for the low activity, if the CHMO was expressed at all. Implementation of an even more stable variant (e.g. as described by Schmidt *et al.*^[88a] or van Beek *et al.*^[88c]) for sure would lead to higher product concentrations especially for long-term reactions. Furthermore, the application of an *in situ* product removal system (e.g. *in situ* polymerization^[28, 177] or absorption^[208]) might nullify the inhibitory effects for the CHMO, although at the used concentrations this enzyme usually not yet underlies this negative effect. In literature the CHMO was described to tolerate up to $60 \text{ mmol} \cdot \text{L}^{-1}$ **6** in combination with an ADH.^[110]

Likewise, the fact that ADHs often prefer the reductive reaction using ketones also has been described.^[111] So that it was not surprising that significant amounts of **5** were detected, especially because the ADH expression was in general quite high. One solution to this problem is obviously to find an ADH, which prefers the oxidative reaction from the alcohol to the ketone, but this might be rather difficult. Also the creation of an ADH mutant by protein engineering with respect to the same purpose is probably difficult. However, lowering the expression of this enzyme by the use of a weaker promoter than for the other ones might lead to avoidance of the observed side-reaction. Alternatively, the detected substances using the cells containing only one single enzyme (Figure 23) suggests that separating the ADH from the other enzymes contributes to avoidance of the unwanted side-reaction as only low amounts of **5** were found here.

Furthermore, in four reactions (COL, LOC, OCL, L+O+C) the intermediate **2** was found in high concentrations up to $9 \text{ mmol} \cdot \text{L}^{-1}$. In these cases the OYE1 either seemed to be inhibited by the substrate and/or product or the expression of it was too low. The data collected for the mixed approach using resting cells with the singly expressed enzymes suggests that the OYE1 indeed might be inhibited by the substrate and/or product, because the measured concentration of intermediate **2** was quite high, although the expression of the enzyme was very high. Of course for this problem the same concepts for improvement might be applied as for the ADH, except that in this case a higher expression of the OYE1 would be desirable to further drive the reaction towards the formation of intermediate **3**.

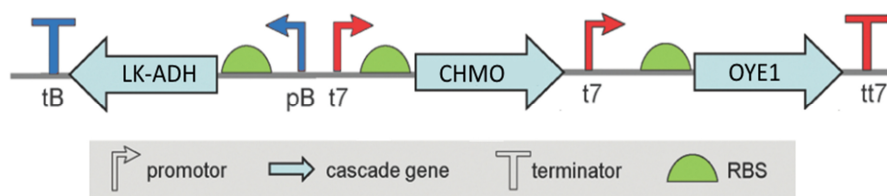


Figure 61: Proposed construct for co-expression of LK-ADH, CHMO and OYE1 (tB: terminator *rrnBT2*, pB: arabinose-inducible promoter *pBAD*, t7: IPTG-inducible *T7/lacO* promoter, tt7: *T7* terminator).

As suggestion for further studies the above construct for co-expression of all three enzymes was proposed (Figure 61). There, the CHMO and OYE1 would be individually under the control of a strong *T7* promoter resulting in pseudo-operon mode expression, which was also used for the original LCO construct. The only change made to this was the inversion of the LK-ADH gene, for which the promoter was changed to the weaker *pBAD* system. An alternative would be a comparable vector, which facilitates an operon mode expression of CHMO and OYE1 under the same *T7* promoter as described by Christin Peters, because this way also high activities were reached.

Although the proposed expression construct was designed rationally, the prediction of the optimal pathway arrangement is up to now very difficult and based only on empirical findings. At least for co-factor independent enzymes an algorithm for the prediction of *in vivo* cascade activities was recently developed by the Damborsky group.^[209] These scientists succeeded in optimizing an *in vivo* cascade for 1,2,3-trichloropropane detoxification by first predicting the optimal intracellular ratios of the involved enzymes by the developed algorithm and verification of these results by

expression using the Duet-vectors from Novagen. Nevertheless, this algorithm cannot be applied for co-factor dependent enzymes according to one of the authors, so that it was not possible to apply it for the cascade reactions used in this thesis.

Other possibilities for balancing the intracellular enzyme levels are fusion engineering (see Chapter 1.2.2), which was already carried out for the described cascade by Christin Peters, or intracellular immobilization of the enzymes by scaffolding. Especially using the latter one should be a very promising approach, because in theory the number of the individual scaffold domains, on which the enzymes are immobilized, could be shuffled and arranged to any necessary extent. The only limitation, which has to be faced when using this method, is the geometrical shape. Usually the scaffolds used so far are only one- (polypeptide chains, DNA or RNA strands)^[151a, 151c, 152a, 153, 210] or two-dimensional ('DNA-origami'),^[152b] but of course a three-dimensional scaffold might be beneficial. The above mentioned bacterial microcompartments are such a scaffold.^[150a-g, 150i-k, 152b] However, only little is known about the exact placement of the enzymes inside the 'protein cage', which makes the design again less rational.

In summary, when working on co-expression optimization there is unfortunately no way to circumvent the classical trial-and-error principle until the prediction tools are also applicable to a broader range of enzymes. Furthermore, the results obtained suggest that next to expression optimization also protein engineering strategies should be applied to open up the identified bottlenecks. Nevertheless, one construct with improved activity for co-expression using the single plasmid strategy in pseudo-operon mode was identified and therefore the basis for further optimization was laid.

4.2 Extension of a Three-Enzyme Redox Cascade

4.2.1 ...by Cytochrome P450-Monooxygenases

By having a closer look at the established three-enzyme cascade (Figure 10) one obvious extension of this reaction would be an initial hydroxylation step. Especially the use of limonene as sustainable chiral precursor has drawn the attention of chemists in the last years, which would be also applicable in this cascade reaction as the use of carveol was already successfully demonstrated for this reaction. The most prominent enzymes for this purpose in biotechnology are P450s, above all the P450-BM3 from *Bacillus megaterium*. The applicability of this P450 and of a homologous one from *Bacillus licheniformis* (CYP102A7), which was described to have slightly better regioselectivity towards C6-hydroxylation,^[189] was studied in this thesis.

At first, the expression of CYP102A7 had to be established. First, it turned out that the use of conical flasks at slow shaking speed and the addition of δ -aminolevulinic acid (δ -ALA) upon induction were crucial for proper P450 expression. Usually baffled flasks are used for the standard expression protocols, especially for CHMO_{Acinetobacter} these ones significantly improved expression.^[208f, 211] This was linked to the high oxygen demand when expressing FAD-dependent enzymes. Unfortunately, the protocol was adopted for the initial P450 expression screenings, because these enzymes also are FAD-respectively FMN-dependent. However, obviously the higher oxygen supply induced by the baffles led to severe decrease of P450 expression. Probably the heme group, especially the coordinated iron, are somehow sensitive towards oxygen. Addition of δ -ALA to improve P450 expression was already described in literature.^[212] This effect

is due to the fact that δ -ALA is an intermediate in heme synthesis and supplementation of the medium leads to improved heme supply within the host.

Furthermore, expression at 30°C was better than at 17°C. In general, when using lower temperatures for protein expression, the amount of inclusion bodies formed is expected to decrease, because the expression rate is slowed down so that the proteins can fold more relaxed.^[213] Nevertheless, the lower temperature leads to an impaired biomass formation. This is no problem when the expressed enzymes are further purified, because the lack of biomass can be compensated by the quantity of cultivated cells. Probably this was also the case for the first characterization of CYP102A7, because there isolated enzyme was used.^[189] Hence, an optimized expression protocol was developed. Nevertheless, in this work the higher temperature was preferred. Especially the use of CO-difference spectra for quantification of the P450 amount enabled the discrimination between the results at 30°C and 17°C as SDS-PAGE analysis was not sufficient enough to do so.

The fact that active P450 was already detectable by eye as indicated by a dark blue color of the cell pellet, was probably due to the formation of indigo. This reaction by P450s is not a new one. It was already reported earlier that these enzymes can hydroxylate indole to indoxyl, of which two molecules react to the dimer indigo.^[214] Additionally it was reported that several P450s are inhibited by indole. Therefore, very recently the group of Rita Bernhardt developed an *E. coli* C43 knock-out strain for improved P450 expression, especially of indole-sensitive ones.^[215] The key to success in this study was the deletion of the gene *tnaA*, which encodes for the tryptophanase. The use of this strain might eventually further improve the P450 activity when used as whole cell catalyst.

The use of either a codon-optimized or the native gene sequence seemed to have not that high impact, because for both ones comparable activities were detected (Table 8). The same trend was observed for the applied His-tag, which could be positioned either at the N- or C-terminus. However, the enzyme without any tag showed significantly lower activities. Reasons for this effect are only speculative. As the N-terminus of the protein is rather closely located to the substrate tunnel, the effect of an N-terminal tag was expected to be more negative than the one of the C-terminal tag, which is located in the CPR domain of the enzyme. One possible explanation for the lower detected activity without tag could be the scavenging effect of reactive oxygen species by histidine,^[216] although this was not yet described for recombinant P450 expression.

After establishment and optimization of expression the P450s were characterized with respect to their regioselectivity by GC. Here it turned out that next to the desired C6-hydroxylation, also epoxidation of the 1,2-double bond and several other unidentified side-products were detected. However, these regio-unspecific reactions were not unknown to date (Figure 62). Although there were successful protein engineering attempts of P450-BM3 with regard to enhanced activity against limonene, the main product of reactions using the described mutants still was limonene-8,9-epoxide^[217] and until now there was no mutant described for the desired regioselective C6-hydroxylation. Only for the synthesis of perillyl alcohol **17** it was possible to create a highly regiospecific variant.^[218] On the contrary, CYP102A7 has not been used as scaffold for protein engineering, so that no hint for hotspots towards regioselectivity were available.

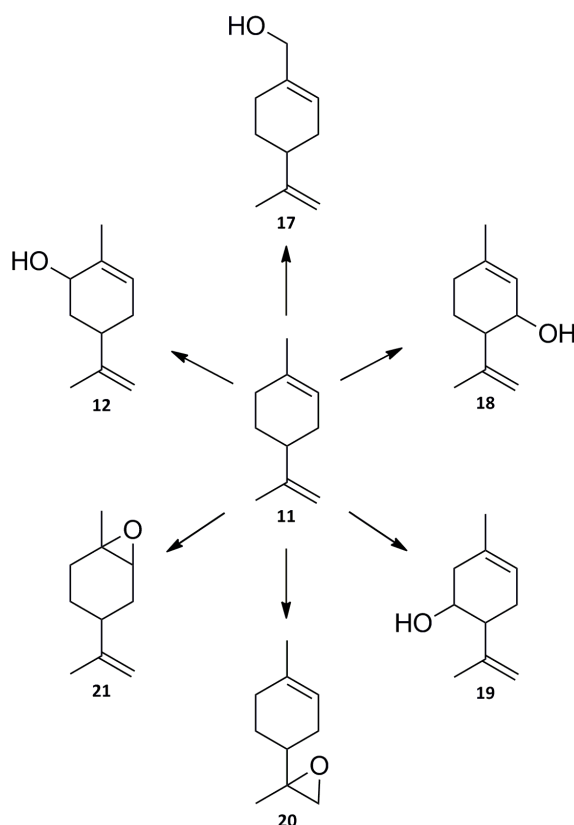


Figure 62: Possible side-products from P450 catalyzed hydroxylation (**11**: limonene, **12**: carveol, **17**: perillyl alcohol, **18**: isopiperitenol, **19**: *p*-menthan-1,8-dien-5-ol, **20**: limonene-8,9-epoxide, **21**: limonene-1,2-epoxide; adapted from ^[189, 219]).

However, there are some alternative enzymes with more specific activities described in literature. One of these is the natural carveol producing limonene-6-hydroxylase (L6H) from *Mentha spicata*, whose essential oil mainly consists of carvone.^[172] To provide a basis for future protein engineering of CYP102A7, possible hotspots responsible for regioselectivity were aimed to be identified by homology modeling of the L6H. Therefore, models of both enzymes were prepared using YASARA, which were further validated using MolProbity. Both models turned out to be acceptable for further analysis, although for L6H the first 15 amino acids were not modeled due to their flexibility. These residues belong to the N-terminal membrane anchor of the enzyme, which of course would also be of certain interest. But modeling the membrane-bound enzyme was by far too laborious for this purpose, so that the model was accepted without membrane anchor. By comparison of both models three loops were identified, which showed significantly different orientation, although according to sequence alignment these belonged to conserved regions (Figure 30 and Figure 31). However, as a matter of fact it is well known that sequence and structure alignments cannot always be compared directly. Therefore, the structure-guided superfamily alignment resulting in a so called 3DM database was developed recently^[220] and setting up of a P450 database would be of certain interest, because this way possible hotspots for control of regioselectivity might be found. The same concept can also be applied for the residues identified as involved in the formation of the distal heme environment. Especially the binding configuration of the heme propionate groups has drawn

attention (Figure 32) and creating a CYP102A7 or P450-BM3 variant with altered binding of the co-factor might be a promising candidate for further protein engineering. Furthermore, prediction of the substrate tunnels of both enzymes led to the conclusion that these are probably completely different (Figure 33). Interestingly, the calculated tunnels were mainly confined by the loops identified before, which further underlines their probable importance. The most interesting CYP102A7 or P450-BM3 variants would be the ones, which feature the alternative ‘tunnel system’ as observed in L6H instead of the native ones. Though introduction of the complete L6H substrate tunnel could have a severe impact on the protein structure, because this cannot be carried out by simply changing some amino acids, but by exchanging complete loops. This structural change might even be too strong to still get properly folded enzyme. An alternative to create a self-sufficient and regioselective P450 is the creation of a fusion enzyme consisting of the CPR from P450-BM3 and L6H. The prepared models already indicated that in theory the CPR domain could be fused to the C-terminus of L6H (Figure 31 C).

After the theoretical studies of L6H the expression of this enzyme was successfully established. However, the activity of L6H could not be reconstituted due to the missing reductase system. Unfortunately, one attempt for the identification of the natural redox chain by gene walking PCR was not further investigated, because only 1% of the identified sequence could be aligned to known ones. Furthermore, due to the fact that also the application of a foreign CPR from *Candida apicola* also failed, the studies involving P450s were stopped at this point. Instead a more promising hydroxylating system was established.

In summary, the expression of CYP102A7 was optimized with respect to sufficient intracellular P450 yield and a possible application of this enzyme and the P450-BM3 was validated. Also the recombinant expression of L6H in *E. coli* was established, which was not trivial since this enzyme is membrane-bound and derived from a plant organism. Finally, homology models of CYP102A7 and L6H suggested that fusion engineering of the L6H with the CPR of an enzyme from the self-sufficient P450s as well as the loop exchange within CYP102A7 or P450-BM3 with the ones from L6H building the substrate channel would be interesting starting points for future protein engineering attempts.

4.2.2 ...by Dioxygenases

This alternative system was the strain *Cellulosimicrobium cellulans* EB-8-4, for which the ability of C6-regioselective hydroxylation of limonene was described.^[195a] The strain was kindly provided by Prof. Dr. Zhi Li (National University of Singapore, Singapore). The results from their publication were reproduced and the ability of using ethyl benzene as sole carbon source was proven. Though the high optical densities described in the original publication were not reached. One fact that might be responsible for this discrepancy could be the different wavelengths (450 nm vs. 600 nm) used for determination of biomass. Nevertheless, the production of carveol from limonene was demonstrated only for ethyl benzene grown cells. To identify the enzyme responsible for this reaction the genome of *C. cellulans* EB-8-4 was partly sequenced in cooperation with Dr. Andrea Thürmer (Göttingen Genomics Laboratory, University of Göttingen). Therefore, the genomic DNA of glucose-grown cells was

isolated, because using this carbon source sufficient biomass could be generated in a reasonable time. After mapping the results to a reference genome by Dr. Johannes Kabisch (Institute of Biochemistry, University of Greifswald) no genes encoding potential oxygenases or other hydroxylating enzymes were found. At this point we got already curious and thought about different methods for identification.

In her M.Sc. thesis Katja Zorn analyzed the protein fractions of *C. cellulans* EB-8-4 either grown on glucose, ethyl benzene or both and could show that the ethyl benzene grown cells had a significant different protein pattern.^[198] That was why we decided to analyze the most prominent bands by ESI-MS in cooperation with Dr. Dirk Albrecht (Institute of Microbiology, University of Greifswald). None of the analyzed proteins could be connected to *Cellulosimicrobium* sp., but all of them were homologous to proteins from *Rhodococcus* sp. At that point it became clear, that a contaminant *Rhodococcus* strain was responsible for the observed hydroxylation reaction and not the *C. cellulans* EB-8-4! After identification of the gene sequence encoding the hydroxylating enzyme it turned out that a benzene-1,2-dioxygenase was responsible for the observed reaction, which was 100% identical to a dioxygenase cluster from *Rhodococcus opacus* B4! As attempts of recombinant expression in *E. coli* by Katja Zorn failed, it was decided to establish the expression in a different host. The expression at least of the small and large subunit of the cluster was successful using *Pseudomonas putida* S12 as host (Figure 39), which was reported to be suitable for expression of a homologous cluster (66.1% identity of the large subunits) from *P. putida* PWD32.^[102] Unfortunately, probably due to the missing expression of reductase and ferredoxin no activity of the cells towards carveol hydroxylation was detectable. Also the introduction of an additional arabinose-inducible promoter in front of the reductase gene did not lead to expression of the reductase, this even led to expression of none of the genes. As alternative the reductase and ferredoxin also might have been expressed under the control of a different promoter encoded on an additional plasmid. For example there is an alkane-inducible one (P_{alkB}) available, which is suitable for expression in *Pseudomonas* sp.^[221]

In summary, the desired cascade reaction was extended successfully to a certain extent by identification of a highly regioselective hydroxylating enzyme, which could be applied for mixed culture reactions for the production of chiral lactones by the project partner in Vienna. However, extending this cascade reaction with a hydroxylating enzyme might be compared to driving a car with the handbrake put on, because these enzymes are in comparison to the other ones very slow in activity. Nevertheless, when comparing the prices of the substrates and intermediates it might become obvious that the establishment of an initial hydroxylation is still of interest (Table 16). Especially the use of carveol as substrate is probably economically not feasible due to its limited availability and connected to that the high price, which is approx. eleven times higher than for *rac*-limonene. Instead carveone might be used directly as substrate, because the prices of the pure enantiomers is only two to six times higher than the respective pure limonene enantiomers.

Table 16: Prices of the substrates and intermediates used for the production of chiral lactones.

Substance	Price [€ · kg ⁻¹]	Reference
(<i>R</i>)-limonene	18.35	a
(<i>S</i>)-limonene	31.88	a
<i>rac</i> -limonene	26.58	a
(-)- <i>cis/trans</i> -carveol	304.00	a
(<i>R</i>)-(-)-carvone	64.00	a
(<i>S</i>)-(+)-carvone	108.80	a
Refined sugar	0.29	b

^aSigma-Aldrich, 2016-03-09^bDeutsche Bank Indikation, 2016-03-09

However, due to the fact that in the last years the limonene biosynthesis pathway was successfully transferred into *E. coli*, the use of sugar or even crude glycerol as substrate for the cascade was enabled.^[222] Especially the production of **17** from these raw materials was successfully implemented by combination of limonene formation and a regiospecific P450 by the working group of Andreas Schmid,^[223] so that coupling of the cascade reaction described here with the limonene producing strain would be an interesting continuation of this project.

4.3 Immobilization of Two Enzymes for Cascade Reactions

As third part of this thesis a cascade reaction for the production of oligo-[caprolactone] (Scheme 14) was aimed to be further optimized by immobilization of the enzymes. Especially the use of a rotating bed reactor (RBR) should be enabled, because the feasibility of this reactor system with respect to recyclability of the catalysts was also shown during this thesis.

Preliminary studies were carried out to demonstrate the general applicability of biocatalysts using an RBR. Therefore, at first the optimal stirring speed of the SpinChem[®] was determined by biocatalysis reactions using the CHMO_{Acineto} and the commercially available lipase CAL-B (Novozyme[®] 435). Unexpectedly, the stirring speed showed no high impact on the conversion. The conversion decreased only very few when using higher spinning rates, so that we decided to use the manufacturer recommendation of 500 rpm for the reactions as standard. However, especially the use of rates >750 rpm led to severe entry of air bubbles into the liquid, which was in general unwanted due to the impaired mass transfer observed when air is going into the voids.

The first model reaction to be studied was the CHMO_{Acineto} catalyzed formation of ϵ -caprolactone **4** from cyclohexanone **3** (Scheme 19) by alginate encapsulated cells carrying the enzyme. In direct comparison of the studied reactor setups the RBR and STR showed the same performance in long-time reactions over 48 h resulting in 66% to 69% conversion respectively. Only the FBR was very insufficient for the use of alginate encapsulated catalysts (Figure 41), which was probably due to the already mentioned drawbacks of such a reactor (Chapter 1.3.2). Especially the squeezability of the alginate beads was a problem, because these were destroyed during the reaction time due to the high occurring pressures. Nevertheless, the RBR's feasibility was definitively shown in recycling studies. Although the catalyst activity in general dropped

down a lot, the one used in RBR still had an approx. three times higher residual activity of 41% than the one used in STR, which showed a residual activity of 13%. The general high activity loss can be explained by the low stability of the CHMO_{Acineto}. However, the advantage of the RBR was obviously the fact that the used particles are protected from any mechanical forces and therefore the morphology is kept. This was not the case for the simply stirred reaction, where the alginate beads were completely destroyed after the 6th batch. Furthermore, the recovery of the catalyst from the RBR was much simpler than for the STR.

Due to the fact that in the desired cascade reaction also a lipase was involved, the general applicability of an immobilized one was demonstrated using the model reaction shown in Scheme 20. Again the comparison of STR and RBR resulted in approx. the same performance in reactions over 4 h with conversions of 45% to 46% respectively and the superiority of the RBR became obvious in recycling studies, although the difference was not as distinct as for the BVMO reaction and even reached the same residual activities of 60% after the 5th batch. At this point probably the only loosely adsorbed lipase molecules were washed away and the tightly bound ones remained. The fact that a kind of minimum residual activity was already reached after the third batch when using the STR underlines this conclusion, so that in this case the use of the RBR simply slowed down the process of leaching from the particles. This is of course again a positive effect.

For further optimization of the catalyst's activity a gas-shear device was applied. Obviously the mass transfer of substrate and/or oxygen inside the large alginate beads produced by the classical 'drop-method' was the reason for the low immobilization yield with respect to activity, because the smaller capsules indeed led to higher activities (Figure 48). Of course decreasing the particle size is a well-known method for improving mass transfer,^[224] but often the expensive equipment for microencapsulation in standard biocatalysis laboratories is missing. Hence, a self-made gas shear device was set up in this thesis using simple laboratory equipment and consumables. As alternative immobilization method very recently the use of so called catalytic 'teabags' and their application in an RBR was described by J. Wachtmeister, *et al.*^[225] In that work the 'teabag' principle even was described to outperform the alginate immobilized catalysts using a cascade reaction featuring a carboligase coupled with an ADH. However, due to the fact that the alginate beads were not compatible with the optimized micro-aqueous reaction conditions, these were used in a non optimal setup, which might have had a negative influence on the catalyst's performance in these reactions. Nevertheless, the 'teabag' principle might also be interesting to the cascade studied in this thesis, because the procedure of immobilizing cells is in this case also very simple.

Despite the fact that the smaller capsules indeed led to improved mass transfer and thereby also to enhanced activity, the reduction of one preparative step before reaction further improved the work-flow. With the now significant smaller capsules it was possible to transfer the immobilization into an *in situ* process, in which the voids of the RBR were packed automatically with the beads formed in the reaction solution. So that now after optimization of the immobilization procedure and the work-flow these could be applied for the described cascade reaction, of which the setting up is expected to be carried out much easier and especially faster by application of the developed procedure.

Therefore, two different approaches of immobilization were investigated and compared to the non-immobilized cells (Figure 51). The main problem, which came up in the first reactions, was the high residual concentration of substrate after 48 h. Here, there were still approx. 60 mM of **6** detectable. Changing the ratio of ADH:BVMO from 1:10 to 1:5 or even 1:2 only slightly improved the reaction performance resulting in residual 40 - 53 mmol · L⁻¹ of **6**. One fact that might have been the rate-limiting factor was probably the high initial substrate concentration, for which it was reported that already 5 mmol · L⁻¹ lead to decreased activity of the CHMO.^[226] That was why the subsequent reactions were carried out using a continuous substrate feed with an initial concentration of 0 mmol · L⁻¹. However, one of the catalysts still seemed to be a rate-limiting factor, because only the exchange of the immobilized cells after 24 h further improved the conversion over 48 h, so that only 14 mmol · L⁻¹ of **6** was left, which resembled based on substrate depletion 93% conversion.

The already described side-activity of the LK-ADH, which prefers the reduction of **3** to **6**,^[111] might be one explanation of the high concentrations of residual substrate as observed in the first reactions. In theory, if the activity of the CHMO was too low, the ADH might simply be catalyzing a so called futile circle, in which the formation of **3** is followed by its reduction again to **6** due to the favored equilibrium by the ADH. To further drive the reaction into the formation of **3**, the overall activities of the CHMO and also of the lipase have to be improved. Although the lipase has really good acyltransferase activity in organic solvent, the one in water is probably not as high as desired. This especially was observed in follow-up studies carried out at one of the project partners, Enzymical^S AG (Greifswald, Germany), where solely the oligomerization reaction was studied using **4** as substrate and the lipase as catalyst in a phosphate buffered system (pH 8) at 30°C. There it turned out that only <50% of 1 mol · L⁻¹ **4** were depleted after five days. Furthermore, at that point it was discovered that the pH severely dropped to approx. 4, at which of course neither the ADH nor the BVMO nor the lipase are still active. So that for future studies the most important parameter to control obviously is the pH value. The simplest way doing this would be the use of a NaHCO₃ solution as reaction medium as reported by Süß *et al.*, because the bicarbonate is able to effectively scavenge protons resulting in the release of CO₂.^[227] Indeed application of this reaction medium for the same reaction and raising the temperature to 50°C led to almost complete conversion after five days. But following studies revealed that the activity of the BVMO and the ADH are significantly lower in this reaction medium, so that in conclusion the pH can only be effectively controlled by titration applying the respective instrumental setup.

Alternatively, a different lipase might be applied for further improvement. The CAL-A is not the only lipase, for which acyltransferase activity in aqueous medium was described. As suggestion also the lipases from *Candida parapsilosis*^[27a, 27b, 27f, 27g] and the one from *Aeromonas hydrophila*^[27h-j] should also be tested for the desired oligomerization reaction. Especially the lipase 2 from *Candida parapsilosis* and the lipase 4 from *Candida tropicalis* exhibited beside the acyltransferase activity in aqueous medium also temperature optima between 30 and 40°C.^[27e] This might be beneficial since the applied CAL-A has a very high temperature optimum >50°C and loses a lot of its activity at temperatures below that.

Furthermore, the oligomers obtained from the sole lipase reaction were used for the production of a prototype PCL. Unfortunately, the PCL produced from the biocatalytically synthesized oligomers were completely unstable due to high amounts

of protein present in the extracted product. In conclusion for transfer of this process into an industrial environment a procedure of effective protein removal has to be developed, which is not trivial as the desired product is acid sensitive. One alternative obviously would be the use of an immobilized lipase instead of the lyophilized one. Of course these were also tested for application in the RBR, but the activity of these are not sufficient for reactions in aqueous media respectively the weight, which can be used, is limited to the available space inside the SpinChem[®]. A promising alternative could be the use of the 'teabag' principle^[225] for immobilization of the lyophilized lipase, if the mesh size of the used material is small enough. Furthermore, the available CLEA preparations of lipases also should be considered, because these are described to have a higher activity than the adsorptive immobilized catalysts.^[228]

So that in summary the way towards a biological process for the synthesis of PCL precursors is paved now and with additional optimizations it might be transferred into an industrial environment at some point in the future. Especially the development of the *in situ* encapsulation process, which in theory might be scaled up to very large volumes, contributed to simplifying of the work-flow and therefore to process intensification. Furthermore, the general demonstration of the RBR's feasibility for enzymatic reactions revealed its superiority to conventional reactor setups and finally the immobilization yield of Ca-alginate encapsulated cells by application of a gas-shear device was significantly improved.

5 Summary

Cascade reactions are not only of interest to chemists and biotechnologists, but also to life in general, because every metabolic reaction resembles a cascade reaction. This principle of substrate/intermediate channeling was only adapted by scientists. That way especially one-pot reactions became very attractive as for this no isolation of intermediates is necessary. Furthermore, unstable or toxic intermediates are only produced in low amounts and directly transformed *in situ*.

In this PhD thesis two previously established cascade reactions were subject of further optimization.

In the first part, a cascade reaction established in a DFG-funded project (Bo1862/6-1) in cooperation with the Vienna Technical University (Austria) for the production of chiral lactones was further optimized and extended. Therefore, on the one hand the genes encoding the needed enzymes were cloned for co-expression into a single plasmid in different arrangements to be expressed in pseudo-operon mode, with the aim to lower the metabolic burden of the cascade host cell. One out of the twelve created constructs showed a reasonable activity of $15.3 \pm 1.2 \text{ U} \cdot \text{g}_{\text{CDW}}^{-1}$.

On the other hand, this cascade reaction was aimed to be extended by the use of a hydroxylating enzyme to enable the use of limonene as renewable and chiral precursor for the proposed production of chiral polymers. Therefore, the feasibility of cytochrome P450-monooxygenases was studied. These turned out to be not applicable due to their bad regioselectivity for the hydroxylation of limonene or due to the difficulties of activity reconstitution. As alternative system for an initial hydroxylation step the use of a *Rhodococcus equi* strain, which was isolated from *Cellulosimicrobium cellulans* EB-8-4 and which is capable of very regioselective limonene-hydroxylation, was investigated. Therefore, the dioxygenase cluster responsible for the desired reaction was identified and especially the recombinant expression in a suitable host (*Pseudomonas putida* S12) was further studied. The results from these experiments revealed that the recombinant expression needs to be further optimized to enable the use of the recombinant dioxygenase in combination with the other enzymes for cascade reactions.

The third part of this PhD thesis dealt with the immobilization of an established cascade reaction for the synthesis of poly-[caprolactone] precursors. Therefore, the use of a rotating bed reactor (RBR) was investigated. Preliminary studies using single enzymes involved in the desired cascade reaction demonstrated the general feasibility of this reactor concept. Especially the reusability of the catalysts was highly improved, because the catalytic particles were protected very effectively from mechanical forces within the voids of the reactor. For further work-flow optimization the immobilization was transformed into an *in situ* process by the application of a gas-shear device, which leads to decreased capsule size and thereby to increased mass transfer inside the particles. The developed methods were applied for encapsulation of the cells containing the enzymes needed for the reaction. After additional improvement of the reaction parameters a conversion of 93% (based on substrate depletion) was reached using catalysts produced by the established encapsulation procedure.

In summary, the described cascade reactions were successfully optimized by either co-expression, extension applying a dioxygenase or immobilization. Furthermore, the general feasibility of an RBR was demonstrated.

5 Zusammenfassung

Kaskadenreaktionen sind nicht nur für Chemiker und Biotechnologen von großem Interesse, sondern auch für Lebensprozesse im allgemeinen, da jede metabolische Reaktion auch eine Reaktionskaskade ist. Dieses Prinzip der Substrat-/Intermediatweiterleitung wurde nun von Wissenschaftlern adaptiert. Auf diese Weise wurden besonders sog. ‚Eintopfreaktionen‘ sehr attraktiv, da hierfür keine Reinigung der Zwischenprodukte mehr notwendig ist. Darüber hinaus werden instabile und/oder toxische Zwischenprodukte nur in geringen Mengen gebildet und *in situ* direkt umgewandelt.

In dieser Doktorarbeit wurden zwei bereits entwickelte Enzymkaskaden einer weiteren Optimierung unterzogen.

Im ersten Teil wurde eine Redoxkaskade für die Synthese von chiralen Laktonen, die im Rahmen eines DFG-geförderten Projekts (Bo1862/6-1) in Zusammenarbeit mit der Technischen Universität Wien (Österreich) entwickelt wurde, optimiert und erweitert. Hierfür wurden einerseits die Gene, die die benötigten Enzyme kodieren, zusammen in allen möglichen Anordnungen auf ein Plasmid kloniert, um diese anschließend im Pseudo-Operon Modus zu exprimieren. Hiermit sollte der metabolische Stress für die Wirtszelle verringert werden. Eines der zwölf erstellten Konstrukte zeigte eine angemessene Aktivität von $15,3 \text{ U} \cdot \text{g}_{\text{CDW}}^{-1}$.

Andererseits sollte dieselbe Kaskade um eine initiale und enzymatische Hydroxylierung erweitert werden, um Limonen als nachwachsendes und chirales Substratmolekül zu verwenden. Dafür wurde zum einen die Anwendbarkeit von Cytochrom P450-Monooxygenasen untersucht. Diese erwiesen sich allerdings als schlecht nutzbar, da sie entweder nur eine schlechte Regioselektivität für die gewünschte Reaktion zeigten oder sich die Aktivität nicht rekonstituieren ließ. Als alternatives System für die initiale Hydroxylierung wurde dann ein *Rhodococcus equi* Stamm verwendet, der aus einer *Cellulosimicrobium cellulans* EB-8-4 Kultur isoliert wurde und in der Lage ist Limonen an der gewünschten Position höchst regioselektiv zu hydroxylieren. Der für die Reaktion verantwortliche Dioxygenase-Cluster konnte identifiziert werden und insbesondere die rekombinante Expression in einem geeigneten Wirt (*Pseudomonas putida* S12) wurde weiter untersucht. Die Ergebnisse aus diesen Versuchen zeigten, dass die Expression allerdings weiter optimiert werden muss, damit die rekombinante Dioxygenase in Kombination mit den anderen Enzymen für eine Kaskadenreaktion eingesetzt werden kann.

Der dritte Teil dieser Arbeit befasste sich mit der Immobilisierung einer anderen bereits entwickelten Kaskadenreaktion für die Synthese von Polycaprolacton Vorstufen. Für diese Reaktion wurde insbesondere die Anwendung eines sog. *rotating bed reactors* (RBR) untersucht. Für diesen konnte in anfänglichen Experimenten gezeigt werden, dass enzymatische Reaktionen in diesem Reaktor prinzipiell möglich sind. Speziell wurde hierbei beobachtet, dass besonders die Wiederverwendbarkeit der Immobilisate stark erhöht wurde, da die katalytischen Partikel in den Hohlräumen des RBR vor jeglichem mechanischen Einfluss geschützt waren. Weiterhin wurde der Arbeitsablauf optimiert, indem das Einschlussverfahren durch die Anwendung einer Gas-Scher Vorrichtung in einen *in situ* Prozess umgewandelt wurde. Dies führte vor allem auch zu einer erhöhten Aktivität der eingeschlossenen Zellen, da die verringerte Kapselgröße den Massentransfer positiv beeinflusste. Abschließend wurden die entwickelten

Verfahren für die zweite Kaskadenreaktion angewendet. Nach weiteren Optimierungen der Reaktionen konnte so ein Umsatz von 93% (bezogen auf Substratabnahme) erzielt werden.

Zusammengefasst konnten die beschriebenen Kaskadenreaktionen entweder mittels Etablierung eines Co-Expressionssystems, der Erweiterung einer Kaskade durch eine Dioxygenase oder die Immobilisierung der benötigten Enzyme erfolgreich optimiert werden. Weiterhin wurde die allgemeine Anwendbarkeit von enzymatischen Reaktionen in einem neuartigen RBR demonstriert.

6 Materials and Methods

6.1 Materials

Chemicals and consumables

All chemicals were purchased from Sigma-Aldrich (Steinheim, Germany), Carl Roth (Karlsruhe, Germany), Alfa Aesar (Karlsruhe, Germany) or Merck (Darmstadt, Germany) and were used without further purification unless stated otherwise.

Consumables were purchased from Sarstedt (Nümbrecht, Germany), Greiner Bio-One (Frickhausen, Germany) or Carl Roth (Karlsruhe, Germany).

Restriction enzymes were purchased from New England Biolabs (Frankfurt/Main, Germany), T4 ligase was purchased from Thermo Fisher Scientific (Waltham, USA) and DNA polymerases were purchased from Roboklon (Berlin, Germany).

Table 17: Used kits.

Kit	Supplier
BCA-Assay Kit	Interchim (Montluçon, Switzerland)
	Thermo Fisher Scientific (Waltham, USA)
DNEasy Blood & Tissue Kit	QIAgen (Hilden, Germany)
Gel Extraction Kit	QIAgen (Hilden, Germany)
innuPREP Plasmid Mini Kit	Analytik Jena (Jena, Germany)
NucleoSpin Gel and PCR Clean-up	Macherey-Nagel (Düren, Germany)
PCR Purification Kit	Roche (Mannheim, Germany)
StrataClone PCR Cloning Kit	Agilent Technologies (Santa Clara, USA)

Strains

Table 18: Used strains (All *E. coli* strains additionally carried a resistance to T¹ phages).

Species	Strain	Genotype/Description	Supplier
<i>Escherichia coli</i>	BL21 (DE3)	<i>dcm ompT hsdS(r_B⁻m_B⁻) gal</i>	New England Biolabs (Frankfurt/Main, Germany)
	TOP10	<i>mcrA</i> , $\Delta(mrr-hsdRMS-mcrBC)$, <i>Phi80lacZ(del)M15</i> , $\Delta lacX74$, <i>deoR</i> , <i>recA1</i> , <i>araD139</i> , $\Delta(ara-leu)7697$, <i>galU</i> , <i>galK</i> , <i>rpsL(SmR)</i> , <i>endA1</i> , <i>nupG</i>	Thermo Fisher Scientific (Waltham, USA)
	C41 (DE3)	F ⁻ <i>ompT gal dcm hsdS_B(r_B⁻ m_B⁻)</i> (DE3)	Sigma-Aldrich (Steinheim, Germany)
	C43 (DE3)	F ⁻ <i>ompT gal dcm hsdS_B(r_B⁻ m_B⁻)</i> (DE3)	Sigma-Aldrich (Steinheim, Germany)

	SHuffle [®] Express	<i>fhuA2 [lon] ompT ahpC gal</i> λ att::pNEB3-r1-cDsbC (SpecR, <i>lacI^f</i>) Δ <i>trxB sulA11 R(mcr-</i> <i>73::miniTn10--Tet^S)2 [dcm] R(zgb-</i> <i>210::Tn10 --Tet^S) endA1 Δgor</i> Δ (<i>mcrC-mrr</i>)114::IS10	Germany) New England Biolabs (Frankfurt/Main, Germany)
<i>Pseudomonas putida</i>	S12 (also ATCC 70801)	Industrially important strain due to its high solvent tolerance	LGC Standards (Wesel, Germany)
<i>Cellulosimicrobium cellulans</i>	EB-8-4	Strain described to be capable of regioselective limonene hydroxylation, when grown on ethyl benzene	Zhi Li (National University of Singapore, Singapore)
	LMG 16121 (also DSM 46030)	Reference strain not capable of growing on ethyl benzene	DSMZ (Braunschweig, Germany)
<i>Rhodococcus equi</i> -		Isolated from <i>C. cellulans</i> EB-8-4 culture	Zhi Li (National University of Singapore, Singapore)

Plasmids and genes

Table 19: Used plasmid (Amp^R: Ampicillin resistance, Kan^R: Kanamycin resistance, Cam^R: Cloramphenicol resistance).

Plasmid	Origin of replication	Marker	Features	Supplier
pBAD/myc-His A	pBR322	Amp ^R	P _{BAD} <i>araC</i> , opt. RBS, C-term. <i>myc</i> epitope tag, C-term. his-tag	Thermo Fisher Scientific (Waltham, USA)
pBTBX-2	pBBR1	Kan ^R	P _{BAD} <i>araC</i> ; broad host-range	Ryan Gill (Addgene plasmid # 26068)
pCYTEX	unknown	Amp ^R	Heat-inducible promoter, his-tag	Vlada Urlacher (University of Düsseldorf, Germany)
pET-21a(+)	f1	Amp ^R	T7 <i>lac</i> , C-term. his-tag, N-term. T7-tag,	Merck (Darmstadt, Germany)
pET-22b(+)	f1	Amp ^R	T7 <i>lac</i> , C-term. his-tag, <i>pe/B</i>	Merck (Darmstadt, Germany)
pET-26b(+)	f1	Kan ^R	T7 <i>lac</i> , C-term. his-tag, <i>pe/B</i>	Merck (Darmstadt, Germany)
pET-28a/b(+)	f1	Kan ^R	T7 <i>lac</i> , N/C-term. his-tag, internal T7 tag, thrombin cleavage site	Merck (Darmstadt, Germany)
pETM6	f1	Amp ^R	T7 <i>lac</i> , C-term. S-tag; pETDuet-1 derivative	Mattheos Koffas (Addgene plasmid # 49795)
pGASTON	ColE1	Amp ^R	P _{RHA} , N-term. his-tag	Matthias Höhne (University of Greifswald, Germany)
pKA1	p15A	Cam ^R	T7 <i>lac</i>	Werner Hummel

(University of Bielefeld,
Germany)

Synthetic genes were either purchased from Genscript (Piscataway, USA) or Eurofins Genomics (Ebersberg, Germany) and ordered already subcloned into the respective vector.

Table 20: Used gene sequences.

Gene	Organism of origin	Plasmid	Supplier
CHMO	<i>Acinetobacter</i> sp.	pET28b(+)	internal
LK-ADH	<i>Lactobacillus kefir</i>	pET21a(+)	Werner Hummel (University of Bielefeld, Germany)
OYE1	<i>Saccharomyces pastorianus</i>	pET26b(+)	Jon D. Stewart (University of Florida, USA)
XenB	<i>Pseudomonas putida</i>	pGASTON	internal
P450-BM3	<i>Bacillus megaterium</i>	pCYTEX	Vlada Urlacher (University of Düsseldorf, Germany)
CYP102A7	<i>Bacillus licheniformis</i>	pET28a(+) pBAD	Vlada Urlacher (University of Düsseldorf, Germany)
CYP102A7	<i>Bacillus licheniformis</i>	pET22b(+)	Synthetic gene, codon optimized
L6H	<i>Mentha spicata</i>	pET22b(+)	Synthetic gene, codon optimized
DOC _{equi}	<i>Rhodococcus equi</i>	pBTBX-2	internal
RR-ADH	<i>Rhodococcus ruber</i>	pKA1	Werner Hummel (University of Bielefeld, Germany)

The plasmid maps of all used and constructed vectors as well as the gene sequences can be found on the supplemented digital raw data disc.

Oligonucleotides

Synthetic oligonucleotides were purchased from Invitrogen (Thermo Fisher Scientific, Waltham, USA).

Table 21: Used oligonucleotides.

#	Name	Sequence (5' → 3')	Use
09003	Seq_cyp102a7_fw	CGCAGTGCTGAAACAGGTCTT	Sequencing of CYP102A7
09004	Seq_cyp102a7_rev	AAACCACGTCCGGCCTGCTG	Sequencing of CYP102A7
09005	Seq2_cyp102a7	GCCGAATCTGAAAGTGGTAACGATCTG CTG	Sequencing of CYP102A7
09006	L6H_optimized_rv	TGCGGGTCTTTGCTGGAATGGTGTACC CATTCATT	Sequencing of L6H
09048	3-hyden	CATCTTATGTTGAACGTATTCCTTAG	Gene walking, 3' primer
09049	5-hyden	TMYTKCTVYTGCTGTTBTTVBGTSTB	Gene walking, 5' primer

09052	TOPO_seq_fw	GAAGAATTATTTGCATTGAGTAGCTG	Sequencing of TOPO TA cloned PCR fragments
09053	TOPO_seq_rv	CAGCGCCGGAAAATGACATTG	Sequencing of TOPO TA cloned PCR fragments
09066	Seq2_TOPO_rv	CTGCCTGCATCTCGGGTATG	Sequencing of TOPO TA cloned PCR fragments
09067	Seq2_TOPO_fw	GAAGCCTTGATTCCTGATGG	Sequencing of TOPO TA cloned PCR fragments
09071	pACYCDuetUP1	GATCTCGACGCTCTCCCTTATG	Sequencing of pETM6
09072	pETDuet Upstream	GATGCGTCCGGCGTAGAG	Sequencing of pETM6
09078	pETM6CHMO-GOIfw	GAAGGAGATATACATATGGGCAGCAGC CATCATCATC	FastCloning into pETM6
09079	pETM6CHMO-GOIr	GACGAGTCCATGTGCTTAGGCATTGGC AGG	FastCloning into pETM6
09080	pETM6CHMO-VOIfw	CCTGCCAATGCCTAAGCACATGGACTC GTC	FastCloning into pETM6
09081	pETM6CHMO-VOIr	GATGATGATGGCTGCTGCCCATATGTA TATCTCCTTC	FastCloning into pETM6
09082	pETM6LK-ADH-GOIfw	GAAGGAGATATACATATGACTGATCGT TTAAAAGGC	FastCloning into pETM6
09083	pETM6LK-ADH-GOIr	GTAGACGAGTCCATGTGTTATTGAGCA GTGTATC	FastCloning into pETM6
09084	pETM6LK-ADH-VOIfw	GATACACTGCTCAATAACACATGGACT CGTCTAC	FastCloning into pETM6
09085	pETM6LK-ADH-VOIr	GCCTTTTAAACGATCAGTCATATGTATA TCTCCTTC	FastCloning into pETM6
09086	pETM6OYE1-GOIfw	GAAGGAGATATACATATGACCAAGTTA CCTATACTAGG	FastCloning into pETM6
09087	pETM6OYE1-GOIr	GACGAGTCCATGTGCTTACTTTTTGTCC CAG	FastCloning into pETM6
09088	pETM6OYE1-VOIfw	CTGGGACAAAAAGTAAGCACATGGACT CGTC	FastCloning into pETM6
09089	pETM6OYE1-VOIr	CCTAGTATAGGTAAGTGGTCATATGTA TATCTCCTTC	FastCloning into pETM6
09090	pETM6RR-ADH-GOIfw	GAAGGAGATATACATATGAAAGCCCTC CAGTACACCGAG	FastCloning into pETM6
09091	pETM6RR-ADH-GOIr	GACTAGTAGACGAGTTCAGCCCGGGA CGAC	FastCloning into pETM6
09092	pETM6RR-ADH-VOIfw	GTCGTCCCGGGCTGAACTCGTCTACTA GTC	FastCloning into pETM6

09093	pETM6RR-ADH-VOIrv	CTCGGTGTA CTGGAGGGCTTTCATATG TATATCTCCTTC	FastCloning into pETM6
09094	pETM6XenB-GOIfw	GGAGATATACATATGACCACGCTTTTC GATC	FastCloning into pETM6
09095	pETM6XenB-GOIrv	GACGAGTCCATGTGCTCAATGATGATG ATG	FastCloning into pETM6
09096	pETM6XenB-VOIfw	CATCATCATCATTGAGCACATGGACTC GTC	FastCloning into pETM6
09097	pETM6XenB-VOIrv	GATCGAAAAGCGTGGTCATATGTATAT CTCC	FastCloning into pETM6
09116	pBAD/myc-His A_BaLi_VU-GOIfw	GCTAACAGGAGGAATTACATATGAACA AGTTAGATGGAATTCCAATC	FastCloning into pBAD/myc-His A
09117	pBAD/myc-His A_BaLi_VU-GOIrv	GGTCGACGGCGCTATTACATTACGTTCT TGCAATGCAGTCC	FastCloning into pBAD/myc-His A
09118	pBAD/myc-His A_BaLi_VU-VOIfw	GGACTGCATTGCAAGAACGTAATGAAT AGCGCCGTCGACC	FastCloning into pBAD/myc-His A
09119	pBAD/myc-His A_BaLi_VU-VOIrv	GATTGGAATTCCATCTAACTTGTTTCATA TGTAATTCCTCCTGTTAGC	FastCloning into pBAD/myc-His A
09146	pBTBX-2_rvseq	AAACTAAAGCGCCACAAGGG	Sequencing of pBTBX-2
09160	DOC_GOI_fw	CTTTAAGAAGGAGATATACCCATGACT GACGTGCAATG	FastCloning into pBTBX-2
09163	DOC_VOI_rv	CATTGCACGTCAGTCATGGGTATATCT CCTTCTTAAAG	FastCloning into pBTBX-2
09164	DOC_GOI_rv_neu	CTCAATACTGACCATTTCATGCCGCTGT TGTTTC	FastCloning into pBTBX-2
09165	DOC_VOI_fw_neu	GAACAACAGCGGCATGAAATGGTCAGT ATTGAG	FastCloning into pBTBX-2
09172	pETM6_CHMO_fw	CCGGTGTTTCAGGTTATTACG	Seq. of co-expr. constructs
09173	pETM6_CHMO_fw2	GGAAATGACCTTATTCCCTAAAGC	Seq. of co-expr. constructs
09174	pETM6_OYE1_fw	AAACGTATTGAAGCTATCCCAC	Seq. of co-expr. constructs
09175	pETM6_OYE1_fw2	TTTCAACAGTATGTCTGGTGG	Seq. of co-expr. constructs
09176	LK_fw	GAAGAATAAAGGACTCGGAGC	Seq. of co-expr. constructs
09177	XenB_fw	GATCGCGCCGAAACCTTTAC	Seq. of co-expr. constructs
09178	FC_LK_insert_GOI_fw	AGCGCTCATGAGCCCGAAGTGGCGAG CCCGATCTTCCCCATCGGTGATG	FastCloning into co-expr. constr.
09179	FC_LK_insert_GOI_rv	CGCGGGATCGAGATCGATCTCGATCCT AGTAGACGAGTCCATGTGTTATTGAGC AG	FastCloning into co-expr. constr.
09180	FC_LK_insert_VOI_fw	CTGCTCAATAACACATGGACTCGTCTA	FastCloning into

		CTAGGATCGAGATCGATCTCGATCCCCG CG	co-expr. constr.
09181	FC_LK_insert_VOI_rv	CATCACCGATGGGGAAGATCGGGCTC GCCACTTCGGGCTCATGAGCGCT	FastCloning into co-expr. constr.
09182	Ara ins VOI rv	CTATGGCATAGCAAAGTGTGACCTAGA AGAAGAAGCTGAG	FastCloning of P _{Ara} into pBTBX-2
09183	Ara ins_GOI rv	GCATATCTTTGTGAGGGCCATGGGTAT ATCTCCTTCTTAAAG	FastCloning of P _{Ara} into pBTBX-2
09184	Ara ins GOI fw	CTCAGCTTCTTCTTCTAGGTCACACTTT GCTATGCCATAG	FastCloning of P _{Ara} into pBTBX-2
09185	Ara ins VOI fw	CTTTAAGAAGGAGATATACCCATGGCC CTCACAAAGATATGC	FastCloning of P _{Ara} into pBTBX-2
09186	LK_downst_GOI_rv	CAGCAGTTTtaggTTAATTAAGCTGCGA CTAGTAGACGAGTCCATGTGTTATTG	SLiCE insertion of LK into pETM6
09187	LK_downst_OCL_GOI_ fw	CAATGCCTAAGCACATGGACTCGTCTA CTAGGATCGAGATCGATCTCGATCCCCG CG	SLiCE insertion of LK into pETM6
09188	CHMO_downst_XLC_G OI_fw	GCTCAATAACACATGGACTCGTCTACT AGGATCGAGATCGATCTCGATCCCCGCG	SLiCE insertion of CHMO in pETM6
09189	CHMO_downst_XLC_G OI_rv	CAGCAGTTTtaggTTAATTAAGCTGCGA CTAGTAGACGAGTCCATGTGCTTAGGC ATTG	SLiCE insertion of CHMO in pETM6
09190	LK_downst_CXL_GOI_ fw	CATCATTGAGCACATGGACTCGTCTAC TAGGATCGAGATCGATCTCGATCCCCG	SLiCE insertion of LK into pETM6
	M13_fw	TGTAAAACGACGGCCAGT	Sequencing of TOPO TA cloned PCR fragments
	M13_rv	CAGGAAACAGCTATGACC	Sequencing of TOPO TA cloned PCR fragments
	T7 fw mod	CCCGCGAAATTAATACGACTCAC	Sequencing of T7- dep. plasmids
	T7 fw	TAATACGACTCACTATAGGG	Sequencing of T7- dep. plasmids
	T7 Term	CTCAAGACCCGTTTAGAGGCCCAAGG G	Sequencing of T7- dep. plasmids
	pBAD fw	ATGCCATAGCATTTTATCC	Sequencing of P _{BAD} -dep. plasmids

Media, buffers and solutions

Table 22: Used media, buffers and solutions (All %-values are given in (v/v) unless stated otherwise).

Medium, buffer or solution	Preparation
10x Running buffer for SDS-PAGE	30.3 g TRIS, 144 g glycine, 10 g SDS in 1000 mL aq. dest., adjust pH to 8.4 with HCl

10x SOC	10 mmol·L ⁻¹ NaCl, 2.5 mmol·L ⁻¹ KCl, 10 mmol·L ⁻¹ MgCl ₂ , 20 mmol·L ⁻¹ MgSO ₄ , 20 mmol·L ⁻¹ glucose
10x TB-salts	164,4 g K ₂ HPO ₄ · 3 H ₂ O, 23,2 g KH ₂ PO ₄ in 1000 mL aq. dest., autoclave at 120°C for 20 min
50x TAE buffer (pH 8.5)	242 g Tris, 57.1 mL glacial acetic acid, 18.6 g EDTA in 1000 mL aq. dest.
Acrylamide solution for SDS-PAGE	30% acrylamide (w/v), 0.8% N,N'-Methylenebisacrylamide (w/v) in aq. dest.
Agarose gel (1%)	1 g agarose in 100 mL 1x TAE buffer, dissolution by heating in microwave oven; lower or higher concentrated gels were prepared by the use of the respective amount of agarose; for DNA visualization by UV of 3 µL RotiStain (Carl Roth) to 50 mL gel solution were added
Alginate stock solution (3.6%)	18 g alginate sodium salt in 500 mL aq. dest., dissolve by extensive stirring and heating up to 100°C
Ampicillin stock solution	100 mg·mL ⁻¹ in aq. dest., sterile filtrated
APS for SDS-PAGE	10% (w/v) ammonium persulfate in aq. dest.
Buffer A	100 mmol·L ⁻¹ Sodium phosphate, 300 mmol·L ⁻¹ NaCl in 1000 mL aq. dest., sterile filtrated and degassed
Buffer B	100 mmol·L ⁻¹ Sodium phosphate, 300 mmol·L ⁻¹ NaCl, 300 mmol·L ⁻¹ imidazole in 1000 mL aq. dest., sterile filtrated and degassed
CaCl ₂ solution (0.1 M)	11.1 g CaCl ₂ (dry) in 1000 mL aq. dest.
Chloramphenicol	50 mg·mL ⁻¹ in ethanol, sterile filtrated
Coomassie staining solution	1 g Coomassie-brilliant-blue G250, 100 mL glacial acetic acid, 300 mL ethanol, 600 mL aq. dest.
Destaining solution	100 mL glacial acetic acid, 300 mL ethanol, 600 mL aq. dest.
DNA Loading buffer	3 mL glycerol, 25 mg bromophenol blue, 2 mL 50x TAE, 5 mL aq. dest.
Glucose stock solution	250 g·L ⁻¹ glucose in aq. dest.
Glycerol stock solution	60% (w/v) glycerol in aq. dest.
IPTG stock solution	1 mol·L ⁻¹ in aq. dest., sterile filtrated
Kanamycin stock solution	100 mg·mL ⁻¹ in aq. dest., sterile filtrated
KP _i buffer (50 mmol·L ⁻¹)	1.97 g KH ₂ PO ₄ , 8,08 g K ₂ HPO ₄ ·3 H ₂ O in 1000 mL aq. dest., adjust pH to 7.5
L-Arabinose stock solution	50% (w/v) in aq. dest., sterile filtrated
LB-medium	1% (w/v) peptone/tryptone, 1% (w/v) NaCl, 0.5% (w/v) yeast extract in aq. dest., autoclave at 120°C for 20 min
Limonene stock solution	4 mol·L ⁻¹ in ethanol
Loading buffer for SDS-PAGE	20% (w/v) glycine, 6% (w/v) 2-mercaptoethanol, 0.0025% bromophenol blue in Upper-TRIS buffer
Lower-TRIS buffer for SDS-PAGE	18.2 g TRIS, 0.1 g SDS in 100 mL aq. dest., adj. pH to

	8.8
L-Rhamnose stock solution	20% (w/v) in aq. dest., sterile filtrated
M9 CaCl ₂	1 mol·L ⁻¹ CaCl ₂ in aq. dest., sterile filtrated
M9 CuCl ₂	1 g CuCl ₂ *2 H ₂ O in 1000 mL diluted sulfuric acid (pH 5.4), sterile filtrated; always prepared freshly prior to use
M9 FeSO ₄	40 g FeSO ₄ *7 H ₂ O in 1000 mL diluted sulfuric acid (pH 5.4), sterile filtrated; always prepared freshly prior to use
M9 glucose (10x)	200 g glucose in 1000 mL aq. dest., sterile filtrated
M9 MgSO ₄	1 mol·L ⁻¹ MgSO ₄ in aq. dest., sterile filtrated
M9 MoO ₄ Na ₂	2 g MoO ₄ Na ₂ *2 H ₂ O in 1000 mL aq. dest., sterile filtrated
M9 salts (5x)	85.5 g Na ₂ HPO ₄ *12 H ₂ O, 15 g KH ₂ PO ₄ , 2.5 g NaCl, 5 g NH ₄ Cl in 1000 mL aq. dest., autoclave at 120°C for 20 min
M9 trace elements	2 g ZnSO ₄ *7 H ₂ O, 4 g CoCl ₂ *6 H ₂ O, 10 g MnSO ₄ *H ₂ O, 1.3 g Al ₂ (SO ₄) ₃ *18 H ₂ O in 1000 mL aq. dest., sterile filtrated
M9-medium	20% M9 salts (5x), 2% M9 glucose (10x), 0.2% M9 MgSO ₄ , 0.01% M9 CaCl ₂ , 0.1% M9 FeSO ₄ , 0.1% M9 CuCl ₂ , 0.1% M9 MoO ₄ Na ₂ , 0.1% M9 trace elements (1000x) in autoclaved MilliQ water
NADPH stock solution	300 mmol·L ⁻¹ in aq. dest.
NaP _i buffer (50 mmol·L ⁻¹)	1.23 g NaH ₂ PO ₄ *H ₂ O, 14.92 g Na ₂ HPO ₄ *12 H ₂ O in 1000 mL aq. dest., adjust pH to 7.5
Separation gel (12%) for SDS-PAGE	3.33 mL acrylamide solution, 2 mL Lower-TRIS buffer, 2.677 mL aq. dest., 40 µL APS, 4 µL TEMED; lower or higher concentrated SDS-PA gels were prepared by the use of the respective acrylamide amount
Stacking gel (4%) for SDS-PAGE	0.52 mL acrylamide solution, 1 mL Upper-TRIS buffer, 2.47 mL aq. dest., 40 µL APS, 4 µL TEMED
TB-medium	24 g yeast extract, 12 g peptone/tryptone, 8 g glycerol in 900 mL aq. dest., autoclave at 120°C for 20 min, add 100 mL 10x TB-salts
TfBI buffer (pH 5.8)	100 mmol·L ⁻¹ RbCl, 50 mmol·L ⁻¹ MnCl ₂ , 30 mmol·L ⁻¹ KOAc, 10 mmol·L ⁻¹ CaCl ₂ , 15% glycerol
TfBII buffer (pH 7.0)	100 mmol·L ⁻¹ RbCl, 75 mmol·L ⁻¹ CaCl ₂ , 10 mmol·L ⁻¹ MOPS, 15% glycerol
TG salts	75 mmol·L ⁻¹ CaCl ₂ , 6 mmol·L ⁻¹ MgCl ₂ , 15% glycerol
TRIS-buffer (20 mM, 1% NaCl)	2.43 g TRIS, 10 g NaCl in 1000 mL aq. dest., adjust pH to 7.5 with HCl
TSB-medium	17 g tryptone, 3 g soytone, 2.5 g glucose, 5 g NaCl, 2.5 g K ₂ HPO ₄ in 1000 mL aq. dest., autoclave at 120°C for 20 min
Upper-TRIS buffer for SDS-PAGE	6 g TRIS, 0.1 g SDS in 100 mL aq. dest., adjust pH to 6.8

Equipment

Table 23: Used equipment.

Equipment	Name	Producer
Balances	PCB350-3	Kern & Sohn GmbH (Belingen, Germany)
	PCB2500-2	
	Explorer E14130	Ohaus (Parsippany, USA)
	MC1 Analytic AC 120S	Sartorius (Göttingen, Germany)
Centrifuges	Biofuge pico	Thermo Fisher Scientific (Waltham, USA)
	Biofuge 400R	
	Multifuge 3S-R	BiozymScientific (Oldendorf, Germany)
	Fresco 17	
Cleanbench	Sprout-Minizentrifuge	Thermo Fisher Scientific (Waltham, USA)
	HeraSafe KS15	
	Mini-Sub Cell GT	Bio-Rad (Munich, Germany)
	Compact XS/S	Biometra GmbH (Göttingen, Germany)
Fermenter/Bioreactor	BioFlo 110	Eppendorf (Hamburg, Germany)
	SpinChem 6530	Nordic ChemQuest AB (Umeå, Sweden)
FPLC	ÄKTApurifier	GE Healthcare (Buckinghamshire, United Kingdom)
	ÄKTAbasic	GE Healthcare (Buckinghamshire, UK)
Gas chromatography	GC-2010(plus) incl. AOC-20i/s	Shimadzu (Duisburg, Germany)
	GCMS-QP2010	Shimadzu (Duisburg, Germany)
Heating-/stirring plate	RCT basic	IKA Labortechnik (Staufen, Germany)
Homogenization	FastPrep-24	MP Biomedicals, Inc. (Eschwege, Germany)
	French Press	Thermo Fisher Scientific (Waltham, USA)
	Sonopuls HD/UW 2070	Bandelin (Berlin, Germany)
Incubation	Incucell	MMM Medcenter Einrichtungen GmbH (Gräfeling, Germany)
	Unitron	HT Infors (Bibra, Germany)
	Multitron	
Membrane Pump	Stepdos 03 RC	KNF (Freiburg im Breisgau, Germany)

Orbital shaker	Polymax 1040	Heidolph (Schwabach, Germany)
Overhead-stirrer	EuroStar digital	IKA Labortechnik (Staufen, Germany)
pH-meter	pH211 Microprocessor	Hanna Instruments (Kehl am Rhein, Germany)
Photometer	V-550	Jasco (Tokyo, Japan)
	Fluostar Optima	bmG-Labtechnologies (Offenburg, Germany)
	UVmini-1240	Shimadzu (Duisburg, Germany)
	EPS EV231	Consort (Turnhout, Belgium)
Power Supply for Electrophoresis	Standard Power Pack 25	Biometra (Göttingen, Germany)
Protein electrophoresis	Minigel-Twin 010-130	Biometra (Göttingen, Germany)
Sterilization	V-120 autoclave	Systec (Bergheim-Glessen, Germany)
	Laboklav	SHP Steriltechnik (Detzel, Germany)
	Dry-Line oven	VWR International (Darmstadt, Germany)
Thermocycler	FlexCycler ²	Analytik Jena (Jena, Germany)
	Flexcycler	Analytik Jena (Jena, Germany)
	Tpersonal	Biometra (Göttingen, Germany)
	Techgene	Techne (Staffordshire, UK)
	DNAEngine (Tetrad 2)	Biorad (Hercules, USA)
Thermoshaker	Thermomixer comfort	Eppendorf (Hamburg, Germany)
UV table	Benchtop UV	UVP (Upland, USA)
	Transilluminators UV-Start	Biometra (Göttingen, Germany)
Vortex	Vortex-Genie 2	Scientific Industries (Bohemia, USA)
Water bath	D8/G	Haake Fissons (Karlsruhe, Germany)

6.2 Microbiological Methods

Strain maintenance

All strains were maintained on agar plates containing the respective antibiotic as selection marker and stored at 4°C for up to two months. For longer storage glycerol stocks were prepared containing 30% glycerol and the desired cells from a pre-culture. These were stored at -80°C.

Preparation of pre-cultures

Pre-cultures for expression were grown in LB supplemented with the respective antibiotic as selection marker at 37°C (*E. coli*) or 30°C (all other bacteria) over night after inoculation with 3 - 5 µl of a glycerol stock or a colony from an agar plate.

Preparation of competent cells

...of *E. coli*

100 mL of LB were inoculated with the respective pre-culture and grown to an optical density of 0.4 - 0.6 at 37°C and 180 rpm. Subsequently the cells were harvested by centrifugation at 4000xg for 10 min at 4°C. The pellet was resuspended in 30 mL pre-cooled Tfb1 solution und incubated on ice for 15 min. Again the cells were harvested by centrifugation as described above, the supernatant was discarded, the pellet was resuspended in pre-cooled Tfb2 solution and the cells were incubated on ice for 15 min. This cell suspension was finally snap-frozen in liquid nitrogen as 50 µL aliquots, which were stored until use at -80°C.

...of *Pseudomonas putida*

Competent cells of *P. putida* were prepared as described by Chuanchuen *et al.*^[199] Therefore, 1 mL of a pre-culture was transferred into a precooled microfuge tube and centrifuged at 13,000xg for 30 s at 25°C. The supernatant was discarded, the cells were resuspended in 1 mL cold 0.1 mol·L⁻¹ MgCl₂ and subsequently centrifuged as before. Again the supernatant was discarded, the cells were resuspended in 1 mL cold TG salts, incubated for 10 min on ice and centrifuged as before. After removal of the supernatant the cells were finally resuspended in 200 µL cold TG salts and snap-frozen in liquid nitrogen or used directly for transformation.

Transformation

...of *E. coli*

One aliquot of competent cells was thawed slowly on ice. After addition of 0.5 - 5 µL DNA solution (approx. 40 ng·µL⁻¹) the cells were incubated on ice for 15 - 30 min. After that the cells were heat-shocked by incubation at 42°C for 30 sec followed by incubation on ice for 2 - 5 min. After addition of pre-warmed LB-SOC medium the cells were incubated under shaking at 37°C for 1 h. Finally the cells were spread on LB agar plates containing the respective antibiotic and incubated over night.

...of *P. putida*

Transformation of *P. putida* was carried out as described by Chuanchuen *et al.*^[199] Briefly, the procedure was the same as used for *E. coli* transformation, except that the heat shock was carried out at 37°C for 2 - 5 min and the shaken incubation after that at 30°C.

Cultivation

E. coli strains were routinely cultured in LB medium and, if necessary, supplemented with ampicillin ($100 \mu\text{g}\cdot\text{mL}^{-1}$), chloramphenicol ($25 \mu\text{g}\cdot\text{mL}^{-1}$) or kanamycin ($50 \mu\text{g}\cdot\text{mL}^{-1}$). Bacterial cultures were incubated in Erlenmeyer flasks in orbital shakers at 180 rpm unless otherwise stated. Bacteria on agar plates were incubated in a certain incubator under air. All materials and biotransformation media were sterilized by autoclaving at 121°C for 20 min. Agar plates for *E. coli* were prepared with LB medium supplemented by 1.5 % (w/v) agar.

P. putida was cultivated as described for *E. coli*, except that routinely TSB medium was used and the cells were incubated at max. 30°C . Agar plates for *P. putida* were prepared with TSB medium supplemented by 1.5 % (w/v) agar.

C. cellulans and *R. equi* were cultivated either aerobically with cotton plug or anaerobically with septum plug in 300 mL Erlenmeyer flasks. 100 mL of M9 medium was used containing either glucose, ethyl benzene or no carbon source. Ethyl benzene was supplied by vaporization from a 15 mL Falcon tube, which was perforated at 6, 7 and 10 mL, and placed inside the flask. The cells were incubated at 30°C with 180 rpm shaking. Agar plates for these bacteria were prepared with LB medium supplemented by 1.5 % (w/v) agar.

Expression of enzymes

In general, the cultivation was carried out by inoculation of 200 mL cultivation medium supplied with the specified antibiotic with 2 mL of a pre-culture (1:100). The cultivation was continued at 37°C until an OD_{600} of 0.6 - 0.7 was reached. Then, expression of the enzymes was induced by addition of the specified inductor. The expression was continued for the specified times at the given temperatures (Table 24).

Table 24: Conditions for enzyme expression.

Enzyme	Expression strain	Inductor	Expression protocol
CHMO	<i>E. coli</i> BL21 (DE3)	$0.1 \text{ mmol}\cdot\text{L}^{-1}$ IPTG	TB _{Kan} , 37°C , 180 rpm; after induction 25°C for 8 h
LK-ADH	<i>E. coli</i> BL21 (DE3)	$0.1 \text{ mmol}\cdot\text{L}^{-1}$ IPTG	TB _{Amp} , 37°C , 180 rpm; after induction 25°C for 8 h
OYE1	<i>E. coli</i> BL21 (DE3)	$0.1 \text{ mmol}\cdot\text{L}^{-1}$ IPTG	TB _{Amp} , 37°C , 180 rpm; after induction 25°C for 8 h
XenB	<i>E. coli</i> BL21 (DE3)	2% L-rhamnose	TB _{Amp} , 37°C , 180 rpm; after induction 25°C for 8 h
P450-BM3	<i>E. coli</i> BL21 (DE3)	heat	TB _{Amp} , 37°C , 180 rpm; for induction 42°C for max. 8 h
CYP102A7 (pET)	Various	$0.1 \text{ mmol}\cdot\text{L}^{-1}$ IPTG	TB _{Amp} , 37°C , 180 rpm; after induction $17/30^\circ\text{C}$ overnight
CYP102A7 (pBAD)	Various	2% L-arabinose	TB _{Amp} , 37°C , 180 rpm; after induction $17/30^\circ\text{C}$ overnight
L6H	<i>E. coli</i> BL21 (DE3)	$0.1 \text{ mmol}\cdot\text{L}^{-1}$ IPTG	TB _{Amp} , 37°C , 180 rpm; after induction 20°C overnight
DOC _{equi}	<i>P. putida</i> S12	0.2 - 2% L-arabinose	TSB _{Kan} , 30°C , 180 rpm; after

			induction 30°C overnight
Co-Expression constructs	<i>E. coli</i> BL21 (DE3) $\Delta nemA$	0.1 mmol·L ⁻¹ IPTG	TB _{Amp} , 37°C, 180 rpm; after induction 25°C for 8 h

Cell disruption

Samples normalized to cell weight (7/OD) were centrifuged at 13,000xg for 5 min, the supernatant was removed and the pellet was stored at -20°C until cell disruption. For preparation of crude cell extracts the pellets were thawed and resuspended in 500 µL phosphate buffer. Subsequently the cells were disintegrated twice by ultrasonication for 30 sec (50% power, 50% cycle). The solution was clarified by centrifugation as before. The supernatant was used as soluble protein fraction and the pellet after resuspension in 500 µL buffer as insoluble protein fraction for SDS-PAGE.

The complete cells from a cultivation, which were used for example for purification, were harvested by centrifugation at 4500xg for 10 - 30 min. The supernatant was discarded and the pellet resuspended in max. 50 mL buffer (1:10 with respect to the actual culture volume). These cells were then disintegrated by ultrasonication for thrice 5 min (50% power, 50% cycle).

6.3 Molecular Biology Methods

Isolation of plasmids

For isolation of plasmids the innuPREP Plasmid Mini Kit (Analytik Jena) was used. The cells from a pre-culture were harvested by centrifugation and subsequently used as described in the manufacturer's manual. Except that for elution 50 µL hot aq. bidest. (70°C) was used and that it was eluted twice using the same water to increase the yield.

Extraction of genomic DNA

Genomic DNA was extracted using the DNEasy Blood and Tissue Kit (Qiagen) according to the manufacturer's instructions.

Agarose gel electrophoresis

For detection, quantification or preparative extraction of DNA fragments these were separated by agarose gel electrophoresis. Therefore, agarose was molten in TAE buffer using a microwave oven. For detection of DNA RotiSafe GelStain (Carl Roth, Darmstadt, Germany) was added after short cooling into the solution (3 µL per 50 mL gel volume). Subsequently the gel solution was poured into the respective gel casting stand. Prior to gel application of the samples these were mixed with DNA sample buffer (5:1). After that 2-50 µL of sample were added into one of the gel pockets. For all agarose gels also a DNA maker (1 kbp DNA ladder, Carl Roth, Darmstadt, Germany) was applied in one of the pockets. The electrophoresis itself was carried out at 90 to 110 V and 400 mA over 30 to 50 min. For visualization of the DNA the gel was illuminated by UV light on a suitable UV table.

Gel extraction of DNA fragments

The DNA fragments were separated as described above. If these were also supplied to gel extraction, it was necessary not to UV-illuminate the gel for a too long time, because this might lead to damage or mutation of the DNA. The gel extraction itself was carried out according to the QIAquick Gel Extraction Kit (Qiagen), PCR Purification Kit (Roche) or the NucleoSpin® Gel and PCR Clean-Up Kit (Macherey-Nagel). As first step the respective bands visualized in the gel were excised using a scalpel and transferred into pre-weighed micro tubes. The residual procedure was carried out as described in the respective manual, except that the elution was done twice with the same 15 µL sterile and hot aq. bidest. (70°C).

PCR-methods

General amplification of DNA

DNA was generally amplified by PCR according to the following procedure.

50 µL PCR-mix: 5 µL PCR-buffer (10x) according to Table 25
 1.5 µL dNTPs (10 mmol · L⁻¹)
 1 µL forward primer (10 pmol · L⁻¹)
 1 µL reverse primer (10 pmol · L⁻¹)
 3 µL template DNA
 0.5 µL polymerase
 38 µL sterile aq. bidest.

Program:	<u>Denaturation</u>	1 min	98°C	} 18 – 30 cycles
	Denaturation	30 - 45 sec	95°C	
	Annealing	30 - 45 sec	50 - 72°C	
	<u>Elongation</u>	1 min · kbp ⁻¹	68 - 72°C	
	Elongation	10 min	68 - 72°C	

The correct annealing temperature was estimated by first calculating the melting temperature either using Geneious or the online tool Melting Temperature (T_m) Calculation^[229] and then subtracting 5°C from this value. If this way no PCR product could be detected a gradient PCR scanning several annealing temperatures was carried out. If still no PCR product could be detected up to 5% of DMSO was added to enhance melting of the DNA strands. If this way still no product could be detected the Q5 polymerase with GC enhancer was used. The correct elongation temperature for the specific polymerases is given in Table 25.

Table 25: Polymerases and the buffers supplied by manufacturer and elongation temperatures to be used.

Polymerase	Buffer	Elongation Temperature [°C]	Purpose
Taq	B	72	General PCR
Taq	C	72	Colony PCR
OptiTaq	C	68	FastCloning/SLiCE PCR
Pfu ⁺	Pfu	68	QuickChange PCR
Q5	Q5	72	PCR for difficult templates

Colony PCR

For identification of positive transformands colony PCR was applied. Therefore the same PCR-mix was used as for the general amplification of DNA, except that the template was left out and generally 5% DMSO was added. The PCR mix was divided into 10 μL portions. In each tube three colonies of interest were pooled. These were prior to application in the PCR tube backup streaked on a new agar plate, so that only very few cells were put into the PCR-mix. The above mentioned PCR program was also used for colonyPCRs, except that the initial denaturation step was elongated to 5 min and always the Taq-polymerase was used. Positive hits were subsequently depooled by repeated colonyPCR using the single backup colonies as template.

QuikChange[®]

The introduction of simple mutations was carried out using the QuikChange[®] method as described before.^[230] Therefore, the desired plasmid was amplified using a pair of primers containing the desired mutation. After digestion of the parental plasmid DNA with *DpnI* the 7 μL of the PCR-mixture were transformed into *E. coli* TOP10, which automatically ligated the nicked DNA strands.

Gene walking PCR

For gene walking PCR the following setup was used. The special fact is that only one primer is used in the reaction. The sequence identified by gene walking can be found on the supplementary digital raw data disc.

200 μL PCR-mix: 20 μL buffer B (RoboKlon)
 10 μL DMSO
 4 μL dNTPs (10 mmol \cdot L⁻¹)
 4 μL primer (10 pmol \cdot L⁻¹)
 3 μL template DNA (approx. 500 ng)
 2 μL OptiTaq-polymerase
 157 μL sterile aq. bidest.

Program:	<u>Denaturation</u>	4 min	95°C	}	30 cycles
	Denaturation	30 sec	95°C		
	Annealing	30 sec	50 - 63°C		
	<u>Elongation</u>	3 min	72°C	}	30 cycles
	Denaturation	30 sec	95°C		
	Annealing	30 sec	40°C		
	<u>Elongation</u>	3 min	72°C	}	30 cycles
	Denaturation	30 sec	95°C		
	Annealing	30 sec	55 - 68°C		
	<u>Elongation</u>	3 min	72°C		
	Elongation	10 min	72°C		

Cloning by FastCloning and SLiCE

Using these techniques any DNA fragment can be cloned into any desired position of a plasmid without the use of a ligase. Therefore, the desired DNA is amplified with additional 16 to 25 bases overhangs. The sequence of these overhangs is identical to the plasmid sequence, which is found up- and downstream of the desired position in the plasmid. The overhangs are simply introduced by PCR using the respective primers containing the additional sequences (Table 21). For FastCloning^[231] the vector itself is also amplified in the same way, except that the overhangs are identical to the respective sequences to be inserted. For SLiCE^[232] the vector is simply cut with a restriction enzyme near the desired position of insertion instead of amplification. In both cases the DNA fragments produced before are purified by gel extraction and mixed in a certain molar ratio (FastCloning: vector:insert=1:4; SLiCE: vector:insert=1:40). Finally, 7 µL of this mixture was transformed directly into *E. coli* TOP10, when using the FastCloning method. The cells automatically ligated the fragments by homologous recombination. If SLiCE was used the vector:insert mixture is 'ligated' for 2 h at 37°C by the SLiCE extract, which mainly consists of a crude *E. coli* TOP10 extract.^[232] Afterwards, 7 µL of this mixture was transformed into *E. coli* TOP10.

Purification of PCR products

For downstream applications the PCR products had to be purified. This was carried out by the use of the PCR Purification Kit (Roche) or the NucleoSpin® Gel and PCR Clean-Up Kit (Macherey-Nagel). The manufacturer's instructions were followed, except that the elution was done twice with the same 20 µL sterile and hot aq. bidest. (70°C).

Sequencing

All modified and cloned DNA fragments or constructs were verified by sequencing. Therefore, either the sequencing service of GATC (Constance, Germany) or Eurofins Genomics (Ebersberg, Germany) was used.

Classical cloning by restriction and ligation

When using the classical cloning method the insert was generally PCR amplified prior to digestion. Both vector and insert (each 1 - 5 µg DNA) were digested with the desired restriction enzymes according to the enzymes' optimal conditions. These were usually identified by using the NEB Double Digest Finder (New England BioLabs) or the DoubleDigest Calculator (Thermo Fisher Scientific) dependent on the manufacturer of the restriction enzyme. In general, the digestion was carried out at 37°C unless a different temperature was mentioned by the supplier for 2 h, followed by 10 min at 80°C for deactivation of the enzyme. Subsequently the fragments were gel extracted for purification. For ligation the fragments were mixed in an approx. vector:insert ratio of 1:4 resulting in a total volume of 8.5 µL. Then 1 µL of T4-ligase buffer (10x) and 0.5 µL T4-ligase were added and the mixture was incubated at room temperature overnight. The following day 7 µL of the ligation mixture was transformed into *E. coli* TOP10.

***DpnI* digestion**

To remove parental plasmid DNA these were digested with the restriction enzyme *DpnI*. This enzyme only cuts methylated DNA, which is produced inside the cell. Therefore, simply 1 µL of the enzyme was added to the desired DNA containing solution and this is subsequently incubated at 37°C for 2 h, followed by 10 min at 80°C for deactivation of the enzyme.

Quantification of DNA

DNA concentrations were in general determined by UV-Vis photometry using the NanoDrop. Furthermore, using this method also the purity of the DNA could be estimated by the calculation of the ratio between absorption at $\lambda = 260$ nm and 280 nm. A quotient between 1.8 and 2.0 was accepted as pure DNA.

6.4 Biochemical Methods

Protein quantification

Protein contents were determined using the BC Assay Protein Quantitation Kit (Uptima) following the delivered kit manual. The assay was carried out in 96-well microtiter plates. One well contained 25 µL of BSA-standard or sample and 200 µL BC Assay working reagent (previously prepared as described in kit manual). The plates were then incubated for 30 min at 37°C. Subsequently, after cooling to room temperature the absorbance at 562 nm was determined. All measurements were conducted in triplicates.

Protein purification via His-tag

Proteins carrying a His-tag were purified using a HisTrap HP column (5 mL column volume (CV), GE Healthcare, Buckinghamshire, UK) attached to a ÄKTA FPLC system. The column was equilibrated prior to sample application with a mixture of

buffer A and B (10:1). Subsequently, the sample was loaded with a flow of $2.5 \text{ mL} \cdot \text{min}^{-1}$ and the column was washed with three CVs of 13% buffer B and a flow of $5 \text{ mL} \cdot \text{min}^{-1}$. The bound protein was eluted with three CVs of 100% buffer B and the same flow. Fractions of 2 mL were collected automatically by the autosampler. Usually, the fraction containing the purified protein could be detected by eye as the enzymes had a significant color (e.g. P450s are red). For further applications the purified proteins had to be desalted, because the imidazole often is interfering with other reagents.

Preparation of *E. coli* membrane fraction

At first the harvested cells were resuspended in 1/7 volume of the respective cultivation of Tris-HCl buffer (0.1 M, pH 7.8, 0.5 mM EDTA, 20% glycerol). The cells were lysed by addition of 0.2 mg Lysozyme and an equal amount of cold aq. dest. and then stirred for 30 min at 4°C. Afterwards the spheroblasts were pelleted by centrifugation (7,000xg, 10 min), which were subsequently resuspended in 1/20 volume of KPi buffer (10 mM, pH 7.5, 0.1 mM EDTA, 20% glycerol, 0.1 mM DTT) by stirring for 30 min at 4°C. For disruption of the cells 0.5 mM PMSF was added and then the cells were sonicated thrice 25 sec (50% power, 50% cycle). Unlysed cells and inclusion bodies were removed by centrifugation (10,000xg, 10 min). Finally, the supernatant was centrifuged (48,000xg, 45 min) and the pellet containing the membrane fraction was resuspended in 1/20 volume of KPi buffer (10 mM, pH 7.5, 0.1 mM EDTA, 20% glycerol) using a pipette.

Desalting

Desalting of purified proteins was done using the PD-10 Desalting Columns (GE Healthcare, Buckinghamshire, UK). The procedure was carried out in accordance with the supplied manual by hand using the gravity protocol.

SDS-PAGE

Enzyme expression levels were analyzed by denaturing SDS-PAGE. Therefore, 15 μL of loading buffer were added to 15 μL sample and subsequently heated to 95°C for 5 min. The centrifuged samples (1 min, 16,000xg) and a protein marker were loaded on the polyacrylamide gel and electrophoresis was performed at 25 mA per gel and 160 - 180 V. The separation was stopped when the samples reached the lower end of the gel after approx. 1 h. The gels were stained with coomassie brilliant blue G250 over night. Afterwards, the gels were rinsed with aq. dest. and incubated in destaining solution until clear blue protein bands were visible. As marker either RotiMark Standard (Carl Roth, Darmstadt, Germany) or PageRuler Unstained Protein Ladder (Thermo Fisher Scientific, Waltham, USA) was used.

NADPH Assay

The activity of crude cell extract was determined by the NADPH-assay in cuvettes. One cuvette contained 949 μL KPi buffer, 1 μL substrate stock solution, 1 μL NADPH stock solution ($0.3 \text{ mmol} \cdot \text{L}^{-1}$ final concentration) and 50 μL crude cell extract. The

activity was determined by observation of absorbance decrease by NADPH consumption at 340 nm. All measurements were conducted in triplicates.

Activity determination of whole free and immobilized cells

The activity of whole free and immobilized cells was determined by biocatalysis in 100 mL Erlenmeyer flasks sealed with a breathable membrane (AeraSeal™ film). The total volume of 10 mL reaction medium of TRIS buffer contained $20 \text{ mmol} \cdot \text{L}^{-1}$ substrate and $20 \text{ mmol} \cdot \text{L}^{-1}$ co-substrate (glucose for BVMO involved reactions, acetone for ADH involved reactions). The reaction was started by addition of approximately 1 g encapsulated cells or 1 mL of cell suspension ($100 \text{ g}_{\text{WCM}} \cdot \text{L}^{-1}$). The flasks were then placed in a shaking incubator at 25 - 30°C and 120 rpm. After 2 h a sample of 500 μL was taken and immediately stored at -20°C for later determination of substrate and product concentration by GC.

6.5 Immobilization and Biocatalysis Reactions in STR, RBR and FBR

Encapsulation in alginate – ‘drop’ method

For encapsulation in alginate fresh cells were resuspended at a concentration of $100 \text{ g}_{\text{WCM}} \cdot \text{L}^{-1}$ in TRIS buffer. An adequate volume of the cell suspension was stored at 4°C for activity determination of the free cells. The residual volume was mixed 1:1 with alginate stock solution (3.6%). This alginate-cell suspension was then passed through a needle (0.8 x 120 mm) using a pump (Stepdos 03 RC, KNF Flodas) at a flow rate between $3 - 6 \text{ mL} \cdot \text{min}^{-1}$ depending on the viscosity of the suspension into a $0.1 \text{ mol} \cdot \text{L}^{-1}$ CaCl_2 solution. The CaCl_2 solution was mixed gently by a magnetic stirring bar and kept on ice during the immobilization procedure. The beads produced this way were separated from the solution using a filter and incubated in fresh CaCl_2 solution at 4°C for at least 30 min. Afterwards, the beads were washed three times with 50 mL TRIS buffer and used directly for biocatalysis.

Encapsulation in alginate – ‘gas-shear’ method

In principle the encapsulation was carried out as described above for the ‘drop’ method. The only addition that had to be made, was the application of the gas-shear device (Figure 45) to the needle, so that the alginate-cell suspension was extruded from the needle as spray.

Biocatalysis reactions

...in RBR

The voids of the SpinChem® (Nordic ChemQuest AB) were filled completely with alginate encapsulated cells. The reaction vessel was thermostated at 25 - 30°C by a heating plate, a waterbath or the BioFlo 110 control unit. Oxygen supply was

performed by continuous aeration of the reaction solution using pure oxygen at 0.25 lpm. The spinning speed of the overhead stirrer was set to 500 rpm. At adequate intervals 500 μL samples were taken from the reservoir and stored immediately at -20°C for later determination of substrate and product concentration.

...in STR

These reactions were carried out in a similar way as the ones using the RBR. Except that in this case the respective amount of cell capsules or cells was placed directly into the reaction medium and stirred at 500 rpm using an overhead stirrer. Oxygen supply was performed by continuous aeration of the reaction solution using pure oxygen at 0.25 lpm. At adequate intervals 500 μL samples were taken from the reservoir and stored immediately at -20°C for later determination of substrate and product concentration.

...in FBR

In average, the fixed bed contained about 46 g of alginate encapsulated cells and was thermostated at 30°C . The beads were fixed with glass wool. The reservoir was thermostated at 18°C to keep evaporation of substrate and product at a low level. Furthermore, the medium reservoir was kept at an oxygen saturation of 100% by the BioFlo 110 (New Brunswick Scientific) control unit. The flow-rate of the reaction medium was set to 100% in the control unit, which corresponded to $2.9 \text{ mL} \cdot \text{min}^{-1}$. At adequate intervals 500 μL samples were withdrawn from the reservoir and stored immediately at -20°C for later determination of substrate and product concentration.

6.6 Analytics

Gas chromatography

Exemplary chromatograms of the analyzed substances can be found on the supplementary digital raw data disc.

The concentrations of all used substrates, intermediates and products were determined by gas chromatography (GC). The substances were separated on the column listed in the respective program (Table 26). Therefore, the samples were extracted with $2 \text{ mmol} \cdot \text{L}^{-1}$ external standard in dichloromethane in a 1:1 ratio and dried afterwards using dry Na_2SO_4 . The GC-analysis was performed by the auto-sampler/-injector of the GC device. The temperature programs used and the retention times of the substances are shown in Table 26 and Table 27.

Table 26: Used GC programs.

Program #	Column	Time [$r = ^\circ\text{C} \cdot \text{min}^{-1}$]	External standard
1	FS-Hydrodex β -3P (25 m x 0.25 mm, Macherey-Nagel)	hold 60°C 5 min 10r to 160°C hold 160°C 10 min	acetophenone
2	FS-Hydrodex β -3P (25 m x 0.25 mm, Macherey-Nagel)	hold 125°C 10 min	(S)-1-phenylethanol
3	FS-LIPODEX® G (50 m x 0.25 mm, Macherey-Nagel)	hold 75°C 13 min 5r to 120°C hold 120°C 5 min 10r to 200°C hold 200°C 5 min	4-methylacetophenone

Table 27: Retention times of the analyzed substances.

Substance	Program #	Retention time [min]
(1 <i>R</i> ,5 <i>R</i>)-carveol	3	30.2
(1 <i>S</i> ,5 <i>R</i>)-carveol	3	30.8
(1 <i>S</i> ,5 <i>S</i>)-carveol	3	31.0
(<i>R</i>)-1-phenylethanol	2	7.1
(<i>R</i>)-1-phenylethylacetate	2	5.0
(<i>R</i>)-carvone	3	28.5
(<i>R</i>)-limonene	3	14.1
(<i>S</i>)-1-phenylethanol	2	7.6
(<i>S</i>)-carvone	3	28.3
(<i>S</i>)-limonene	3	14.6
(<i>S</i>)-perillyl alcohol	3	32.8
4-methylacetophenone	3	26.7
acetophenone	1	18.2
<i>cis/trans</i> -(-)-limonene-1,2-epoxide	3	21.0/21.3
cyclohexanol	1	16.3
cyclohexanone	1	14.2
cyclohexenone	1	15.5
<i>rac</i> -cyclohexenol	1	16.4/16.6
<i>trans</i> -(+)-limonene-1,2-epoxide	3	21.3
ϵ -caprolactone	1	20.4

6.7 Bioinformatic Methods

Table 28: Used software.

Name	Purpose	Developer
MS Office Pro Plus 2010	Creation of Word-documents and Excel-sheets	Microsoft Corporation
SigmaPlot 12.0	Creation of graphs	Systat Software, Inc.
Caver 3.0 ^[192]	Computation of protein tunnels	J. Damborsky
ChemBioDraw Ultra 12.0	Creation of reaction schemes	CambridgeSoft
HYDEN ^[235]	Design of degenerated primers	C. Linhart & R. Shamir
PyMol 1.5.0.4	Visualization of protein structures	Schrödinger, LLC.
Geneious 8.0.4	Sequence management and virtual cloning	Biomatters, Ltd.
YASARA 15.11.18 ^[233]	Homology modelling	E. Krieger

Creation of homology models by YASARA

Homology models were prepared by using the internal YASARA homology modeling function. Therefore, simply a protein sequence in FASTA format is submitted to the program. This automatically performs a BLAST search and picks a set number of sequences sharing the highest homology with the submitted one and for which the structure has been solved. On each of these sequences the submitted one is aligned onto for a set number of times, so that in the end several models are prepared. Out of these models again from the best ones a chimera model is created, which was in general accepted as homology model. In the end, this homology model was refined using the YASARA macro `md_refine` with the standard parameters. The model with the lowest energy was finally accepted as final model. All models prepared were submitted to MolProbity^[190a] for evaluation. The YASARA outputs can be found on the supplementary digital raw data disc.

Computation of protein tunnels using Caver 3.0

Caver 3.0 is a plugin for PyMol. This calculates cavities, which are present in protein structures. This was used for the computation of the tunnels in the described P450s. Therefore the heme was defined as starting point. For calculation the standard parameters of the plugin were used and only the amino acid chain was defined as scaffold. The raw data for the calculations can be found on the supplementary digital raw data disc.

7 References

- [1] a) R. H. Michel, P. E. McGovern, V. R. Badler, *Nature* **1992**, 360, 24-24; b) R. H. Michel, P. E. McGovern, V. R. Badler, *Anal. Chem.* **1993**, 65, 408A-413A; c) P. E. McGovern, *Uncorking the Past: The Quest for Wine, Beer, and Other Alcoholic Beverages*, University of California Press, **2010**; d) S. H. Katz, M. M. Voigt, *Expedition Mag.* **1986**, 28, 23-34; e) R. J. Braidwood, *Am. Anthropol.* **1953**, 55, 515-526.
- [2] M. Dixon, in *Multi-Enzyme Systems*, University Press, Cambridge, **1949**, pp. 5-6.
- [3] G. Köhler, C. Milstein, *Nature* **1975**, 256, 495-497.
- [4] nobelprize.org, **2014**, accessed on 2016-01-21, http://www.nobelprize.org/nobel_prizes/medicine/laureates/1984/press.html
- [5] gene.com, **2016**, accessed on 2016-01-21, <http://www.gene.com/media/company-information/chronology>
- [6] nobelprize.org, **2014**, accessed on 2016-01-21, http://www.nobelprize.org/nobel_prizes/chemistry/laureates/1980
- [7] a) K. Itakura, T. Hirose, R. Crea, A. Riggs, H. Heyneker, F. Bolivar, H. Boyer, *Science* **1977**, 198, 1056-1063; b) H. G. Khorana, K. L. Agarwal, H. Büchi, M. H. Caruthers, N. K. Gupta, K. Kleppe, A. Kumar, E. Ohtsuka, U. L. RajBhandary, J. H. van de Sande, V. Sgaramella, T. Tebao, H. Weber, T. Yamada, *J. Mol. Biol.* **1972**, 72, 209-217.
- [8] a) K. Kleppe, E. Ohtsuka, R. Kleppe, I. Molineux, H. G. Khorana, *J. Mol. Biol.* **1971**, 56, 341-361; b) R. Saiki, S. Scharf, F. Faloona, K. Mullis, G. Horn, H. Erlich, N. Arnheim, *Science* **1985**, 230, 1350-1354; c) nobelprize.org, **2014**, accessed on 2016-01-21, http://www.nobelprize.org/nobel_prizes/chemistry/laureates/1993
- [9] D. G. Gibson, J. I. Glass, C. Lartigue, V. N. Noskov, R.-Y. Chuang, M. A. Algire, G. A. Benders, M. G. Montague, L. Ma, M. M. Moodie, C. Merryman, S. Vashee, R. Krishnakumar, N. Assad-Garcia, C. Andrews-Pfannkoch, E. A. Denisova, L. Young, Z.-Q. Qi, T. H. Segall-Shapiro, C. H. Calvey, P. P. Parmar, C. A. Hutchison, H. O. Smith, J. C. Venter, *Science* **2010**, 329, 52-56.
- [10] a) biotechnologie.de, **2016**, accessed on 2016-01-20, <http://www.biotechnologie.de/BIO/Navigation/DE/Hintergrund/studien-statistiken,did=180726.html>; b) biotechnologie.de, **2016**, accessed on 2016-02-01, <http://www.biotechnologie.de/BIO/Navigation/DE/Hintergrund/studien-statistiken,did=95732.html?listBIId=74636&sortSelect=DescendingDocumentDate&searchActionPage3=searchActionPage3>
- [11] U. T. Bornscheuer, G. W. Huisman, R. J. Kazlauskas, S. Lutz, J. C. Moore, K. Robins, *Nature* **2012**, 485, 185-194.
- [12] S. Lutz, U. T. Bornscheuer (Eds.), *Protein Engineering Handbook*, Vol. 3, Wiley-VCH, **2012**.
- [13] a) rcsb.org, **2016**, accessed on 2016-02-01, <http://www.rcsb.org/pdb/home/home.do>; b) uniprot.org, **2016**, accessed on 2016-02-01, <http://www.uniprot.org>
- [14] N. Perdigão, J. Heinrich, C. Stolte, K. S. Sabir, M. J. Buckley, B. Tabor, B. Signal, B. S. Gloss, C. J. Hammang, B. Rost, A. Schafferhans, S. I. O'Donoghue, *Proc. Natl. Acad. Sci. U.S.A.* **2015**, 112, 15898-15903.
- [15] M. Dörr, M. P. C. Fibinger, D. Last, S. Schmidt, J. Santos-Aberturas, D. Böttcher, A. Hummel, C. Vickers, M. Voss, U. T. Bornscheuer, *Biotechnol. Bioeng.* **2016**, doi: 10.1002/bit.25925.
- [16] A. Nobili, M. G. Gall, I. V. Pavlidis, M. L. Thompson, M. Schmidt, U. T. Bornscheuer, *FEBS J.* **2013**, 280, 3084-3093.
- [17] Y. Ni, D. Holtmann, F. Hollmann, *ChemCatChem* **2014**, 6, 930-943.
- [18] R. A. Sheldon, *Chem. Commun.* **2008**, 29, 3352-3365.
- [19] K. Buchholz, V. Kasche, U. T. Bornscheuer, in *Biocatalysts and Enzyme Technology*, 2nd ed., Wiley-VCH, **2005**, p. 19.
- [20] D. Rozzell, in *Enzyme Catalysis in Organic Synthesis Vol. 3* (Eds.: K. Drauz, H. Gröger, O. May), Wiley-VCH, **2012**, pp. 1849-1938.
- [21] a) F. Steffen-Munsberg, C. Vickers, H. Kohls, H. Land, H. Mallin, A. Nobili, L. Skalden, T. van den Bergh, H.-J. Joosten, P. Berglund, M. Höhne, U. T. Bornscheuer, *Biotechnol. Adv.* **2015**, 33, 566-604; b) H. Kohls, F. Steffen-Munsberg, M. Höhne, *Curr. Opin. Chem. Biol.* **2014**, 19, 180-192; c) J. M. Janey, in *Sustainable Catalysis*:

- Challenges and Practices for the Pharmaceutical and Fine Chemical Industries* (Eds.: P. J. Dunn, K. K. (Mimi) Hii, M. J. Krische, M. T. Williams), John Wiley & Sons, Inc., Hoboken, **2013**, pp. 75-87.
- [22] F. van Rantwijk, A. Stolz, *J. Mol. Catal. B: Enzym.* **2015**, *114*, 25-30.
- [23] U. Schörken, P. Kempers, *Eur. J. Lipid Sci. Technol.* **2009**, *111*, 627-645.
- [24] U. T. Bornscheuer, *Eur. J. Lipid Sci. Technol.* **2014**, *116*, 1322-1331.
- [25] a) U. Biermann, U. Bornscheuer, M. A. R. Meier, J. O. Metzger, H. J. Schäfer, *Angew. Chem., Int. Ed.* **2011**, *50*, 3854-3871; b) J. O. Metzger, U. Bornscheuer, *Appl. Microbiol. Biotechnol.* **2006**, *71*, 13-22; c) U. T. Bornscheuer (Ed.), *Enzymes in Lipid Modification*, Wiley-VCH, Weinheim, **2005**; d) R. L. O. R. Cunha, E. A. Ferreira, C. S. Oliveira, Á. T. Omori, *Biotechnol. Adv.* **2015**, *33*, 614-623; e) A. S. de Miranda, L. S. M. Miranda, R. O. M. A. de Souza, *Biotechnol. Adv.* **2015**, *33*, 372-393; f) D. Romano, F. Bonomi, M. C. de Mattos, T. de Sousa Fonseca, M. da Conceição Ferreira de Oliveira, F. Molinari, *Biotechnol. Adv.* **2015**, *33*, 547-565.
- [26] K. Buchholz, V. Kasche, U. T. Bornscheuer, in *Biocatalysts and Enzyme Technology*, 2nd ed., Wiley-VCH, **2005**, p. 127.
- [27] a) L. Brunel, V. Neugnot, L. Landucci, H. Boze, G. Moulin, F. Bigey, E. Dubreucq, *J. Biotechnol.* **2004**, *111*, 41-50; b) A.-H. Jan, M. Subileau, C. Deyrieux, V. Perrier, É. Dubreucq, *Biochim. Biophys. Acta, Proteins Proteomics* **2016**, *1864*, 187-194; c) J. Müller, M. A. Sowa, M. Dörr, U. T. Bornscheuer, *Eur. J. Lipid Sci. Technol.* **2015**, *117*, 1903-1907; d) J. Müller, M. A. Sowa, B. Fredrich, H. Brundiek, U. T. Bornscheuer, *ChemBioChem* **2015**, *16*, 1791-1796; e) P. M. Neang, M. Subileau, V. Perrier, E. Dubreucq, *Appl. Microbiol. Biotechnol.* **2014**, *98*, 8927-8936; f) N. M. Osório, E. Dubreucq, M. M. R. da Fonseca, S. Ferreira-Dias, *Eur. J. Lipid Sci. Technol.* **2009**, *111*, 120-134; g) M. Subileau, A.-H. Jan, H. Nozac'h, M. Pérez-Gordo, V. Perrier, E. Dubreucq, *Biochim. Biophys. Acta, Proteins Proteomics* **2015**, *1854*, 1400-1411; h) A. de Kreij, S. Mampusti Madrid, J. D. Mikkelsen, J. B. Søre, DuPont Nutrition Biosciences APS (DK), Patent *US 2010/0285525 A1*, **2010**; i) J. D. Mikkelsen, K. M. Kragh, R. Mikkelsen, P. M. F. Derkx, S. Yu, H. Mulder, I. Nikolaev, DuPont Nutrition Biosciences APS (DK), Patent *US 2011/0236935 A1*, **2011**; j) J. B. Søre, J. D. Mikkelsen, A. de Kreij, Danisco A/S (DK), Patent *US 2005/0196766 A1*, **2005**.
- [28] S. Schmidt, C. Scherkus, J. Muschiol, U. Menyess, T. Winkler, W. Hummel, H. Gröger, A. Liese, H.-G. Herz, U. T. Bornscheuer, *Angew. Chem., Int. Ed.* **2015**, *54*, 2784-2787.
- [29] J. H. Sattler, M. Fuchs, F. G. Mutti, B. Grischek, P. Engel, J. Pfeffer, J. M. Woodley, W. Kroutil, *Angew. Chem., Int. Ed.* **2014**, *53*, 14153-14157.
- [30] a) H. Gröger, W. Hummel, S. Borchert, M. Krauß, in *Enzyme Catalysis in Organic Synthesis Vol. 2* (Eds.: K. Drauz, H. Gröger, O. May), Wiley-VCH, **2012**, pp. 1037-1110; b) K. Buchholz, V. Kasche, U. T. Bornscheuer, in *Biocatalysts and Enzyme Technology*, 2nd ed., Wiley-VCH, **2005**, p. 112.
- [31] W. Hummel, *Appl. Microbiol. Biotechnol.* **1990**, *34*, 15-19.
- [32] C. Filling, K. D. Berndt, J. Benach, S. Knapp, T. Prozorovski, E. Nordling, R. Ladenstein, H. Jörnval, U. Oppermann, *J. Biol. Chem.* **2002**, *277*, 25677-25684.
- [33] H. Jörnval, B. Persson, M. Krook, S. Atrian, R. Gonzalez-Duarte, J. Jeffery, D. Ghosh, *Biochemistry* **1995**, *34*, 6003-6013.
- [34] F. Hollmann, K. Bühler, B. Bühler, in *Enzyme Catalysis in Organic Synthesis Vol. 3* (Eds.: K. Drauz, H. Gröger, O. May), Wiley-VCH, **2012**, pp. 1325-1437.
- [35] A. Weckbecker, W. Hummel, *Biocatal. Biotransform.* **2006**, *24*, 380-389.
- [36] J. Haberland, A. Kriegesmann, E. Wolfram, W. Hummel, A. Liese, *Appl. Microbiol. Biotechnol.* **2002**, *58*, 595-599.
- [37] M. Krauß, W. Hummel, H. Gröger, *Eur. J. Org. Chem.* **2007**, *2007*, 5175-5179.
- [38] K. Abokitse, PhD thesis, University of Düsseldorf **2004**.
- [39] T. M. Poessl, B. Kosjek, U. Ellmer, C. C. Gruber, K. Edegger, K. Faber, P. Hildebrandt, U. T. Bornscheuer, W. Kroutil, *Adv. Synth. Catal.* **2005**, *347*, 1827-1834.
- [40] A. Díaz-Rodríguez, W. Borzęcka, I. Lavandera, V. Gotor, *ACS Catal.* **2014**, *4*, 386-393.
- [41] G. de Gonzalo, I. Lavandera, K. Faber, W. Kroutil, *Org. Lett.* **2007**, *9*, 2163-2166.
- [42] D. J. Bougioukou, J. D. Stewart, in *Enzyme Catalysis in Organic Synthesis Vol. 2* (Eds.: K. Drauz, H. Gröger, O. May), Wiley-VCH, **2012**, pp. 1111-1163.
- [43] O. Warburg, W. Christian, *Naturwissenschaften* **1932**, *20*, 688-688.
- [44] a) E. Haas, *Biochem. Z.* **1938**, *298*, 378-390; b) O. H. Warburg, W. Christian, *Biochem. Z.* **1938**, *298*, 368-377.

- [45] a) F. G. Fischer, O. Wiedemann, *Justus Liebigs Ann. Chem.* **1934**, 513, 260-280; b) F. G. Fischer, O. Wiedemann, *Justus Liebigs Ann. Chem.* **1935**, 520, 52-70.
- [46] P. A. Karplus, K. M. Fox, V. Massey, *FASEB J.* **1995**, 9, 1518-1526.
- [47] H. S. Toogood, J. M. Gardiner, N. S. Scrutton, *ChemCatChem* **2010**, 2, 892-914.
- [48] K. Saito, D. J. Thiele, M. Davio, O. Lockridge, V. Massey, *J. Biol. Chem.* **1991**, 266, 20720-20724.
- [49] C. Peters, R. Kölsch, M. Kadow, L. Skalden, F. Rudroff, M. D. Mihovilovic, U. T. Bornscheuer, *ChemCatChem* **2014**, 6, 1021-1027.
- [50] D. S. Blehert, B. G. Fox, G. H. Chambliss, *J. Bacteriol.* **1999**, 181, 6254-6263.
- [51] P. van Dillewijn, R.-M. Wittich, A. Caballero, J.-L. Ramos, *Appl. Environ. Microbiol.* **2008**, 74, 6820-6823.
- [52] R. E. Williams, D. A. Rathbone, N. S. Scrutton, N. C. Bruce, *Appl. Environ. Microbiol.* **2004**, 70, 3566-3574.
- [53] a) CYPED v6.0, **2016**, accessed on 2016-02-09, <https://cyped.biocatnet.de/>; b) Ł. Gricman, C. Vogel, J. Pleiss, *Proteins: Struct., Funct., Bioinf.* **2013**, 82, 491-504.
- [54] D. R. Nelson, in *Cytochrome P450 Protocols, Methods in Molecular Biology Vol. 320*, 2 ed. (Ed.: I. R. Phillips), Humana Press, **2006**, pp. 1-10.
- [55] a) D. Garfinkel, *Arch. Biochem. Biophys.* **1958**, 77, 493-509; b) M. Klingenberg, *Arch. Biochem. Biophys.* **1958**, 75, 376-386.
- [56] a) R. Sato, T. Omura, in *Proceedings of the Fifth International Congress of Biochemistry Vol. 9*, Pergamon Press, Oxford, **1961**, p. 529; b) T. Omura, R. Sato, *J. Biol. Chem.* **1962**, 237, PC1375-PC1376.
- [57] a) T. Omura, R. Sato, *J. Biol. Chem.* **1964**, 239, 2370-2378; b) T. Omura, R. Sato, *J. Biol. Chem.* **1964**, 239, 2379-2385.
- [58] V. B. Urlacher, M. Girhard, in *Enzyme Catalysis in Organic Synthesis Vol. 3* (Eds.: K. Drauz, H. Gröger, O. May), Wiley-VCH, **2012**, pp. 1227-1267.
- [59] J. Rittle, M. T. Green, *Science* **2010**, 330, 933-937.
- [60] a) P. C. Cirino, F. H. Arnold, *Angew. Chem., Int. Ed.* **2003**, 42, 3299-3301; b) A. C. Kotze, *Int. J. Parasitol.* **1999**, 29, 389-396; c) K. S. Rabe, K. Kiko, C. M. Niemeyer, *ChemBioChem* **2008**, 9, 420-425; d) K. S. Rabe, M. Spengler, M. Erkelenz, J. Müller, V. J. Gandubert, H. Hayen, C. M. Niemeyer, *ChemBioChem* **2009**, 10, 751-757.
- [61] B. Hu, C. Sun, S. Xu, W. Zhou, in *On Biomimetics*, doi: 10.5772/19279 (Ed.: L. Pramatarova), InTech, under CC BY-NC-SA 3.0 license, **2011**.
- [62] C. A. Tyson, J. D. Lipscomb, I. C. Gunsalus, *J. Biol. Chem.* **1972**, 247, 5777-5784.
- [63] T. Kido, T. Kimura, *J. Biol. Chem.* **1981**, 256, 8561-8568.
- [64] Y. Kumagai, K. A. Wickham, D. A. Schmitz, A. K. Cho, *Biochem. Pharmacol.* **1991**, 42, 1061-1067.
- [65] C. J. C. Whitehouse, S. G. Bell, L.-L. Wong, *Chem. Soc. Rev.* **2012**, 41, 1218-1260.
- [66] G. A. Roberts, G. Grogan, A. Greter, S. L. Flitsch, N. J. Turner, *J. Bacteriol.* **2002**, 184, 3898-3908.
- [67] a) R. Bernhardt, in *Encyclopedia of Biological Chemistry Vol. 1*, Elsevier, **2004**, pp. 544-549; b) R. Bernhardt, *J. Biotechnol.* **2006**, 124, 128-145.
- [68] F. P. Guengerich, A. W. Munro, *J. Biol. Chem.* **2013**, 288, 17065-17073.
- [69] a) M. J. Cryle, J. E. Stok, J. J. De Voss, *Aust. J. Chem.* **2003**, 56, 749-762; b) F. P. Guengerich, *Curr. Drug Metab.* **2001**, 2, 93-115; c) E. M. Isin, F. P. Guengerich, *Biochim. Biophys. Acta, Gen. Subj.* **2007**, 1770, 314-329; d) V. B. Urlacher, R. D. Schmid, *Curr. Opin. Chem. Biol.* **2006**, 10, 156-161.
- [70] a) C. Duport, R. Spagnoli, E. Degryse, D. Pompon, *Nat. Biotechnol.* **1998**, 16, 186-189; b) F. M. Szczepara, C. Chandelier, C. Villeret, A. Masurel, S. Bourot, C. Duport, S. Blanchard, A. Groisillier, E. Testet, P. Costaglioli, G. Cauet, E. Degryse, D. Balbuena, J. Winter, T. Achstetter, R. Spagnoli, D. Pompon, B. Dumas, *Nat. Biotechnol.* **2003**, 21, 143-149.
- [71] K. Petzoldt, K. Annen, H. Laurent, R. Wiechert, Schering AG (D), Patent *US4353985*, **1982**.
- [72] P. K. Ajikumar, W.-H. Xiao, K. E. J. Tyo, Y. Wang, F. Simeon, E. Leonard, O. Mucha, T. H. Phon, B. Pfeifer, G. Stephanopoulos, *Science* **2010**, 330, 70-74.
- [73] C. J. Paddon, P. J. Westfall, D. J. Pitera, K. Benjamin, K. Fisher, D. McPhee, M. D. Leavell, A. Tai, A. Main, D. Eng, D. R. Polichuk, K. H. Teoh, D. W. Reed, T. Treynor, J. Lenihan, H. Jiang, M. Fleck, S. Bajad, G. Dang, D. Dengrove, D. Diola, G. Dorin, K. W. Ellens, S. Fickes, J. Galazzo, S. P. Gaucher, T. Geistlinger, R. Henry, M. Hepp, T.

- Horning, T. Iqbal, L. Kizer, B. Lieu, D. Melis, N. Moss, R. Regentin, S. Secrest, H. Tsuruta, R. Vazquez, L. F. Westblade, L. Xu, M. Yu, Y. Zhang, L. Zhao, J. Lievense, P. S. Covello, J. D. Keasling, K. K. Reiling, N. S. Renninger, J. D. Newman, *Nature* **2013**, *496*, 528-532.
- [74] amyris.com, **2016**, accessed on 2016-02-11, <https://amyris.com/collaborations/artemisinin/>
- [75] A. Baeyer, V. Villiger, *Ber. Dtsch. Chem. Ges.* **1899**, *32*, 3625-3633.
- [76] R. Criegee, *Justus Liebigs Ann. Chem.* **1948**, *560*, 127-135.
- [77] a) H. Leisch, K. Morley, P. C. K. Lau, *Chem. Rev.* **2011**, *111*, 4165-4222; b) W. v. E. Doering, L. Speers, *J. Am. Chem. Soc.* **1950**, *72*, 5515-5518.
- [78] K. P. C. Vollhardt, N. E. Shore, *Organic Chemistry*, Vol. , 5 ed., Wiley-VCH, Weinheim, **2011**.
- [79] G. E. Turfitt, *Biochem. J.* **1948**, *42*, 376-383.
- [80] a) H. E. Conrad, R. DuBus, M. J. Namtvedt, I. C. Gunsalus, *J. Biol. Chem.* **1965**, *240*, 495-503; b) F. W. Forney, A. J. Markovetz, *Biochem. Biophys. Res. Commun.* **1969**, *37*, 31-38.
- [81] a) A. J. Willetts, *Trends Biotechnol.* **1997**, *15*, 55-62; b) K. Balke, M. Kadow, H. Mallin, S. Saß, U. T. Bornscheuer, *Org. Biomol. Chem.* **2012**, *10*, 6249-6265.
- [82] F. Fiorentini, M. Geier, C. Binda, M. Winkler, K. Faber, M. Hall, A. Mattevi, *ACS Chem. Biol.* **2016**, doi: 10.1021/acscchembio.5b01016.
- [83] M. D. Mihovilovic, in *Enzyme Catalysis in Organic Synthesis Vol. 3* (Eds.: K. Drauz, H. Gröger, O. May), Wiley-VCH, **2012**, pp. 1439-1485.
- [84] B. J. Yachnin, T. Sprules, M. B. McEvoy, P. C. K. Lau, A. M. Berghuis, *J. Am. Chem. Soc.* **2012**, *134*, 7788-7795.
- [85] a) F. Hollmann, I. W. C. E. Arends, K. Bühler, A. Schallmeyer, B. Bühler, *Green Chem.* **2011**, *13*, 226-265; b) N. M. Kamerbeek, D. B. Janssen, *Adv. Synth. Catal.* **2003**, *345*, 667-678.
- [86] a) W. Labet, W. Thielemans, *Chem. Soc. Rev.* **2009**, *38*, 3484-3504; b) F. J. van Natta, J. W. Hill, W. H. Carothers, *J. Am. Chem. Soc.* **1934**, *56*, 455-457.
- [87] P. Schlack, *Pure Appl. Chem.* **1967**, *15*, 507-523.
- [88] a) S. Schmidt, M. Genz, K. Balke, U. T. Bornscheuer, *J. Biotechnol.* **2015**, *214*, 199-211; b) L. P. Parra, J. P. Acevedo, M. T. Reetz, *Biotechnol. Bioeng.* **2015**, *112*, 1354-1364; c) H. L. van Beek, H. J. Wijma, L. Fromont, D. B. Janssen, M. W. Fraaije, *FEBS Open Bio* **2014**, *4*, 168-174; d) H. L. van Beek, G. de Gonzalo, M. W. Fraaije, *Chem. Commun.* **2012**, *48*, 3288-3290; e) D. J. Opperman, M. T. Reetz, *ChemBioChem* **2010**, *11*, 2589-2596.
- [89] Y. K. Bong, M. D. Clay, S. J. Collier, B. Mijts, M. Vogel, X. Zhang, J. Zhu, J. Nazor, D. Smith, S. Song, Codexis Inc. (USA), Patent WO 2011/071982 A2, **2011**.
- [90] a) *Drug and Therapeutics Bulletin* **2006**, *44*, 73-77; b) *Pharmainformation* **2007**, *22*, 1.
- [91] D. T. Gibson, R. E. Parales, *Curr. Opin. Biotechnol.* **2000**, *11*, 236-243.
- [92] T. Senda, T. Yamada, N. Sakurai, M. Kubota, T. Nishizaki, E. Masai, M. Fukuda, Y. Mitsui, *J. Mol. Biol.* **2000**, *304*, 397-410.
- [93] C. L. Colbert, M. M. J. Couture, L. D. Eltis, J. T. Bolin, *Structure* **2000**, *8*, 1267-1278.
- [94] Y. Furusawa, V. Nagarajan, M. Tanokura, E. Masai, M. Fukuda, T. Senda, *J. Mol. Biol.* **2004**, *342*, 1041-1052.
- [95] D. J. Ferraro, L. Gakhar, S. Ramaswamy, *Biochem. Biophys. Res. Commun.* **2005**, *338*, 175-190.
- [96] a) A. R. McDonald, L. Que, *Nat. Chem.* **2011**, *3*, 761-762; b) I. Prat, J. S. Mathieson, M. Güell, X. Ribas, J. M. Luis, L. Cronin, M. Costas, *Nat. Chem.* **2011**, *3*, 788-793.
- [97] S. M. Barry, G. L. Challis, *ACS Catal.* **2013**, *3*, 2362-2370.
- [98] a) T. Hudlicky, D. Gonzalez, D. T. Gibson, *Aldrichim. Acta* **1999**, *32*, 35-62; b) D. J. Leak, Y. Yin, J.-J. Zhang, N.-Y. Zhou, in *Enzyme Catalysis in Organic Synthesis Vol. 3* (Eds.: K. Drauz, H. Gröger, O. May), Wiley-VCH, **2012**, pp. 1487-1533.
- [99] a) C. Evans, D. Ribbons, S. Thomas, S. Roberts, Enzymatix Ltd. (GB), Patent WO 9012798 A2, **1990**; b) S. C. Taylor, ICI (GB), Patent EP 0076606A1, **1983**.
- [100] a) C. M. Serdar, D. C. Murdock, B. D. Ensley, Amgen Inc. (USA), Patent US 5173425, **1992**; b) D. C. Murdock, B. D. Ensley, C. M. Serdar, M. Thalen, *Bio/Technology* **1993**, *11*, 381-385.
- [101] W. Duetz, A. Fjällman, S. Ren, C. Jourdat, B. Witholt, *Appl. Environ. Microbiol.* **2001**, *67*, 2829-2832.

- [102] M. Groeneveld, H. L. van Beek, W. A. Duetz, M. W. Fraaije, *Tetrahedron* **2016**, doi: 10.1016/j.tet.2015.12.061
- [103] R. Robinson, *J. Chem. Soc., Trans.* **1917**, 111, 762-768.
- [104] a) S. Moriyama, S. Mogi, Y. Ishimatsu, Denka Engineering Co., Ltd. (JP), Patent *JP53091187A*, **1978**; b) S. Moriyama, S. Mogi, Y. Ishimatsu, Denka Engineering Co., Ltd., Patent *JP53091186A*, **1978**.
- [105] M. Dixon, in *Multi-Enzyme Systems*, University Press, Cambridge, **1949**, p. 1.
- [106] a) I. Oroz-Guinea, E. García-Junceda, *Curr. Opin. Chem. Biol.* **2013**, 17, 236-249; b) E. Ricca, B. Brucher, J. H. Schrittwieser, *Adv. Synth. Catal.* **2011**, 353, 2239-2262; c) P. A. Santacoloma, J. M. Woodley, in *Cascade Biocatalysis: Integrating Stereoselective and Environmentally Friendly Reactions* (Eds.: S. Riva, W.-D. Fessner), Wiley-VCH, Weinheim, **2014**, pp. 231-247; d) T. Sehl, J. Kulig, R. Westphal, D. Rother, in *Industrial Biocatalysis Vol. 1* (Ed.: P. Grunwald), CRC Press, Boca Raton, **2014**, pp. 887-930; e) R. A. Sheldon, in *Multi-Step Enzyme Catalysis* (Ed.: E. García-Junceda), Wiley-VCH, Weinheim, **2008**, pp. 109-135.
- [107] M. Dixon, in *Multi-Enzyme Systems*, University Press, Cambridge, **1949**, pp. 6-8.
- [108] J. Muschiol, C. Peters, N. Oberleitner, M. D. Mihovilovic, U. T. Bornscheuer, F. Rudroff, *Chem. Commun.* **2015**, 51, 5798-5811.
- [109] I. Ardao, A.-P. Zeng, *Chem. Eng. Sci.* **2013**, 87, 183-193.
- [110] a) H. Mallin, H. Wulf, U. T. Bornscheuer, *Enzyme Microb. Technol.* **2013**, 53, 283-287; b) S. Staudt, U. T. Bornscheuer, U. Menyes, W. Hummel, H. Gröger, *Enzyme Microb. Technol.* **2013**, 53, 288-292.
- [111] N. Oberleitner, C. Peters, F. Rudroff, U. T. Bornscheuer, M. D. Mihovilovic, *J. Biotechnol.* **2014**, 192, Part B, 393-399.
- [112] N. Oberleitner, C. Peters, J. Muschiol, M. Kadow, S. Sass, T. Bayer, P. Schaaf, N. Iqbal, F. Rudroff, M. D. Mihovilovic, U. T. Bornscheuer, *ChemCatChem* **2013**, 5, 3524-3528.
- [113] a) R. P. Shetty, D. Endy, T. F. Knight, Jr., *J. Biol. Eng.* **2008**, 2, 5; b) P. Xu, A. Vansiri, N. Bhan, M. A. G. Koffas, *ACS Synth. Biol.* **2012**, 1, 256-266.
- [114] S. Krauser, C. Weyler, L. Blaß, E. Heinze, in *Fundamentals and Application of New Bioproduction Systems* (Ed.: A.-P. Zeng), Springer, Berlin, Heidelberg, **2013**, pp. 185-234.
- [115] a) P. Cernuchova, M. D. Mihovilovic, *Org. Biomol. Chem.* **2007**, 5, 1715-1719; b) M. J. Fink, T. C. Fischer, F. Rudroff, H. Dudek, M. W. Fraaije, M. D. Mihovilovic, *J. Mol. Catal. B: Enzym.* **2011**, 73, 9-16; c) T. Reignier, V. de Berardinis, J. L. Petit, A. Mariage, K. Hamze, K. Duquesne, V. Alphand, *Chem. Commun.* **2014**, 50, 7793-7796.
- [116] a) R. Agudo, M. T. Reetz, *Chem. Commun.* **2013**, 49, 10914-10916; b) J. Liu, Z. Li, *ACS Catal.* **2013**, 3, 908-911; c) J.-W. Song, J.-H. Lee, U. T. Bornscheuer, J.-B. Park, *Adv. Synth. Catal.* **2014**, 356, 1782-1788.
- [117] C. Peters, F. Rudroff, M. D. Mihovilovic, U. T. Bornscheuer, *submitted*.
- [118] G. Gourinchas, E. Busto, M. Killinger, N. Richter, B. Wiltschi, W. Kroutil, *Chem. Commun.* **2015**, 51, 2828-2831.
- [119] C. Schmidt-Dannert, F. H. Arnold, *Trends Biotechnol.* **1999**, 17, 135-136.
- [120] C. Wandrey, in *Immobilized Cells: Basics and Application* (Eds.: R. H. Wijfels, R. M. Buitelaar, C. Bucke, J. Tramper), Elsevier Science B.V., Amsterdam, **1996**, pp. 3-16.
- [121] H. A. Conner, R. J. Allgeier, *Adv. Appl. Microbiol.* **1976**, 20, 81-133.
- [122] a) Y. Levin, M. Pecht, L. Goldstein, E. Katchalski, *Biochemistry* **1964**, 3, 1905-1913; b) G. Manecke, S. Singer, *Makromol. Chem.* **1960**, 37, 119-142.
- [123] T. Tosa, T. Mori, N. Fuse, I. Chibata, *Enzymologia* **1966**, 31, 214-224.
- [124] a) A. M. Klibanov, *Science* **1983**, 219, 722-727; b) S. Ramakrishna, R. Prakasham, *Curr. Sci. India* **1999**, 77, 87.
- [125] a) Y.-M. Ko, C.-I. Chen, C.-J. Shieh, Y.-C. Liu, *Biochem. Eng. J.* **2012**, 61, 20-27; b) A. Percot, X. X. Zhu, M. Lafleur, *Bioconjugate Chem.* **2000**, 11, 674-678.
- [126] a) T. Hattori, C. Furusaka, *J. Biochem.* **1960**, 48, 831-837; b) T. Hattori, C. Furusaka, *J. Biochem.* **1961**, 50, 312-315.
- [127] J. Klein, H. Ziehr, *J. Biotechnol.* **1990**, 16, 1-15.
- [128] M. Martienssen, habil. thesis, Martin-Luther-University Halle Wittenberg **2001**.
- [129] a) J. M. Goddard, J. H. Hotchkiss, *Prog. Polym. Sci.* **2007**, 32, 698-725; b) M. Ozdemir, C. U. Yurteri, H. Sadikoglu, *Crit. Rev. Food Sci. Nutr.* **1999**, 39, 457-477.
- [130] F. Secundo, *Chem. Soc. Rev.* **2013**, 42, 6250-6261.

- [131] a) R. A. Sheldon, *Adv. Synth. Catal.* **2007**, *349*, 1289-1307; b) R. A. Sheldon, in *Pharmaceutical Process Chemistry* (Eds.: T. Shioiri, K. Izawa, T. Konoike), Wiley-VCH, **2010**, pp. 159-181; c) R. A. Sheldon, *Org. Process Res. Dev.* **2011**, *15*, 213-223; d) R. A. Sheldon, R. Schoevaart, L. M. Langen, in *Immobilization of Enzymes and Cells*, (Ed.: J. M. Guisan), Humana Press, Totowa, NJ, **2006**, pp. 31-45; e) R. A. Sheldon, R. Schoevaart, L. M. van Langen, *Biocatal. Biotransform.* **2005**, *23*, 141-147; f) R. A. Sheldon, S. van Pelt, *Chem. Soc. Rev.* **2013**, *42*, 6223-6235; g) R. A. Sheldon, S. van Pelt, S. Kanbak-Aksu, J.-A. Rasmussen, M. H. A. Janssen, *Aldrichim. Acta* **2013**, *46*, 81-93, 13 pp.
- [132] a) Z. Liu, B. Liu, M. Zhang, J. Kong, J. Deng, *Anal. Chim. Acta* **1999**, *392*, 135-141; b) D. Chen, Y. Cao, B. Liu, J. Kong, *Anal. Bioanal. Chem.* **2002**, *372*, 737-739.
- [133] a) E. Stanford, *Am. J. Pharm.* **1883**, *55*; b) E. Stanford, *J. Chem. Soc., Abstr.* **1883**, *44*, 943-944; c) E. C. C. Stanford, *Chem. News* **1883**, *47*, 254-257, and 267-259.
- [134] a) A. Jensen, in *Algae, Environment and Human Affairs* (Eds.: W. Wiessner, E. Schnepf, R. C. Starr), Biopress, Bristol, **1995**, pp. 79-92; b) A. H. King, in *Food Hydrocolloids Vol. 2* (Ed.: M. Glicksman), CRC Press, Boca Raton, **1983**, pp. 115-188; c) A. C. J. Voragen, W. Pilnik, in *Ullmann's Encyclopedia of Industrial Chemistry Vol. 5* (Eds.: B. Elvers, S. Hawkins, W. Russey), Wiley-VCH, Weinheim, **1994**, pp. 21-57.
- [135] a) F. G. Fischer, H. Dörfel, *Z. Physiol. Chem.* **1955**, *302*, 186-203; b) W. L. Nelson, L. H. Cretcher, *J. Am. Chem. Soc.* **1929**, *51*, 1914-1922; c) W. L. Nelson, L. H. Cretcher, *J. Am. Chem. Soc.* **1930**, *52*, 2130-2132; d) A. I. Usov, *Russ. Chem. Rev.* **1999**, *68*, 957-966.
- [136] O. Smidsrød, G. Skjåk-Braek, *Trends Biotechnol.* **1990**, *8*, 71-78.
- [137] D. A. Rees, E. J. Welsh, *Angew. Chem., Int. Ed.* **1977**, *16*, 214-224.
- [138] U. Prüße, J. Dalluhn, J. Breford, K. D. Vorlop, *Chem. Eng. Technol.* **2000**, *23*, 1105-1110.
- [139] J. K. Park, H. N. Chang, *Biotechnol. Adv.* **2000**, *18*, 303-319.
- [140] I. Nilsson, S. Ohlson, L. Häggström, N. Molin, K. Mosbach, *Eur. J. Appl. Microbiol.* **1980**, *10*, 261-274.
- [141] S. C. Musgrave, N. W. Kerby, G. A. Codd, W. D. P. Stewart, *Biotechnol. Lett.* **1982**, *4*, 647-652.
- [142] J. A. Fujii, D. T. Slade, K. Redenbaugh, K. A. Walker, *Trends Biotechnol.* **1987**, *5*, 335-339.
- [143] M. Decleire, N. van Huynh, J. C. Motte, W. Cat, *Appl. Microbiol. Biotechnol.* **1985**, *22*, 438-441.
- [144] molekularkuche.de, **2016**, accessed on 2016-03-01, <http://www.molekularkuche.de/spharenbildung/5-algin-texturas-natriumalginat-8435261900004.html>
- [145] X. Zhu, Patent CN20081026095 20080128, **2009**.
- [146] C. Yao, T. Zhu, Y. Qi, Y. Zhao, H. Xia, W. Fu, *Sensors* **2010**, *10*, 5859-5871.
- [147] a) M. Amounas, C. Innocent, S. Cosnier, P. Seta, *J. Membr. Sci.* **2000**, *176*, 169-176; b) M. Amounas, V. Magne, C. Innocent, E. Dejean, P. Seta, *Enzyme Microb. Technol.* **2002**, *31*, 171-178.
- [148] A. Fishman, I. Levy, U. Cogan, O. Shoseyov, *J. Mol. Catal. B: Enzym.* **2002**, *18*, 121-131.
- [149] C.-I. Chen, Y.-M. Ko, C.-J. Shieh, Y.-C. Liu, *J. Membr. Sci.* **2011**, *380*, 34-40.
- [150] a) Y. Azuma, R. Zschoche, M. Tinzl, D. Hilvert, *Angew. Chem., Int. Ed.* **2016**, *55*, 1531-1534; b) F. Cai, M. Sutter, S. L. Bernstein, J. N. Kinney, C. A. Kerfeld, *ACS Synth. Biol.* **2014**, *4*, 444-453; c) S. Cheng, S. Sinha, C. Fan, Y. Liu, T. A. Bobik, *J. Bacteriol.* **2011**, *193*, 1385-1392; d) J. L. Chorchero, J. Cedano, *Microb. Cell Fact.* **2011**, *10*, 92; e) C. Fan, T. A. Bobik, *J. Bacteriol.* **2011**, *193*, 5623-5628; f) C. Fan, S. Cheng, Y. Liu, C. M. Escobar, C. S. Crowley, R. E. Jefferson, T. O. Yeates, T. A. Bobik, *Proc. Natl. Acad. Sci. U. S. A.* **2009**, *107*, 7509-7514; g) C. Fan, S. Cheng, S. Sinha, T. A. Bobik, *Proc. Natl. Acad. Sci. U. S. A.* **2012**, *109*, 14995-15000; h) J. B. Parsons, S. Frank, D. Bhella, M. Liang, M. B. Prentice, D. P. Mulvihill, M. J. Warren, *Mol. Cell* **2010**, *38*, 305-315; i) F. Sargent, F. A. Davidson, C. L. Kelly, R. Binny, N. Christodoulides, D. Gibson, E. Johansson, K. Kozyrskaya, L. L. Lado, J. MacCallum, R. Montague, B. Ortmann, R. Owen, S. J. Coulthurst, L. Dupuy, A. R. Prescott, T. Palmer, *Microbiology* **2013**, *159*, 2427-2436; j) B. Wörsdörfer, Z. Pianowski, D. Hilvert, *J. Am. Chem. Soc.* **2012**, *134*,

- 909-911; k) B. Wörsdörfer, K. J. Woycechowsky, D. Hilvert, *Science* **2011**, 331, 589-592.
- [151] a) K. Cameron, S. Najmudin, V. D. Alves, E. A. Bayer, S. P. Smith, P. Bule, H. Waller, L. M. A. Ferreira, H. J. Gilbert, C. M. G. A. Fontes, *J. Biol. Chem.* **2015**, 290, 13578-13590; b) X. Gao, S. Yang, C. Zhao, Y. Ren, D. Wei, *Angew. Chem., Int. Ed.* **2014**, 53, 14027-14030; c) K. Cameron, J. Y. Weinstein, O. Zhivin, P. Bule, S. J. Fleishman, V. D. Alves, H. J. Gilbert, L. M. A. Ferreira, C. M. G. A. Fontes, E. A. Bayer, S. Najmudin, *J. Biol. Chem.* **2015**, 290, 16215-16225.
- [152] a) Y. Hu, F. Wang, C.-H. Lu, J. Girsh, E. Golub, I. Willner, *Chem. - Eur. J.* **2014**, 20, 16203-16209; b) V. Linko, M. Eerikäinen, M. A. Kostianen, *Chem. Commun.* **2015**, 51, 5351-5354.
- [153] C. J. Delebecque, A. B. Lindner, P. A. Silver, F. A. Aldaye, *Science* **2011**, 333, 470-474.
- [154] H. Mallin, J. Muschiol, E. Byström, U. T. Bornscheuer, *ChemCatChem* **2013**, 5, 3529-3532.
- [155] C. W. Pilo, S. W. Dahlbeck, Patent *US2941872*, **1960**.
- [156] a) J. J. Carberry, *Ind. Eng. Chem.* **1964**, 56, 39-46; b) J. A. Mahoney, *J. Catal.* **1974**, 32, 247-253; c) J. R. Pereira, P. H. Calderbank, *Chem. Eng. Sci.* **1975**, 30, 167-175.
- [157] N. B. Havewala, H. H. Weetall, Corning Glass Works (USA), Patent *US3767535*, **1973**.
- [158] a) J. Persson, K. Öberg, F. Almqvist, K. Irgum, Nordic Chemquest AB (Sweden), Patent *WO 2011/098570*, **2011**; b) E. Byström, H. Scherman, U. T. Bornscheuer, K. Irgum, Nordic Chemquest AB (Sweden), Patent *WO 2015/050491*, **2015**.
- [159] gruenenthal-opfer.de, **2016**, accessed on 2016-02-22, <http://www.gruenenthal-opfer.de/Contergan>
- [160] T. Eriksson, S. Björkman, B. Roth, P. Höglund, *J. Pharm. Pharmacol.* **2000**, 52, 807-817.
- [161] V. Günzler, *Drug Saf.* **1992**, 7, 116-134.
- [162] a) M. Reist, P.-A. Carrupt, E. Francotte, B. Testa, *Chem. Res. Toxicol.* **1998**, 11, 1521-1528; b) V. Jacques, A. W. Czarnik, T. M. Judge, L. H. T. Van der Ploeg, S. H. DeWitt, *Proc. Natl. Acad. Sci. U.S.A.* **2015**, 112, E1471-E1479.
- [163] F. Weber, G. Sedelmeier, *Nachr. Chem.* **2014**, 10, 997.
- [164] M. Quintanar-Audelo, E. Eberhard, J. Nazor, D. Smith, C. Wang, Codexis Inc. (USA), Patent *WO 2014/133960 A1*, **2014**.
- [165] M. Fuchs, J. E. Farnberger, W. Kroutil, *Eur. J. Org. Chem.* **2015**, 2015, 6965-6982.
- [166] T. Matsui, Y. Dekishima, M. Ueda, *Appl. Microbiol. Biotechnol.* **2014**, 98, 7699-7706.
- [167] a) B. H. Guo, G. Y. Kai, H. B. Jin, K. X. Tang, *Afr. J. Biotechnol.* **2006**, 5, 15-20; b) S. Howat, B. Park, I. S. Oh, Y.-W. Jin, E.-K. Lee, G. J. Loake, *New Biotechnol.* **2014**, 31, 242-245.
- [168] C. K. Savile, J. M. Janey, E. C. Mundorff, J. C. Moore, S. Tam, W. R. Jarvis, J. C. Colbeck, A. Krebber, F. J. Fleitz, J. Brands, P. N. Devine, G. W. Huisman, G. J. Hughes, *Science* **2010**, 329, 305-309.
- [169] M. J. Fink, F. Rudroff, M. D. Mihovilovic, *Bioorg. Med. Chem. Lett.* **2011**, 21, 6135-6138.
- [170] a) M. Girhard, K. Machida, M. Itoh, R. D. Schmid, A. Arisawa, V. B. Urlacher, *Microb. Cell Fact.* **2009**, 8, 36; b) S. Schulz, M. Girhard, S. K. Gaßmeyer, V. D. Jäger, D. Schwarze, A. Vogel, V. B. Urlacher, *ChemCatChem* **2015**, 7, 601-604.
- [171] W. Tassaneeyakul, L.-Q. Guo, K. Fukuda, T. Ohta, Y. Yamazoe, *Arch. Biochem. Biophys.* **2000**, 378, 356-363.
- [172] T. J. Leitereg, D. G. Guadagni, J. Harris, T. R. Mon, R. Teranishi, *J. Agric. Food. Chem.* **1971**, 19, 785-787.
- [173] a) H. J. Bouwmeester, M. C. J. M. Konings, J. Gershenzon, F. Karp, R. B. Croteau, *Phytochemistry* **1999**, 50, 243-248; b) H. J. Bouwmeester, J. Gershenzon, M. C. J. M. Konings, R. B. Croteau, *Plant Physiol.* **1998**, 17, 901-912.
- [174] a) C. Haudenschield, M. Schalk, F. Karp, R. B. Croteau, *Arch. Biochem. Biophys.* **2000**, 379, 127-136; b) S. L. Lupien, F. Karp, M. Wildung, R. B. Croteau, *Arch. Biochem. Biophys.* **1999**, 368, 181-192.
- [175] M. Schalk, R. B. Croteau, *Proc. Natl. Acad. Sci. U. S. A.* **2000**, 97, 11948-11953.
- [176] plasticseurope.org, **2016**, accessed on 2016-02-25, <http://www.plasticseurope.org/plastics-industry/market-and-economics.aspx>

- [177] S. Schmidt, H. C. Büchsenschütz, C. Scherkus, A. Liese, H. Gröger, U. T. Bornscheuer, *ChemCatChem* **2015**, 7, 3951-3955.
- [178] a) S. C. Knight, C. P. Schaller, W. B. Tolman, M. A. Hillmyer, *RSC Adv.* **2013**, 3, 20399-20404; b) J. R. Lowe, W. B. Tolman, M. A. Hillmyer, *Biomacromolecules* **2009**, 10, 2003-2008; c) C. L. Wanamaker, L. E. O'Leary, A. L. Nathaniel, M. A. Hillmyer, W. B. Tolman, *Biomacromolecules* **2007**, 8, 3634-3640; d) D. Zhang, M. A. Hillmyer, W. B. Tolman, *Biomacromolecules* **2005**, 6, 2091-2095.
- [179] L. Jiang, J. Zhang, in *Handbook of Biopolymers and Biodegradable Plastics* (Ed.: S. Ebnesajjad), William Andrew Publishing, Boston, **2013**, pp. 109-128.
- [180] R. A. Gross, B. Kalra, *Science* **2002**, 297, 803-807.
- [181] B. Liu, S. Bhaladhare, P. Zhan, L. Jiang, J. Zhang, L. Liu, A. T. Hotchkiss, *Ind. Eng. Chem. Res.* **2011**, 50, 13859-13865.
- [182] Y. Tokiwa, T. Suzuki, *Nature* **1977**, 270, 76-78.
- [183] C. L. Ventola, *Pharm. Ther.* **2014**, 39, 704-711.
- [184] R. T. MacDonald, S. K. Pulapura, Y. Y. Svirkin, R. A. Gross, D. L. Kaplan, J. Akkara, G. Swift, S. Wolk, *Macromolecules* **1995**, 28, 73-78.
- [185] P. Inprakhon, P. Panlawan, T. Pongtharankul, E. Marie, L. O. Wiemann, A. Durand, V. Sieber, *Colloids Surf., B* **2014**, 113, 254-260.
- [186] S. Namekawa, S. Suda, H. Uyama, S. Kobayashi, *Int. J. Biol. Macromol.* **1999**, 25, 145-151.
- [187] F. Chen, L. Liu, P. H. Cooke, K. B. Hicks, J. Zhang, *Ind. Eng. Chem. Res.* **2008**, 47, 8667-8675.
- [188] a) E. Boisselier, M.-L. Audet, L. Cantin, C. Salesse, *BioTechniques* **2011**, 51, 193-194; b) thermofisher.com, **2015**, accessed on 2015-11-05, <https://www.thermofisher.com/us/en/home/life-science/protein-biology/protein-biology-learning-center/protein-biology-resource-library/pierce-protein-methods/gst-tagged-proteins-production-purification.html>
- [189] M. Dietrich, S. Eiben, C. Asta, T. A. Do, J. Pleiss, V. B. Urlacher, *Appl. Microbiol. Biotechnol.* **2008**, 79, 931-940.
- [190] a) V. B. Chen, W. B. Arendall, III, J. J. Headd, D. A. Keedy, R. M. Immormino, G. J. Kapral, L. W. Murray, J. S. Richardson, D. C. Richardson, *Acta Crystallogr., Sect. D: Biol. Crystallogr.* **2010**, 66, 12-21; b) I. W. Davis, A. Leaver-Fay, V. B. Chen, J. N. Block, G. J. Kapral, X. Wang, L. W. Murray, W. B. Arendall, J. Snoeyink, J. S. Richardson, D. C. Richardson, *Nucleic Acids Res.* **2007**, 35, W375-W383.
- [191] C. J. C. Whitehouse, S. G. Bell, L.-L. Wong, *Chem. Soc. Rev.* **2012**, 41, 1218-1260.
- [192] E. Chovancova, A. Pavelka, P. Benes, O. Strnad, J. Brezovsky, B. Kozlikova, A. Gora, V. Sustr, M. Klvana, P. Medek, L. Biedermannova, J. Sochor, J. Damborsky, *PLoS Comput. Biol.* **2012**, 8, e1002708.
- [193] B. A. Halkier, H. L. Nielsen, B. Koch, B. L. Møller, *Arch. Biochem. Biophys.* **1995**, 322, 369-377.
- [194] C. Linhart, R. Shamir, in *PCR Primer Design, Methods in Molecular Biology Vol. 402* (Ed.: A. Yuryev), Humana Press, **2007**, pp. 220-244.
- [195] a) Z. Wang, F. Lie, E. Lim, K. Li, Z. Li, *Adv. Synth. Catal.* **2009**, 351, 1849-1856; b) T. K. Cheong, P. J. Oriel, *Appl. Biochem. Biotechnol.* **2000**, 84-86, 903-915.
- [196] P. Schumann, E. Stackebrandt, in *Bergey's Manual of Systematic Bacteriology Vol. 5: The Actinobacteria* (Eds.: W. Whitman, M. Goodfellow, P. Kämpfer, H.-J. Busse, M. Trujillo, W. Ludwig, K.-I. Suzuki, A. Parte), Springer-Verlag, New York, **2012**, pp. 1002-1005.
- [197] P. Jones, D. Binns, H.-Y. Chang, M. Fraser, W. Li, C. McAnulla, H. McWilliam, J. Maslen, A. Mitchell, G. Nuka, S. Pesseat, A. F. Quinn, A. Sangrador-Vegas, M. Scheremetjew, S.-Y. Yong, R. Lopez, S. Hunter, *Bioinformatics* **2014**, 30, 1236-1240.
- [198] K. Zorn, M.Sc. thesis, Greifswald University **2015**.
- [199] R. Chuanchuen, C. T. Narasaki, H. P. Schweizer, *BioTechniques* **2002**, 33, 760-763.
- [200] H. Mallin, U. Menyes, T. Vorhaben, M. Höhne, U. T. Bornscheuer, *ChemCatChem* **2013**, 5, 588-593.
- [201] J. Muschiol, Dipl. thesis, Greifswald University **2012**.
- [202] H. Mallin, PhD thesis, Greifswald University **2014**.
- [203] a) M. B. Abdul Rahman, N. M. M. Yunus, M. Z. Hussein, R. N. Z. R. Abdul Rahman, A. B. Salleh, M. Basri, *Biocatal. Biotransform.* **2005**, 23, 233-239; b) R. George, S. Sugunan, *J. Mol. Catal. B: Enzym.* **2014**, 105, 26-32.

- [204] S. Becker, B.Sc. thesis, Greifswald University **2013**.
- [205] a) Y. G. Li, J. M. Xing, X. C. Xiong, W. L. Li, H. S. Gao, H. Z. Liu, *J. Ind. Microbiol. Biotechnol.* **2008**, *35*, 145-150; b) D. B. Seifert, J. A. Phillips, *Biotechnol. Prog.* **1997**, *13*, 562-568; c) D. Serp, E. Cantana, C. Heinzen, U. Von Stockar, I. W. Marison, *Biotechnol. Bioeng.* **2000**, *70*, 41-53.
- [206] H. Büchsenschütz, M.Sc. thesis, University of Greifswald **2015**.
- [207] C. Peters, PhD thesis, University of Greifswald **2015**.
- [208] a) I. Hilker, V. Alphand, *Org. Lett.* **2004**, *6*, 1955-1958; b) I. Hilker, V. Alphand, R. Wohlgemuth, R. Furstoss, *Adv. Synth. Catal.* **2004**, *346*, 203-214; c) I. Hilker, M. C. Gutiérrez, R. Furstoss, J. Ward, R. Wohlgemuth, V. Alphand, *Nature Protocols* **2008**, *3*, 546-554; d) I. Hilker, R. Wohlgemuth, V. Alphand, R. Furstoss, *Biotechnol. Bioeng.* **2005**, *92*, 702-710; e) H. D. Simpson, V. Alphand, R. Furstoss, *J. Mol. Catal. B: Enzym.* **2001**, *16*, 101-108; f) K. Geitner, J. Rehdorf, R. Snajdrova, U. T. Bornscheuer, *Appl. Microbiol. Biotechnol.* **2010**, *88*, 1087-1093.
- [209] a) P. Dvorak, N. P. Kurumbang, J. Bendl, J. Brezovsky, Z. Prokop, J. Damborsky, *ChemBioChem* **2014**, *15*, 1891-1895; b) N. P. Kurumbang, P. Dvorak, J. Bendl, J. Brezovsky, Z. Prokop, J. Damborsky, *ACS Synth. Biol.* **2014**, *3*, 172-181.
- [210] J. E. Dueber, G. C. Wu, G. R. Malmirchegini, T. S. Moon, C. J. Petzold, A. V. Ullal, K. L. J. Prather, J. D. Keasling, *Nat. Biotechnol.* **2009**, *27*, 753-761.
- [211] J. Rehdorf, M. D. Mihovilovic, M. W. Fraaije, U. T. Bornscheuer, *Chem. - Eur. J.* **2010**, *16*, 9525-9535.
- [212] M. Sugiura, T. Sakaki, Y. Yabusaki, H. Ohkawa, *Biochim. Biophys. Acta, Gene Struct. Expression* **1996**, *1308*, 231-240.
- [213] a) A. L. Demain, P. Vaishnav, *Biotechnol. Adv.* **2009**, *27*, 297-306; b) C. H. Schein, *Nat. Biotechnol.* **1989**, *7*, 1141-1149.
- [214] E. M. J. Gillam, L. M. Notley, H. Cai, J. J. De Voss, F. P. Guengerich, *Biochemistry* **2000**, *39*, 13817-13824.
- [215] S. Brixius-Anderko, F. Hannemann, M. Ringle, Y. Khatri, R. Bernhardt, *Biotechnol. Appl. Biochem.* **2016**, doi: 10.1002/bab.1488.
- [216] Q. Cai, G. Takemura, M. Ashraf, *J. Cardiovasc. Pharmacol.* **1995**, *25*, 147-155.
- [217] R. Fasan, Y. T. Meharena, C. D. Snow, T. L. Poulos, F. H. Arnold, *J. Mol. Biol.* **2008**, *383*, 1069-1080.
- [218] A. Seifert, M. Antonovici, B. Hauer, J. Pleiss, *ChemBioChem* **2011**, *12*, 1346-1351.
- [219] a) F. Karp, C. A. Mihaliak, J. L. Harris, R. Croteau, *Arch. Biochem. Biophys.* **1990**, *276*, 219-226; b) M. Wüst, R. B. Croteau, *Biochemistry* **2002**, *41*, 1820-1827.
- [220] R. K. Kuipers, H.-J. Joosten, W. J. H. van Berkel, N. G. H. Leferink, E. Rooijen, E. Ittmann, F. van Zimmeren, H. Jochens, U. Bornscheuer, G. Vriend, V. A. P. Martins dos Santos, P. J. Schaap, *Proteins: Struct., Funct., Bioinf.* **2010**, *78*, 2101-2113.
- [221] T. H. M. Smits, M. A. Seeger, B. Witholt, J. B. van Beilen, *Plasmid* **2001**, *46*, 16-24.
- [222] J. Alonso-Gutierrez, R. Chan, T. S. Batth, P. D. Adams, J. D. Keasling, C. J. Petzold, T. S. Lee, *Metab. Eng.* **2013**, *19*, 33-41.
- [223] a) C. Willrodt, C. David, S. Cornelissen, B. Bühler, M. K. Julsing, A. Schmid, *Biotechnol. J.* **2014**, *9*, 1000-1012; b) C. Willrodt, A. Hoschek, B. Bühler, A. Schmid, M. K. Julsing, *Biotechnol. Bioeng.* **2015**, *112*, 1738-1750.
- [224] a) F. Benyahia, R. Polomarkaki, *Process Biochem.* **2005**, *40*, 1251-1262; b) M. N. Kathiravan, R. Karthiga Rani, R. Karthick, K. Muthukumar, *Bioresour. Technol.* **2010**, *101*, 853-858; c) D. Lewińska, S. Rosiński, D. Hunkeler, D. Poncelet, A. Weryński, *J. Membr. Sci.* **2002**, *209*, 533-540.
- [225] J. Wachtmeister, P. Mennicken, A. Hunold, D. Rother, *ChemCatChem* **2016**, *8*, 607-614.
- [226] C. Scherkus, PhD thesis, Technical University Hamburg-Harburg **in preparation**.
- [227] P. Süß, S. Illner, J. von Langermann, S. Borchert, U. T. Bornscheuer, R. Wardenga, U. Kragl, *Org. Process Res. Dev.* **2014**, *18*, 897-903.
- [228] P. López-Serrano, L. Cao, F. van Rantwijk, R. A. Sheldon, *Biotechnol. Lett.* **2016**, *24*, 1379-1383.
- [229] biophp.org, **2016**, accessed on 2016-03-17, http://www.biophp.org/minitools/melting_temperature/demo.php
- [230] a) M. Sugimoto, N. Esaki, H. Tanaka, K. Soda, *Anal. Biochem.* **1989**, *179*, 309-311; b) M. A. Vandeyar, M. P. Weiner, C. J. Hutton, *Gene* **1988**, *65*, 129-133; c) J. W. Taylor, J. Ott, F. Eckstein, *Nucleic Acids Res.* **1985**, *13*, 8765-8785.

- [231] C. Li, A. Wen, B. Shen, J. Lu, Y. Huang, Y. Chang, *BMC Biotechnol.* **2011**, *11*, 92.
- [232] Y. Zhang, U. Werling, W. Edelmann, *Nucleic Acids Res.* **2012**, *40*, e55.
- [233] E. Krieger, G. Vriend, *Bioinformatics* **2014**, *30*, 2981-2982.
- [234] X. Dai, G. Wang, D. S. Yang, Y. Tang, P. Broun, M. D. Marks, L. W. Sumner, R. A. Dixon, P. X. Zhao, *Plant Physiol.* **2010** *152*, 44-54.
- [235] C. Linhart, R. Shamir, *J. Cell Biol.*, **2005**, *12*, 431-456.

List of Publications

Articles in peer review journals

1. J. Muschiol*, C. Peters*, N. Oberleitner, M. D. Mihovilovic, U. T. Bornscheuer, F. Rudroff, **2015**: Cascade catalysis – strategies and challenges *en route* to preparative synthetic biology, *Chemical Communications* 51:5798-5811.
2. S. Schmidt, C. Scherkus, J. Muschiol, U. Menyes, T. Winkler, W. Hummel, H. Gröger, A. Liese, H.-G. Herz, U. T. Bornscheuer, **2015**: An Enzyme Cascade Synthesis of ϵ -Caprolactone and its Oligomers, *Angewandte Chemie International Edition* 54(9):2784-2787.
3. H. Mallin*, J. Muschiol*, E. Byström, U. T. Bornscheuer, **2013**: Efficient Biocatalysis with Immobilized Enzymes or Encapsulated Whole Cell Microorganism by Using the SpinChem Reactor System, *ChemCatChem* 5(12):3529-3532.
4. N. Oberleitner*, C. Peters*, J. Muschiol, M. Kadow, S. Saß, T. Bayer, P. Schaaf, N. Iqbal, F. Rudroff, M. D. Mihovilovic, U. T. Bornscheuer, **2013**: An Enzymatic Toolbox for Cascade Reactions: A Showcase for an *In Vivo* Redox Sequence in Asymmetric Synthesis, *ChemCatChem* 5(12):3524-3528.

*Equal contribution/Shared first authorship

Contributions to monographs and other journals

5. N. Oberleitner, C. Peters, J. Muschiol, F. Rudroff, M. D. Mihovilovic, U. T. Bornscheuer, **2015**: A three Enzyme mediated RedOx Cascade for the production of Normal Carvo-Lactone, in *Practical Methods for Biocatalysis and Biotransformations 3, Vol. 3* (ed. J. Whittall, P. W. Sutton, W. Kroutil).
6. H. Mallin, J. Muschiol, E. Byström, U. T. Bornscheuer, **2013**: SpinChem: A Novel Reactor Concept For Biocatalysis, *BRG Newsletter* 12:4-5.

Conference Contributions

7. J. Muschiol, C. Peters, N. Oberleitner, S. Schmidt, C. Scherkus, E. Byström, U. Menyes, F. Rudroff, A. Liese, M. D. Mihovilovic, U. T. Bornscheuer, Poster: Production of Chiral Lactones and Oligomers by Enzyme Cascades and Application of a Rotating Flow Cell, *12th Biotrans*, 2015-07-26 – 30, Vienna, Austria.
8. J. Muschiol, H. Mallin, C. Peters, E. Byström, N. Oberleitner, F. Rudroff, M. D. Mihovilovic, U. T. Bornscheuer, Poster: Heterogeneous biotransformation using a novel mass transfer concept, *3rd Multistep Enzyme Catalyzed Processes Congress*, 2014-04-07 – 10, Madrid, Spain.
9. N. Oberleitner, C. Peters, J. Muschiol, M. Kadow, S. Saß, T. Bayer, P. Schaaf, N. Iqbal, F. Rudroff, M. D. Mihovilovic, U. T. Bornscheuer, Poster: Development of an Enzymatic *In Vivo* Redox Cascade for Asymmetric Synthesis, *Molecular Life Sciences*, 2013-10-03 – 06, Frankfurt (Main), Germany.
10. J. Muschiol, H. Mallin, E. Byström, U. Menyes, U. T. Bornscheuer, Poster: Heterogeneous biotransformation using a novel mass transfer concept, *3rd Int. Bielefeld-CeBiTec Research Conference – Advances in Industrial Biotechnology: Synthetic Pathways and Reaction Cascades*, 2013-09-22 – 25, Bielefeld, Germany.

11. J. Muschiol, H. Mallin, D. Böttcher, U. Menyes, K. Geitner, T. Vorhaben, E. Byström, U. T. Bornscheuer, Poster: Heterogeneous Baeyer-Villiger biotransformation applying a novel mass transfer concept, *International Workshop on New and Synthetic Bioproduction Systems*, 2012-12-06 – 07, Hamburg, Germany.

Danksagung

An erster Stelle möchte ich mich herzlich bei Uwe bedanken. Nicht nur für die Überlassung des interessanten Themas, sondern besonders auch für die exzellente Betreuung in den letzten Jahren. Hierzu zählen natürlich nicht nur die vielen Meetings, Telefonkonferenzen und Seminare, sondern auch dass du immer für neue Ideen deiner Doktoranden offen bist und vor allem dass du uns auch immer mit deinen neuen Ideen weitere Möglichkeiten eröffnest (Beispiel SpinChem).

Als zweites möchte ich mich bei der DFG (Projekt Bo1862/6-1) und der Europäischen Kommission (FP7 Programm 289350) für die finanzielle Unterstützung während der Doktorarbeit bedanken.

Des Weiteren geht ein besonderer Dank an unsere Projektpartner aus Wien. Die Zusammenarbeit mit euch hat immer Spaß gemacht und vor allem für das Vorankommen des Projekts beigetragen. Danke Nikolin, Florian und Marko.

Allerherzlichst möchte ich mich auch bei Christin bedanken. Im Prinzip könnte ich hier jetzt genau das Gleiche schreiben, was du an mich in deiner Danksagung geschrieben hast. Vielen Dank für die tolle Zusammenarbeit, dafür dass ich noch vieles von dir lernen konnte, für das Korrekturlesen, für die ab und zu notwendige Aufmunterung und alles andere.

Genauso herzlichst bedanke ich auch bei Sandy. Irgendwie bin ich ja in dein Projekt mit reingerutscht und trotzdem hat die Zusammenarbeit mit dir immer wieder Spaß gemacht. Ich hoffe, dass ich in Zukunft wieder mit euch beiden zusammenarbeiten kann.

Ein großer Dank geht auch an meine Masterandin Katja und meine Bachelorette Stefanie. Ihr habt wesentlich zum Gelingen dieser Arbeit beigetragen. Natürlich bedanke ich mich auch bei all meinen anderen Schützlingen für die spaßige Arbeit mit Euch: Regina, Sven, Jenny und Lea.

Vlada Urlacher danke ich für die Überlassung der CYP102A7, Werner Hummel für die Bereitstellung der LK-ADH und RR-ADH, Jon Stewart für die Bereitstellung der OYE1 und Zhi Li für die zur Verfügungstellung des *C. cellulans* EB-8-4.

Nina Beyer und Dick Janssen danke ich für die Hilfe mit den P450s und die Möglichkeit eines kurzen Aufenthalts.

Hugo van Beek und Marco Fraaije danke ich für die Hilfe mit den Dioxygenasen.

Anna Kluza und Lisa Morlock danke ich für die Arbeiten mit der L6H.

Bei Emil Byström und Hendrik Mallin möchte ich mich herzlich für die super Zusammenarbeit im SpinChem-Projekt bedanken.

Weiterhin danke ich Johannes und Javier für die Teilhabe an eurem geballten molekularbiologischen Wissen. Ihr konntet mich tatsächlich für PCRs begeistern.

Vielen Dank geht auch an Andrea Thürmer für Genomsequenzierung und Dirk Albrecht für die MS-Analysen, ebenso wie an Christine Stöhr und Tim Wendlandt für die Möglichkeit die Gewächshäuser zu nutzen.

Natürlich bedanke ich mich bei den gesamten Arbeitskreisen „Biotechnologie & Enzym Katalyse“, „Proteinbiochemie“ und „DropIn Biofuels“. Hervorzuheben sind hier aber sicherlich Dominique, Ina, Angelika und Fr. Großmann, die im Hintergrund mehr Fäden ziehen als man halten kann; Anita für all die synthetische Leistung und auch für so manchen Klönschnack; Micha, Lilly, HSi, Paulette und Claudi für alles was man außerhalb des Labors machen kann; und Gandi, der wohl weltbeste Verkuppler und sehr guter Freund.

Prelast, but not least, möchte ich mich bei all meinen anderen Freunden und meiner Familie bedanken, die mich in den letzten Jahren immer tatkräftig unterstützt haben und wahrscheinlich auch so manches ertragen mussten.

Zu guter Letzt bedanke ich mich von ganzem Herzen bei Jule und Juris, meiner eigenen kleinen Familie, für das Verständnis und die Geduld. Vor allem musstest du, Jule, in den letzten Wochen zu oft zurückstecken. Aber letzten Endes ward ihr es, die mich immer wieder motiviert haben, die Arbeit auch schnell abzuschließen. Ich freue mich jetzt einfach auf unsere gemeinsame Zukunft. Ich liebe euch.